

**POLYMERIC MATERIALS FROM CELLULOSE AND ITS
DERIVATIVES: PREPARATION, CHARACTERIZATION
AND DURABILITY OF THEIR BLENDS AND COMPOSITES**

A thesis submitted to the
University of Pune

for the degree of
Doctor of Philosophy
in
CHEMISTRY

by
ANNAMALAI PRATHEEP KUMAR

Research supervisor: Dr. R.P. SINGH

Division of Polymer Science and Engineering
National Chemical Laboratory
Pune 411 008, INDIA

June 2008

CERTIFICATE

This is to certify that the work presented in the thesis entitled “*Polymeric Materials from Cellulose and its Derivatives: Preparation, Characterization and Durability of Their Blends and Composites*” submitted by **Mr. A. PRATHEEP KUMAR**, was carried out by the candidate at National Chemical Laboratory, Pune, under my supervision. Such materials as obtained from other sources have been duly acknowledged in the thesis.

Dr. RAJ PAL SINGH, F.R.S.C.
RESEARCH SUPERVISOR,
DEPUTY DIRECTOR,
DIVISION OF POLYMER SCIENCE AND ENGINEERING
NATIONAL CHEMICAL LABORATORY
PUNE – 411 008, INDIA

Declaration of the candidate

I, **Mr. A. PRATHEEP KUMAR**, hereby declare that the thesis entitled “***Polymeric Materials From Cellulose and Its Derivatives: Preparation, Characterization and Durability of Their Blends and Composites***” submitted for the degree of Doctor of Philosophy to the University of Pune, has been carried out by me at Division of Polymer Science and Engineering, National Chemical Laboratory, Pune 411 008, India, under the supervision of **Dr. R. P. Singh**. The work is original and has not been submitted to in part or full by me for any other degree or diploma to this or any other university.

(A. PRATHEEP KUMAR)

To

*Smt. V.A. Kasthuri, (Late) Sri V. Annamalai (my parents),
Mr. A. Senthil Kumar (my brother),
My teachers*

&

To those feet



*whose sheer genius serve as the pillars of the advancement of
science and society...*

Acknowledgements

*It was a Pongal (in Tamil: boiling over) festival in January 2002, when I first met my research supervisor **Dr. Raj Pal Singh**, Polymer Science and Engineering (PSE) Division, National Chemical Laboratory (NCL), Pune since then he has been guiding and teaching me all the dimensions of research field. I would like to express my sincerest thanks to him for his guidance, patience, time, and stimulation that has enabled me to complete my research work successfully.*

I am grateful to Dr. Sivaram, the Director, NCL, Pune, for providing the infrastructure and facilities for my research work. I am very much grateful to Dr. M. G. Kulkarni, Head, PSE division, for providing me access to the facilities in the division. I am very thankful to Dr C. Ramesh and Dr. Baskaran for their valuable suggestions for my research work, esp. in absence of Dr. Singh. I am also very thankful to other scientists in the division namely, Dr. P. P. Wadgaonkar, Dr. C. V. Avadhani, Dr. B.D. Sarwade, Dr. U. Natrajan, Mr. K.G. Raut, Dr S. Ponrathnam, Mr. S. K. Menon, Mrs. D. A. Dhoble, and Mrs. S. Poorvi, for their timely help, fruitful discussions and support.

Additional thanks to Dr. K. Guruswamy and Dr M. Badiger, coordinators of the Polymer Physics and Chemistry, Pre-PhD course work and Prof. S. Ramakrishnan (IISc), Prof. Anil Kumar (IIT-B), Prof. Chabra (IIT-K), Prof Shankar (IIT-K), Prof Nanavati (IIT-B), Dr. V.V. Ranade (NCL), and A.K. Lele (NCL) for their help, fruitful discussions and teaching the subjects. This course work has been vital role for understanding the polymers.

It is an immense pleasure to express my heartiest gratitude to Prof. H. Kothandaraman (Ex-Head) and Dr. A. Raghavan, Department of Polymer Science, University of Madras, for extending their constant moral support and advice from M. Sc days to date. I would like to express affectionate thanks to my friends, Mr. Gandhi (who has motivated me during my M. Sc days for doing research in science) and Mr. Sandeep for their constant support, care and advice.

I also acknowledge CSIR, New Delhi for financial assistance for my research work and medical expenses as Senior Research Fellowship. For earlier funding, I would like to acknowledge M/s Bio-D Plastics, M/s. Bharati-Duraline and IFCPAR, New Delhi on whose projects I was involved as project assistant.

How can I forget my colleagues! Without their support, cooperation, discussions and timely help, my research work could not have matured enough. So I extend my gratitude to my earlier and present labmates Shrojal, Shailendra, Jitendra, Amit Patwa, Kailash, Raghunath, Dilip, Mukesh,

Sravendra, Sunil and Rupali. I also express my sincere thanks to my divisional colleagues Malli, Mahesh, Ravi, Munirasu, Gnyaneshwar, Dhyaneshwar, Arun, Arvind, Asutosh, Vijay, Kedar, Vivek, Smitha, Sachin, Dharma, and all others. I also thank Mr. Mahesh, Mr Zine, Mr. U. Dhavale and Mr. Silas S. Kakade for their assistance.

I am also thankful to Mr. A.B. Gaikwad, Mr. Gholap (CMC) for SEM and TEM facilities and fruitful discussions. I express my thanks to Mr. Deenadayalan, and Harsharvardhan, (PPC) for their timely help in processing and measurement facilities.

Then, once again I recall that festive day of Pongal, since then, I have been into the network of very good friendships. For their moral support and love, I would like to express thanks to Mr. M. Balakrishnan and Mr P. Muthukumar, whom I got as first room mates at NCL, are best friends for the life.

I would like to express my immense thanks to all of my NCL friends,, Vijayanand, Khaja, Selva, Pujari, Vivek, Dr. Chidambaram, Malli, Kannan, Munirasu, Elangovan, Sankar, Marivel, Thirunavukarasu, Marimuthu (C-MET), Murugan, Govind, Shrikant, Swaroop, Kishore, Sarvesh, Kamendra, Sampa, Arshad, Sunil, Sasi, and etc. for their moral support and timely help.

Nobody would have forgotten about an accident happened to me. During those moments, lots of friends at NCL have helped and taken care of my family members and me. I express my sincere thanks to all of my friends including Satyanarayana, Amar and an Iranian couple, Dr. Umesh, Dr. Gijjini(Ruby Hall), Dr. Siddharth (Kotbagi) and the nurses for their hospitality. Especially, I would like to express my thanks to Dr A. Murugan (E-41) Mrs. Durgesh, Mrs. Singh (E-40), Mr. Balaji (RPBD) and his family for their timely help and making our stay peaceful.

Apart from NCL, there is a huge list of friends who are my well wishers. To mention here: Dr. Srisailas, Thirumoorthy, Vijaygopal, Supriya, Rakee, Gokulakrishnan, Manikandan, Geeroopa and Anusuya. I am thankful to all of them for their support.

I am indebted to my parents and brothers (Senthil, Raj & Ashok) who have constantly supported and encouraged me all the time. I am always thankful to them for their love, care and all sacrifices. In the same period, I am fortunate to have Ms. Agila Gopal as my life-partner and my-everything now and then and I am in immense pleasure to express my gratitude for her love, sacrifice, encouragement and support.

I would like to express my thanks to my uncle Sri. C.. Samipillai and his family for their inspiration and family support since my childhood. I extend my thanks to my uncle Sri DM. Gopal, my aunty Smt. Radhabhai and my in-laws Bharathi, Sujatha and Kanimozhi for their love, care, inspiration, encouragement and constant support.

I also express my thanks to Microsoft Inc. for the MS-Office software used for thesis preparation.

I have been fortunate from my prelapsarian childhood as I met really nice people who helped and inspired me time to time. I would like to all of them for their help and inspirations.

Finally, I express my prayers and gratitude to the Almighty (Unified force) for the lead.

(PRATHEEP KUMAR. A)

Contents

Contents	i
Abstract	ix
Abbreviations	xi
List of Tables	xii
List of Figures	xiii
List of Schemes	xviii

Chapter 1: Introduction

1.1	Overview of Polymers: Polymer age	3
1.2	Polymer Applications in Daily Life	4
1.2.1	Overview on Plastics in India	5
1.3	Environmental Impact of Polymers	6
1.3.1	Environmental Advantages of Polymers	7
1.3.2	Environmental Disadvantages of Polymers	8
1.4	Polymer Waste Management	8
1.4.1	Indian Scenario of Plastic Waste Management	10
1.5	Biodegradation and Biodegradable Polymers	12
1.5.1	Biodegradation	12
1.5.1.1	Biological Agents for Degradation	12
1.5.1.2	Mode of Degradation	12
1.5.2	Abiotic Degradation: Precursor for Biodegradation	13
1.5.3	Biodegradability	16
1.5.3.1	Definitions	16
1.5.3.2	Standard Test Methods	17
1.5.3.3	Compostability	18
1.5.3.4	Life Cycle Assessment (LCA)	19
1.5.4	Biodegradable Polymers and Biopolymers	19
1.5.4.1	Biobased Polymers	20

1.5.4.1.1	Derivation of Polymers Directly from Biomass	20
1.5.4.1.2	Synthesis of Polymers using Biobased Monomers	23
1.5.4.1.3	Polymers Synthesized by Microorganisms and Genetically Modified Microorganisms	23
1.5.4.2	Synthetic Biodegradable Polymers	24
1.5.4.3	Polymer Modification to Facilitate Biodegradation	25
1.5.4.4	Blending of Biodegradable with Non-Biodegradable Polymers	25
1.5.5	Applications of Biodegradable Polymers	26
1.6	Cellulose	26
1.6.1	Structural Characteristics	27
1.6.2	Cellulose Production Scenario	28
1.6.3	Cellulose Utilization	29
1.6.4	Applications of Cellulose Fibers	30
1.6.4.1	In Structural and Semi-Structural Applications	30
1.6.4.2	Biocomposites as Eco-Friendly Composites	30
1.6.5	Applications of Cellulose Derivatives	31
1.6.6	Degradation of Cellulose and Its Derivatives	31
1.7	Polymeric Composite Materials	32
1.7.1	Polymer Nanocomposites	33
1.7.2	Growth and Importance of Polymer Nanocomposites	34
1.7.3	Polymer-Layered Silicates Nanocomposites	36
1.7.4	Characterization Techniques	39
1.7.5	Nanocomposites of Biodegradable Polymers: Bionanocomposites	39
1.7.5.1	Cellulose and Its Nanocomposites	39
1.7.5.1.1	Cellulose Whiskers as Nanoscale Fillers	40
1.7.5.1.2	Cellulose Derivatives as Matrices	41
1.7.5.2	Starch Based Nanocomposites	41
1.7.5.3	Chitin/Chitosan Based Nanocomposites	41

1.7.5.4	Polylactic Acid Nanocomposites	42
1.7.5.5	Natural Oil Based Nanocomposites	42
1.7.5.6	Other Polyesters Nanocomposites	42
1.8	The Importance of This Study	42
	References	44

Chapter 2: Scope and Objectives of the Present Investigation

2.1	Introduction: Motivation of the Study	52
2.2	Approaches and Objectives	54
	References	56

Chapter 3: Effect of the Treatment of Cellulose Fiber on the Properties and Durability of Natural-Fiber Reinforced Composites

3.1	Introduction	58
3.2	Experimental	59
3.2.1	Materials	59
3.2.2	Alkaline Treatment and Lignin Content Measurement	59
3.2.3	Maleation of EP Copolymer and Preparation of Composites	60
3.2.4	Characterization	61
3.2.4.1	FTIR Spectroscopy	61
3.2.4.2	Color Index	61
3.2.4.3	Mechanical Properties Measurements	62
3.2.4.4	Thermal Properties Measurements	62
3.2.4.5	Microscopic Measurements	62
3.2.5	Performance Evaluation	62
3.2.5.1	Photo-Degradation	62
3.2.5.2	Biodegradation: Composting Method	63
3.3	Results and Discussion	63
3.3.1	Characterization	63

3.3.1.1	Fiber Characterization	63
3.3.1.2	Preparation	64
3.3.2	Color Index	66
3.3.3	Mechanical Properties	69
3.3.4	Thermal Stability	71
3.3.5	Evaluation of Durability / Degradability	71
3.3.5.1	Photo-Irradiation Induced Changes	71
3.3.5.1.1	FTIR Spectral Changes	71
3.3.5.1.2	Color Index	74
3.3.5.1.3	Surface Morphological Aspects	75
3.3.5.1.4	Mechanical Properties	78
3.3.5.2	Composting	80
3.4	Conclusion	84
	References	85

Chapter 4: Effect of Nano-Clay Reinforcement on the Properties and Durability of Cellulose - Reinforced Composites

4.1	Introduction	88
4.2	Experimental	91
4.2.1	Materials	91
4.2.2	Maleation of Polymers	91
4.2.3	Preparation of Composites	91
4.2.4	Characterization	92
4.2.4.1	FTIR Spectroscopy	92
4.2.4.2	Mechanical Properties Measurements	92
4.2.4.3	Thermal Analysis	92
4.2.4.4	X-Ray Diffraction Measurements	93
4.2.4.5	Microscopic Measurements	93
4.2.4.6	Water Absorption	93
4.2.5	Durability Evaluation	94

4.2.5.1	Photo-Degradation	94
4.2.5.2	Biodegradation: Composting Method	94
4.3	Results and Discussion	95
4.3.1	Characterization	95
4.3.2	Structure and Morphology	97
4.3.3	Thermal Properties	101
4.3.4	Mechanical Properties	103
4.3.5	Water Absorption Behavior	107
4.3.6	Durability Evaluation	108
4.3.6.1	Photo-Irradiation	108
4.3.6.1.1	FTIR Spectral Changes	108
4.3.6.1.2	Morphological Aspects	113
4.3.6.1.3	Changes in Mechanical Properties	116
4.3.6.2	Biodegradation: Composting	118
4.3.6.2.1	Weight Loss during Composting	118
4.3.6.2.2	Surface Morphological Aspects	121
4.4	Conclusion	123
	References	124

Chapter 5: Improvement of Properties of Cellulose Reinforced Starch Composites by Photo-Induced Crosslinking

5.1	Introduction	127
5.2	Experimental	128
5.2.1	Materials	128
5.2.2	Preparation and Photo-Irradiation of Composite Films	128
5.2.3	Characterization	129
5.2.3.1	Water Absorption	129
5.2.3.2	Swelling Degree and Gel Fraction Measurement	130
5.2.3.3	Thermal Analysis	130
5.2.3.4	Mechanical Properties Measurement	130

5.2.3.5	Microscopic Analysis	130
5.3	Results and Discussion	131
5.3.1	Characterization	131
5.3.2	Sorption behavior	132
5.3.2.1	Water Absorption Behavior	132
5.3.2.2	Swelling Degree and Gel Fraction in Dimethylsulphoxide (DMSO)	134
5.3.3	Thermal Properties	136
5.3.3.1	Anti-Plasticization Effect	137
5.3.3.2	Reduction in Anti-Plasticization by Photo-Irradiation	138
5.3.4	Mechanical Properties	139
5.4	Conclusion	144
	References	145

Chapter 6: Preparation and Characterization of Bionanocomposites based on Cellulose esters and Clay

6.1	Introduction	147
6.2	Bionanocomposites from Polyethylene Glycolated Cellulose Esters and Organically Modified Montmorillonite	148
6.2.1	Experimental	149
6.2.1.1	Materials	149
6.2.1.2	Preparation of Isocyanate Terminated Polyethylene Glycol Prepolymer	149
6.2.1.3	Grafting of PEG on Cellulose Acetate	150
6.2.1.4	Preparation of Nanocomposites	150
6.2.1.5	Characterization	151
6.2.1.5.1	FTIR Spectroscopy	151
6.2.1.5.2	NMR Spectroscopy	151
6.2.1.5.3	Wide Angle X-Ray Diffraction	151
6.2.1.5.4	Thermal Properties	151

	6.2.1.5.5	Dynamic Mechanical Properties	151
	6.2.1.5.6	Tensile Properties	152
	6.2.1.5.7	Biodegradation: Composting	152
6.2.2		Results and Discussion	152
	6.2.2.1	Synthesis of Isocyanate-terminated Prepolymer	152
	6.2.2.2	Grafting of Isocyanate-Terminated PEG with Cellulose Ester	153
	6.2.2.3	Wide Angle X-Ray Diffraction Pattern	156
	6.2.2.4	Thermal Properties	157
	6.2.2.5	Dynamic Mechanical Analysis	159
	6.2.2.6	Tensile Properties	161
	6.2.2.7	Biodegradation: Compostability	162
6.3		Bionanocomposites from Polylactic Acid Grafted Cellulose Esters and Organically Modified Montmorillonite	164
	6.3.1	Experimental	164
	6.3.1.1	Materials	164
	6.3.1.2	Grafting of Lactide on Cellulose Acetate and Cellulose Acetate Butyrate	164
	6.3.1.3	Preparation of Nanocomposites	165
	6.3.1.4	Characterization	166
	6.3.2	Results and Discussion	166
	6.3.2.1	FTIR Spectroscopy	166
	6.3.2.2	¹³ C NMR-Spectroscopy	166
	6.3.2.3	Wide Angle X-Ray Diffraction Pattern	167
	6.3.2.4	Dynamic Mechanical Properties	168
	6.3.2.5	Mechanical Properties	169
	6.3.2.6	Biodegradation: Compostability	170
6.4		Conclusion	172
		References	173

Chapter 7: Biomimetic Synthesis of Nanohybrids based on Calcium Hydroxyapatite and Carboxymethyl Cellulose

7.1	Introduction	175
7.2	Experimental	177
7.2.1	Materials	177
7.2.2	Synthesis of Nanohybrids	177
7.2.3	Characterization	178
7.3	Results and Discussion	179
7.3.1	FTIR Spectroscopy	179
7.3.2	³¹ P-NMR Spectroscopy	180
7.3.3	Thermogravimetric Analysis (TGA)	182
7.3.4	Wide Angle X-Ray Diffraction (WAXD)	183
7.3.5	Scanning Electron Microscopy (SEM) and Energy Dispersive X-ray Analysis (EDAX)	186
7.3.6	Transmission Electron Microscopy (TEM)	188
7.4	Conclusion	191
	References	192

Chapter 8: Conclusions

8.1	Summary and Conclusions	195
8.2	Future perspectives	197

Polymeric Materials from Cellulose and its Derivatives:

Preparation, Characterization and Durability of Their Blends and Composites

Abstract

Renewable resources, which had been of central importance with respect to the economy and agricultural policy before the Industrial Revolution, are again of importance in our modern society because of their positive effects on agriculture, the environment and the economy. From the current point of view, cellulose is the most common organic polymer, representing about 1.5×10^{12} tons of the total annual biomass production, and is considered an almost inexhaustible source of raw material for the increasing demand for environmentally friendly and biocompatible products. Thus, the present research work is aimed to refocus or revisit the possibilities of utilization of cellulose for various applications esp. structural and semi-structural fields. *Chapter 1* gives an **introduction** and literature background on this area. *Chapter 2* reveals the **scope and objective** of the present study. The present study has been divided into three parts. The first part is on utilizing cellulose fibers as reinforcing materials. The second part is on utilization of cellulose after some chemical modification as matrix. The third part is to give an example of utilizing cellulose derivative to in the bionanomaterial field as template material for synthesizing nanoparticles.

In the first part, the *Chapter 3* is focused on **the effect of fiber treatment on material properties and their durability under biotic and abiotic conditions**. Jute fiber is one of the natural fibers abundantly available in India. Jute fiber was treated with aqueous NaOH (3-40%) solution and incorporated into thermoplastic polyolefin matrix. It was found that alkali treatment had significant effect on the performance and durability. Depending on content of fiber components (esp. lignin), durability was affected. It is summarized that for various applications of natural fiber reinforced composites, the treatments on the fiber have to be optimized depending on their durability requirement.

Recently, possibilities of reinforcing polymers with layered silicates are highly explored. The polymer-clay nanocomposites have shown drastic improvement in thermal, mechanical properties, because of their platelet nature high surface and aspect ratio. The

Chapter 4 discusses **the possibilities of incorporating layered silicates into the cellulose-fiber reinforced composites**, by preparing ternary composites of clay, cellulose and polyolefin (thermoplastic) matrix.

It was also decided to prepare the green composite materials using cellulose fiber natural biopolymer as matrix. The *Chapter 5* reveals the strategy of **improving material properties by biopolymer (starch) matrix by cellulose fiber reinforcement and photo-induced crosslinking**.

The second part is on utilization of cellulose after some chemical modification as matrix. Cellulose esters have been used as thermoplastics after external plasticization. There are some drawbacks in using external plasticizers while processing and usage such as leaching out of plasticizer apparently harms the environment. To evade this problem, it has been planned to graft the polymer chains, which are also biodegradable on cellulose esters. In *Chapter 6*, **the preparation, characterization and applications of nanocomposite materials of polyethylene glycol (via urethane linkage) and lactide (ring opening polymerization) grafted cellulose esters (cellulose acetate (CA) and cellulose acetate butyrate (CAB) with layered silicates**. The prepared materials were carefully characterized and found to show various structural morphology and mechanical properties depending on the preparation methodologies involved.

In the third part of the study, modified cellulose was used for preparing bioinspired nanoparticles. The *Chapter 7* discusses the study on **biomimetic synthesis of nanosized hydroxyapatite (HA) using a cellulose derivative**. The nanohybrids having different sizes of HA nanoparticles were prepared by varying the concentration of carboxymethylcellulose (CMC).

The *Chapter 8* **summarizes** and briefly discusses the **future perspectives** in the area of the study.

Abbreviations

^{13}C -NMR	Carbon Nuclear Magnetic Resonance Spectroscopy
^1H -NMR	Proton Nuclear Magnetic Resonance Spectroscopy
C30	Cloisite 30 B (Modified montmorillonite)
CA	Cellulose Acetate
CAB	Cellulose Acetate Butyrate
CI	Carbonyl Index
CMC	Carboxymethyl Starch
DMA	Dynamic Mechanical Analysis
DSC	Differential Scanning Calorimetry
EDAX / EDX	Energy Dispersive X-ray Analysis
ED	Electron Diffraction
FTIR	Fourier Transform Infra-red Spectroscopy
HA	Hydroxyapatite
IPDI	Isophorone diisocyanate
LCA	Life Cycle Assessment
MC	Microcrystalline Cellulose
MMT	Montmorillonite
MPa	Mega Pascal (unit)
PEG	Polyethylene glycol
SEM	Scanning Electron Microscopy
TEM	Transmission Electron Microscopy
TGA	Thermogravimetric Analysis
UV	Ultraviolet Spectroscopy
WAXD	Wide Angle X-Ray Diffraction
YI	Yellow Index

List of Tables

Tab. 1.1	Demand scenario for key commodity plastics in India (in thousand tones)	6
Tab. 1.2	The energy requirement for production of general packaging materials	7
Tab. 1.3	International standard methods for testing biodegradability	17
Tab. 1.4	Chemical structure of some polysaccharides	21
Tab. 1.5	Composition in the fibers	29
Tab. 1.6	Primary and additional functions of fillers	33
Tab. 1.7	Worldwide volume and value for polymer nanocomposites 2003 - 2008 (millions)	36
Tab. 1.8	Global projection for materials demand in a ‘ <i>business-as-usual</i> ’ scenario	42
Tab. 3.1	Characteristics of fibers	59
Tab. 3.2	Composition of the composites	61
Tab. 3.3	Characteristics of treated fibers	64
Tab. 3.4	Trends in properties of composites	83
Tab. 4.1	d-spacing values of 001-basal plane	98
Tab. 4.2	Weight loss (%) of 50-h photo-irradiated samples during composting	120
Tab. 5.1	Formulations of the composites prepared	129
Tab. 6.1	Tensile properties of externally plasticized and polyethylene glycolated cellulose esters (copolymer) and their nanocomposites	161
Tab. 6.2	Tensile properties of externally plasticized and polylactide grafted cellulose esters (copolymer) and their nanocomposites	170
Tab. 7.1	Calcium phosphates (CaPs) of biomedical significance	175
Tab. 7.2	The observed 2θ ($^{\circ}$), d-values and corresponding indices from WAXD pattern of as-synthesized and calcined samples of HA-05	185
Tab. 7.3	Crystallite size of as-synthesized and calcined hydroxyapatite nanoparticles	185

List of Figures

Fig 1.1.	Distribution of polymer used in a) USA and b) European countries	4
Fig 1.2.	General pathways plastic waste management	9
Fig 1.3.	Schematic representation of polymer auto-oxidation and stabilization	14
Fig 1.4.	Schematic representation of mechanism bioassimilation of oxidized products	15
Fig 1.5	Schematic representation of origin and method of production of biobased polymers	20
Fig. 1.6	Chemical Structure of few biodegradable polymers	24
Fig. 1.7	From molecular structure to microfibers formation	27
Fig. 1.8	Schematic representation of general synthesis of cellulose	28
Fig. 1.9	Schematic representation of various shapes and dimensions of nanoscale materials	34
Fig. 1.10	Schematic representation of 2:1 phyllosilicates	37
Fig. 1.11	Schematic representation of preparation and types of nanocomposites based on polymer and nanoscale layers	38
Fig. 3.1	Influence of alkaline treatment on acid insoluble lignin content	63
Fig. 3.2	Optical micrograph of a) microcrystalline powder and b) alkali treated jute fibers (with x50 magnification).	64
Fig. 3.3	FTIR spectra of composites a) carbonyl region and b) hydroxyl region	65
Fig. 3.4	Optical micrograph of the composite a) J1C05, b) J2C05 and c) MC05 (with x50 magnification)	66
Fig. 3.5	Picture of the prepared composites	67
Fig. 3.6	Color Index of the prepared composites.	67
Fig. 3.7	UV spectra of acid soluble lignin extracted 17.5 % NaOH treated Jute fiber.	68
Fig. 3.8	Influence of loading of different fibers on a) tensile Modulus, b) yield Stress, c) stress at break and d) elongation [%] at break.	69

Fig. 3.9	Derivative thermogram of the composites with 5% fiber content.	71
Fig. 3.10	FTIR spectra of 100 hrs UV irradiated composites at a) carbonyl region and b) hydroxyl region	72
Fig. 3.11	Yellowing of samples upon photo-irradiation	74
Fig. 3.12	SEM of photo irradiated samples a) J1C05, b) J2C05 and c) MC05.	76-77
Fig. 3.13	Effect of photo-irradiation on the mechanical properties a) Tensile Modulus, b) Yield Stress, c) Stress at break and d) Elongation at break [%] of composites	78
Fig. 3.14	Weight loss [%] of the non-irradiated films composites with a) 5% of fibers b) 10% of fibers and c) 15, 25 and 40% of fibers during composting	80
Fig. 3.15	Optical micrograph of one month composted samples a) J1C25 and b) J2C25.	81
Fig. 3.16	Weight loss (%) values during composting of 50 h photo-irradiated samples.	82
Fig. 3.17	SEM images of 50h irradiated and 2 month composted specimen of a) MC05 and b) J1C05	83
Fig. 4.1	FTIR spectra of neat polymer, maleated polymer and composites of a) PE, b) PE samples at carbonyl region, and c) EP copolymer	96
Fig. 4.2	WAXD pattern of composites of a) PE, b) PP, c) EP (2-30°) and d) EP (2-10°)	98
Fig. 4.3	Bright field TEM image of EP-TC05	100
Fig. 4.4	DSC thermogram of composites of a) PE and b) EP copolymer	101
Fig. 4.5	TGA thermograms of composites	102
Fig. 4.6	Tensile properties of PE and PP samples a) Tensile modulus, b) Yield stress c) Elongation (%) of PE samples and d) Elongation (%) at break for PP samples.	104
Fig. 4.7	Influence of clay on the tensile properties of cellulose composites of EP	105
Fig. 4.8	Water absorption behavior of composite samples	107

Fig. 4.9	FTIR spectral changes at a) carbonyl region and b) hydroxyl region of PE and maleated PE samples upon photo-irradiation	109
Fig. 4.10	FTIR spectra of EP-composite samples upon photo-irradiation at a) carbonyl region and b) hydroxyl region	110
Fig. 4.11	FTIR spectra at carbonyl region of PE samples upon photo-irradiation	111
Fig. 4.12	Effect of photo-irradiation on samples as carbonyl index in FTIR spectra of a) PE, b)PP and c) EP samples	112
Fig. 4.13	Scanning electron micrographs of 0h and 50h photo-irradiated samples of PE	114
Fig. 4.14	Scanning electron micrographs of 50 h photo-irradiated samples of EP	115
Fig. 4.15	Scanning electron micrographs of 50 h photo-irradiated samples of PP	116
Fig. 4.16	Effect of photo-irradiation on the mechanical properties a) Tensile modulus, b) Stress at break and c) elongation at break of PE samples	117
Fig. 4.17	Weight loss (%) of non-irradiated samples upon incubation in compost.	119
Fig. 4.18	Scanning electron micrographs of non-irradiated samples of PE after 1 month of composting	121
Fig. 4.19	Scanning electron micrographs of 50h-irradiated composite samples of PE after 1 month of composting	122
Fig. 5.1	a) Polarized optical micrograph (x50 magnification) and b) Scanning electron micrograph of microcrystalline cellulose powder	131
Fig. 5.2	Picture of a) NeatSt (faster) dried at 50-60 °C and 20 min irradiated, b) StCell5 (slowly) dried at 30 °C and 20 min irradiated, and c) StCell5 (faster) dried at 50-60 °C and 20 min irradiated	133
Fig. 5.3	Water absorption % of samples a) after 48 h of storage as a	133

	function of UV irradiation time and b) as a function of storage time, under 100 % relative humidity.	
Fig. 5.4	Picture of specimens of a) controlled ‘NeatSt’, b) controlled ‘Stcell5’, c) 30-min. irradiated ‘Stcell5’ and d) swollen gel of c, after 24 h soaking in DMSO.	134
Fig. 5.5	Swelling degree of prepared composite films as a function of irradiation time.	135
Fig. 5.6	Effect of photo-irradiation on the gel fraction (%)	136
Fig. 5.7	Thermal gravimetric (TGA) thermograms of controlled and 30min irradiated specimen of plasticized starch and composite films.	136
Fig. 5.8	Differential scanning calorimetric (DSC) thermograms of controlled and 30min irradiated specimen of plasticized starch and composite films.	137
Fig. 5.9	Schematic representation of reduced retrogradation a) plasticized amylopectin and b) photoirradiated amylopectin. Ovals / coils are to symbolize retrogradation and dotted lines represent inter-/ intra-molecular crosslinking	139
Fig. 5.10	Effect of photo-irradiation on tensile modulus of composite films	140
Fig. 5.11	Effect of photo-irradiation on a) stress at break and b) yield stress	141
Fig. 5.12	Elongation (%) a) at break and b) yield of controlled and (10, 30 min) irradiated composite films	142
Fig. 6.1	FTIR spectra of a) isocyanate terminated polyethylene glycol, and b) cellulose acetate and grafted copolymer	153
Fig. 6.2	¹ H-NMR spectra of a) isocyanate terminated polyethylene glycol, b) cellulose acetate and c) grafted copolymer	154- 155
Fig. 6.3	Wide angle X-ray Diffraction pattern of prepared samples of a) CA and b) CAB	156
Fig. 6.4	Derivative thermogram of samples	157
Fig. 6.5	DSC thermograms of samples based on a) cellulose acetate and b) cellulose acetate butyrate esters.	158

Fig. 6.6	Dynamic mechanical properties (storage modulus (Δ), loss modulus (\square) and tan delta (\diamond))	159-160
Fig. 6.7	Weight loss (%) of the samples upon composting	163
Fig. 6.8	FTIR Spectra of neat cellulose acetate butyrate and grafted copolymer	166
Fig. 6.9	^{13}C -NMR Spectrum of lactide grafted copolymer of cellulose acetate butyrate	167
Fig. 6.10	WAXD pattern of nanocomposite polylactide grafted copolymer and C30B	168
Fig. 6.11	Dynamic mechanical properties (storage modulus (Δ), loss modulus (\square) and tan delta (\diamond))	169
Fig. 6.12	Weight loss (%) of samples upon composting	171
Fig. 7.1	FTIR Spectra of a) as-synthesized and b) calcined hydroxyapatite-CMC nanohybrid samples	180
Fig. 7.2	^{31}P -NMR spectra of a) <i>as-synthesized</i> and b) calcined hydroxyapatite-CMC nanohybrid samples	181
Fig. 7.3	Thermograms hydroxyapatite-CMC nanohybrids	182
Fig. 7.4	WAXD patterns of spectra of a) as-synthesized and b) calcined hydroxyapatite-CMC nanocomposite samples	184
Fig. 7.5	Scanning electron micrographs (SEM) of a) as-synthesized and b) calcined of HA-05, c) as-synthesized and b) calcined of HA-1 (50x magnification)	186
Fig. 7.6	EDAX spectra of as-synthesized and calcined HA-05	187
Fig. 7.7	Bright field TEM images of a) as-synthesized HA-005, b) calcined HA-005, c) as-synthesized HA-05, d) as-synthesized HA-01 and e) electron diffraction of HA-05.	188

List of Schemes

Sch. 2.1	Flowchart of the present investigation	55
Sch. 3.1	Radical formation on a) cellulose and b) lignin components under UV irradiation	73
Sch. 3.2	Formation of quinonoid structures upon photo-irradiation	75
Sch. 4.1	Schematic representation of three types of composites	90
Sch. 4.2	General reaction mechanism of maleic anhydride grafting on a polyolefin PP	95
Sch. 4.3	Schematic representation of possible interactions between polymer, compatibilizer and fillers.	99
Sch. 6.1	Grafting reaction of polyethylene glycol on cellulose acetate via urethane linkage	150
Sch. 6.2	Pathways for preparation of nanocomposites based on polyethylene glycolated cellulose acetate and clay	151
Sch. 6.3	Pathways for preparation of nanocomposites based on polyethylene glycolated cellulose acetate and clay	166
Sch. 7.1	Chemical Structure of Sodium Carboxymethyl cellulose (CMC)	177
Sch. 7.2	Schematic representation of nucleation and induction of hydroxyapatite crystals by carboxyl groups of CMC.	190

Chapter 1

Introduction

Summary

Renewable resources and issues of sustainability are receiving increasing attention from academia, industry and government. The evolution and the success of the chemical industry have intimately been related to the introduction of fossil feedstocks as a basis for synthesis. Today fossil feedstocks are the most important raw materials for the chemical industry, accounting for more than 90%. In the 21st century, major changes are coming in automobile industry and materials will be a key enabling technology. Since about 90% of the total energy consumption by an automobile in its lifetime is from fuel¹⁻², the automobile parts made of metals cause the higher exploitation of petroleum resources. The high expectations for fuel economy and low emissions for manufacturing and transportation are creating a demand for new low cost and high-performance lightweight materials. Not only in automobile industry, almost in every applications from agriculture to transport and from aerospace to food packaging, the use of polymeric materials has become an integral part of our modern daily living. The success of plastics based on petroleum resources can be attributed not only to the reliable raw materials basis and to their versatile applications properties, but also to their melt-processability³. Their real problem is disposal. In landfills, they will occupy the land for indefinite amounts of time due to very slow degradation. As a result of the fossil fuel crisis, alternative energy and raw materials sources such as biomass are propagated and investigated intensely. From the current point of view, cellulose is the most common organic polymer, representing about 1.5×10^{12} tons of the total annual biomass production, and is considered an almost inexhaustible source of raw material for the increasing demand for environmentally friendly and biocompatible products⁴⁻⁵.

The present thesis is aimed to re-focus or re-visit the possibilities of utilization of cellulose for various applications esp. structural and semi-structural fields by preparing the polymeric materials using cellulose and its derivatives as reinforcing fiber and matrix, respectively, and studying their durability in abiotic and biotic environmental conditions. Additionally, using cellulose derivative, the biomedical important inorganic nanoparticles have also been prepared. This chapter portrays the historical background and literature survey on biopolymers and biodegradation of polymers.

Chapter 1

1.1. Overview of Polymers: Polymer age

The polymer industry has revolutionized the quality of life through the generation of new materials that have transformed everything from transportation to communication to recreation. The story of how the human race gained mastery over metals is well known and has been enshrined in terms of “Bronze age” and “Iron age”. Now, it is difficult to imagine our society without polymers. From plastic soda bottles to automobile parts, from medical implants to bulletproof vests, polymers are an integral part of our daily lives. New polymers and new uses for existing polymers are constantly being developed. Fully half of the new chemicals entering commerce in the United States (US) each year are polymers. In addition, ethylene, primarily used as a monomer for plastics, is second only to sulfuric acid in production volume. The plastics industry plays a major role in the economy of the US and the world. In 1996, shipments of plastics in the US totaled \$274.5 billion, a 55% increase since 1991. In the same year, globally 95.6 million metric tons of the five leading thermoplastics (high-density polyethylene, low-density polyethylene, polypropylene, polystyrene and polyvinyl chloride) were consumed⁶. The growth of polymers and plastics has had remarkable parallels to the growth of the environmental movement. Both of these movements have their origins in the early part of this century; however, it was during 1960s that a widespread explosion in awareness and adoption of these two new frontiers occurred. Whether it was in 1962 when Rachel Carson penned ‘Silent Spring’ or in 1967 when the film ‘The Graduate’ advised popular culture that future was just one word “PLASTICS”, these two areas have been developing industries ever since, and since their origins they have tracked one another in other aspects as well⁷. As consciousness about the environmental issues rose, so a desire to change people’s littering behavior along with the materials that continue the litter. During this period, the polymer-based industries first began to focus on designing materials that biodegrade in the natural environment. To this day, efforts continue to make a wide range of synthetic materials that do not persist in the environment intact but break down into innocuous degradation products.

Chapter 1

1.2. Polymer Applications in Daily Life

The versatility of polymers has been the central to their extensive use in a wide range of applications. Polymers are altogether more complex than metals, and the history of evolution of our familiarity with polymers, from the first wooden club to the latest carbon baseball bat, is still largely untold. Polymers have almost replaced materials such as metal, glass, wood, paper, fiber, ceramics etc. in packaging, automobiles, building construction, biomedical fields, electronics, electrical equipments, appliances, furniture, pipes and heavy industrial equipments. In a nutshell, from agriculture to transport and from aerospace to food packaging, the use of plastics has become an integral part of our modern daily living⁸. Their growth is almost matching with the need of our growing world population. *Figure 1.1* shows the utilization of plastics for various applications in USA⁶ and Europe⁷.

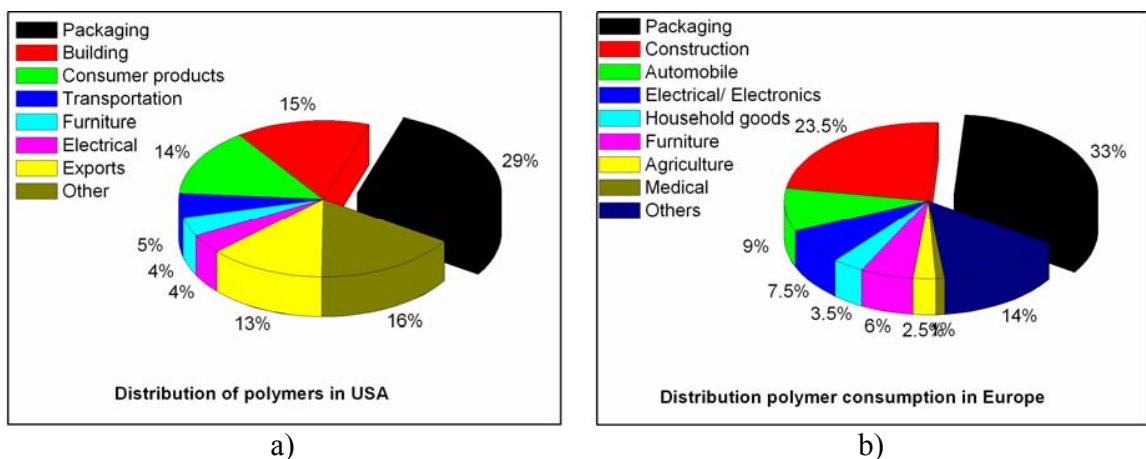


Figure 1.1: Distribution of polymer used in a) USA and b) European countries

Then phenomenal rise in the use of plastics is the result their extraordinary versatility and low cost. For example, for making beverage containers, 3 pounds of aluminium or 27 pounds of glass can be replaced by 2 pounds, for delivering eight gallons of juice. The mechanical properties of plastics allow less packaging materials to be used, decreasing production, shipping and energy costs. As it can be seen in the *Figure 1.1*, one third of polymers are utilized for packaging only. Plastic packaging is popular on account of its low cost and performance properties, which make them to use in any forms, from shopping bags to different types of loose-fill packaging materials including peanut-shaped variety. One-half of the plastic packaging materials are used for containers, such as soft drink,

Chapter 1

bottles, and jugs for milk, water, laundry detergents, and bleach. One third is in the form of plastic sheeting or films and remainder is for closures, coatings, and other purposes. Since the plastic packaging has increased, in order to main compatibility, the use of synthetic adhesives has also grown. Now we have become a partly plastic-oriented society, since the society has become packaging-oriented. However, over 60% of post-consumer plastics waste is produced by households; as single-use packaging materials. In addition, plastics perform a critical function in life-saving devices used in hospitals ad emergency rooms. Syringes are used to deliver essential drugs; IV bags dispense vital fluids, and plastic tubing transfer oxygen to assist with breathing. The inertness of plastics also makes them ideal candidates for use in prosthetic limbs and pacemakers. Biodegradable stitches are commonly used to eliminate the need for subsequent removal. Improved medical devices and procedures have benefited from better polymer products⁷.

1.2.1. Overview on Plastics in India

The polymer industry in India has moved a long way and has diversified to serve key sectors like agriculture, telecom, transport and packaging. As the per capita consumption of plastics (4kg) in India is very low as compared to the world average of 18 kg consumption, India is still a scarcely tapped market and the number of potential consumers is enormous. So the industry believes that the demand for plastic products can be vastly increased in India⁹. Further, liberalization of the Indian economy and petrochemical industry being a high priority area for the Government, there is bound to be an increase in plastic production and consumption in the years to come. The growth of the Indian plastic industry has been phenomenal - the growth rate (17%) is higher than for the plastic industry elsewhere in the world⁹. India has a population of over 1 billion and a plastic consumption of 4 million tonnes. One third of the population is the middle class whose aspirations could be molded to increase consumption. Plastic manufacturers create needs for this segment of population. The rising needs of the middle class, and abilities of plastics to satisfy them at a cheaper price as compared to other conventional materials like glass and metal, has contributed to an increase in the consumption of plastics in the last few years. The consumption trends for key commodity plastics are presented in *Table 1.1*, as estimated in 1997.

Table 1.1: Demand scenario for key commodity plastics in India (in thousand tones)⁹⁻¹⁰

Polymer	1995-1996	2001-2002	2006-2007	2009-2010
Polyethylene (PE)	823	1835	3267	-
Polypropylene (PP)	340	885	1790	-
Polyvinyl chloride (PVC)	489	867	1287	-
Polyethyleneterephthalate (PET)	34	140	289	-
Others	203	647	1415	-
Total	1889	4374	8054	12000
Plastics in Packaging – (% of total plastics)	976 (52%)	2272 (52%)	4037 (50%)	-

Of the total consumption of plastics, commodity plastics account for 85% with engineering and other plastics accounting for the balance¹¹. Packaging presents a major growth area where there has been a spiraling demand for plastics. Major share (52%) of the plastics produced in India are utilized for packaging. Among the commodity plastics, polyethylene and PET are predominantly used in packaging. The rise in PET is mainly associated with the non-availability of clean water in the country. Since the durability of plastics has helped them in market-place, increasing their durability has also been a major goal of polymer research. The resistance towards degradation was touted as an out standing and attractive property in the course of this country¹².

1.3. Environmental Impact of Polymers

Advances in petroleum based fuels and polymers have benefited mankind in numerous ways. Since 1950s not only polymers, synthetic dyes, light-stable colorants and drugs have become accessible to larger portions of the population for the first time³. However, environmental concerns extend polymers beyond the products, to synthesis and manufacturing. Very first concern is the raw materials and energy requirement. Traditionally, these processes have utilized non-renewable feedstocks, volatile organic solvents, or hazardous reagents. Sometimes the reaction may require a large energy input or may generate a significant quantity of waste. Most of polymer syntheses, like 98% of

Chapter 1

organic synthesis, begin with petroleum-based feedstocks. After 1970s, contemporary geopolitical and economical developments have brought back to mind the disadvantages of a dependence on crude oil and its limited availability. The range of proven oil reserves accessible with conventional recovery techniques is currently estimated to be 40 years¹³. This may be pessimistic estimation in hindsight, on the other hand without doubt the dependence on the oil reserves in the Middle East will substantially increase³. In addition, the ultimate formation of the greenhouse gas CO₂ from fossil feedstocks has unpredictable and irreversible consequences on the global climate.

1.3.1. Environmental Advantages of Polymers

The low production cost (labor and energy) of plastic materials from crude oil is attributed to their ease of processability and production. *Table 1.2* compares the energy requirement for production of general packaging materials¹⁴.

Table 1.2: The energy requirement for production of general packaging materials¹⁴

Material	Energy required (kWh/kg)	Container	Energy required per container (kWh)
Aluminium	74.1	Aluminium	3.00
Steel	13.9	Steel can	0.70
Glass	7.9	Glass beverage bottle	2.00-2.40
Paper	7.1	Paper milk carton	0.18
Plastic	3.1	Plastic beverage container	0.11

The processing of conventional materials (metal, glass, wood and paper) requires more energy than that needed for plastics. Thus, as far as energy concerned for the processing, the plastics make their use as a positive contribution to environmental resources. However, the long life and desirability of plastics which have made them a material of choice for many applications is seemingly a disadvantage when it comes to their disposal.

1.3.2. Environmental Disadvantages of Polymers

The disposal of items made of petroleum-based plastics, such as fast-food utensils, packaging containers, and trash bags, also creates an environmental problem. First problem is the litter. The beautiful parks, lawns and gardens, streets, highways, railways, seashore, river-banks, health resorts and hill-shots are spoiled by plastic littering. Since the discarded plastic materials are lighter in weight, they are easily carried away by winds and waves to distant places. In cities, these discarded plastic materials may choke the street gutters, manholes and sewage drainage systems and serious water logging problems. Some of the plastic additives are highly reactive even toxic to the environment (water and land) and life. Upon atmospheric oxidation, they may generate hazardous gases. For example, PVC liberates corrosive HCl gas. Open burning of plastics is even more dangerous. Ultimately, polymer waste if dumped or discarded haphazardly, will pose serious problems (litter, toxic, blocking of sewage /drainage)¹⁵.

1.4. Polymer Waste Management

Plastic goods after completion of their useful life find their way into waste. Waste generation rates are often affected by socio-economic development, degree of industrialization, and climatic conditions. Generally, greater the economic prosperity and the higher percentage of urban population, greater the amount of solid waste produced¹⁶. The phenomenal growth of plastics and their consumption in terms of products of short and intermediate life spans have resulted in significant generation of waste. Depending on their generation stage, polymer waste can be classified as industrial polymer waste (IPW) and post-consumer polymer waste (PCPW). IPW includes waste generated at i) production, ii) processing, and iii) service or repairing stages. Their handling was tackled by the respective industries, primarily to aid the economics of the process. The real problem with PCPW and the cost associated with its management. The discarded polymer products are handled through usual municipal solid waste management methods such as landfill, incineration, recycling and degradation as shown in *Figure 1.2*¹⁷.

Landfill is most widely used method of disposal of polymeric materials. It is economical and requires less energy. Many plastic materials are found to undergo a degree of degradation after certain time period. However, once land-filled, the energy invested for

manufacture and use of the products is lost. This method provides no solid waste diversion or any energy recovery¹⁸.

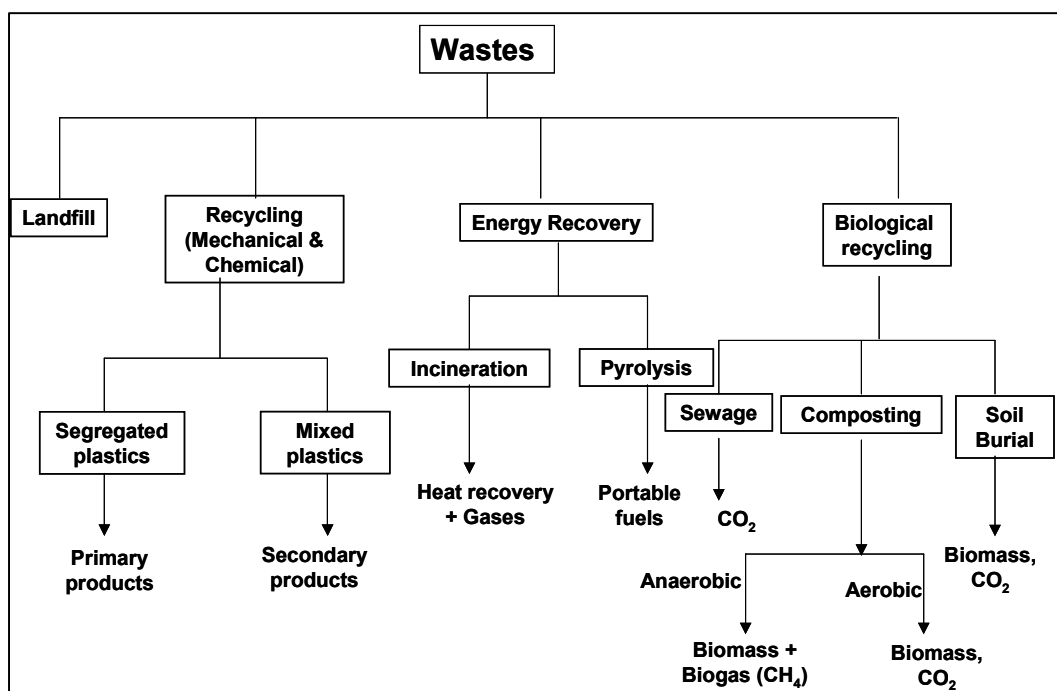


Figure 1.2: General pathways plastic waste management

Moreover, in case of open-dumping, serious threat to public health, marine life and wildlife can be encountered. Nevertheless, economic reality continues to favor this option against the technology as mean to manage polymeric waste. However it requires very large-scale land area for landfill¹⁹. This situation coupled with environmental concern is making the option gradually impractical. **Incineration** involves controlled combustion of polymeric waste with or without energy recovery. Among many municipal solid waste materials, polymers generate proportionately higher amount of energy upon incineration. The prospect of energy recovery for steam or electricity production is undeniable. The combustion reduces polymer wastes by 90 % in volume (80 % in mass)²⁰. When the polymeric wastes are seen from the perspective of sustainable development, the advantages of **recycling** become obvious as for conservation of materials and the energy savings²¹. Broadly, recycling can be done in two ways, namely, chemical recycling and mechanical recycling. The chemical recycling is done using chemicals (catalysts, solvents) and it

Chapter 1

involves like chemical decomposition, depolymerization through hydrolysis and solvolysis²²⁻²³. For mechanical recycling, PCPW have to be collected first, transported to recycling centre for further processing. Technology is available for each operation these days but adds the cost to regenerated materials. Upon reprocessing, polymers are prone to mechanochemical oxidation²⁴. As far as environmental benefits considered, recycling is triggered, because it diverts waste from landfill. Recent emphasis on mechanical recycling has enhanced plastic recycling to 7 %. Since the raw chemicals employed in polymer industry come from petroleum-fuels and their resources are finite, recycling would become worth-pursuing²⁵. Polymers can be *degraded* in several ways. Among them, biodegradation has received greater attention for few decades. Biodegradation takes place through enzymatic actions associated with living (micro-/ macro-) organisms or their secretion products. *Compost*²⁶ is an organic soil conditioner obtained by biodegradation of a mixture consisting principally of various vegetable residues, occasionally with other organic material and having a limited mineral content. Composting is nowadays a general treatment method for municipal solid waste.

1.4.1. Indian Scenario of Plastic Waste Management

Urbanization and rising incomes, which lead to more use of resources and therefore more waste, are the two most important trends that factor into rising waste generation rates and this is exactly the case with India's urban population. The predominant sources of post consumer plastic waste are a) municipal sources (residential households, markets, small commercial establishments, hotels and hospitals), b) distribution and industry sector and c) Other sources include automotive wastes, agricultural wastes, industrial waste and construction debris. A total of 36.5 million tonnes/year (36.5 kg/individual) of municipal solid waste is generated in the country²⁷. The plastic content in the MSW depends on the consumption pattern, which varies from zone to zone, and level of urbanization.

The plastic content is reported to be in the range of 1-4% (0.37kg/individual – 1.5kg/individual). Major part (60%) of the post consumer waste is collected for recycling and the remaining 40% waste is uncollected and left⁹. Considering the post consumer waste available for current year, then 800,000 tonnes of waste remains as litter, posing a huge problem, or finds its way to open dumping grounds. Process of collection,

Chapter 1

transportation and disposal of waste is not systematically structured in any Indian city. Garbage makes its way to neighborhood dumps. These are usually open vats where the garbage festers and spills out to the street. The waste could lie there for days together with cows and stray dogs foraging through it. Some of it gets transported to landfill sites¹². Low calorific value, high moisture content, and high quantity of non-combustibles characterize the Indian municipal waste. Waste is the responsibility of the municipal authorities in India, but since the non-biodegradable garbage presents a value for the poor who eke out a living from the waste, it is often taken care of by the informal sector. The biodegradable waste along with the uncollected non-biodegradable garbage is taken care of by the municipal authority. The level of service for waste collection is also very poor in many developing countries like India where municipal services are limited. Open dumping is the most commonly accepted way of disposing waste in India. Dumping is also carried out illegally on private farmlands located in the city vicinity. One reason for this is the lack of landfill space in the cities²⁸. These pits of rotting waste generate methane, which cannot be tapped or used without regular soil cover. During monsoons, rain dissolves the toxins present in the waste that permeates the soil and pollutes groundwater²⁹. An important feature of waste recovery and recycling in India is the involvement of the informal sector. This sector is mainly engaged in the recovery and re-sale of most of the recyclables and is highly labor intensive. They form the core for plastic waste management in India but their role in waste management is yet to be recognized.

Generally, around the world, the biomedical polymer wastes are mostly incinerated. Incineration of polymers, which needs higher energy input, emits toxic gases and great deal of energy, which may damage the furnace. For landfill, it requires more land-space and finding of acceptable sites near urban areas is becoming difficult but, from an economic point of view, plastics to disappear in the soil would be environmentally acceptable method³⁰. Bio-recycling / biodegradation can be an alternative to overcome the problem of plastic waste disposal^{3, 16, 20, 25, 31-32}.

1.5. Biodegradation and Biodegradable Polymers

1.5.1. Biodegradation

Polymer degradation is an irreversible process leading to a significant change of structure of a material, typically characterized by a loss of properties (e.g. integrity, molecular weight, structure and mechanical properties) and / or fragmentation. Degradation is affected by environmental conditions and proceeds over a time comprising one or more steps. *In biodegradation, process is mediated at least one step / partially by a biological system*³³⁻³⁴. It is a natural process by which organic chemicals in the environment are converted to simpler compounds, mineralized redistributed thorough elemental cycles such as carbon, nitrogen and sulphur cycles³⁵.

1.5.1.1. Biological Agents for Degradation

The biological environment, i.e. the biological surroundings in which polymers are present, includes the biological agents (micro- /macro-organisms and their enzymes) responsible for the deterioration of polymeric materials. Microorganisms (bacteria, fungi and actinomycetes) and their enzymes are of particular interest in the biodegradation of natural and synthetic polymers. They use / consume polymers as a food source so that its properties deteriorate. Under appropriate conditions of moisture, temperature, and oxygen availability, biodegradation is a relatively rapid process³⁶. When the invertebrates and insects such as crickets, snails and slugs consume the polymers as food, then the process can be called as ‘macro-organism degradation’. It involves a) mastication, b) digestion and c) exo-corporeal degradation. Very few reports have been made still on ‘macro-organism degradation’³⁷.

1.5.1.2. Mode of Degradation

Bio-degradation occurs in two steps: Initially, polymeric chains (carbon nutrients) are converted into low molecular metabolites by extracellular enzymatic or abiotic reactions and these fragments can be resorbed by cells and are mineralized into carbon dioxide and water³⁸. The degradation of a polymeric material depends on its chemical structure, morphology, crystallinity, hydrophobicity and its environmental factors (light, heat, oxygen and moisture). In most of the cases, the abiotic degradation of polymer acts as precursor

Chapter 1

for its biodegradation. Abiotic reactions which lead to the formation of cell nutrients fall into two main chemical classes; namely, hydrolysis and oxidation³⁹. The heterochain polymers (which contains functional groups like ester, ether, urethanes, amides) undergo through hydrolysis, whereas, the biodegradation of carbon chain polymers is predominantly initiated by oxidation. Though any one of these reactions dominates with one polymer, both oxidation and hydrolysis can also occur. For example, polyether polyurethanes can be degraded abiotically by both oxidation and hydrolysis⁴⁰. It has become evident that the rate of initiating step is dominated by the physical accessibility of the polymer structure to the abiotic attack. As erosion usually occurs faster in amorphous regions than in crystalline regions, crystallinity can have a strong impact on the degradation rate. However, once fragmentation has occurred, the surface area available for further reaction and hence biodegradation is considerably increased and autoaccelerating degradation occurs⁴¹. Thus, the distinction between *biodegradable* and *non-biodegradable* is not always clear, but above-mentioned arguments suggest that the difference lies in the rate of abiotic processes, which precede biological attack.

1.5.2. Abiotic Degradation: Precursor for Biodegradation

From polymer production to its usage, abiotic oxidation processes can occur at any stages, which are principally during processing, storage and service. It can be initiated by chemicals (impurities, metals, catalyst residues, additives and etc.), energy (light, heat, sound) and environmental factors^{23, 31-32, 39, 42-45}.

The ‘mechanochemical’ oxidation of polymers occurs in viscous molten state by shear forces at high processing temperatures by the introduction of sensitizing oxygen-containing species⁴⁶. The heat energy or higher temperature can also cause the oxidation, which is called ‘thermal’ degradation. During their service life, the ultraviolet light is most important is environmental influence. The degradation action caused by natural daylight is called ‘photo-degradation’. The abiotic degradation process can also be initiated by some other sources such as ozone, high-energy radiations (X-ray, α -, β -, and γ -rays), electric field / discharge and plasma^{29, 47-50}. *Figure 1.3* shows the generally accepted pathways of degradation and stabilization where radical formation is initiating and vital step for polymer degradation.

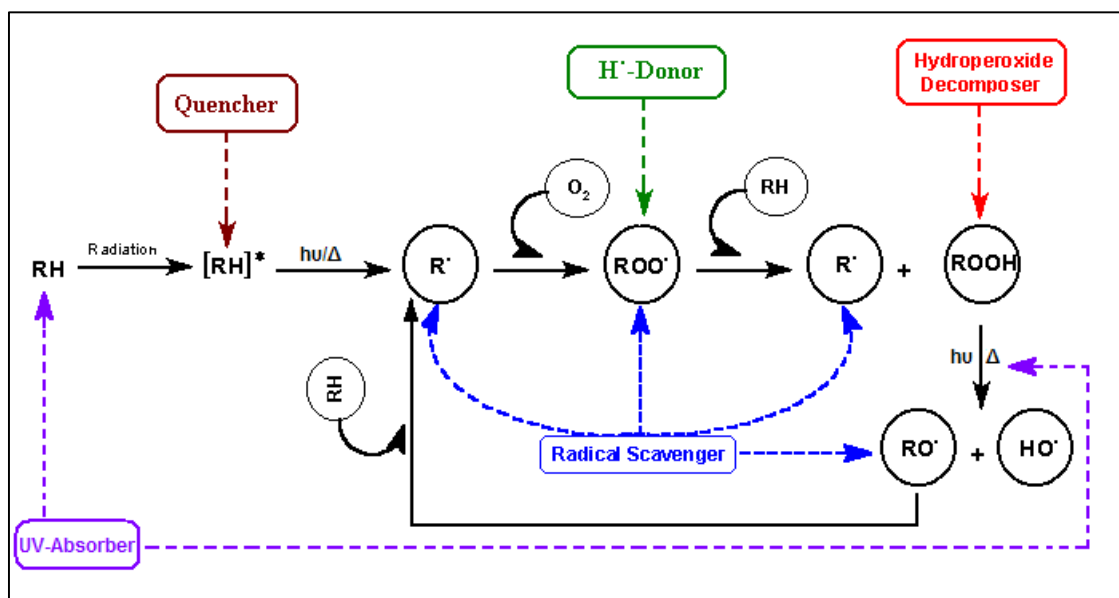


Figure 1.3: Schematic representation of polymer auto-oxidation and stabilization⁵⁰⁻⁵¹

This is based on an original scheme for autocatalytic oxidation of hydrocarbons. The oxidation of polymers begins during processing (mechano-oxidation), and the hydroperoxide formation during fabrication affects further the rate of thermal / photo-oxidation during subsequent use (aging and weathering). These abiotic oxidative degradation processes of polymers results in oxidized low molecular weight metabolites. For example, the end products of polyolefins, upon oxidative degradation are long chain carboxylic acids, esters, aldehydes and ketones. They are bioassimilated into biological cycle as shown below (*Figure 1.4*)⁵²⁻⁵³. This mechanism shows the similarities with the typical β -oxidation of fatty acids and paraffins in animals and man. The distribution of oxidized products is non-uniform across the sample. This gives a very conducive environment for microbial colonization. The induction period observed for such microbial growth (and ultimate rate of degradation) is certainly related with diffusion outwards of oxidized products. It will be evident that the oxidation must precede in case of carbon chain polymers and crystalline heterochain polymers. Thus, the control over oxidation rate, the controlled biodegradation can be obtained. In *Figure 1.3*, the dotted arrows show steps where oxidation processes are slowed down and / or terminated by the antioxidants and stabilizers. They can be a) quenchers, b) light absorbers, c) hydrogen donars, and peroxide decomposers.

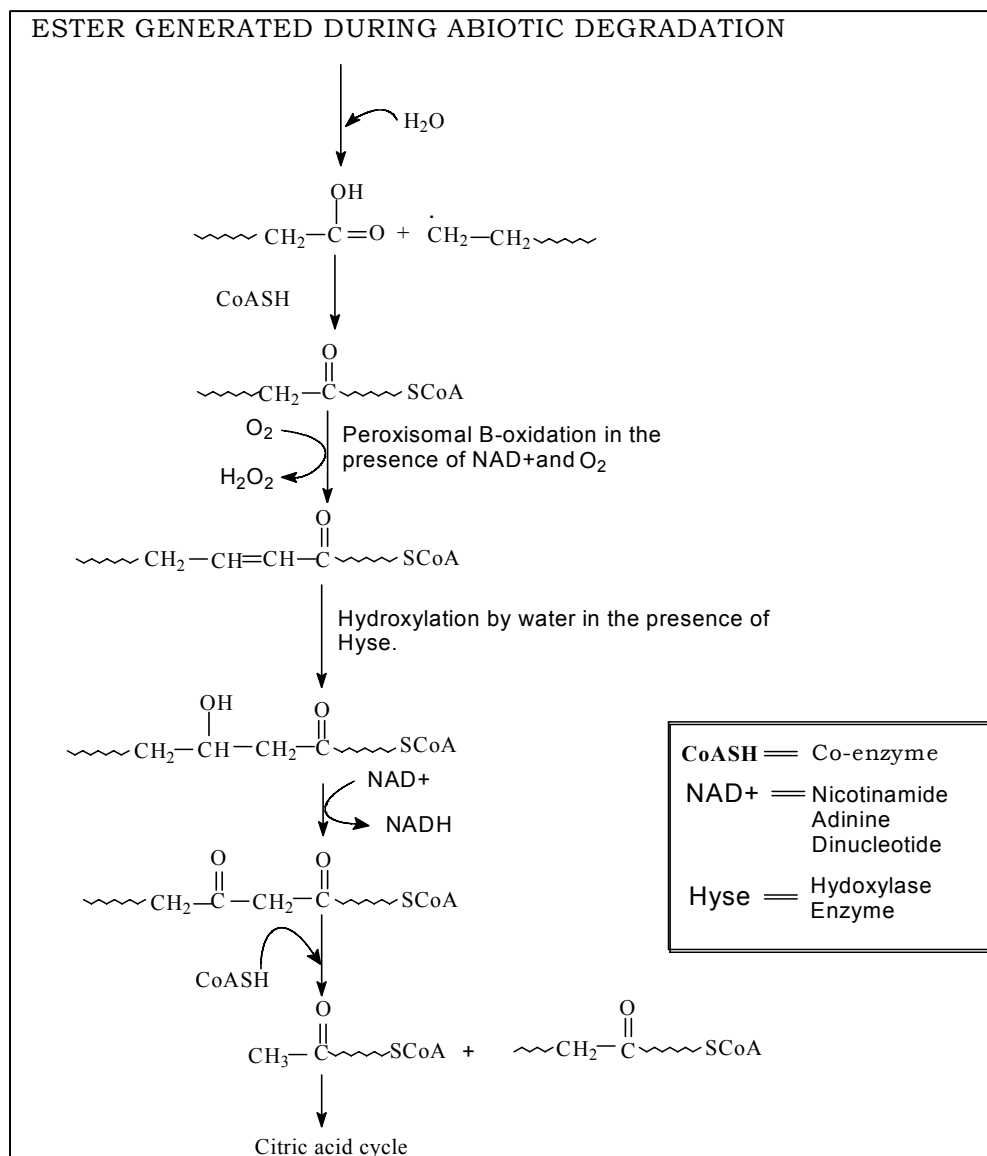


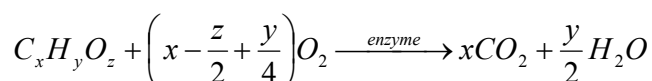
Figure 1.4: Schematic representation of mechanism bioassimilation of oxidized products

Similarly, in order to induce and promote oxidation of polymers, the sensitizers, which transfer the energy to polymer or decompose itself to give singlet oxygen ($^1\text{O}_2$) molecule which can initiate the oxidation, are also added⁸. Certain organic and inorganic compounds are excited in presence of light, heat, high-energy radiations, and transfer energy to polymers or free radicals. For various applications, the service life of polymeric materials can be tuned by incorporating additives externally.

Chapter 1

1.5.3. Biodegradability

The chemistry of biodegradation process varies with the substrates. The obvious direct measure of biodegradation will be the loss of polymer from the system. The process of complete biodegradation of polymers or any organic material can be expressed by following simple chemical process⁵⁴.



In principle, an aerobic biodegradation can be evaluated by monitoring the carbon dioxide evolved. In an anaerobic process, methane or some other product might be measured. The percent conversion of carbon into carbon dioxide / methane is good measure of biodegradation. As the microorganism metabolize the substrate, their growth and reproduction will increase the biomass / living tissue in the system. Measuring the biomass growth can also represent the biodegradation. In some cases, the changes (loss) in properties (mechanical, physical and thermal) upon biosphere exposure are also evaluated to assess the biodegradability⁵⁵.

1.5.3.1. Definitions

Although a number of standard committees have sought to produce definitions of biodegradable plastics, each gives its own definition of biodegradable polymer⁵⁶⁻⁵⁸.

Inherent biodegradability: The potential of a material to be biodegraded, established under laboratory conditions.

Ultimate biodegradability: The breakdown of an organic chemical compound by microorganisms in the presence of oxygen to biodegradability carbon dioxide, water and mineral salts of any other elements present (mineralization) and new biomass or in the absence of oxygen to carbon dioxide, methane, mineral salts and new biomass.

Degradable Plastic: A plastic designed to undergo a significant change in its chemical structure under specific environmental conditions resulting in a loss of some properties that may vary as measured by standard test methods appropriate to the plastic and its applications in a period of time.

Biodegradable Plastic: A degradable plastic in which the degradation results from the action of naturally occurring microorganisms such as bacteria, fungi and algae.

Chapter 1

Compostability: Compostability is a property of a packaging to be biodegraded in a composting process. To claim compostability it must have been demonstrated that a packaging can be biodegraded in a composting system as can be shown by standard methods. The end product must meet the relevant compost quality criteria.

Disintegration is the falling apart into very small fragments of packaging or packaging material caused by environmental degradation mechanisms. Very often disintegration is misunderstood and is claimed as biodegradation.

An important part of assessing biodegradability is testing for disintegration in the form in which it will be ultimately used. Either a controlled pilot-scale test or a test in a full-scale aerobic composting treatment facility can be used. Due to the nature and conditions of such disintegration tests, the tests cannot differentiate between biodegradation and abiotic disintegration, but instead demonstrates that sufficient disintegration of the test materials has been achieved within the specified testing time.

1.5.3.2. Standard Test Methods

Standard test methods are available from international [American Society for Testing and Materials⁵⁶, European Standardisation Committee (CEN)⁵⁷, International Standards Organisation (ISO)⁵⁹] and various national organizations⁶⁰ [National Institute for Standards Research (ISR, USA), German Institute for Standardisation (DIN), Organic Reclamation and Composting Association (ORCA, Belgium), Association Française de Normalization (AFNOR, France)] that employ the abovementioned approaches for measuring biodegradability as given in *Table 1.3*.

Table 1.3: International standard methods for testing biodegradability

<i>Standard</i>	<i>Description</i>
ISO 14851 (EN ISO 14851)	Determination of the ultimate aerobic biodegradability in an aqueous medium- method by determining the oxygen demand in a closed respirometer
ISO 14852 (EN ISO 14852)	Determination of the ultimate aerobic biodegradability in an aqueous medium-method by analysis of released carbon dioxide
ISO 14855	Determination of the ultimate aerobic biodegradability and

Chapter 1

(EN ISO 14855)	disintegration of plastics under controlled composting conditions- method by analysis of released carbon dioxide
ASTM D 5247	Determining the Aerobic Biodegradability of Degradable Plastics by Specific Microorganisms
ASTM D 6002-96	Guide for Assessing the Compostability of Environmentally Degradable Plastics
ASTM D 5338-98	Test Method for Determining Aerobic Biodegradation of Plastic materials under controlled composting conditions.
ASTM D 6340-98	Test Methods for Determining Aerobic Biodegradation of Radiolabeled Plastic Materials in an Aqueous or Compost Environment.
ASTM D 5210	Test Methods for Determining the Anaerobic Biodegradation of Plastic Materials in the presence of Municipal Sewage Sludge
ASTM D 5152	Water Extraction of Residual Solids from Degraded Plastics for Toxicity Testing.
European Standard CEN TC 261	Evaluation of the compostability, biodegradability and disintegration of packaging materials
German Standard Method DIN V 54900	Prüfung der Kompostierbarkeit von Kunststoffen (<i>Probing the compostability of plastics</i>)

1.5.3.3.Compostability (DIN V 54900)

A German standard method (DIN V 54900) is a typical example of standard for assessing the biodegradability. In addition to an analysis of the chemical composition (e.g. heavy metals) this standard test includes probing the complete degradability in laboratory experiments, probing the degradability under real-life conditions and the quality of the resulting compost, and probing the ecotoxicity of the compost for barley, rain worms, and daphnia. To be classified as biodegradable, in laboratory experiments more than 60 % of the organic carbon must be converted within a maximum of six months; moreover under real-life conditions of composting more than 90 % of the plastic is required to be degraded to fragments not more than 2 mm in size.

1.5.3.4. Life Cycle Assessment (LCA)

Life cycle assessment⁶¹ describes the design of ecologically acceptable material. In general, there is a correlation between ecological acceptability and cost which is of primary concern to the manufacturer of polymer products. This is a ‘*cradle-to-grave*’ assessment of alternative strategies for a given application. This process includes three as follows; i) an inventory of the raw materials, energy and wastes associated with the manufacture, use and disposal of a product, ii) An estimation of the impact of raw material extraction and emissions, and iii) an improvement of analysis. Since the procedure generally involves a comparison of alternative manufacturing and disposal techniques, it is essentially an assessment of the overall energetic and environmental impact of a product.

1.5.4. Biodegradable Polymers and Biopolymers

Biodegradable polymers are designed to degrade by the action of living organism. Earlier studies on biodegradable polymers were motivated for biomedical applications such as controlled release of drug, fertilizers and pesticides, absorbable surgical plants, skin grafts and bone plates. In recent decades, polymer waste management through biodegradation and bioconversion has become more important. It has also motivated the development and manufacture of polymers from biomass. Biodegradable polymers can be derived from both petroleum and renewable resources. However, petroleum resources are finite, and prices are likely to continue to rise in the future⁶². It is necessary to find new ways to secure sustainable world development. Renewable biomaterials that can be used for both bioenergy and bioproducts are a possible alternative to petroleum-based and synthetic products. The polymers derived from renewable resources are also called as ‘biopolymers’. The biodegradability is an added advantage. There are also many biobased materials which do not show inherent biodegradability⁶³.

1.5.4.1. Biobased Polymers

The polymers can be derived in following three ways (Figure 1.5) from renewable resources^{5, 35, 64-65}.

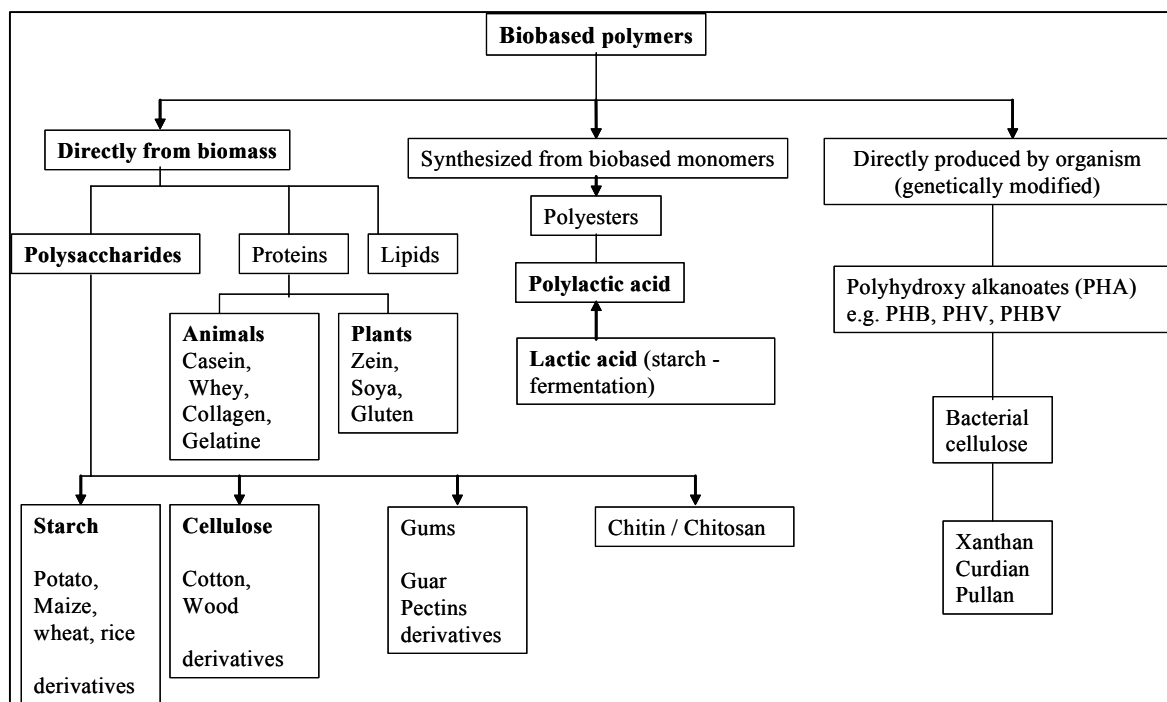


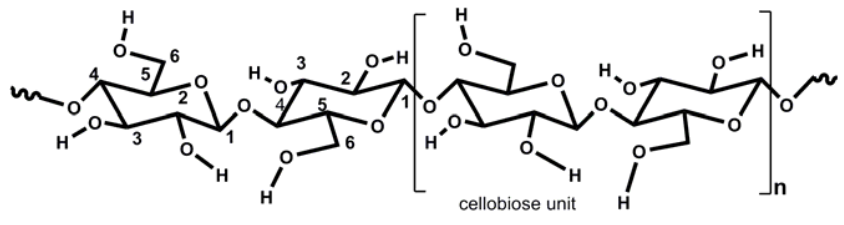
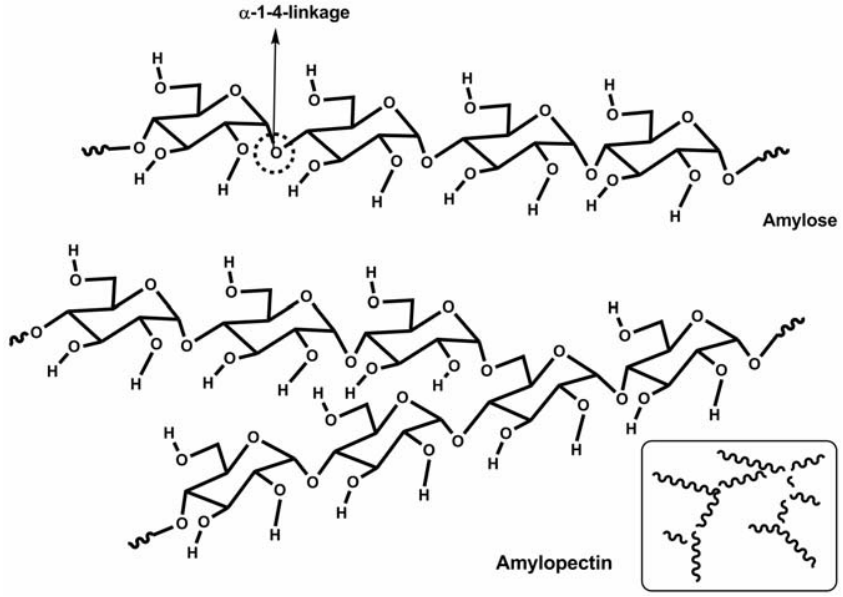
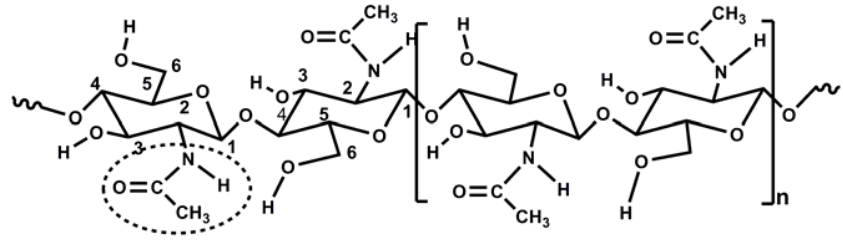
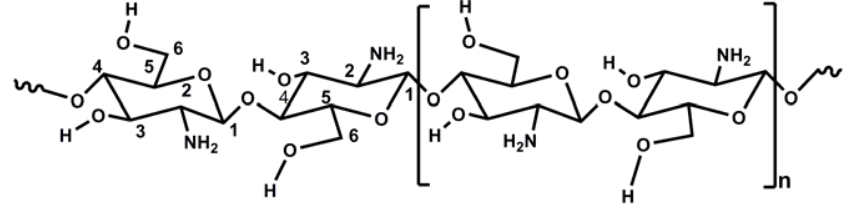
Figure 1.5: Schematic representation of origin and method of production of biobased polymers

1.5.4.1.1. Derivation of Polymers Directly from Biomass

The polymers, which are most commonly available in nature, are derived / extracted from marine and agricultural animals and plants. They are produced naturally during the growth cycles of organisms. Examples are polysaccharides such as cellulose, starch, chitin and gums, proteins such as soya, gelatin and lipids.

Polysaccharides: For materials applications, to date, the principal polysaccharides used are cellulose and starch. They are composed of D-anhydroglucose unit as shown in Table.1.4. Cellulose, which occurs in high crystalline state in cell walls, is consists of repeating D-anhydroglucose (AGU) through β -1-4-linkage. Since it is a very highly crystalline, high molecular weight polymer in all forms, it is infusible and insoluble in common organic solvents. Thus, cellulose is usually converted into derivatives to make it processable⁶⁶⁻⁶⁸.

Table 1.4: Chemical structure of some polysaccharides

Cellulose	
Starch	
Chitin	
Chitosan	

Chapter 1

Because of its regular structure and inter and intra molecular hydrogen bonds, cellulose tend to form highly crystalline microfibrils and fibers. These natural fibers are most widely used for reinforcing synthetic thermoplastics⁶⁹. Detailed description is separately given below about cellulose and derivatives. Starch, which is combination of amylose (linear polymer) and amylopectin (branched), occurs in plants as granules. As shown in scheme, amylose is composed of AGU through only α -1-4 linkage, whereas in amylopectin, branched structure is additionally formed through α -1-6 linkage. Starch is not truly a thermoplastic as are most synthetic polymers, but it can be melted / processed using conventional plastic processing equipment with the addition of water and / or other plasticizers (generally polyols, such as glycerol) and made to flow at high temperatures under pressure and shear⁷⁰⁻⁷¹. Blending and / or reinforcing with some synthetic polymers are few ways to improve material properties⁷²⁻⁷⁵. Then, chemical modifications (e.g. esterification, etherification, grafting and crosslinking) are able to limit the excessive water uptake and macromolecular reorganizations (aging)⁷⁶. Vinyl monomers have been grafted by radiative grafting processes using high-energy sources such as gamma irradiation⁷⁷ and electron beam⁷⁸⁻⁷⁹. Chitin, which is generally found in the shells of crabs, lobsters, shrimps and insects, consists of 2-acetamide-2-deoxy- β -D-glucose through the β -(1-4)-glycoside linkage. It can be degraded by chitinase. Chitin fibers have been utilized for making artificial skin and absorbable sutures. Chitin is insoluble in its native form but chitosan, the partly deacetylated form, is water-soluble. Due to its biocompatibility, biodegradability and avirulence, chitosan has been used in many biomedical applications⁸⁰⁻⁸³. Because of its properties, such as high mechanical strength, hydrophylicity, good adhesion and non-toxicity, it is usually applied as food additive and as anticoagulant or wound healing accelerator. The ability of chitosan to form films may permit its extensive use in the formulation of film dosage forms or as drug delivery systems⁸⁴. It also has antimicrobial activities as well as the ability to absorb heavy metals.

Proteins: Proteins can be derived from animals (casein, whey, collagen) and plants (zein, soy, gluten). The proteins that have found applications as materials are, for the most part, neither soluble nor fusible without degradation, so they are used in the form in which they are found in nature. This description is especially true for the fibrous proteins wool, silk

Chapter 1

and collagen. All proteins are specific copolymers with regular arrangements of different types of α -amino acids. The side chains are suitable for chemical modification for tailoring the required properties for material applications⁸⁵⁻⁸⁷.

1.5.4.1.2. Synthesis of Polymers using Biobased Monomers

A wide range of polymers is synthesized by classical chemical synthesis method using bio-based monomers⁸⁸. Example: polyesters, polyurethanes, polyamides and etc. They can also be called as 'semi-synthetic polymers'. To date, polylactic acid has been proved to be commercially viable successful in this category because of its potential for major scale production⁸⁹. Its monomer, lactic acid, can be easily produced by fermentation of carbohydrate feedstock (corn, maize, wheat). The properties of PLA are highly related to the D/L mesoform ratio. It can be plasticized using its monomer or oligomer. It can be processed into blown films, molded objects and coatings. Since long, castor oil has been recognized as starting material for producing polyurethanes⁹⁰⁻⁹¹. Some seed crops and flax also contain fatty acids and oils in which, linoleic acid, oleic acid and β -linolenic acids are major components. These unsaturated fatty acids are of interest for application in coatings and paintings and others utilizing air drying process⁹²⁻⁹³. Oleochemicals have long been recognized as useful precursors in preparing polymeric materials (polyesters, polyamides)⁹⁴. Diols and diacids can also be derived from carbohydrates by fermentation⁹⁵. Furan resin can be derived from biomass (wood) through biotechnological transformation⁹⁶.

1.5.4.1.3. Polymers Synthesized by Microorganisms and Genetically Modified Microorganisms

These polymers are generated by microorganisms as byproduct of their biochemical cycles. Example: *polyhydroxyalkanoates*, *bacterial cellulose*. Polyhydroxyalkanoates (PHAs) are polyesters that accumulate as inclusions in a wide variety of bacteria. These bacterial polymers have properties ranging from stiff and brittle plastics to rubber-like materials⁹⁷⁻⁹⁸. Bacterial or microbial cellulose (BC) can be produced from some bacteria such as *Acetobacter xylinum*, vinegar or acetic acid as an extracellular product. BC has found their way as reinforcement in composites⁹⁹⁻¹⁰⁰.

1.5.4.2. Synthetic Biodegradable Polymers

Recently, a broad range of synthetic biodegradable resins have commercialized by various companies. They are generally produced by classical chemical reactions (e.g. condensation, ring opening polymerization). They break down rapidly into carbon dioxide, water, and humus in appropriate conditions by microorganisms.

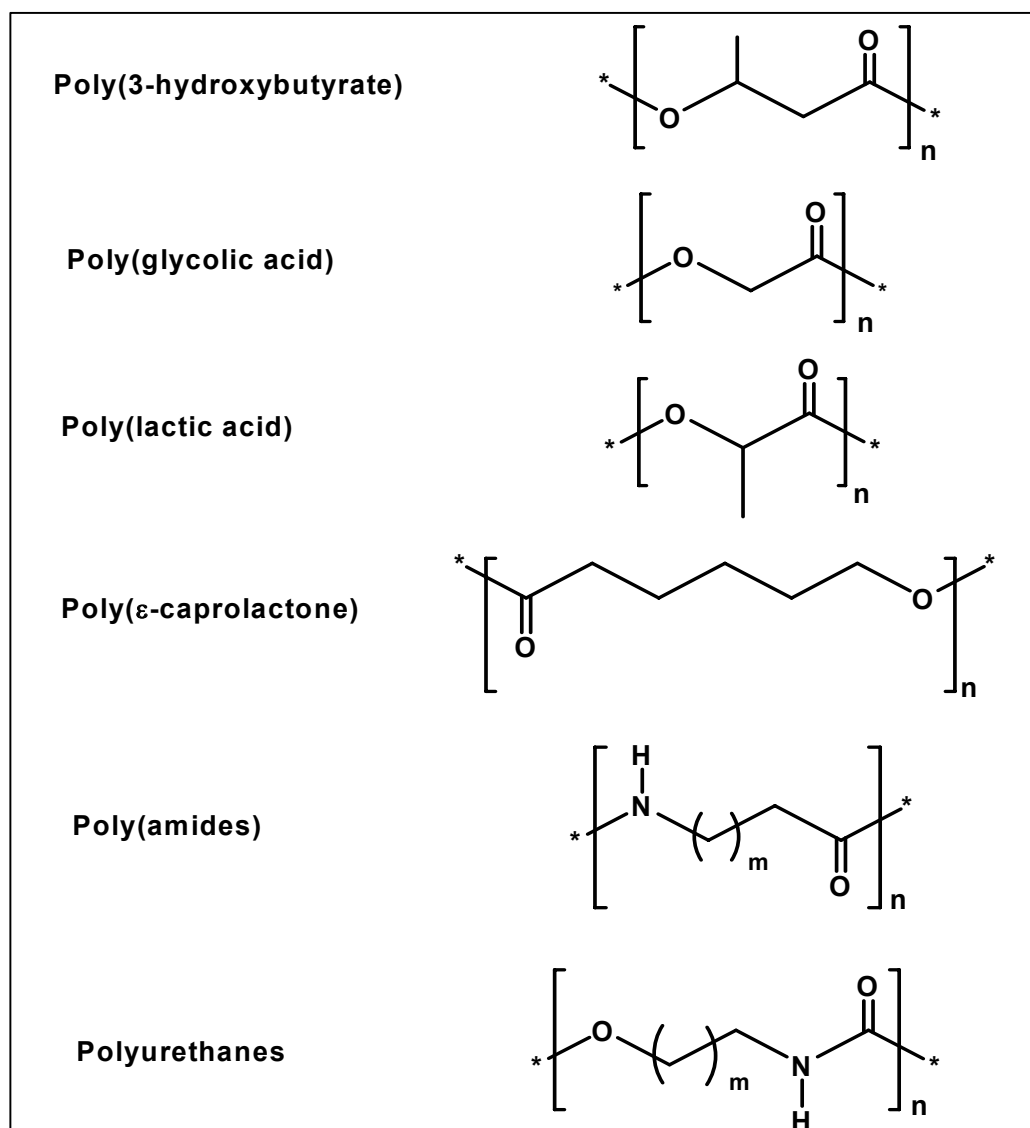


Figure 1.6: Chemical Structure of few biodegradable polymers

Polyesters, polyurethanes, polyamides, polyanhydrides, polycarbonates, polyesteramides, polyphosphazenes, and their copolymers are major class of synthetic biodegradable

polymers (*Figure 1.6*)¹⁰¹. Their synthetic methods, properties and applications have been several times reviewed¹⁰²⁻¹⁰⁴.

1.5.4.3. Polymer Modification to Facilitate Biodegradation

The carbon chain polymers and oligomers (except for those with large numbers of polar groups on the main chain such as poly(vinyl alcohol)) show little or no susceptibility to enzymatic degradation, especially at higher molecular weights. Biodegradation can be facilitated by inserting polar groups / functional groups within or immediately attached to the backbones of such polymers¹⁰⁵. These functional groups are designed to permit the controlled degradation of an initially high molecular weight, hydrophobic polymer into lower molecular weight metabolites, which can be utilized and consumed by microorganisms. The insertion of hydrolysable functional groups in the main chain can result in low molecular weight compounds upon hydrolytic cleavage. A clever method for inserting main chain ester groups into vinyl-type polymers including polystyrene and polyethylene is to carry out a free radical copolymerization of the appropriate vinyl monomer (e.g. styrene or ethylene) with a special monomer (e.g. methylene-substituted cyclic acetal and ortho-ester monomers) that undergoes free radical, ring-opening reaction to generate a main chain ester group¹⁰⁶. The insertion of functional groups such as carbonyl groups in or on the main chain that can undergo photochemical chain-cleavage reactions, is another approach. This can also be done by free radical copolymerization reaction with the monomer, which will create carbonyl group in or immediately attached to the main chain. The comonomers such as carbon monoxide and vinyl monomers with carbonyl groups have been used effectively in small amounts to prepare useful photodegradable copolymers with a variety of vinyl-type monomers¹⁰⁵. As mentioned earlier, upon irradiation, these polymers can produce low molecular metabolites for further bioassimilation. The addition of sensitizers, which can induce photo-oxidation, is also an important and commercially viable method¹⁰⁷.

1.5.4.4. Blending of Biodegradable with Non-Biodegradable Polymers

Blending of biodegradable polymers with non-biodegradable polymers is another approach to induce biodegradability¹⁰⁸. In principal, in case of blends and composites where one

Chapter 1

component degrades faster than other in biotic conditions, after its removal from the material by microorganisms, the non-biodegradable component can lose its integrity, then disintegrate and later degrade slowly¹⁰⁹. The biopolymers such as cellulose, starch, proteins and their derivatives are generally blended with nonbiodegradable polymers like polyethylene^{67, 110}. Blends of biodegradable polymers such as, PHA, PCL, PLA, PGA are also produced and commercialized¹¹¹. This approach is useful to produce environmentally degradable materials.

1.5.5. Applications of Biodegradable Polymers

The biodegradable polymers are used in numerous applications from biomedical to conventional thermoplastics¹¹². Because of their specialized nature and greater unit value, biodegradable plastics based *medical device applications*^{104b} have developed faster than others. They have generally been used as surgical implants, implantable matrices and absorbable surgical sutures for repairing and replacing the diseased or nonfunctional tissues, replacing the function of the major organs as whole or part and for controlled / targeted delivery of drugs¹¹³. *In packaging applications*^{65, 114}, as mentioned earlier, biodegradable polymers are widely used. Then, they are also widely used in *agricultural applications* such as mulching, plant container, controlled release of pesticides, fertilizers and nutrients, soil conditioning, seed coatings, gel plantings and plant protection¹¹⁵. Agricultural plastic mulches help growers in plant growth and then photodegrade in the fields thereby avoiding the cost of removal. They conserve moisture, reduce weeds and increase soil temperatures, thus improving the rate of growth in plants. They are designed to photodegrade and biodegrade after their service time using light-sensitizers. The plastics used for mulch films are generally low density polyethylenes, poly(1-butene), poly(vinylchloride), polybutylene or copolymers of ethylene with vinyl acetate¹¹⁵. By controlled release (CR) method, agricultural chemicals are made available to a target species at a specified rate and for a predetermined time. The polymer serves primarily to control the rate of delivery, mobility, and period of effectiveness of the chemical component. A small niche for degradable plastics is for small agricultural planting containers. Recently, using biodegradable polymers, photovoltaic cells are also prepared¹¹⁶.

1.6. Cellulose

The present work is focused on the utilization of cellulose as raw materials for various applications. From the current point of view, cellulose is the most common organic polymer, representing about 1.5×10^{12} tons of the total annual biomass production, and is considered an almost inexhaustible source of raw material for the increasing demand for environmentally friendly and biocompatible products⁴⁻⁵. As a chemical raw material, it has been used for 150 years. In 1870, the first thermoplastic material called ‘celluloid’ was synthesized and demonstrated as new materials could be produced on industrial-scale by *Hyatt Manufacturing Company*. With this knowledge came an increased use of synthetic fibers from wood cellulose for textile and technical products.

1.6.1. Structural Characteristics

Cellulose is polydisperse homopolymer consisting of β -D-glucopyranose residues linked by glycoside bond at their C1 and C4 hydroxyl groups (*Figure 1.7*). Cellulose differs from synthetic polymers by virtue of its distinct polyfunctionality, high stiffness, and sensitivity toward the hydrolysis and oxidation.

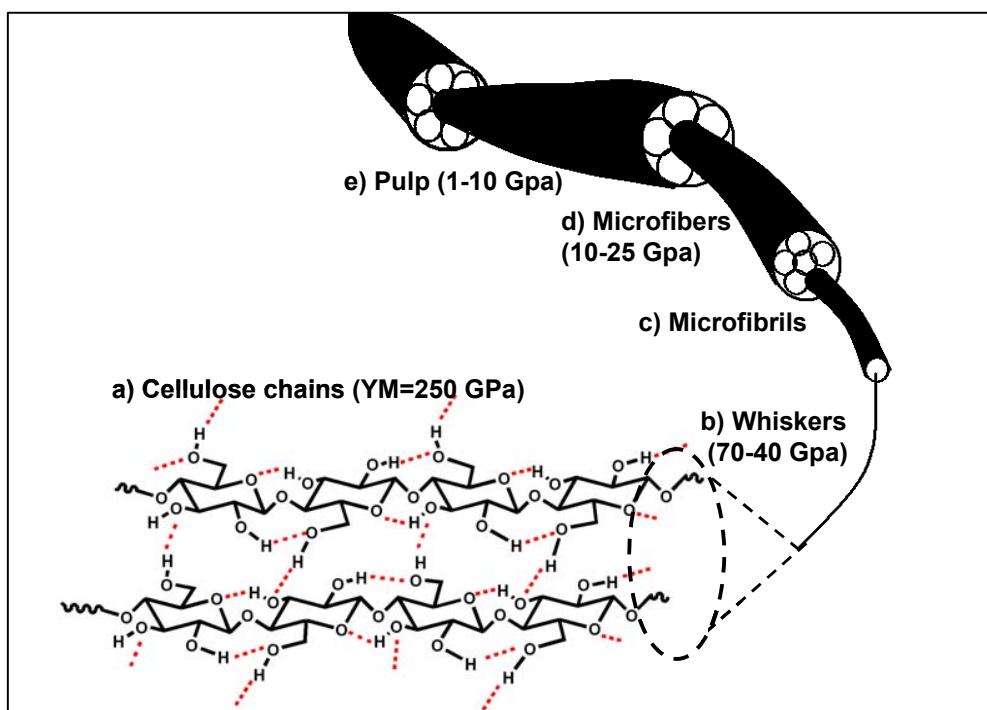


Figure 1.7: From molecular structure to microfibrils formation

Chapter 1

It has three hydroxyl groups per anhydroglucose unit (AGU) at C2, C3 and C6 atoms. It forms the intramolecular hydrogen bond between the proton of C3-OH and C5-O of adjacent glucose ring, and thereby linearity of cellulose chains may appear not only in solid states but also in solution ones. To accommodate the preferred bond angles of the acetal oxygen bridges, every second AGU is rotated 180 in the plane. In this manner, two adjacent structural units define the disaccharide cellulose. The chain length, expressed in the number of AGUs (degree of polymerization, DP), depends on the origin and treatment of the raw material¹¹⁷. It is worth to mention that the molecular structure imparts cellulose with its characteristic properties: hydrophilicity, chirality, degradability and broad chemical variability initiated by the high donor reactivity of the OH groups¹¹⁸.

1.6.2. Cellulose Production Scenario

The cellulose can be synthesized in four different pathways as shown *Figure 1.8*⁴.

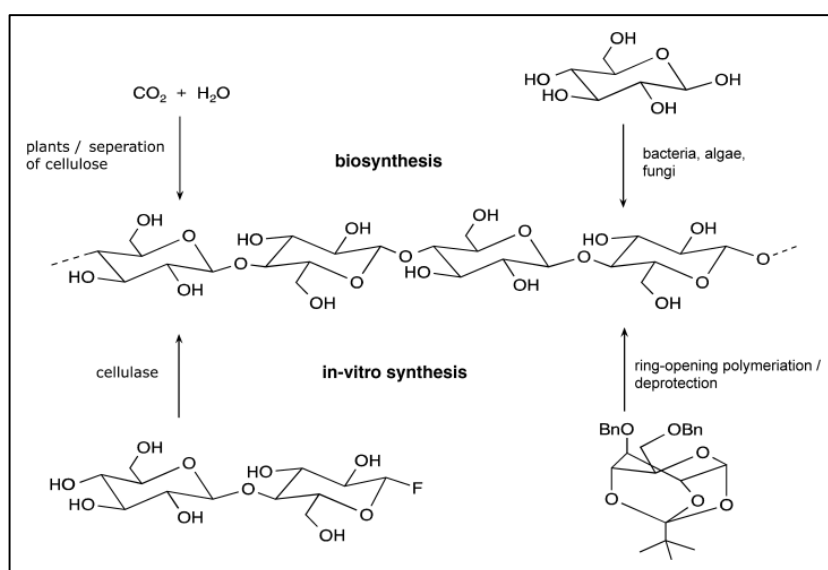


Figure 1.8: Schematic representation of general synthesis of cellulose⁴

The predominant source of cellulose is plant fibers. In wood, the cellulose forms native composite materials with lignin and hemicelluloses from which cellulose is isolated by large-scale chemical pulping, separation, and purification processes. As it can be seen in *Figure 1.7*, the inter- and intra-molecular hydrogen bonds result the linearity, the stiffness, the rigidity, strength and ultimately to form thread like material called micro-fibrils that are

Chapter 1

apparently bound to form natural fibers. They are often referred to as *cellulosic fibers*, related to the main chemical component cellulose, or as *lignocellulosic fibers*, since the fibers usually contain a natural polyphenolic polymer, lignin also, in their structure. Depending on the source, the composition in the fiber varies, as given in *Table 1.5*.¹¹⁹

Table 1.5: Composition in the fibers¹¹⁹⁻¹²⁰

Source	Composition (%)			
	Cellulose	Hemicellulose	Lignin	Extract / Water solubles
Cotton	95	2	0.9	0.4
Ramie	76.2	16.7	0.7	6.4
Henequen	77.6	4-8	13.1	3.6
Jute	71.5	13.6	13.1	1.8
Flax (retted)	71.2	20.6	2.2	6.0
Hardwood	43-47	25-35	16-24	2-8
Softwood	40-44	25-29	25-31	1-5
Bagasse	40	30	20	10
Wheat straw	30	50	15	5

Depending on the compositions, the fibers exhibit wide range of physical and chemical properties.

1.6.3. Cellulose Utilization

Due to their molecular structure, crystallinity, inter- and intra-molecular hydrogen bondings, cellulose is poorly soluble in common solvents and is not melt-processible. It decomposes before it undergoes melt flow. Thus, conversion of cellulose to its esters affords materials that are processible into various useful forms such as three dimensional objects, fibers, and solutions to be used for coating or casting (as films, membranes). All of the important derivatives of cellulose are reaction products of one or more of the three hydroxyl groups, which are present in each glucopyranoside repeating unit, including: (1) ethers, e.g. methyl cellulose and hydroxyl-ethyl cellulose; (2) esters, e.g. cellulose acetate

and cellulose xanthate, and (3) acetals. Another reason for modifying cellulose is that the physical properties of modified cellulose give entry into range of applications⁶⁷.

1.6.4. Applications of Cellulose Fibers:

1.6.4.1. In Structural and Semi-Structural Applications

The history of fibre-reinforced plastics began in 1908 with cellulose fibre in phenolics, later extending to urea and melamine and reaching commodity status with glass fibre reinforced plastics. The fibre-reinforced composites market is now a multibillion-dollar business¹²¹. In recent years, the consumption of natural fiber-reinforced composites has been skyrocketed not only for environmental concerns (*renewability, availability of vast array of fillers throughout the world, nonfood agricultural based economy*) but also for yielding a unique combination of low energy consumption, low cost, low density, high specific strength and modulus, high performance, great versatility and processing advantages at favorable cost¹²²⁻¹²⁴. They exhibit many advantages including low density, little damage during processing, comparatively easy processability due to their nonabrasive nature, which allows high filling levels, resulting in significant cost savings and relatively reactive surface, which can be used for grafting specific groups¹²⁵⁻¹²⁶. In addition, the recycling by combustion of lignocellulosic filled composites is easier in comparison with inorganic fillers systems. Therefore, the possibility of using lignocellulosic fillers in the plastic industry has received considerable interest. Potential applications of agro-fiber based composites in railways, aircraft, irrigation systems, furniture industries, and sports and leisure items are currently being researched¹²⁷.

1.6.4.2. Biocomposites as Eco-Friendly Composites

Biopolymers or synthetic polymers reinforced with natural or bio fibres (termed as biocomposites) are a viable alternative to glass fibre composites. Broadly defined, biocomposites are composite materials made from natural / biofibre and petroleum derived non-biodegradable polymers (PP, PE) or biodegradable polymers (PLA, PHA). The latter category i.e. biocomposites derived from plant derived fibre (natural/biofibre) and crop/bioderived plastic (biopolymer/bioplastic) are likely to be more eco-friendly and such composites are termed as green composites¹²⁸. Another aspect that has gained global

Chapter 1

attention is the development of biodegradable plastics from vegetable oils like soybean oil, peanut oil, walnut oil, sesame oil and sunflower oil. Green composites from soy protein based bioplastics and natural fibres show potential for *rigid packing and housing and transportation applications*¹²⁹. Fish oil based polymers have also attracted the attention of researchers due to their high degree of unsaturation. Fish oil based polymers also possess unique good damping and shape memory properties¹³⁰.

1.6.5. Applications of Cellulose Derivatives

As mentioned earlier, cellulose derivatives were the basis of the original synthetic plastics. Till early part of 20th century, they enjoyed the commercial importance and success. The synthesis of cellulose derivatives (i.e. dissolution, esterification, etherification, deoxyhalogenation, and other reactions) has been reviewed¹³¹. The inter-/intra-molecular hydrogen bondings, crystallinity, crystal size, crystal structures, interactions with water, molecular mass and molecular mass distributions, presence of lignin or hemicelluloses, shape and size of cellulosic materials and others, greatly influence the reactivity of cellulose, efficiency of reactions and finally the properties of chemically modified materials¹¹⁸. Among the derivatives, cellulose esters are most widely used ones in various applications^{67, 132}. Cellulose derivatives are applied in various applications esp. as medical polymers¹³³

1.6.6. Degradation of Cellulose and Its Derivatives

Some fungi can secrete enzymes that catalyze oxidation reactions of either cellulose or its low molecular weight oligomers. For example, the peroxidases can provide hydrogen peroxide for free radical attack on the C2–C3 positions to form ‘aldehyde’ cellulose, which is very reactive and can be hydrolyzed into low molecular weight fragments while other oxidative enzymes can oxidize glucose and related oligomers to glucuronic acids. Bacteria also secrete both endo-/exo-enzymes, which form complexes that act jointly in degrading cellulose into carbohydrate nutrients, which are utilized by microorganisms for survival. In aerobic soil environments, consortia of several degrading bacteria and fungi operate cooperatively. Primary microorganisms degrade cellulose to glucose and cellodextrins, a portion of which is consumed by secondary microorganisms. The final products from

Chapter 1

aerobic biodegradation are ultimately CO₂ and water. In anaerobic environments, a variety of final products are formed, including CO₂ hydrogen, methane, hydrogen sulphide and ammonia¹³⁴.

Cellulose esters represent a class of polymers that have the potential to participate in the carbon cycle via microbiologically catalyzed *de-esterification* and decomposition of the resulting cellulose and organic acids. Based on film disintegration and film weight loss, cellulose acetates having DS < 2.20 compost at rates comparable to that of PHBV. Reese¹³⁵ presented evidence of esterase activity on soluble cellulose acetates with a low degree of substitution (DS, 0.76 sites esterified per anhydroglucose monomer). Recently, Buchanan et al.¹³⁶ presented evidence supporting the inherent biodegradability of cellulose acetate with naturally occurring microorganisms in activated sludge and in aerobic microbial cultures. The biodegradation of cellulose ethers has been studied extensively and it is known that cellulose ethers with a DS of less than 1 will degrade readily. Depending on the chemical nature of modifications, the degradability of cellulose is obviously affected due to the lack of accessibility.

1.7. Polymeric Composite Materials

The concept of reinforcing thermoplastics with fillers like minerals, metals and fibers has been for many years to improve thermal (esp. flame retardancy), mechanical and physical properties of the materials with low processing requirements and low production cost. Their practical applications are well known over a long period. Conventional micro-sized fillers are generally incorporated by melt-compounding methods. *Table 1.6*, represents the typical fillers used for plastics reinforcement and their additional function in the resulting materials¹³⁷. Rapid advances in synthesis and characterization tools coupled with recognition of increased surface area by decreasing particle size have shifted attention towards developing nano-scale fillers. Thus, polymer nanocomposites, in last few decades, have become worldwide research interest for developing polymeric materials with improved / desired properties by incorporation of these nanoscale materials into polymer matrix¹³⁸⁻¹³⁹. Numerous research papers, patents and funding are generated out of this field.

Table 1.6: Primary and additional functions of fillers¹³⁷

Example of fillers	Primary function	Additional function
Glass fibers, mica, nanoclay, carbon nanotubes, graphite, natural and synthetic fibers	Modification of mechanical properties	Control of permeability
Hydrated fillers (e.g. hydroxyapatite, tricalcium phosphate, Al(OH) ₃ , Mg(OH) ₂)	Enhanced of fire retardancy	Bioactivity (e.g. Bone regeneration)
Conductive, non-conductive and ferromagnetic fillers (e.g. metals, carbon fibers and nanotubes, carbon black, mica)	Modification of electrical and magnetic properties	Degradation and stabilization
Antiblock and lubricating fillers (e.g. silica, CaCO ₃ , PTFE, MoS ₂ , graphite)	Modification of surface properties	Radiation and absorption
Thixotropic, anti-sag, thickeners and acid scavengers (e.g. colloidal silica, bentonite, hydrotalcite)	Enhancement of processability	Improved dimensional stability Modification of optical properties Control of damping

1.7.1. Polymer Nanocomposites

The composite materials that combine one or more separate components in order to improve performance properties, for which at least one dimension of the dispersed particles is lesser than 100nm¹⁴⁰⁻¹⁴¹. As shown in *Figure 1.9*, nanoscale particles are classified into three categories depending on their dimensions as follows; a) Nanoparticles: When the three dimensions of particulates are in the order of nanometers, they are referred as equi-axed (isodimensional) nanoparticles or nanogranules or nanocrystals. Example

Chapter 1

silica, titania, calcium carbonate, magnesium oxide, b) Nanotubes: When two dimensions are in the nanometer scale and the third is larger, forming an elongated structure, they are generally referred as ‘nanotubes’ or nanofibers / whiskers. (e.g. Carbon nanotubes (CNTs), cellulose whiskers) c) Nanolayers: The particulates which are characterized by only one dimension in nanometer scale are nanolayers / nanosheets (e.g. clay (layered silicates), layered double hydroxides (LDH)). These particulate is present in the form of sheets of one to a few nanometer thick to hundreds to thousands nanometers long.

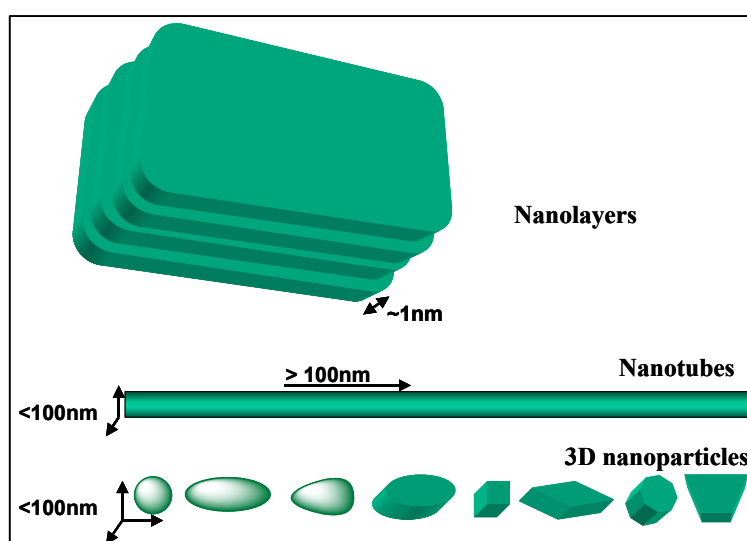


Figure 1.9: Schematic representation of various shapes and dimensions of nanoscale materials¹⁴²

In principle, any kind of material can be produced to appear in a nano-scaled shape and size, but in last few decades, none of these particles has gained as much attention as clay (esp. layered silicates) and carbon nanotubes. This is because of the fact that they can simultaneously improve both physical, mechanical properties and flammability, unlike conventional fillers, these nanosized particles have exhibited tremendous improvement in properties with very low amount of loading (upto 10 wt. %).

1.7.2. Growth and Importance of Polymer Nanocomposites

Recently, a big window of opportunities has opened for polymer nanocomposites just to overcome the limitations of traditional micro-composites. Although, the chemistry of clay

Chapter 1

minerals and composites based on some nano-scale particles are known for a several decades, the research and development of nanoscale-filled polymers has been skyrocketed in recent years, for numerous reasons. First, unprecedented combinations of properties have been observed in some polymer nanocomposites. For example, incorporation of isodimensional nanoparticles, into thermoplastics, increases the modulus, the yield stress and the ultimate tensile strength¹⁴³. A volume fraction of 0.04 layered silicates (MTS) in epoxy polymer the modulus below glass transition region temperature by 58% and the modulus in the rubbery region by 450%¹⁴⁴. The permeability was shown to decrease by an order of magnitude with 4.8% of layered silicates in poly- ϵ -caprolactone¹⁴⁵. The discovery of carbon nanotubes is a second reason. Though, the carbon nanotubes has the history since 1960s¹⁴⁶, in mid 1990s only, it was shown by Ijima¹⁴⁷ that the carbon nanotubes can be made in the quantities required for the reinforcement of polymer and their evaluation. The properties of these carbon nanotubes, particularly strength and electrical properties are significantly different from those of carbon black or graphite and lead to new class of composite materials. Third, the significant development in preparing and processing of nanoparticles and nanocomposites (esp. *In-situ* methods) has directed to good control over the interface between the inter-phases, morphology and ultimately the properties of such composites¹⁴⁸.

In application point of view, the nanocomposites have been studied for their improved flammability. It is well known that commercially available, traditional flame-retardants such as aluminium trihydrate or halogen-containing compounds are highly effective. However, the mechanical properties and processing of flame retardant polymers are often negatively influenced by the large quantities of halogen-free flame-retardants. Conversely halogen-containing flame-retardants are under pressure in many countries because of environmental considerations. The addition of many flame-retardants often increases the production of soot and carbon monoxide during combustion. Nanocomposites have many advantages over these traditional flame-retardants. Processing of nanocomposites is straightforward and as the nanocomposites contain no additional halogen, they are considered to be an environmentally friendly alternative. In nanoscale particle filled polymer systems, the char formation, which insulates the base polymer from heat and forms a barrier, reduce the escape of volatile gases from the polymer combustion, is

Chapter 1

explained to be responsible for improved flame retardancy. As a result of the enhancements, nanocomposites have the potential to play a significant role in future space systems. Launch vehicles would greatly benefit from appropriately designed nanocomposites that could provide improved barrier properties and gradient morphologies enabling linerless composite cryogenic fuel tanks. Self-rigidizing, self-passivating nanocomposite materials could be used to construct space vehicle components that are both highly resistant to space-borne particles and resistant to degradation from electromagnetic radiation, while reducing the overall weight of the spacecraft. Nanocomposite materials also offer the unique opportunity for improved tailorability of physical and structural properties such as the coefficient of thermal expansion (CTE), which would be especially useful in constructing large aperture telescopes and antennas using inflatable membranes¹⁴⁹. In an earlier estimation, Business Communications Company, Inc. reported¹⁵⁰ the worldwide growth of polymer nanocomposites as summarized in *Table 1.7*.

Table 1.7: Worldwide volume and value for polymer nanocomposites 2003 - 2008 (millions)

Polymer	2003		2008		AAGR (%)
	Volume (Kg)	Value (\$)	Volume (Kg)	Value (\$)	2003-2008
Thermoplastics	5.7	70.7	27.7	178.9	20.4
Thermosets	5.4	20.1	8.2	32.2	9.9
Total	11.1	90.8	35.9	211.1	18.4

It can be noted that total worldwide market for polymer nanocomposites reached 11.1 million kg valued at \$90.8 million in 2003 and projected to grow at an average annual growth rate (AAGR) of 18.4% to reach \$211.1 million by 2008.

1.7.3. Polymer-Layered Silicates Nanocomposites

Clay minerals based on phyllosilicates have extensively been for last few decades, most probably because the starting materials are easily available and their intercalation chemistry has been studied for a long time. These clay can be synthesized from precursors. In the family of phyllosilicates, 2:1 type layered silicates are most popular among

Chapter 1

industries and academia. Natural montmorillonite (MMT) is smectite (2:1) type clay minerals whose one layer contains one central octahedral sheet (of either aluminium hydroxide or magnesium hydroxide) condensed to two parallel tetrahedral sheets (of silica), via silica oxygen apices to octahedral hydroxyl planes. These layers are attracted by van der Waals forces. The negative charges that arise due to isomorphous substitution of cations (Al^{3+}) on the surface of layers are compensated by hydrated cations (e.g. Na^+ , K^+ , Ca^{2+} and Mg^{2+}) which are exchangeable¹⁵¹⁻¹⁵² as shown in *Figure 1.10*.

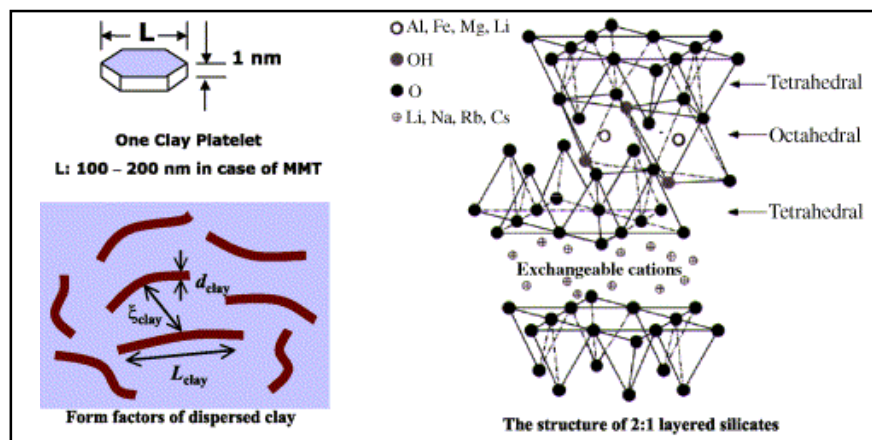


Figure 1.10: Schematic representation of 2:1 phyllosilicates

The natural clay minerals are hydrophilic. It is well established that these cations can be replaced by organic cations such as alkyl-ammonium ions to render the organophilicity for lowering the surface energy of the silicate layers and improving the wetting with polymer chains. These organophilic montmorillonite (OMMT) clays whose surface energy is lowered and is more compatible with organic polymers, polymer molecules may be able to intercalate within the galleries, under well-defined experimental conditions¹⁴⁴⁻¹⁴⁵. When these layered silicates are associated with a polymer, depending on the nature of the components used (layered silicate, organic cation and polymer matrix) and the method of preparation, different structure / morphologies of composites can be obtained¹⁴⁰⁻¹⁴¹ as shown in *Figure 1.11*.

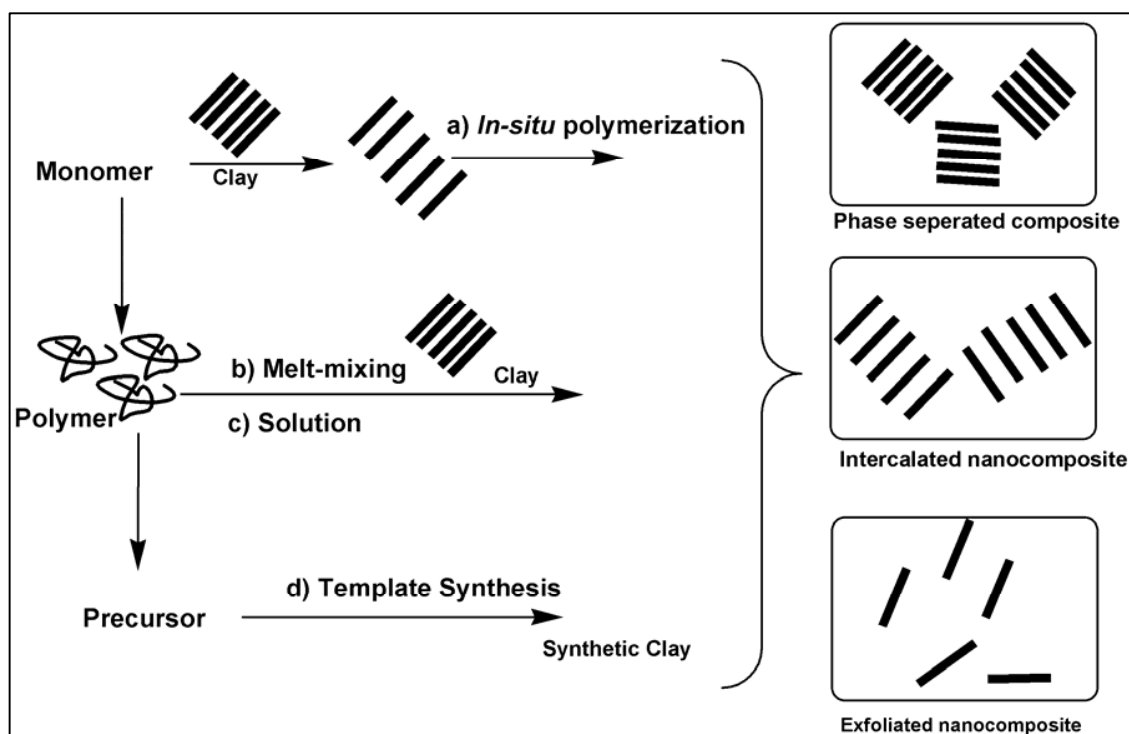


Figure 1.11: Schematic representation of preparation and types of nanocomposites based on polymer and nanoscale layers

a) *Phase-separated composites:* If the polymer is unable to intercalate between the silicate sheets, the obtained composite can be considered as phase-separated composite. Their properties stay in the same range as traditional microcomposites.

b) *Intercalated nanocomposites:* When a single and / or more than one extended polymer chain is inserted in a crystallographically regular fashion between the silicate layers resulting in a well-ordered multilayer morphology built up with alternating polymeric and inorganic layers, the obtained composites can be called as ‘intercalated nanocomposites’. In this type of nanocomposites, if silicate layers are flocculated due to hydroxylated *edge-edge* interaction of the silicate layers, they can be called as *flocculated nanocomposites*.

c) *Exfoliated nanocomposites:* When the individual silicate layers are completely and uniformly dispersed in a continuous polymer matrix, an exfoliated or delaminated structure is obtained. Usually, the clay content of an exfoliated nanocomposite is much lower than that of an intercalated nanocomposite.

1.7.4. Characterization Techniques

The crystallographic interactions of layered silicates / nanoscale fillers with polymers, state of dispersion and have generally characterized by X-ray diffraction (XRD) analysis and transmission electron micrographic (TEM) observation.

X-ray Diffraction: Due to its easiness and availability XRD is most commonly used to probe the nanocomposite structure and occasionally to study the kinetics of the polymer melt intercalation. By analyzing the basal reflections (i.e. position, shape, and intensity) of silicate layers, the nanocomposite structure may be identified. The intercalation can be observed in terms of expansion in *d-spacing* of interlayer corresponding to the larger gallery height. The exfoliation results in the eventual disappearance of any coherent X-ray diffraction from the distributed silicate layers because of the extensive layer separation associated with the delamination of the original silicate layers in the polymer matrix.

Transmission Electron Microscopy: TEM allows a qualitative understanding of the internal structure, spatial distribution and dispersion of the nanoparticles within the polymer matrix, and views of the defect structure through direct visualization. However, special care must be exercised to guarantee a representative cross section of the sample.

1.7.5. Nanocomposites of Biodegradable Polymers: Bionanocomposites

Biodegradable polymers have great commercial potential for bio-plastic, but some of the properties such as brittleness, low heat distortion temperature, high gas permeability, low melt viscosity for further processing etc. restrict their use in a wide-range of applications. On the other hand, nanoreinforcement of polymers has already proven to be an effective way to improve these properties concurrently. So, preparation to processing of biodegradable polymer-based nanocomposites, that is, *green nanocomposites* are the wave of the future and considered as the next generation materials.

1.7.5.1. Cellulose and Its Nanocomposites

The nanocomposites based on cellulose can be made in two ways. a) The disintegrated microfibrils / nanoscale whiskers can be used for reinforcing polymers; b) Cellulose or cellulose derivatives can be reinforced by other nanoscale particles. In nanoscience and

nanotechnology, cellulose and its derivatives are used for synthesizing important nanoparticles and for their coating for many applications.

1.7.5.1.1. Cellulose Whiskers as Nanoscale Fillers

The biosynthesis of cellulose has led to highly crystalline microfibrils, which are defect-free, with the consequence of axial physical properties approaching perfect crystals. The research group at CERMAV-CNRS has shown that these microfibrils can be disintegrated and used nano-scale fillers for reinforcing polymers¹⁵³. They have presented numerous studies based on cellulose whiskers reinforced nanocomposites¹⁵⁴. The microfibrils (10–50 nm width), are typically disintegrated from an edible tunicate (a sea animal) and parenchyma cells of sugar beet, potato tuber^{155, 156}. Cellulose nanocomposites are usually fabricated by utilizing these whiskers in to polymers such as starch, cellulose derivatives, natural rubber and etc. A review of the recent research into cellulosic whiskers, their properties and their application in nanocomposite field has been presented by the same group¹⁵⁷. The control over properties (*e.g.*, wettability, chemical resistance, biocompatibility, *etc.*) of the resultant composite materials can be achieved surface coating such as layer-by-layer assembly of polyelectrolytes.

Recently, Huang *et al.*¹⁵⁸ achieved uniform polypyrrole nanocoating on cellulose fibres without disrupting the hierarchical network structures of microfibrils. Using low-cost plant primary cell walls, the high performance composites, were developed by Bruce *et al.*¹⁵⁹, which gave the best tensile properties. As mentioned above, Bacterial or microbial cellulose (BC) have also found their way as reinforcement in composites. An interesting study concentrated on the preserving the microfibril organization of wood veneer in composites¹⁶⁰. Cellulose whiskers were incorporated in a polyvinyl alcohol matrix using solution casting with water as the solvent¹⁶¹. Xiaodong *et al.*¹⁶² have reported nanocomposite materials reinforced with flax cellulose nanocrystals in waterborne polyurethane. The films showed a significant increase in Young's modulus and tensile strength from 0.51 to 344 MPa and 4.27 to 14.96 MPa, respectively, with increasing filler content from 0 to 30-wt%, with better dispersion.

1.7.5.1.2. Cellulose Derivatives as Matrices

Cellulose ester powders in the presence of different plasticizers and additives are extruded to produce various grades of commercial cellulose plastics in pelletized form. The nanoscale fillers can be mixed with these thermoplastic cellulose derivatives with aid of plasticizers. Recently, Park et al.¹⁶³ successfully used melt intercalation technique for the fabrication of cellulose nanocomposites from cellulose acetate (CA), triethylcitrate (TEC, as plasticizers) and organically modified clay.

1.7.5.2. Starch Based Nanocomposites

By analogy with works on cellulose whiskers, starch microcrystals can be processed by partial acid hydrolysis of the amorphous domains of starch granules into nanocrystals¹⁶⁴. The objective of this treatment is to dissolve away regions of low lateral order so that the water-insoluble and highly crystalline residue may be converted into a stable suspensoid by subsequent vigorous mechanical shearing action. Later it has been incorporated into natural polymers such as polyhydroxyalkanoates¹⁶⁵ and natural rubber¹⁶⁶. In addition, starch nanocrystals were incorporated into starch itself.¹⁶⁷ On the other hand, starch has been reinforced by other nanofillers also. Cellulose nanowhiskers have been incorporated into starch to prepare biocomposites ‘green composites’¹⁵⁴. De Carvalho et al. reported the first preparation of TPS/kaolin hybrids by melt intercalation technique using a twin screw extruder¹⁶⁸. Then, Park et al. reported the preparation of TPS/clay nanocomposites by melt intercalation in detail¹⁶⁹. Later, nanocomposites starch blends¹⁷⁰ have also been made. It has been reinforced with other nanoscale fillers also.

1.7.5.3. Chitin/Chitosan Based Nanocomposites

Similarly, the chitin whiskers are made by partial hydrolysis, and incorporated polymers such as poly (styrene-*co*-butylacrylate)¹⁷¹, polycaprolactone¹⁷², natural rubber¹⁷³ and soy protein isolate¹⁷⁴. Using carbon nanotubes¹⁷⁵, clay¹⁷⁶ and other inorganic nanoparticles¹⁷⁷, many biologically important nanocomposites have been made.

1.7.5.4. Polylactic Acid Nanocomposites

The commercially successful biopolymer from renewable resource is polylactic acid. First, Ogata et al.¹⁷⁸ prepared PLA / organically modified layered silicates (OMLS) blends by dissolving polymer and found that the silicate layers forming the clay could not be intercalated in the PLA/MMT blends. After that Bandyopadhyay et al.¹⁷⁹ reported the preparation of intercalated PLA/OMLS nanocomposites with much improved mechanical and thermal properties. Then, many reports have been made PLA / clay nanocomposites by Ray et.al.¹⁸⁰.

1.7.5.5. Natural Oil Based Nanocomposites

Uyama et al.¹⁸¹ synthesized new green nanocomposites consisting of plant oils and clay with much improved properties. They used epoxidized soybean oil (ESO) as an organic monomer. Miyagawa et al.¹⁸² prepared nanocomposites from functionalized vegetable oil (anhydride-cured epoxidized linseed oil (ELO)) and organically-modified layered silicate clay.

1.7.5.6. Other Polyesters Nanocomposites

Maiti et al.¹⁸³ reported the first preparation of PHB/OMLS nanocomposites (PHBCNs) by melt intercalation method. Sinha Ray et al.¹⁸⁴ reported the first preparation of polybutylene succinate (PBS)/OMLS nanocomposites by melt extrusion of PBS and OMLS. Similarly, the biodegradable nanocomposites based on other aliphatic polyesters are also prepared.

1.8. The Importance of This Study

Considering the demand and applications of biodegradable polymers, the shortage of landfill availability and petroleum resources and CO₂ neutrality, development of polymeric materials from renewable resources is a revived research interests around the world. Table 1.8 shows the Global projection for materials demand in a ‘*business-as-usual*’ scenario¹⁸⁵. It can be understood that the portion of biobased polymeric materials has to be increased according to the projected materials demand.

Table 1.8: Global projection for materials demand in a ‘business-as-usual’ scenario¹⁸⁵

	Total global demand (Mt / Yr)					Of which from biomass in 2100	
	2000	2020	2030	2050	2100	%	Mt
Wood	306	530	670	1010	1620	100	1620
Paper	320	600	760	1110	1750	100	1750
Polymers	180	370	490	820	1880	10-100	190-1880
Total	806	1500	1920	2940	5250	68-100	3560-5250

From the current point of view, cellulose is the most common organic polymer, representing about 1.5×10^{12} tons of the total annual biomass production, and is considered an almost inexhaustible source of raw material for the increasing demand for environmentally friendly and biocompatible products⁴⁻⁵. The present thesis is aimed to re-focus or re-visit the possibilities of utilization of cellulose for various applications esp. structural and semi-structural fields. The present study has been divided into three parts. In the first part, which is on cellulose fibers as reinforcing materials, various aspects of natural fiber reinforcement have been presented in three chapters (**Chapter 3, Chapter 4 and Chapter 5**). The second part is on the utilization of chemically modified cellulose as matrix. The grafting of the polymer chains, which are also biodegradable, on cellulose esters and their nanocomposites preparation are studied (**Chapter 6**). The third part of the study is on utilizing cellulose in bionanomaterial field as template material for biomineralization process. The derivative of cellulose has been demonstrated to have control over the nucleation and growth of biomineral nanoparticles (**Chapter 7**).

Chapter 1

References

1. Powers, W. F., *Adv. Mater. Process*, **2000**, May, 38
2. Mohanty, A.K.; Drzal, L.T.; Misra, M., *Polym. Mater. Sci. Engineering*. **2003**, 88, 60
3. Mecking S, *Angew. Chem., Int. Ed.* **2004**, 43, 1078
4. Klemm, D; Schmauder H.-P.; Heinze T. in *Biopolymers*, Vandamme E.; De Beats S.; Steinbchel A., Wiley-VCH, Weinheim, **2002**, 6, 290
5. Kaplan D.L. in *Biopolymers from Renewable Resources*, Kaplan D. L Ed., Springer, Berlin, **1998**, 1
6. Stevens E.S. *Green Plastics*, **2002**, Princeton University Press, New Jersey, Chapter 1, p6
7. Anastas P.T.; Bickart P.H.; Kirchhoff M.M., *Designing Safer Polymers*, **2000**, Wiley -Interscience, John-Wiley & Sons, Inc. New York, Chapter 1, 1
8. Singh R.P.; Thanki P.N.; Solanky S.S; Desai S.M, in *Advanced Functional Molecules and Polymers*, Nalwa H.S (ed.), **2001**, Vol.4, Chapter1
9. *National Plastic waste management Task Force Report*, **1997**, Ministry of Environment and Fertilizers (MOEF), Government of India, New Delhi,
10. Alperowicz, N, *Chemical Week*, **2006**, 168(5), 25
11. CDC Study report, *Technology Status and Prospects of Biodegradable Plastics in India*. **2001**, Ministry of Science and Technology, New Delhi, India
12. Narayan P 'Analysing Plastic Waste Management in India' M.Sc Thesis, Lund Univeristy, Sweden, **2001**, September
13. BP Statistical Review of World Energy, 51st ed., **2002**
14. Guillet J.E, *Plastics Engineering*, **1974**, Aug. 47
15. Maiti S.; Jana. S., *Biodegradable Polymers Polymer Recycle And Waste Management*, Anusandhan Publishers, Midnapore, **2005**, Chapter 2, 53
16. Hoornweg D; Thomas L; *World Bank. Report: What a Waste: Solid Waste Management in Asia*. **1999**, 1, Report No 19328
17. Mukhopadhyay P; Tanguy P.A., *Intern. Plastic. Engg. Technol.* **1995**, 2, 55
18. Franklin W.E.; Sauer B.J.; Franklin M.A., *Proc. ANTEC*, **1995**, 3504
19. Hunt R.G. *Resources, Conservation and Recycling*, **1995**, 14, 225
20. A report on *Management of plastic waste in ECE region*, **1992**, United Nations, New York
21. Perugini F.; Mastellone, M.L.; Arena U. *Environmental Progress* **2005**, 24, 137
22. Gintis D, *Die Macromol. Chem. Macromol. Symp.*, **1992**, 57, 185
23. Brandrup, J.; Bittner M; Michaeli W.; Menges G; (Eds.) *Recycling and Recovery of Plastics*, Hanser, New York, **1996**,
24. Scott G, in *Atmospheric Oxidation and Antioxidants*, II Edn, Scott. G, Ed., Vol. II, Elsevier Applied Science, **1993**, Chapter 3.
25. Scheirs, J. *Polymer recycling science, technology, and applications*, Wiley, New York., **1998**
26. Griffin G.J.L, *Chemistry and Technology of Biodegradable Polymers*, Griffin G.J.L, Ed. 1st Edn, Blackie Academic and Professional (C&H), UK, **1994**, 18
27. Down to Earth: Plastic Unlimited, **2000**, 9, December 31

Chapter 1

28. a) Report of the WHO Commission on Health and the Environment: *Our Planet, Our Health*, World Health Organization (WHO), Geneva, **1992**, b) Beukering P.; Sehker M.; Gerlagh R.; Kumar V., *Analyzing Urban Solid Waste in Developing Countries: a Perspective on Bangalore, India*, International Institute of Environment and Development (IIED), **1999**, CREED Working Paper: 24.
29. Down to Earth: *Garbage: Your Problem*, **2001**, Jan. 31
30. Scott, G. In *Degradable Polymers principles and Applications*; Scott, G. Gillead, D., Eds.; Chapman and Hall: London, **1995**; Chapter 1.
31. Pandey, J.K.; Kumar, A.P.; Singh, R.P, *Macromol. Symp.* **2003**, 197, 411.
32. Alariqi, S.A.S.; Kumar, AP.; Rao, B.S.M.; Singh, R.P, *Polym Degrad Stab.* **2006**; 91, 1105
33. Ottenbritte R.M.; Albertsson A.C; Scott G., in *Biodegradable Polymers and Plastics*, Vert M Ed., Royal Society of Chemistry, Cambridge, **1992**, 73
34. Albertsson A.C; Karlsson S., in *Degradable Materials: Perspectives, Issues and Opportunities*, Barenberg S.A; Brash J.L; Narayan R; Redpath A.E., Ed: CRC Press, Boca Raton, **1990**, 263-286
35. Chandra R.; Rustgi R, *Prog Polym Sci*, **1998**, 23, 1273
36. a) Albertsson A.C; Karlsson S, *J. Appl. Polym. Sci.*, **1988**, 35, 1289, b) Albertsson A.C; Karlsson S, *Polym. Mater. Eng.* **1988**, 58, 65
37. Wool R.P.; Peanasky J.; Long J.M. Goheen S.M. *Proceedings of the First International Scientific Consensus Workshop on Degradable Plastics*, Toronto, Canada. **1989**, November 4
38. Vert M., *Biodegradable Polymers and Plastics*, Vert M., Ed. Royal Society of Chemistry, Cambridge, **1992**, 1.
39. Grassie N.; Scott G. *Degradation and Stabilization of Polymers*, Cambridge University Press. **1985**,
40. Kawai F., *Biodegradable Polymers and Plastics*, Vert, M. Ed., Royal Society of Chemistry, Cambridge, **1992**, 1.
41. Scott G., in *Atmospheric Oxidation and Antioxidants*, 1st Edn, Scott G., Ed. Elsevier Applied Science, **1965**, 387.
42. Scott G., in *Atmospheric Oxidation and Antioxidants*, 1st Edn, Scott G., Ed. Elsevier Applied Science, **1965**, 272
43. Osawa Z, *Developments in Polymer Stabilization-7*, Elsevier Applied Science, 1984, 193.
44. Iring, M.; Kelen, T.; Tudos, F., *Polym. Degradn. Stab.* **1979**, 1, 297
45. Mikheev Yu.A.; Zaikov, G.E.; Zaikov, V.G., *Polym. Degradn. Stab.* **2001**, 72, 1
46. Colin X.; Verdu J, *Comptes Rendus Chimie*, **2006**, 9, 1380
47. Berezhanskii, V.B.; Bykov, V.M.; Gorodov, V.V.; Zakrevskii, V.A.; Slutsker, A.I., *Polym. Sci. USSR*, **1986**, 28, 2404
48. Fuse, N.; Fujita, S.; Hirai, N.; Tanaka, T.; Kozako, M.; Kohtoh, M.; Okabe, S.; Ohki, Y. *IEEJ Transactions on Fundamentals and Materials*, **2007**, 127, 459
49. Friedrich, J.; Loeschke, I.; Frommelt, H.; Reiner, H.D.; Zimmermann, H.; Lutgen, P, *Polym. Degradn. Stab.* **1991**, 31, 97
50. Alariqi, S.A.S.; Kumar, A.P.; Rao, B.S.M.; Tevtia, A.K. Singh R.P., *Polym Degrad Stab.* **2006**, 91, 2451
51. Malik J; Kröhnke C, *Comptes Rendus Chimie*, **2006**, 9, 1330

Chapter 1

52. Albertsson A.C.; Andersson S.O.; Karlsson S, *Polym Degrad Stab*, **1987**, 18, 73
53. Albertsson A.C.; Barenstedt, C.; Karlsson S.; Lindberg, T, *Polymer*, **1995**, 36, 3075
54. Andrady A.L. in *Plastics Additives: An A-Z Reference*, Pritchard G Ed. Chapman & Hall, London, **1998**, 32
55. Andrady A.L. *Macromol Sci. Rev. in Macromol. Chem. Phys*, **1994**, C34, 25
56. ASTM D20.96 on *Environmentally Degradable Plastics and Biobased Products 1996* (www.astm.org)
57. European Standards a) CEN/TC 261 – Packaging b) CEN/TC 249-Plastics (www.http://www.cen.eu/cenorm/homepage.htm)
58. Pagga, U.; Beimborn, D. B.; Yamamoto M, *J Environ. Polym Degradn.* **1996**, 4, 173
59. www.iso.org
60. a) USA, www.nist.gov, b) Germany, www2.din.de, c) Belgium, www.orca.be and d) France, www.afnor.org
61. Scott G. in *Polymers and the Environment*, Royal Society of Chemistry, Cambridge, **1999**, 78
62. Chiellini E.; Chiellini F.; Cinelli P.; Ilieva V.I., in *Biodegradable Polymers and Plastics* Chiellini E.; Solaro R., Ed. Kluwer Academic /Plenum Publishers, New York, **2003**, 85
63. Steinbchel A, *Current opinion in Biotechnol.* **2005**, 16, 607
64. Petersen K.; Nielsen P.V.; Bertelsen G; Lawther M.; Olsen M.B.; Nilsson N.H.; Mortensen G., *Trend. Food Sci. Technol.* **1999**, 10, 52
65. Tuil. R.v.; Fowler P.; Lawther M.; Weber C.J.; Properties of Biobased Packaging Materials, in *Biobased packaging Materials for the food industry* Ed. Weber C.J, **2000**, EU Project Report (www.biomatnet.org/publications/f4046fin.pdf)
66. Krochta J.M.; De Mulder-Johnston C.L.C., in *Agricultural Materials and Renewable Resources*, Fuller G.; McKeon T.A.; Bills D.D. (Eds), American Chemical Society, Washington, **1996**, 120
67. Edgar K.J.; Buchanan C.M.; Debenham J.S.; Rundquist P.A.; Seiler B.D.; Shelton M.C; Tindall D., *Prog. Polym. Sci.*, **2001**, 26: 1605
68. Gloor W.E.; Gilbert C.B., *Indust. Engg. Chem.* **1941**, 33, 597
69. Bledzki A.K.; Gassan J., *Prog. Polym. Sci.*, **1999**, 24, 221
70. Dufresne A.; Vignon M.R., *Macromolecules*, **1998**, 31, 2693
71. Mathew, A.P.; Dufresne A., *Biomacromolecules*, **2002**, 3, 1101
72. Griffin G.J.L., Brit. Pat. 1485833. **1972**.
73. Westhoff, R.P.; Otey, F.H.; Mehlretter, C.L.; Russell, C.R.; *Ind. Eng. Chem. Prod. Res. Dev.* **1974**, 13, 123.
74. Otey, F.H.; Westhoff, R.P.; Doane, W.M., *Ind. Eng. Chem. Prod. Res. Dev.*, **1980**, 19, 592
75. Lenz R.W., *Adv. Polym. Sci.*, **1993**, 107, 1
76. Fringant, C.; Debrieres, J.; Rinaudo, M., *Polymer*, **1996**, 37, 2663
77. Fanta, G.F.; Burr, R.C.; Doane, W.M.; Russell, C.R., *J. Polym. Sci.: Symposia*, **1974**, 45, 89
78. Olivier A.; Cazaux F.; Gors C.; Coqueret X., *Biomacromolecules*, **2000**, 1, 282
79. Zhai, M.; Yoshii, K.; Kume, T., *Carbohydr. Polym.*, **2003**, 52, 311
80. Khor E.; Lim L.Y., *Biomater.* **2003**, 24, 2339

Chapter 1

81. Lee K.Y.; Ha W.S.; Park W.H., *Biomater*, **1995**, *16*, 1211
82. Miyazaki S.; Ishii K.; Nadai K., *Chem. Pharam. Bull* (Tokyo) **1981**, *29*, 3067.
83. Roller S, Corill N. *Intern. J Food Microbiol* **1999**; *47*, 67.
84. Miyazaki S.; Yamaguchi H. *Acta Pharm. Nord.*, **1990**, *2*, 401
85. Cuq, B., Gontard, N., Guilbert, S., *Cereal Chem.* **1998**, *75*, 1
86. Nagapudi, K., Brinkman, W.T., Leisen, J., Thomas, B.S., Wright, E.R., Haller, C., Wu, X., Chaikof, E.L., *Macromolecules*, **2005**, *38*, 345
87. Zelikin A.N.; Quinn J.F.; Caruso F., *Biomacromolecules*, **2006**, *7*, 27
88. Lindblad, M.S.; Liu, Y.; Albertsson, A.-C.; Ranucci, E.; Karlsson, S., *Adv. Polym. Sci.* **2002**, *157*, 139
89. a) *Chem. Eng. News* **2002**, *80*, 13; b) S.K. Ritter, *Chem. Eng. News* **2002**, *80*, 19. c) *Chem. Eng. News* **2003**, *81*, 11. b) Drumright R.E.; Gruber P.R.; Henton D.E., *Adv. Mater.* **2000**, *12*, 1841
90. a) Nayak, P.L.; Lenka, S.; Panda, S.K.; Pattnaik, T., *J. Appl. Polym. Sci.* **1993**, *47*, 1089, b) Oertel, G. *PU Based on Castor Oil Polyols in Telecommunications.* in *Polyurethane Handbook*, Hanser Publisher, New York. **1985**
91. a) Wang, H.J., Rong, M.Z., Zhang, M.Q., Hu, J., Chen, H.W., Czigány, T. *Biomacromolecules*, **2008**, *9*, 615, b) Kumar A.P.; Reddy KR.; Rana S.; Lonkar S.P.; Raut K.G.; Singh RP. *J. Vinyl. Additive. Technol.* **2005**, *11*, 13
92. Höfer, R.; Daute, P.; Grützmacher, R.; Westfechtel, A.; *J. Coat. Technol.* **1997**, *69*, 65
93. Watkins, C. *INFORM - International News on Fats, Oils and Related Materials* **2003**, *14*, 518
94. a) Mol, J.C. *J. Mol. Cat. A: Chem* **2004**, *213*, 39, b) Hill K, *Pure Appl. Chem.*, **2007**, *79*, 1999
95. Gandini, A.; Belgacem, M.N. *Prog. Polym. Sci.*, **1997**, *22*, 1203
96. Poirier, Y.; Nawrath, C.; Somerville, C. *Bio/Technology* **1995**, *13*, 142
97. Steinbüchel, A.; Hein, S. *Adv. Biochem. Eng. / Biotechnol.* **2001**, *71*, 81
98. Brown, R.M. *Pure Appl. Chem.*, **1996**, *33*, 1345
99. Iguchi, M.; Yamanaka, S.; Budhioni, A. *J. Mater. Sci.*, **2000**, *35*, 1
100. Gea S.; Torres F.G.; Troncoso O.P.; Reynolds C.T.; Vilasecca F.; Iguchi, M.; Peijs T., *Internat. Polym. Process.* **2007**, *22*, 497
101. Okada M., *Prog. Polym. Sci.*, **2002**, *27*, 87
102. Albertsson, A.-C.; Varma, I.K. *Adv. Polym. Sci.* **2002**, *157*, 1
103. a) Williams, C.K. *Chem. Soc. Rev.* **2007**, *36*, 1573, b) Gunatillake, P.; Mayadunne, R.; Adhikari, R., *Biotechnol. Ann. Rev.* **2006**, *12*, 301, c) Varma I.K.; Albertsson A.C.; Rajkhowa R.; Srivastava R.K., *Prog. Polym. Sci.* **2005**, *30*, 949
104. a) Vert M, *Prog. Polym. Sci.* **2007**, *32*, 755 b) Middleton, J.C., Tipton, A.J. *Biomaterials* **2000**, *21*, 2335, c) Kumar, N. Langer, R.S., Domb, A.J. *Adv. Drug Deliv. Rev.* **2002**, *54*, 889
105. a) Brubaker M. M., Coffman D. D., Hoehn H. H., *J. Am. Chem. Soc.*; **1952**, *74*, 1509, b) Swift G; *Acc. Chem. Res.*; **1993**, *26*, 105
106. Bailey W.J., Kuruganti V. K. Angle J. S., *Macromolecules* **1990**, *23*, 149.
107. a) Amin M.U.; Scott G., *Euro. Polym. J.*, **1974**, *10*, 1019, b) Morsi, S.E.; Zaki, A.B.; Etaiw S.H.; Khalifa W.M; Salem M. Al-S., *Polymer*, **1981**, *22*, 942
108. Griffin G.J.L., *J. Polym. Sci.* **1976**, *57*, 281.

Chapter 1

109. Bikiaris D.; Aburto J.; Alric I.; Borredon E.; Botev M.; Betchev C.; Panayiotou C. *J. Appl. Polym. Sci.* **1999**, *71*, 1089
110. Yu L.; Dean K.; Li L., *Prog. Polym. Sci.* **2006**, *31*, 576
111. a) Avella, M., Martuscelli, E., Raimo, M. J. *Mater. Sci.* **2000**, *35*, 523, b) Yao, J.-Y.; Yang, Q.-F.; Ma, Q., *Gaofenzi Cailiao Kexue Yu Gongcheng / Polym. Mater. Sci. Eng.* **2004**, *20*, 28
112. a) Nair, L.S.; Laurencin, C.T. *Prog. Polym. Sci.* **2007**, *32*, 762, b) Hernandez-Izquierdo V.M.; Krochta J.M., *J. Food Sci.* **2008**, *73*, R30-R39
113. Navarro, M.; Aparicio, C.; Charles-Harris, M.; Ginebra, M.P.; Engel, E.; Planell, J.A. *Adv. Polym. Sci.* **2006**, *200*, 209
114. a) Brandl, H.; Gross, R.A.; Lenz, R.W.; Fuller, R.C., *Adv. Biochem. Eng. / Biotechnol.* **1990**, *41*, 77, b) Bastioli, C. *Starch/Staerke* **2001**, *53*, 351
115. a) Chiellini, E., Cinelli, P., D'Antone, S., Ilieva, V.I. *Polimery/Polymers* **2002**, *47*, 538, b) Kyrikou, I., Briassoulis, D. *J. Polym. Environ.* **2007**, *15*, 125
116. Strange M.; Plackett D.; Kaasgaard M.; Krebs F.C., *Solar Energy Mater. Solar Cells*, **2008**, *In Press*
117. a) Honjo, G.; Watanabe, M. *Nature* **1958**, *181*, 326, b) Marchessault R.H.; Morehandi, F.F.; Walter, N.M., *Nature*, **1959**, *184*, 632
118. Meshitsuka G.; Isogai A., in *Chemical Modifications of Lignocellulosic materials*, Ed. Hon. D.N.S. Marcel Dekker Publications Inc. New York, **1996**, Chapter 2, 11
119. Gassan J.; Bledzki A.K., *Die Angew Makromol Chem* **1996**, *236*, 129.
120. Mohanty, A.K; Misra, M.; Hinrichsen, G. *Macromol. Mater. Eng.* **2000**, *276-277*, 1
121. Material Thoughts, Fiber reinforced plastics use. *Plastics News.* **2002**, August
122. Eichhorn, S.J.; Baillie, C.A.; Zafeiropoulos, N.; Mwaikambo, L.Y.; Ansell, M.P.; Dufresne, A.; Entwistle, K.M.; Herrera-Franco P.J.; Escamilla G.C.; Groom L.; Hughes M.; Hill C.; Rials, T.G.; Wild, P.M. *J. Mater. Sci.* **2001**, *36*, 2107
123. Joyly C, Kofman M, Gauthier R. *J Macromol Sci*, **1996**; *A33*, 1981
124. Zadorecki P, Michell AJ. *Polym. Compos*, **1989**; *10*: 69
125. Beshay, Hoa SV. *Sci Engng Compos Mater*, **1992**; *2*: 86
126. George J, Sreekala M.S.; Thomas S, *Polym Sci & Engg.* **2001**, *41*, 1071
127. a) Azizi Samir, M.A.S.; Alloin, F.; Dufresne, A. *Biomacromolecules*, **2005**, *6*, 612. b) Pal. P.K. *Plastics Rubber Process Appl* **1984**, *4*, 215. c) Winfield A.G. *Plastics and Rubber Int* **1979**, *4*, 23. d) Herrmann, A. S.; Nickel, J.; Riedel, U. *Polym. Degrad. Stab.* **1998**, *59*, 251.
128. John M.J.; Thomas S., *Carbohydr. Polym.*, **2008**, *71*, 343
129. Tummala, P., Mohanty, A.K.; Misra, M., Drzal, L.T., *Proceedings of 14th international conference on composite materials (ICCM-14)*, **2003**
130. Technology International Exchange Inc. *Certificate of analysis for pronova fish oil*, Pronoval Biocare, **1996**, 6
131. a) Clasen C.; Kulicke W.-M., *Prog. Polym. Sci.*, **2001**, *26*, 1839, b) Rosenau T.; Potthast, A; Sixta H.; Kosma P, *Prog. Polym. Sci.*, **2001**, *26*, 1763, c) Heinze T. Liebert T. *Prog. Polym. Sci.*, **2001**, *26*, 1689, d) Fink H. -P., Weigel P., Purz H. J.; Ganster J., *Prog. Polym. Sci.*, **2001**, *26*, 1473
132. a) El Seoud, O.A. Heinze, T. *Adv. Polym. Sci.* **2005**, *186*, 103 b) Glasser W.G. *Macromol. Symposia*, **2004**, *208*, 371, c) Dixon J, Andrews P.;Butler L.G., *Biotechnol. Bioeng.* **1979**, *21*, 2113

Chapter 1

133. a) Sakellariou P. Rowe. R. C *Prog. Polym. Sci* **1995**, 20, 889, b) Kumar, V.; Banker, G.S., *Drug Develop. Indus. Pharm.* **1993**, 19,, 1
134. Aubert, J.P.; Beguin, P.; Millet, J.; *Biochemistry and Genetics of Cellulose Degradation*. Academic, New York, **1988**.
135. Reese E. T. *Ind. Eng. Chem.* **1957**,49, 89.
136. a) Buchanan, C.M., Gardner, R.M., Komarek, R.J., Gedon, S.C. and White, A.W., in *Fundamentals of Biodegradable Polymers and Materials*. Technomic, Lancaster, Philadelphia. **1993**, b) Buchanan C.M., Gardner R.M. Komarek R.J., *J. Appl. Polym. Sci.* **1993**, 47, 709
137. Xanthos M. in *Functional Fillers for Plastics*, Xanthos, M., Wiley-VCH Verlag GmbH and co, Weinheim, **2005**, Chapter 1, 14
138. Vaia RA.; Wagner H.D., *Mater. Today*, **2004**, 7, 32
139. a) LeBaron P.C; Wang Z; Pinnavaia T.J, *Appl Clay Sci* **1999**, 15, 11, b) Pinnavaia T.J.; *Polymer- Clay Nanocomposites*, John Wiley & Sons, Pinnavaia T.J.; Beall G.W., (Eds) **2000**, c) Dennis H.R; Hunter D.L; Chang D; Kim S; White J.L; Cho JW; Paul DR, *Polymer*, **2001**, 42, 9513
140. Alexandre M.; Dubois. P., *Mater Sci Engg: R: Reports*, **2000**, 28, 1
141. Ray S.S.; Okamoto, M., *Prog. Polym. Sci.* **2003**, 28, 1539
142. Kumar. A.P.; Depan D.; Singh R.P., *Prog. Polym. Sci.* **2008**, (Communicated)
143. Sumita M., Tsukumo Y., Miyasaka K., Ishikawa K., *J. Mater. Sci.* **1983**, 18, 1758
144. Messersmith P.B., Giannelis E.P., *Chem. Mater* **1994**, 6, 1719
145. Messersmith P.B., Giannelis E.P., *J. Polym Sci. Part A. Polym Chem* **1995**, 33,1047.
146. Colbert D.T., Smalley R.E., *Past, Present and Future of fullerenes workshop*, Tokyo, Japan, Febraury 20-21, **2001**, Kluwer Dordrecht, Netherlands
147. Ijima S., *Nature*, **1991**, 354, 56
148. Ajayan P.M.; Schadler L.S.; Braun P.V., *Nanocomposite Science and Technology*, Wiley-VCH Verlag, Weinheim, Germany, **2003**, Chaper 2.
149. Lincoln, D.M.; Vaia, R.A.; Brown, J.M.; Benson Tolle, T.H. in *IEEE Aerospace Conference Proceedings*, **2000**, 4, 183
150. RP-234 *Polymer Nanocomposites: Nanoparticles, Nanoclays and Nanotubes* Business Communications Company, Inc.
151. Carrado K.A.; in *Handbook of Layered Materials*, Auerbach S.M.; Carrado K.A.; Dutta P.K., Eds. Marcel Dekker Inc. New York, **2004**, Chapter 1, 1
152. Newman, A.C.D.; Brown. G, in: *Chemistry of Clays and Clay Minerals*. Newman, A.C.D. Ed. Wiley-Interscience, New York: **1987**, 1.
153. Favier, V.; Chanzy, H.; Cavaillé, J.Y. *Macromolecules*, **1995**, 28, 6365
154. a) Dufresne A.; Cavaille, JY, Helbert W, *Macromolecules*, **1996**, 29, 7624, b) Dufresne A.; Vignon M.R. *Macromolecules*, **1998**, 31, 2693, c) Dufresne A.; Kellerhals M.B.; Witholt B. *Macromolecules*, **1999**, 32, 7396, d) Mathew, A.P., Dufresne, A. *Biomacromolecules* **2002**, 3, 609.
155. Helbert, W.; Cavaillé, J.Y.; Dufresne, A. *Polym. Compos.* **1996**, 17, 604
156. Dufresne, A., Cavaillé, J.-Y., Vignon, M.R. *J. Appl. Polym. Sci.* **1997**, 64, 1185,
157. Azizi Samir, M.A.S.; Alloin, F.; Dufresne, A. *Biomacromolecules*, **2005**, 6, 612
158. Huang J.; Ichinose I.; Kunitake T., *Chem Comm.* **2005**, 13, 1717

Chapter 1

159. Bruce D.M.; Hobson R.N.; Farrent J.W.; Hepworth, D.G., *Composites Part A* **2005**, 36, 1486
160. Yano H.; Hirose A.; Collins P.J.; Yazaki Y.J., *J. Mater Sci Lett* **2001**, 20, 1125
161. Kvien.; Oksman K., *Appl. Phys. A: Mater. Sci.Process.* **2007**, 87, 641
162. Xiaodong C.; Hua D.; Chang, M.L., *Biomacromolecules* **2007**, 8, 899
163. a) Park, H.-M.; Misra, M.; Drzal, L. T.; Mohanty, A. K. *Biomacromolecules*; **2004**, 5, 2281 b) Park H.-M., Liang X., Mohanty A.K., Misra M. Drazal L.T., *Macromolecules*, **2004**, 37, 9076
164. Dufresne, A.; Cavaille, J.-Y.; Helbert, W. *Macromolecules*; **1996**; 29, 7624.
165. Dubief, D.; Samain, E.; Dufresne, A. *Macromolecules*; **1999**; 32, 5765.
166. Angellier, H.; Molina-Boisseau, S.; Lebrun, L.; Dufresne, A. *Macromolecules*, **2005**, 38, 3783
167. Angellier, H.; Molina-Boisseau, S.; Dole, P.; Dufresne, A. *Biomacromolecules*; **2006**, 7, 531.
168. de Carvalho A.J.F.; Curvelo A.A.S.; Agnelli J.A.M., *Carbohydr. Polym* **2001**, 45, 189.
169. a) Park H.M.; Li X.; Jin C.Z.; Park C.Y.; Cho W.J.; Ha C.K., *Macromol Mater Eng* **2002**, 287, 553, b) *J Mater Sci* **2003**, 38, 909.
170. Pérez, C.J.; Alvarez, V.A.; Mondragón, I.; Vázquez, A. *Polym. Internat.* **2008**, 2, 247
171. Paillet, M.; Dufresne, A. *Macromolecules*; **2001**, 34, 6527.
172. Morin, A.; Dufresne, A. *Macromolecules*; **2002**, 35, 2190.
173. Nair, K.G.; Dufresne, A. *Biomacromolecules*; **2003**, 4, 657.
174. Lu, Y.; Weng, L.; Zhang, L. *Biomacromolecules*; **2004**, 5, 1046.
175. Huang, H., Yuan, Q., Yang, X. *J. Colloid Inter. Sci.* **2005**, 282, 26
176. Wang, S.; Chen, L., Tong, Y. *J. Polym. Sci., Part A: Polym. Chem.* **2006**, 44, 686
177. Hu, Q., Li, B., Wang, M. Shen, J. *Biomaterials* **2004**, 25, 779-785
178. Ogata N; Jimenez G.; Kawai H.; Ogihara T., *J Polym Sci Part B: Polym Phys* **1997**, 35, 389
179. Bandyopadhyay S.; Chen R.; Giannelis E.P., *Polym Mater Sci Eng* **1999**, 81, 159
180. a) Ray S.S.; Okamoto K.; Yamada K.; Okamoto M, *Nano Lett* **2002**, 2, 423. b) Ray S.S.; Yamada K.; Okamoto M.; Ueda K, *Nano Lett* **2002**, 2 1093. c) Ray S.S.; Maiti, P.; Okamoto M.; Yamada K.; Ueda K., *Macromolecule* **2002**, 35 3104.
181. Uyama H.; Kuwabara M.; Tsujimoto T.; Nakano M.; Usuki A.; Kobayashi S., *Chem Mater* **2003**, 15, 2492.
182. Miyagawa H.; Misra, M.; Drazal L.T.; Mohanty A.K., *Polymer*, **2005**, 46, 445.
183. Maiti P.; Batt C.A.; Giannelis E.P., *Polym Mater Sci Eng* **2003**, 88, 58.
184. Ray S.S. Okamoto K.; Maiti P; Okamoto M., *J Nanosci Nanotech* **2002**, 2,171.

Scope and Objectives of the Present Investigation

2.1. Introduction: Motivation of the study

In the 21st century, major changes are coming in automobile industry and materials will be a key enabling technology. Since about 90% of the total energy consumption by an automobile in its lifetime is from fuel, the automobile parts made of metals cause the higher exploitation of petroleum resources. The high expectations for fuel economy and low emissions for manufacturing and transportation are creating a demand for new low cost and high-performance lightweight materials to replace the metals¹⁻². Not only in automobile industry, almost in every applications from agriculture to transport and from aerospace to food packaging, the use of polymeric materials has become an integral part of our modern daily living. Biopolymers currently achieve high interest in materials science since they offer reductions of landfill space during waste management as well as new end-user benefits in various fields of applications³. Among these materials, those from renewable resources such as polysaccharides, additionally offer CO₂-neutrality, partial independence from petrochemistry-based products and the exploitation of nature's synthesis capabilities via photosynthesis. From the current point of view, cellulose is the most common organic polymer, representing about 1.5 x 10¹² tons of the total annual biomass production by natural photosynthesis from CO₂ and water, and is considered an almost inexhaustible source of raw material for the increasing demand for environmentally friendly and biocompatible products⁴. Thus, the present research work is aimed to refocus or revisit the possibilities of utilization of cellulose for various applications esp. structural and semi-structural fields. Cellulose which is a linear condensation polymer consisting of D-anhydroglucopyranose units (AGU) linked together by β 1, 4 – glycoside bond, is highest constituent of the natural fiber. The inter and intra molecular hydrogen bonds result the linearity, the stiffness, the rigidity, strength and ultimately to form thread like material called micro-fibrils which are apparently bound to form natural fibers⁵. Basically two main groups of cellulose-materials can be distinguished: natural / regenerated celluloses are suitable only for fibre and film production from conventional and new processes. Secondly, melt-processable cellulose derivatives such as esters can be used for extrusion and molding⁶. The present study has been divided in three parts, which are expanded in five working chapters.

Chapter 2

The first part is on utilizing cellulose fibers as reinforcing materials. Jute fiber is one of the natural fibers abundantly available in India. In this study, it is aimed to study the effect of treatment on fibers on the properties of final composite materials. Recently, possibilities of reinforcing polymers with layered silicates or clay are highly explored⁷⁻⁸. The polymer clay nanocomposites have shown drastic improvement in thermal, mechanical properties, because of their high aspect ratio (platelet nature). Thus, another aim is to study effect of the incorporation of clay on the properties of cellulose-fiber reinforced composites. Next to cellulose, starch is most abundant polymer. Because of branching and inter- and intra-molecular hydrogen bonding, melt processing of starch is difficult. In order to extrude it is generally processed using plasticizers. However, thermoplastic starch exhibits poor properties because of its water absorption, brittleness, and dependence of mechanical properties on the environmental conditions esp. relative humidity⁹. Thus, our aim has been extended to improve the water resistance of starch by reinforcing with microcrystalline cellulose and further improving the properties by photo-induced crosslinking.

The second part is on utilization of cellulose after some chemical modification as matrix. In fact, cellulose derivatives were the basis of the original synthetic plastic. It could readily be used to form many useful articles, including film, sheet, and molded objects. Cellulose acetate and its mixed esters have had to find their place in the spectrum of plastic properties¹⁰. Cellulose ester plastics have, however, continued to satisfy significant marketplace needs and their properties have continued to attract interest. As with all materials, the properties of cellulose esters are often an advantage in one application but a detriment in another. Some of the detrimental properties include a relatively narrow window between the melt flow temperature and the decomposition temperature. This quality means that in most commercial applications, plasticizers are used in conjunction with cellulose esters¹¹. There are some drawbacks in using external plasticizers while processing and usage such as leaching out of plasticizer apparently harms the environment¹². To evade this problem, it has been planned to graft the polymer chains, which are also biodegradable on cellulose esters.

Though they have commercial potential as bioplastics, but some of the properties such as brittleness, low heat distortion temperature, high gas permeability, low melt viscosity for

Chapter 2

further processing etc. restrict their use in a wide-range of applications. Therefore, modification of these biopolymers with nanoreinforcement to prepare nanocomposite has can be an effective way to improve these properties concurrently. It is also planned to incorporate clay (layered silicates) into these grafted matrices expecting that the grafted chains may crawl into silicate galleries to improve the materials properties.

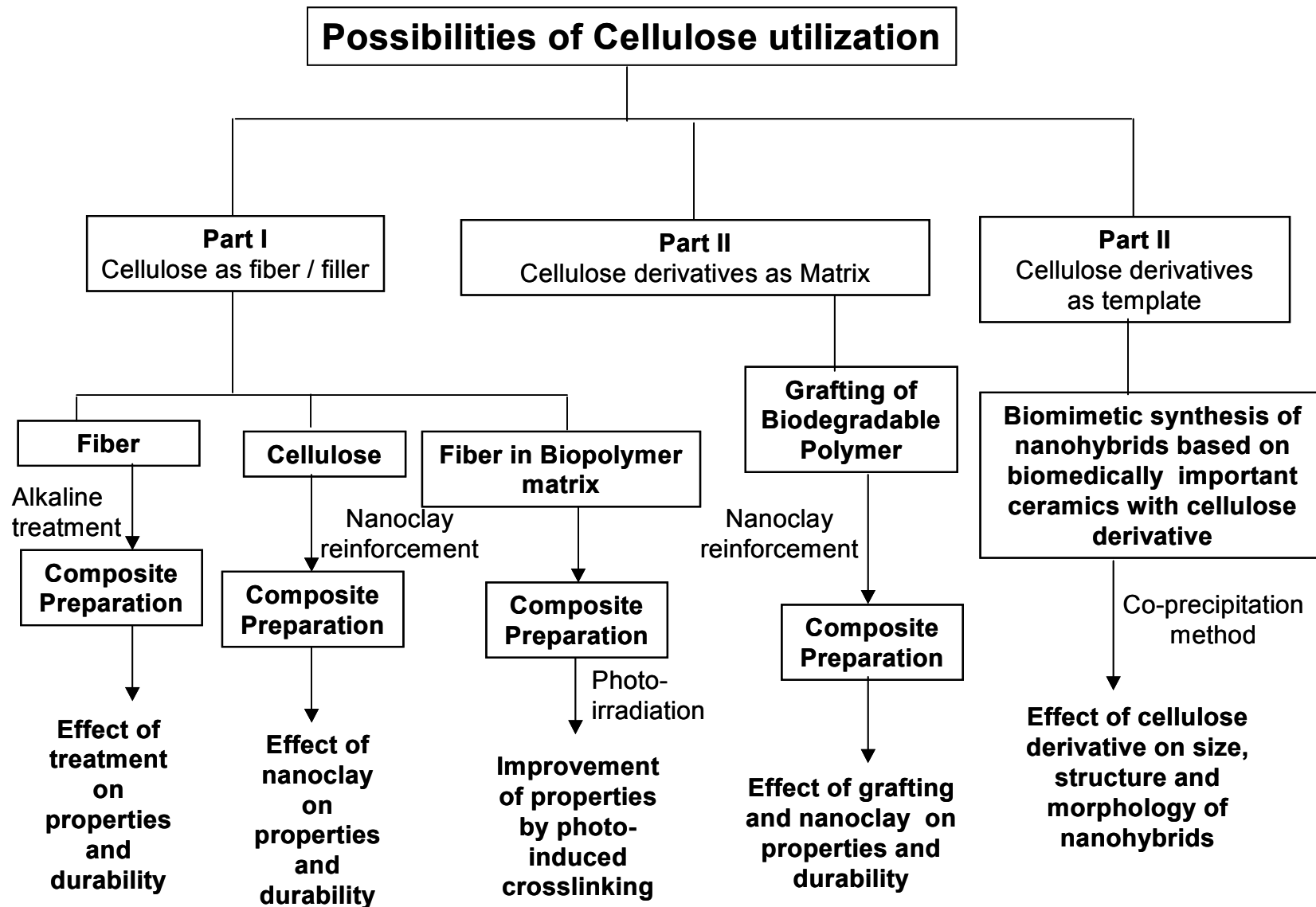
The third part of the study is on utilizing cellulose in bionanomaterial field. The main goal of bone tissue engineering has been to develop biodegradable materials as bone graft substitutes for filling large bone defects¹³. Owing to their small size and high specific surface area of nanoscale bioceramics, the proliferation of osteoblasts has been greater on the nanoscale hydroxyapatite (HA) than that on the conventional ceramics¹⁴. Nanoscale bioceramics open up unique possibilities of treating some complex bone defects¹⁵. In addition solubility in biological fluids is also important factor for enhancing the proliferation.

2.2. Approaches and Objectives

With the above-mentioned background information, the following main objectives were drawn for the present study:

- To prepare the natural fiber reinforced composites with polyolefin (thermoplastics) using various fibers and to study their properties and durability under abiotic and biotic environmental conditions
- To reinforce polyolefin (thermoplastics) with both natural fibers and nanoclay and to study the properties and durability of obtained composites under abiotic and biotic environmental conditions
- To prepare the natural fiber reinforced composites using a biopolymer matrix and to improve the properties by photo-induced crosslinking
- To graft the cellulose derivatives with biodegradable polymer chains and to prepare nanocomposites of grafted cellulose derivatives with nanoclay
- To prepare nanohybrids based on cellulose derivative with biologically important nanoparticles and to study the effect of cellulose derivative on the size, morphology of nanoparticles.

These objectives have been summarized as flowchart in *Scheme 2.1*.



Scheme 2.1: Flowchart of the present investigation

Chapter 2

References

1. Powers, W. F., *Adv. Mater. Process*, **2000**, May, 38
2. Mohanty, A.K.; Drzal, L.T.; Misra, M., *Polym. Mater. Sci. Engineering*. **2003**, 88, 60
3. Klemm, D; Schmauder H.-P.; Heinze T. in *Biopolymers*, Vandamme E.; De Beats S.; Steinbchel A., Wiley-VCH, Weinheim, **2002**, 6, 290
4. Kaplan D.L. in *Biopolymers from Renewable Resources*, Kaplan D.L Ed., Springer, Berlin, **1998**, 1
5. Marchessault R.H.; Morehandi, F.F.; Walter, N.M., *Nature*, **1959**, 184, 632
6. Simon J.; Müller H. P.; Koch R. Müller V. *Polym. Degradn Stab*, **1998**, 59, 107
7. Alexandre M.; Dubois. P., *Mater Sci Engg: R: Reports*, **2000**, 28, 1
8. Ray S.S.; Okamoto, M., *Prog. Polym. Sci.* **2003**, 28, 1539
9. Dufresne A.; Vignon M.R., *Macromolecules*, **1998**, 31, 2693
10. Malm C.J.; Mench J.W.; Kendall D.L.; Hiatt G.D., *Ind Engg Chem* **1951**, 43, 688.
11. Edgar K.J.; Buchanan C.M.; Debenham J.S.; Rundquist P.A.; Seiler B.D.; Shelton M.C; Tindall D., *Prog. Polym. Sci.*, **2001**, 26: 1605
12. a) Maramorosch K., *Sceince* **1952**, 115, 236, b) M.Yoshika, N. Hagiwara and N.Shiraishi *Cellulose* **1999**, 6, 193-212
13. Stupp S.I.; Braun P.V., *Science*, **1997**, 277, 1242.
14. Doi Y.; Horiguchi T, *J. Biomed. Mater. Res.* **1996**, 31, 43
15. Webster T.J.; Siegel R.W.; Bizios R, *Biomaterials*, **2000**, 21, 1803

Effect of the treatment of cellulose fiber on the properties and durability of natural-fiber reinforced composites*

* *Mater. Chem. Phys.* 2005; 92 (2-3): 458-469

3.1. Introduction

In recent years, the consumption of natural fiber-reinforced composites has been skyrocketed not only for environmental concerns but also for yielding a unique combination of high performance, great versatility and processing advantages at favorable cost¹⁻³. In these materials, to evade the major problem that is incompatibility between the hydrophilic (polar) polysaccharides and hydrophobic (non polar) polymer matrix, many efforts have been focused to optimize / influence the quality of the fiber-matrix interface by some physical and chemical methods such as change of the surface energy, impregnation, coatings, coupling agents and graft copolymerization⁴. Among many other additives used for this purpose, MAH-PP has been found to be very efficient in improving the filler dispersion and the compatibility in polypropylene-cellulose composites⁵⁻⁹.

There are many reports^{4-9, 10} which have been documented on the processing conditions, mechanical property variations and fiber modifications. Now-a-days, it is a tendency to use the mercerization of natural fibers in the industries which is one of the cheapest and old methods. Its effectiveness has been found to depend on the concentration of the alkaline solution, its temperature, time of treatment, tension of the material as well as on the additives present¹¹⁻¹². According to Lai and Sarkanen's estimation¹³, the peeling process which is degradation at the reducing ends of cellulose chains, is relatively rapid at 150-190 °C and Gentile et. al.¹⁴ also detected the decrease in concentration of alkaline solution and temperature which were reduced due to the peeling factor by hydrolysis of amorphous cellulose. On the other hand, it is well evident from the results of theoretical calculations of fibers¹⁵, that the quality of fibers in terms of mechanical properties depends on the degree of polymerization, crystallinity, orientation of chains (spiral angle) and fiber diameter. According Hermans¹⁶ and Roy et. al.¹⁷⁻¹⁸, the alkali treatment will also affect the fiber orientation by swelling, stretching and reorientation. Thus, it will be worthwhile to study the effect of concentration of alkaline solution on the mechanical properties of fiber-reinforced composites. In the present chapter, the study has been focused on the effect of size and treatment of the natural fibers on the mechanical properties, thermal stability and durability of their composites in biotic and accelerated aging conditions.

There is a vast array of potential of long and short fibers for composite production. One of the stem / bast fibers is jute fiber which is renewable, versatile, non-abrasive, porous,

Chapter 3

hydroscopic, viscoelastic, combustible and biodegradable¹⁹. Table 3.1 shows the technical information on jute fibers^{20,21}.

Table 3.1: Characteristics of fibers^{20,21}

Physical and Mechanical properties				
Density [g/cm ³]	Elongation [%]	Tensile Modulus [MPa]	Young Modulus [MPa]	Moisture absorption
1.3	1.5-1.8	393-773	26500	12
Composition (%)				
Cellulose	Hemi-cellulose	Pektin	Lignin	Water solubles
64.4	12.0	0.2	21 -24	1.1

These jute fibers were treated with low and higher concentrations of alkali to differentiate lignin content in the fibers. The ethylene-propylene copolymers have a wide range of applications by varying in composition of monomers from soft elastomers to rigid thermoplastics. One of the ethylene-propylene copolymers is used as matrix with treated jute fibers. For comparison, composites were also prepared by using commercially available microcrystalline cellulose powder.

3.2. Experimental

3.2.1. Materials

The ethylene-propylene copolymer [ethylene 15.1% mole] with melt-flow index about 3.5 g/10 min and density about 0.9 g/cm³ was obtained from M/s. Montell Ferrara, Italy. Maleic anhydride, benzoyl peroxide, sodium hydroxide and xylene were obtained from M/s. SD. Fine Chemicals Ltd., India. The jute fiber was purchased from local market and used after alkaline treatment. The microcrystalline cellulose powder for TLC grade was obtained from M/s. LOBA Chemie, Mumbai, India

3.2.2. Alkaline Treatment and Lignin Content Measurement

The jute fibers were immersed in various concentration of aqueous solution of NaOH for ~ 3 hr at 80 °C. Then, they were washed with deionized water up-to the pH of filtrate reaches to 7.0, dried in vacuum oven at 50 °C for one week. The alkali treated and neat fibers were dried at 50 °C in vacuum oven for 12 hr. Their acid insoluble lignin content was measured using following procedure (TAPPI-T222 om-88)²².

Chapter 3

In a test tube, 1g of fiber (W_1) was weighed accurately using *Precisa 205 A* SCS balance with .0000g accuracy. To this test tube, 15 ml of 72% H_2SO_4 was added and cooled to 4 °C and slowly stirred (to wet sample thoroughly) for 2-3 minutes. First stage of hydrolysis was done at room temperature (~ 25 °C) for 2 hr with stirring. Second hydrolysis was done after diluting this mixture to 3% H_2SO_4 concentration with deionized water by gentle boiling followed refluxing for 4 hr. After cooling and rinsing with deionized water, the mixture was filtered and washed with warm water and dried at 60 °C in vacuum oven till obtaining constant weight (W_2). Then the crucible was calcined at 575 °C with heating rate 20 °C / min for 4 hr in a muffle furnace. The crucible was cooled in desiccator and weighed (W_3). The acid insoluble lignin (%) was calculated as follows,

$$\text{Acid insoluble lignin (\%)} = \frac{W_2 - W_3}{W_1} \times 100$$

The fibers, which were treated with 3 % and 17.5 % of NaOH solution were chosen for further study of reinforcement and labeled as J1 and J2, respectively. These fibers were cut into short fibers with 6 mm in length. The third fiber MC was commercial grade cellulose powder, which is generally used for TLC.

3.2.3. Maleation of EP Copolymer and Preparation of Composites

The dried EP copolymer was maleated in a melt blender (Brabendar Plasticorder - 487106) by melting in presence of benzoyl peroxide (0.15 % wt/wt) and maleic anhydride (3 % wt/wt) at 170 °C at 65 rpm for 1.5-2 min. Crude maleated ethylene-propylene copolymer (MEP) (5g) was dissolved in 250 ml of xylene at 125 °C, for 3-5 hours and then added to 750 ml of cold acetone. The precipitated MEP was washed with acetone, filtered and dried in vacuum oven at 50 °C for 12 hours. The mercerized fibers were dried before preparation of composites in vacuum oven at 50 °C for one week. The melt mixing of polymers and fibers was performed in the same Brabendar. Keeping the weight ratio between neat EP copolymer and maleated EP copolymer (Neat EP/MEP) 9/1 as constant, the composites were prepared with varying the concentration of jute fibers at 170 °C with 70 rpm for 3 min. *Table 3.2* depicts the composition of all the composites.

Table 3.2: Composition of the composites

S.No	Fiber content (%)	EP copolymer (%)	MEP (%)	Code
1.	-	100	-	EP
2.	-	-	100	MEP
Composites of 3 % NaOH treated jute fiber (J1C)				
3.	5	85.5	9.5	J1C05
4.	10	81.0	9.0	J1C10
5.	15	86.5	8.5	J1C15
Composites of 17.5 % NaOH treated jute fiber (J2C)				
6.	5	85.5	9.5	J2C05
7.	10	81.0	9.0	J2C10
8.	15	76.5	8.5	J2C15
9.	25	67.5	7.5	J2C25
10.	40	54	6.0	J2C40
Composites of microcrystalline cellulose powder (MC)				
11.	5	85.5	9.5	MC05
12.	10	81.0	9.0	MC10
13.	15	76.5	8.5	MC15

Due to the practical difficulties in the melt-mixing and hydraulic press molding of the samples with higher content of the jute fibers, the maximum J2 fiber content used in this study was 40% and others were up to 15 %wt. The samples were molded to obtain films (thickness $\approx 100 \mu\text{m}$) in electrically heated hydraulic Carver press at $180 \text{ }^\circ\text{C}$ for 1.5 min and quench-cooled to room temperature ($27 \text{ }^\circ\text{C}$).

3.2.4. Characterization

3.2.4.1. FTIR Spectroscopy

The functional group analysis was done using Perkin-Elmer 16 PC FTIR spectrophotometer and our interest was focused on the changes in hydroxyl ($3600\text{-}3100 \text{ cm}^{-1}$) and carbonyl region ($1800\text{-}1600 \text{ cm}^{-1}$) to follow the photo-oxidation of the samples.

3.2.4.2. Color Index

Yellowness index (YI) was determined in accordance with ASTM-D1925 by reflectance measurements using Color Mate HDS Colorimeter (Milton Roy, USA) with integrating

Chapter 3

sphere. The samples were placed in the reflectance part of a sphere using a standard white ceramic as reference tile. The instrument is designed to give direct yellowness index value on the basis of CIE standard illumination C (CIE 1931) 2° standard observer viewing²³. It was obtained from the tristimulus values X_{CIE} , Y_{CIE} and Z_{CIE} relative to source C using the equation $YI = [100(1.28 X_{CIE} - 1.06 Z_{CIE})] / Y_{CIE}$. Several values of YI obtained from different parts of the samples were used to obtain an average value of YI.

3.2.4.3. Mechanical Properties Measurements

Specimens were cut according to IS: 2508-1984:A4 for material properties estimations. The static tensile behavior of composites was investigated at room temperature (27 ± 2 °C) and 65 ± 5 % relative humidity using a Universal Testing Machine (Instron model 4204) at crosshead speed at 10 mm / min. Average value out of six measurements was reported for each composition.

3.2.4.4. Thermal Properties Measurements

Perkin-Elmer TGA-7 was used to study the thermal stability of these composites and their constituents. They were heated to 600 °C with a typical rate of 10 °C/min under nitrogen flow with at a rate of 20 ml/min.

3.2.4.5. Microscopic Measurements

Surface morphological changes of photo-irradiated and composted samples were examined by staining the samples with osmium tetroxide, drying under vacuum at 50 °C for 24 h and scanning under electron microscope (Leica Cambridge Stereoscan 440 Model). The dimensions of fibers were determined by using optical microscope (Olimpus, Model Bx50 F4, Japan) with x50 magnification.

3.2.5. Performance Evaluation

3.2.5.1. Photo-degradation

The specimens were irradiated (≥ 290 nm) in a polychromatic irradiation chamber (SEPAP 12/24 M/s. Material Physico Chimique, Neuilly, Marne, France) at 60 °C under air. It consists of (4 x 400W) medium-pressure mercury vapor lamps supplying radiation longer

Chapter 3

than 290 nm²⁴⁻²⁶. The photo-degradation was monitored by changes in functional groups and mechanical properties.

3.2.5.2. Biodegradation: Composting method

The compostability tests of 4 x 4 cm² specimens were done in a laboratory-scale composting bin^{24-26, 27}. The constitution of solid waste mixture (compost) used for biodegradability testing of samples was as follows (in dry weight): 40.8% shredded leaves, 11.4% cow manure/dung, 15.8% newspaper and computer paper, 2% white bread, 7.8% sawdust, 19.2% food waste (dry milk, potato, carrot, banana, and other vegetables), and 3.0% urea. The total dry solid content of compost was 50-60 %. The compost bin was covered with green grass around and moisture content was maintained by spraying water periodically. To avoid anaerobic conditions, the bin was constantly aerated with oxygen through a hollow tube. Through out the study, the carbon/nitrogen (C/N) ratio was measured by elemental microanalysis of dry solid to follow the quality of compost. It was observed to be ~ 10/1 to 30/1. The temperature of compost was observed to be slightly higher (up to 42 ±1 °C) than that of atmosphere (35 ±1) °C. Compostability was measured in terms of weight loss (%), which is calculated using the following formula:

$$\text{Weight Loss (\%)} = [(\text{Initial weight (g)} - \text{Final weight (g)}) / \text{Initial weight (g)}] \times 100$$

3.3. Results and Discussion

3.3.1. Characterization

3.3.1.1. Fiber characterization

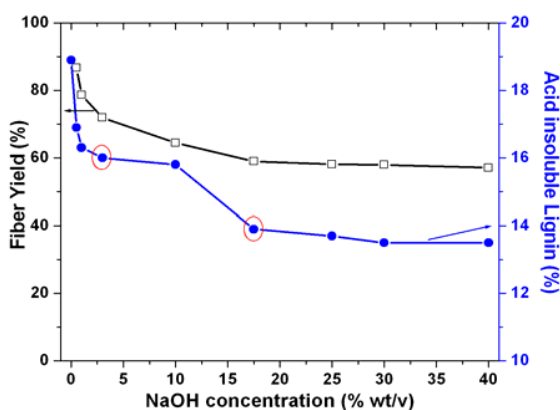


Figure 3.1: Influence of alkaline treatment on acid insoluble lignin content

Chapter 3

Figure 3.1 shows the acid insoluble lignin content versus alkaline concentration, where, the two fibers, which are used in the present study, are circled. Optical micrographs of them can also be found in Figure 3.2.

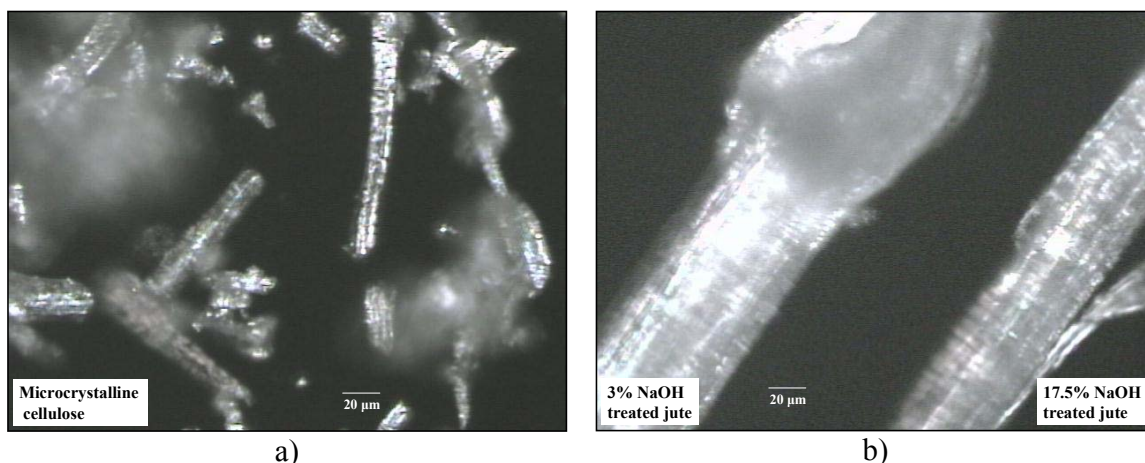


Figure 3.2: Optical micrograph of a) microcrystalline powder and b) alkali treated jute fibers (with x50 magnification)

The average values of their dimensions are presented in Table 3.3 where the MC was observed to be smaller in size and the aspect ratio of J2 fiber was observed to be higher than others.

Table 3.3: Characteristics of treated fibers

Parameters	J1	J2	MC
Yield (%)	70.01	58.05	-
Alkali treatment			
Length (μm)	6000	6000	38.8±0.2
Diameter (μm)	70.4±0.2	47.2±0.2	14.8±0.2
Aspect ratio (l/d)	85.22±0.02	127.11±0.02	2.62±0.02
Lignin content	Higher	Moderate	Low/nil

3.3.1.2. Preparation

Figure 3.3a shows the FTIR spectra of maleated EP copolymer where the peaks at 1780 cm^{-1} for cyclic anhydride and 1714 cm^{-1} for carboxylic acid groups are observed. After melt mixing of fibers with Neat EP / MEP, the absorption peak at 1780 cm^{-1} of MEP can be found to be decreased / reduced in Figure 3.3a, whereas the increase at 1740-1720 cm^{-1} region is observed for ester groups. This absorption was found to be varied for different

fibers, for example absorbance at ester region was observed to be higher for MC composites. The ester formation which is one of the supporting evidences for the chemical compatibility⁵, depends on the availability of hydroxyl groups on the surface of the fibers.

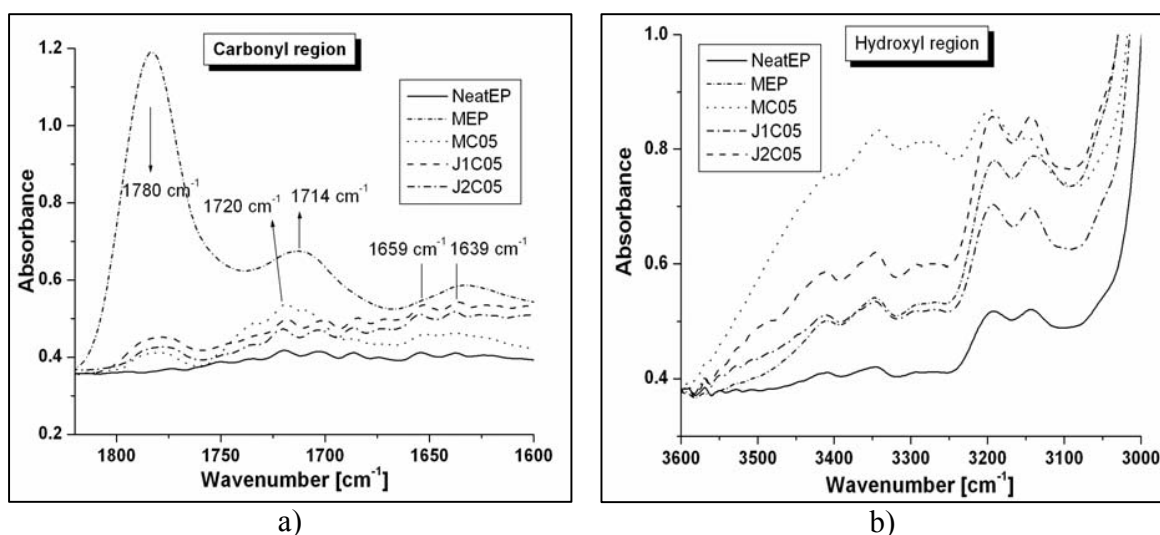


Figure 3.3: FTIR spectra of composites a) carbonyl region and b) hydroxyl region

The MC composites were found to show higher absorbance at 3500-3100cm⁻¹ for hydroxyl groups in FTIR spectrum (*Figure 3.3b*) than other two composites. This variation in the hydroxyl groups may be attributed to the extent of treatments on the fibers. For example, the commercial cellulose powder (MC) is generally prepared by multistage processes, like water retting, alkali-mercerization, bleaching (with hypochlorite solution) and milling processes while the fibers J1 and J2 have been treated with sodium hydroxide aqueous solution. On alkali treatment, the lignin which make the natural fibers stiff and strong by acting as adhesive between cellulose micro-fibrils through covalent and hydrogen bonds with hydroxyl groups of cellulose, were removed in particular extent depending upon the concentration of alkaline solution used¹¹⁻¹² and leaving free hydroxyl groups. With lower concentration of alkaline concentration (3%), lignin could be removed minutely only. This can be evidenced from the absorption bands at 1700-1630 cm⁻¹ esp. at 1659 and 1639 cm⁻¹ which are assignable for acidic and aldehydic carbonyl stretching of lignin and other extractives for jute fiber composites (J1C05 and J2C05) in *Figure 3.3 a*. These peaks were hardly detectable for MC05. *Figures 3.4 a-c* shows the optical micrograph of the composites.

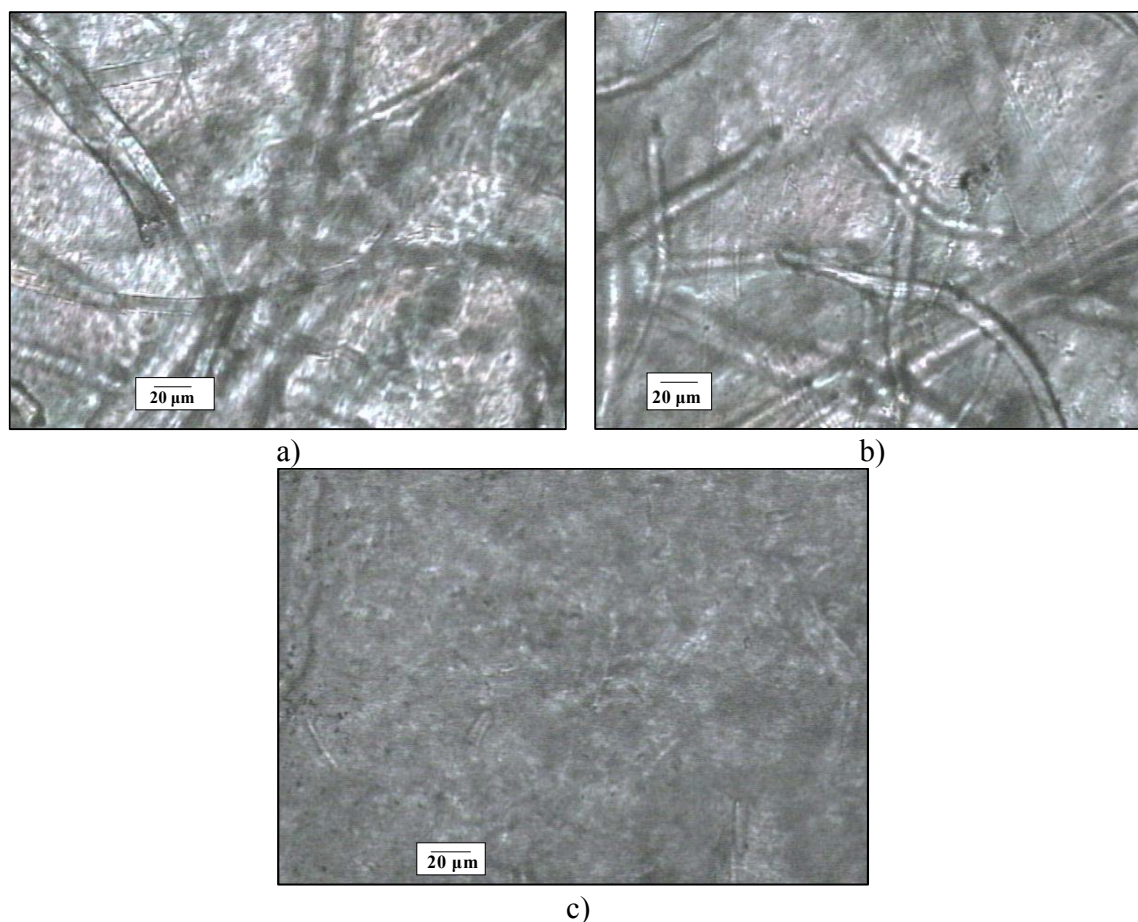


Figure 3.4: Optical micrograph of the composite a) J1C05, b) J2C05 and c) MC05 (with x50 magnification)

It could be noted in comparison with *Figure 3.2* and *3.4*, that after melt processing, microfibrils were defibrillated / ruptured. The dispersion of the micro-fibers in the film of MC composites that was made under the carver press was observed even at the edges of the film.

3.3.2. Color Index

Figure 3.5 shows the photograph of the composite strips. It can be seen with increasing fiber content, the intensity of the yellowing increases. The jute fiber reinforced composites (J1C & J2C) show higher intensity than microcrystalline fiber reinforced composites (MC). The color / yellowing intensity has been quantified plotted in *Figure 3.6* as a function of fiber content.

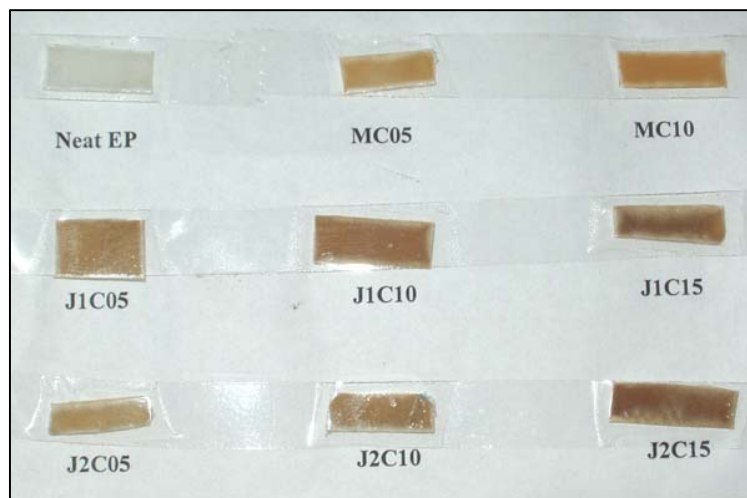


Figure 3.5: Picture of the prepared composites

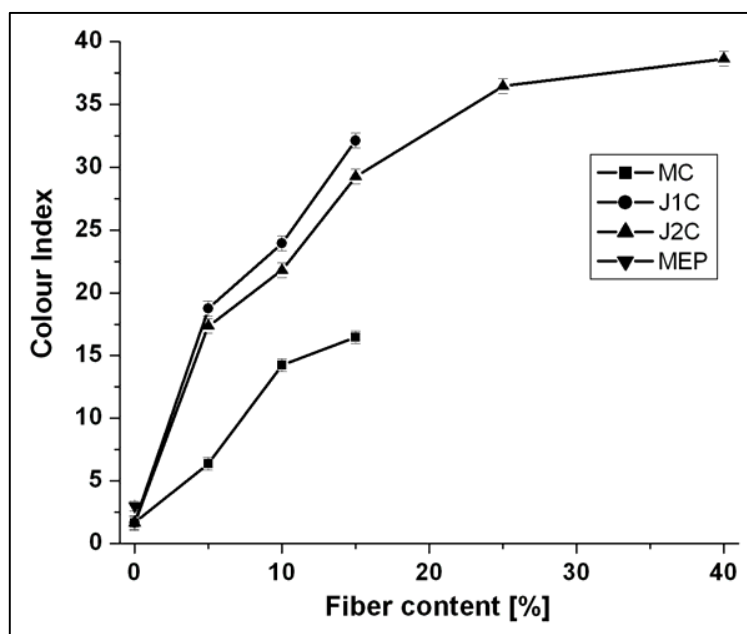


Figure 3.6: Color Index of the prepared composites

It can be seen that the color index increase with the content fiber. Thus, in the natural fiber reinforced composites, the fibers might be a light absorber which can be attributed to the presence of lignin in the fibers, which was further confirmed by UV spectral analysis. The *Figure 3.7* shows the UV spectra of acid soluble lignin extracted from 17.5 % NaOH treated fiber.

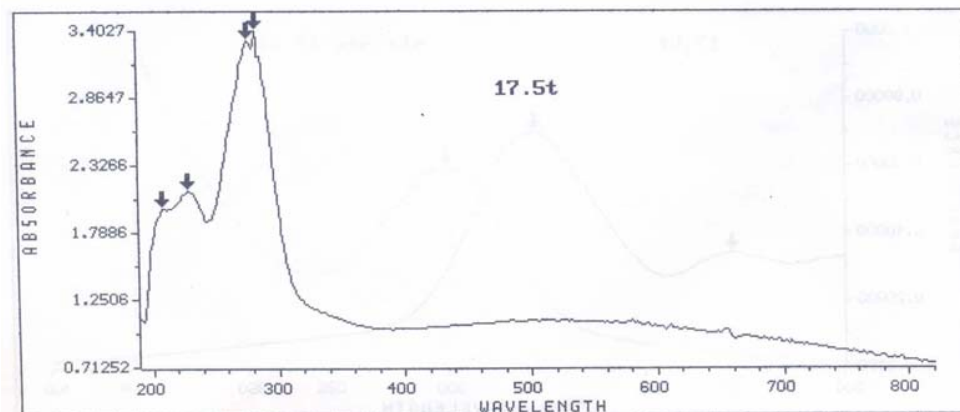


Figure 3.7: UV spectra of acid soluble lignin extracted 17.5 % NaOH treated Jute fiber

An inspection reveals that cellulose absorbs light strongly between 200-300nm, with a tail of absorption extending to 400nm. Lignin and polyphenols, i.e. absorb light strongly below 200nm and have a strong peak at 280nm, with absorption through the visible region.

According to Norrstrom ²⁸, lignin contributes 80-95%, the carbohydrates 5-20%, and the extractives about 2% of the absorption co-efficient. Pure cellulose is not a good light absorber. The absorption by cellulose may be due to the presence of carbonyl group that accidentally introduces into cellulose during its treatment. In addition to the carbonyl group, it has been suggested that absorption chromophores in cellulose can also be contributed by acetal / ketonic carbonyl groups at C₁ position of glucose unit at the non-reducing end ²⁹. Because of the structural similarity, the light-absorption characteristics of hemicelluloses should resemble those of cellulose. Unlike cellulose and hemicelluloses, lignin is a good light absorber. The absorption occurs at chromophoric structural elements within the molecular network of lignin. They are as i) Chromophoric functional groups: phenolic hydroxyl groups, double bonds, carbonyl groups, etc., ii) Chromophoric systems; quinines, quinonemethides, biphenyls, etc., and iii) Leuco-chromophoric systems; methylenequinones, phenanthraene-quinones, phenylanthraquinones, bimethylenequinones etc. Because of its light-absorption properties, it absorbs predominant light and imparts color to the fibers. In addition, during the processing, the composites can undergo thermal-induced degradation, which may also impart the yellowing to final composites.

3.3.3. Mechanical Properties

The effect of treatments of the fibers and their loading on the mechanical properties can be seen in *Figure 3.8*.

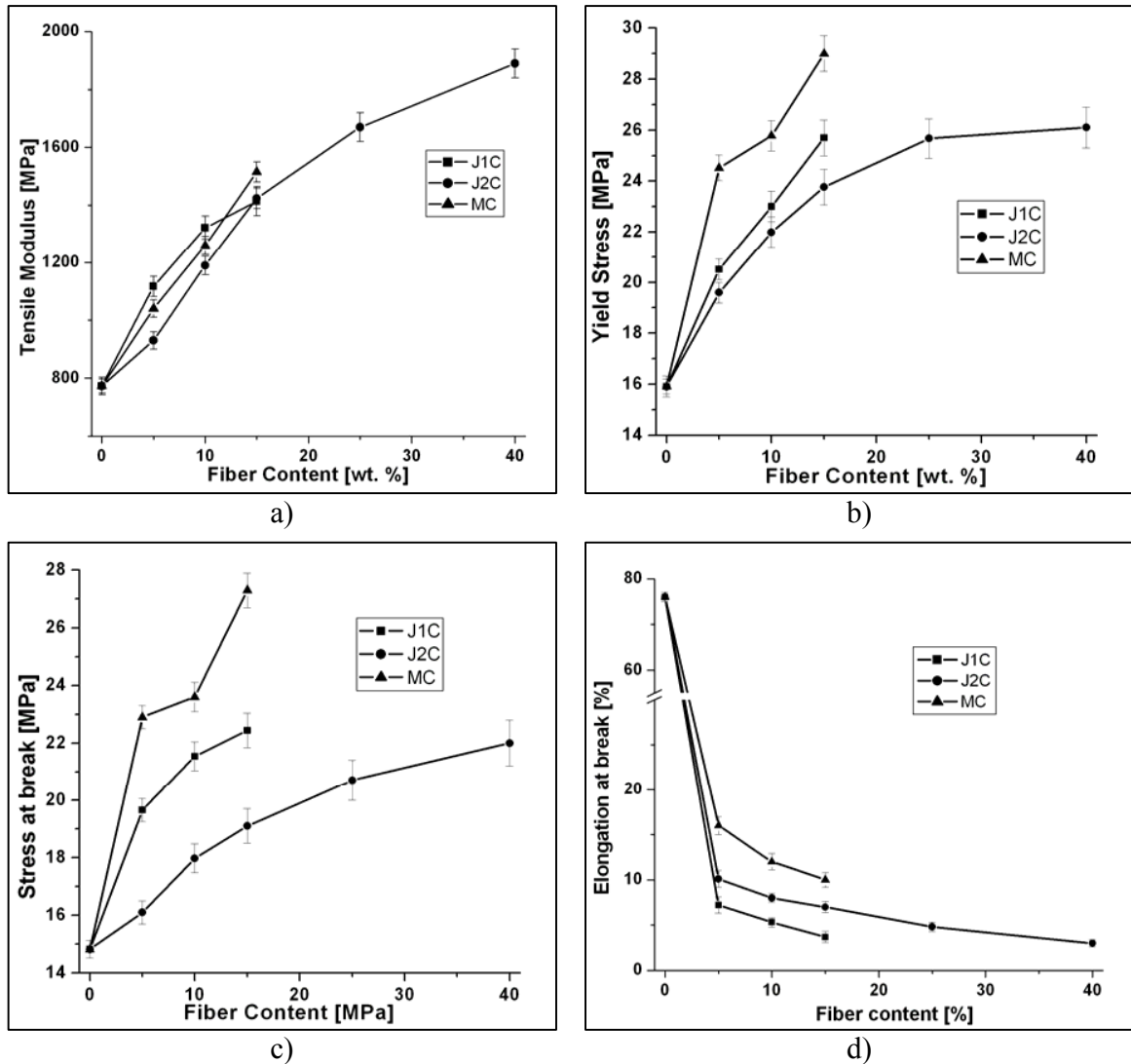


Figure 3.8: Influence of loading of different fibers on a) tensile Modulus, b) yield Stress, c) stress at break and d) elongation [%] at break

The modulus which denotes the stiffness of the material was found to be increased with increasing content of the fibers. Among jute composites (*Figure 3.8a*), J1 composites are relatively stiffer than J2 composites, since J1 is richer in lignin content than J2. The MC composites showed higher modulus than jute composites, though it is less in lignin content.

Chapter 3

This could be attributed to its better dispersion throughout polymer matrix, as being smaller in size than other fibers.

The yield stress which indicates the hardness of the material has been found to be increased with increasing content of the fibers (*Figure 3.8b*). MC composites have shown higher yield stress than other composites. This may be attributed to the better dispersion of microcrystalline powder, as being smaller in size with same amount of compatibilizer. It is well reported³⁰ that better dispersion of smaller size fillers will yield the applied stress in higher extent. Among jute composites, J1 composites were found to show higher yield stress values than J2, since J1 is richer in lignin content which makes the fiber stiff and strong by gumming the microfibrils. The similar behavior can be observed for stress at break, which is the ultimate tensile strength of the composites (*Figure 3.8c*).

The effect of higher lignin content and bigger size was found to be adverse in the other property i.e. elongation (%) at break which is directly related to the toughness of the materials. This could be seen in *Figure 3.8d* where the J1 composites were observed to elongate comparatively lesser. MC composites were found to be stretched out longer. The increasing fiber content also decreases the elongation (%) at break. The increasing fiber size and content with constant ratio of compatibilizer creates the incompatible centers where failure mechanism initiated by causing the local stress in their vicinity to exceed the strength of the sample and the samples break at earlier stages of the tensile tests. Predominantly, the mechanical properties (other than elongation (%)) of the composites were found to be higher than neat ethylene propylene copolymer matrix.

However, the usefulness of the polymeric material in many applications is largely determined by its predominant failure mechanism under the conditions of applications. In the tensile test, the neat polymer films were believed to follow the craze failure mechanism which requires the mobility of molecular chains to absorb more energy while the fiber-reinforced composites could be considered to follow the crack mechanism³¹.

3.3.4. Thermal Stability

Figure 3.9 shows the derivative thermogram of the samples where the thermal stability of the fiber reinforced composites is found to be higher than neat polymer due to heat deflection property of the fibers.

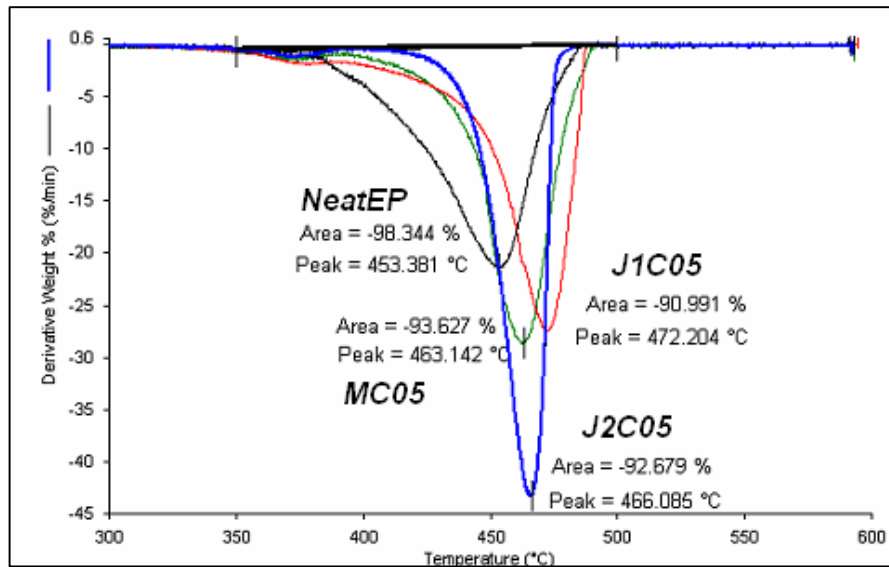


Figure 3.9: Derivative thermogram of the composites with 5% fiber content

The jute fiber-reinforced composites (J1C & J2C) were found to be more stable than commercial cellulose composites and this may be attributed to the presence of aromatic ring based lignin. Antioxidant behavior of lignin in thermal aging was recently supported by Pouteau et al.³² in case of better compatibilization with polyolefin matrix.

3.3.5. Evaluation of Durability / Degradability

3.3.5.1. Photo-irradiation Induced Changes

3.3.5.1.1. FTIR Spectral Changes

It is well documented³³⁻³⁴ that on photo-oxidation, polyolefins generate carbonyl, hydroxyl, hydro-peroxyl groups via radical formation and Norrish type I and type II photochemical reactions and it is conventional technique to focus on the carbonyl and hydroxyl regions by FTIR spectroscopy to follow the photo-oxidation. Though, these

functional groups are already present, the increase in the absorbance can be relatively found in these composites.

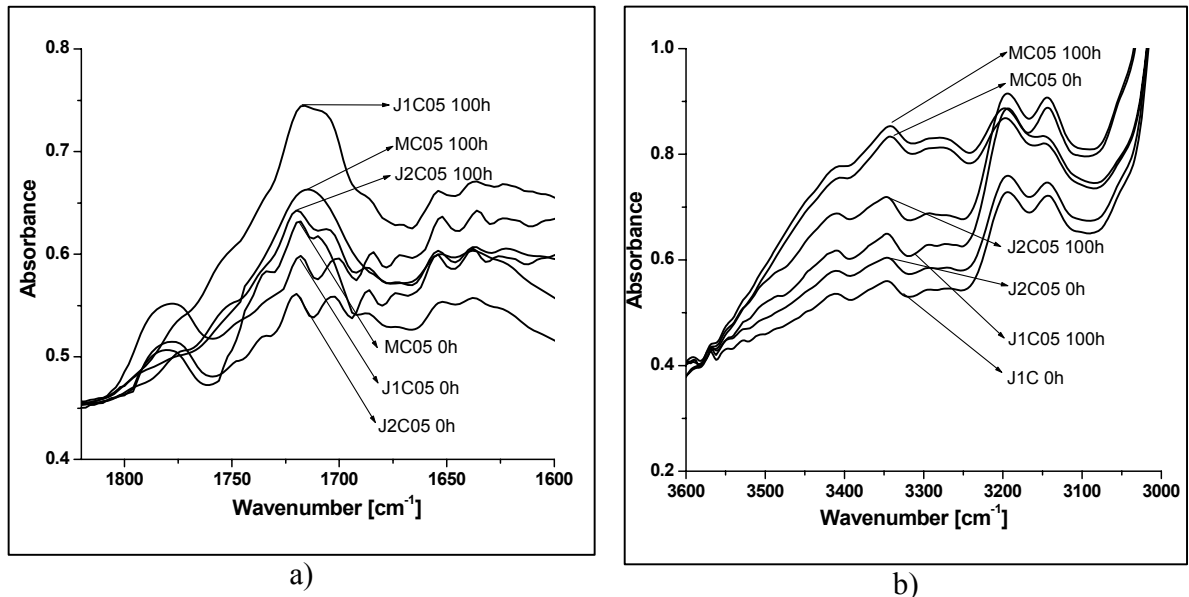


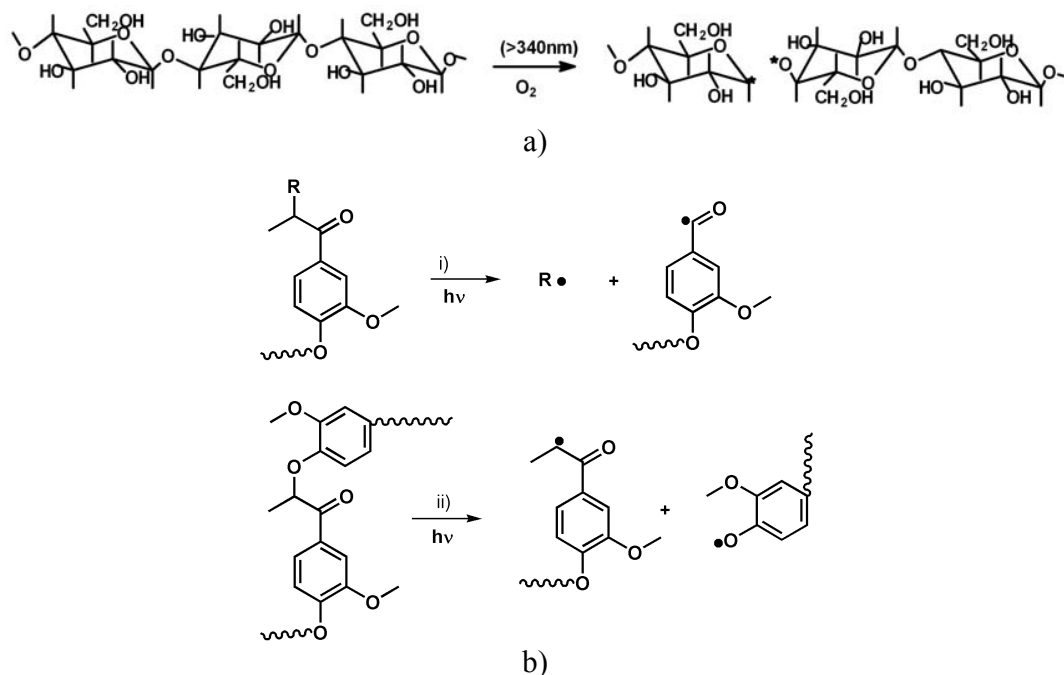
Figure 3.10: FTIR spectra of 100 hrs UV irradiated composites at a) carbonyl region and b) hydroxyl region

Figure 3.10a shows the increase in absorbance of carbonyl region with maximum at 1720 cm⁻¹ in the composites. During photo-irradiation, the decrease in absorption at 1780 cm⁻¹ of cyclic anhydride of MEP, was found after 25 h of UV irradiation and it may be attributed to the ester formation with hydroxyl groups of the fibers. The presence of carbonyl groups of MEP and fibers would sensitize and accelerate the photo-oxidation. The rate of increase in absorption band at 1720 cm⁻¹ was observed higher for J1-composites than other composites. This may be due to the presence of lignin, aromatic ring structures in the fiber that is most sensitive component to the photo-degradation. This fact was supported by recent investigation³⁵ with different kinds of wood fibers. The MC composites which are free of lignin, show lower increase in the absorbance of carbonyl region. The same effect can also be found in hydroxyl region in Figure 3.10b.

The increase in absorption bands at 3500 – 3100 cm⁻¹ was hardly detectable for MC composites whereas, the increase was clearly seen for jute composites. Since the composites are multi-component systems, the separation and characterization of degraded products are difficult and proper mechanism of photo-oxidation of natural fiber reinforced

Chapter 3

composites are yet to be studied. According to Hon et. al.³⁶, pure cellulose is not influenced in vacuo by the irradiation of light longer than 340 nm and cellulose degradation by light is confined to a narrow band of the electromagnetic spectrum. However, in the presence of air (mainly oxygen) and light of wavelengths longer than 340 nm, oxidative degradation of cellulose chains may take place at a slower rate through free radical formation as shown in *Scheme 3.1.a*.



Scheme 3.1: Radical formation on a) cellulose and b) lignin components under UV irradiation^{36,37}

These radicals readily undergo secondary termination reactions e.g. hydrogen abstraction to stabilize themselves in the presence of oxygen and they are transformed rapidly into hydroperoxide radicals to build up hydroperoxide concentration. This rapid oxygenation is further accelerated when the excited oxygen is presented³⁷. Because of structural similarity, hemicelluloses can also follow the similar radical formation mechanism. As seen earlier, lignin which is a predominant light absorber of the fiber has an absorption peak at 280nm with its tail extending to over 400nm. Upon UV irradiation, it absorbs most of the energy and forms radicals as shown in *Scheme 3.1b*. These radicals are capable of accelerating the rate of photo-oxidation. As lignin content of the J1 fiber is higher than that

of the other fibers (Table 3.3), the higher /faster rate of photo-oxidation is observed for the J1 composites. The detrimental effect of the free radical formation in composite materials can be seen as fading (yellowing).

3.3.5.1.2. Color Index

Figure 3.11 shows the yellowness index values upon photo-irradiation.

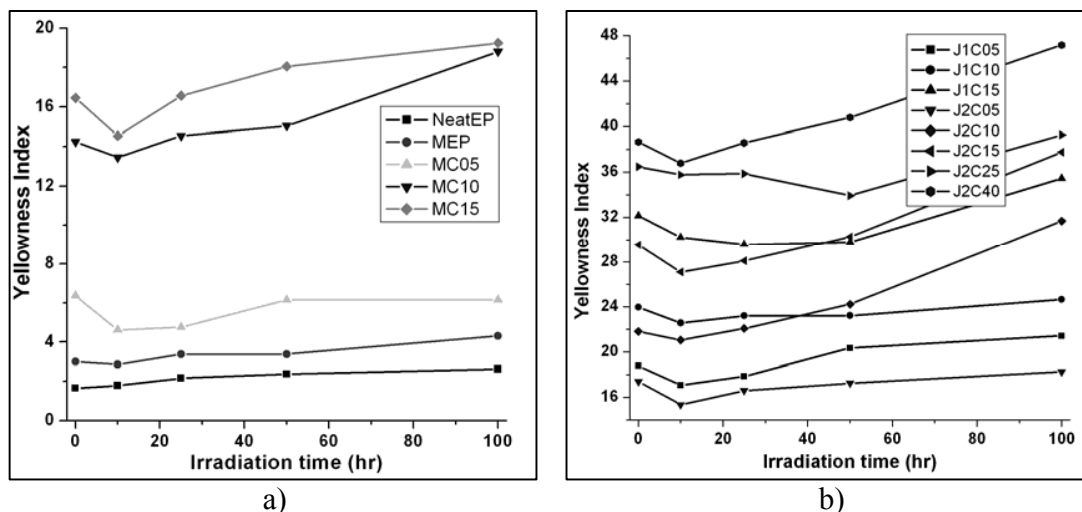
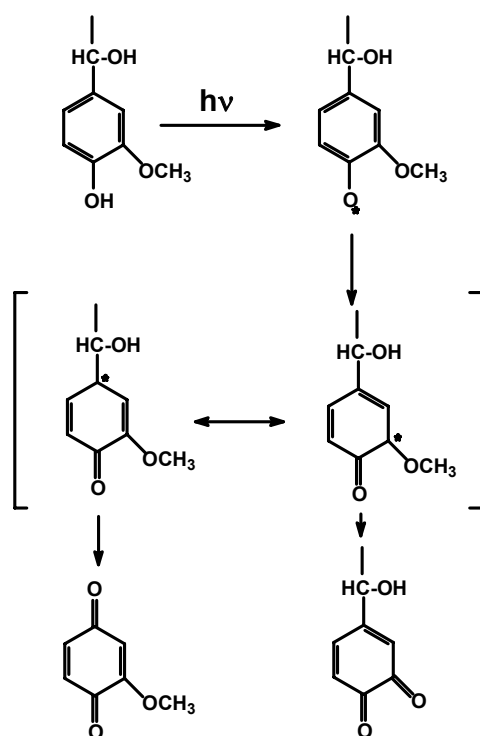


Figure 3.11: Yellowing of samples upon photo-irradiation

The neat polymer (NeatEP) matrix has shown slower fading (in terms of yellowness index) than composite materials. The composites containing alkali treated jute fibers have shown higher yellowness index than microcrystalline cellulose fiber. This can be attributed to the chromophore formation upon photo-irradiation.

The significant contribution to yellowing is expected from lignin component. The formation of radicals is rapid on the lignin component of the fiber. The formed free radical can undergo transformations to form chromophores as shown in Scheme 3.2. It can be observed that the phenolic hydroxyl group is an important source that interacts with light rapidly to produce a phenolic radical, which in turn transforms into *o*- and *p*-quinonoid structures by demethylation or by cleavage of the side chain. These transformations could be attributed for the yellowing in jute fiber composites.



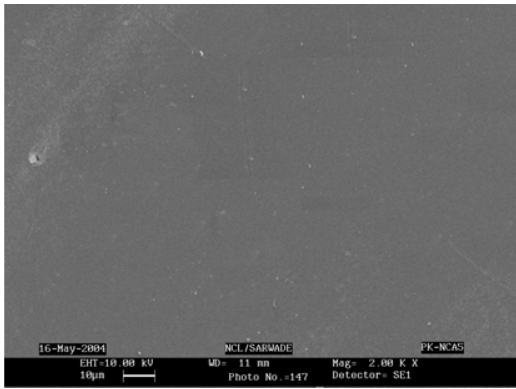
Scheme 3.2: Formation of quinonoid structures upon photo-irradiation ^{36, 37}

3.3.5.1.3. Surface morphological aspects

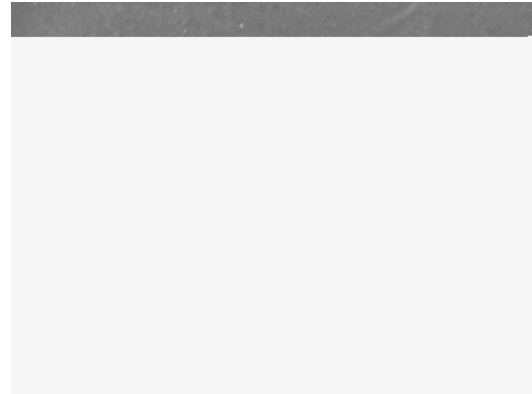
In addition to wavelengths and sensitizers, other factors that are morphology, humidity and wetness have significant effect on free radical formation and degradation rate. *Figure 3.12* shows the surface morphological changes (SEM images) of the unirradiated and (50-150h) photo-irradiated samples. It can be observed that with increasing time of photo-irradiation, the crack formation on the surface of samples increased.

It is obvious that crack formation (amorphous) on the surface may accelerate considerably and the further rate of auto-photo-oxidation, since any kind of degradation (hydrolysis or oxidation) is initiated at amorphous surface of the polymer samples ³⁸.

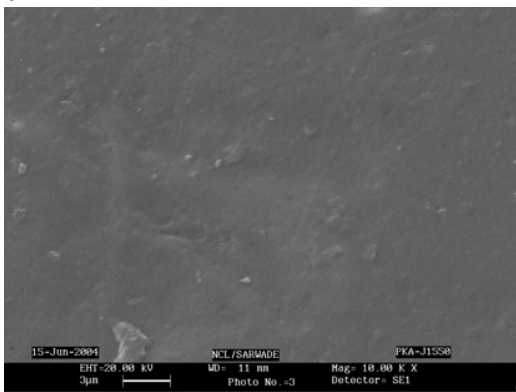
Chapter 3



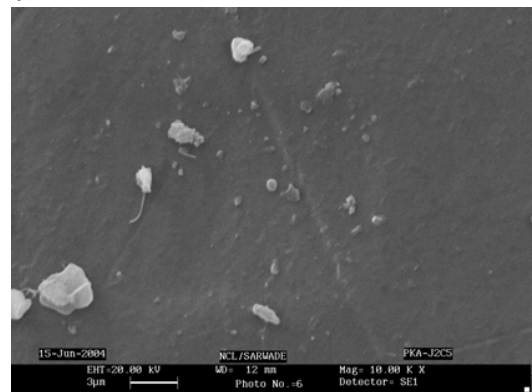
0h



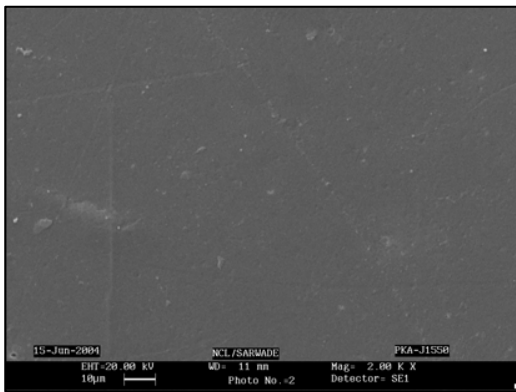
0h



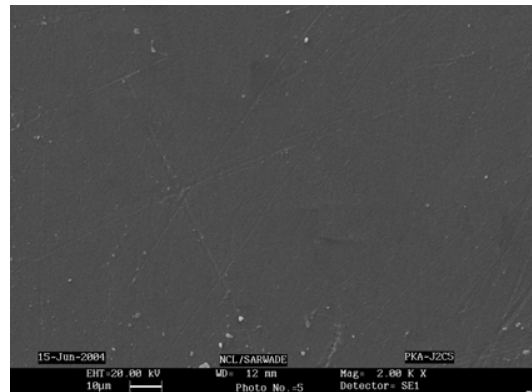
50h



50h



150h

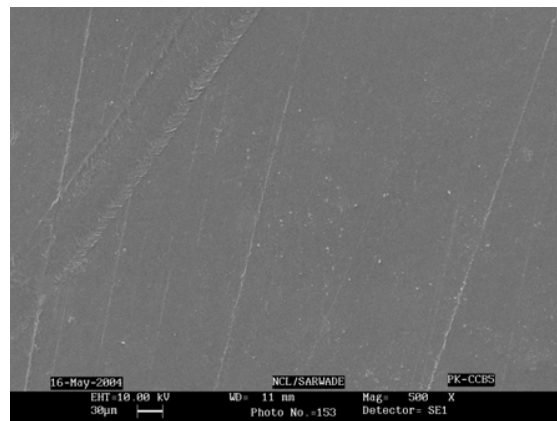


150h

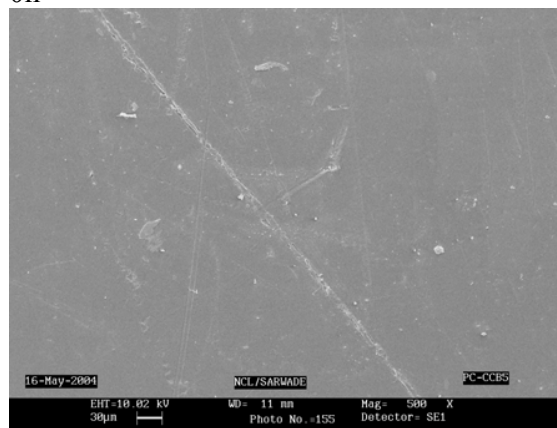
a)

b)

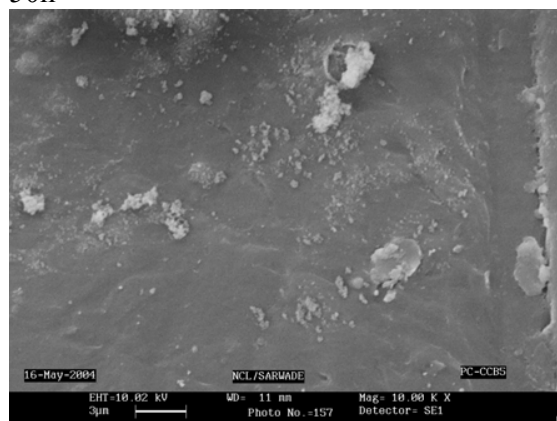
Chapter 3



0h



50h



150h

c)

Figure 3.12: SEM of photo irradiated samples a) J1C05, b) J2C05 and c) MC05

The detrimental effect of photo-irradiation can also be observed on the mechanical properties of these composites also.

3.3.5.1.4. Mechanical Properties

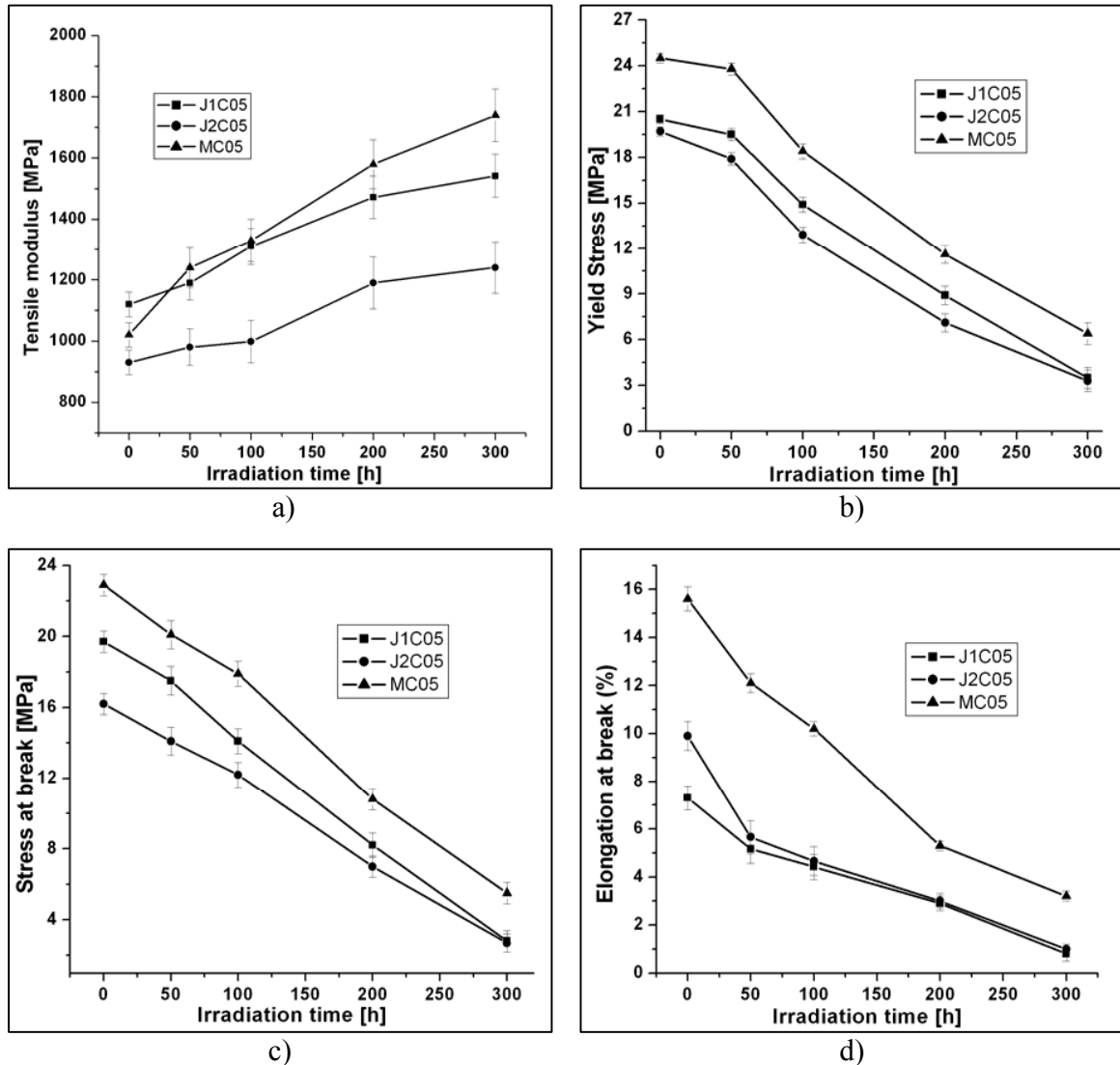


Figure 3.13: Effect of photo-irradiation on the mechanical properties a) Tensile Modulus, b) Yield Stress, c) Stress at break and d) Elongation at break [%] of composites

The ultimate mechanical characteristics (especially elongation at break) of polyolefins are more sensitive to irradiation than the methods reflecting chemical changes³⁹. *Figure 3.13a* shows the increase in tensile modulus but at the same time, the drastic dropping in their strength values which can be seen in *Figure 3.13b* and *3.13c*. *Figure 3.13d* shows the decrease in the elongation (%) at break point. In *Figure 3.13a*, it can be seen that the

Chapter 3

tensile modulus shows wide deviations because of their brittle nature and during photo-irradiation handling photo-irradiated films was little difficult. According to earlier reports³⁹⁻⁴¹, the changes in tensile modulus had not been a vital determinant parameter of mechanical properties due to its inconsistency for neat polyolefin matrix.

On the long duration of irradiation, yield point and break point are found to drop at the same as well as least point. Increase in tensile modulus and decrease in strength values are somewhat peculiar behavior of photo-irradiated films. The changes in the mechanical properties can be explained by two possible structural modes, viz., crosslinking and additional crystallization. Under UV irradiation, the formation of radicals, leads to oxidation products, breaking chain but/and also crosslinking reactions due to radical recombination. It should be noted that photodegradation proceeds preferentially in a comparatively localized region near the initiation site (such as, e.g., photosensitive carbonyl groups, cellulose fiber). Such a localization of the process is a consequence of the low molecular mobility both of the polymer and of the photoactive site in the solid state⁴⁰. This will disfavor the entanglement of polymer chains under applied stress and ultimately reduce the elongation (%) at break. Chemical reasons are also involved here, e.g., the zip mechanism of degradation along the polymer chain. The probability of the occurrence of such degradation sites is higher in the surface layer of the specimen, in particular in the case of polyolefins⁴¹, but such sites may also lie inside the bulk of the material. When the specimen is subjected to mechanical stress, the degraded weak sites act as stress concentrators and crack nuclei.

The overall embrittlement of the material is a result of the formation of cracks which act qualitatively similarly to macroscopic incisions introduced into the test piece. The surface morphological changes i.e. crack formation and chain scission, were also observed to lead to deterioration in elongation (%) at break. The brittle nature is unlike crazing and shear yielding depends on crack failure mechanism while the non-irradiated neat polymer films were observed to follow the craze mechanism⁴². This embrittlement was also found to increase with increasing content and in the order of fibers as J1C>J2C>MC.

3.3.5.2. Composting

Figures 3.14 a-c show the biodegradability of the samples in the composting environment in terms of weight loss (%).

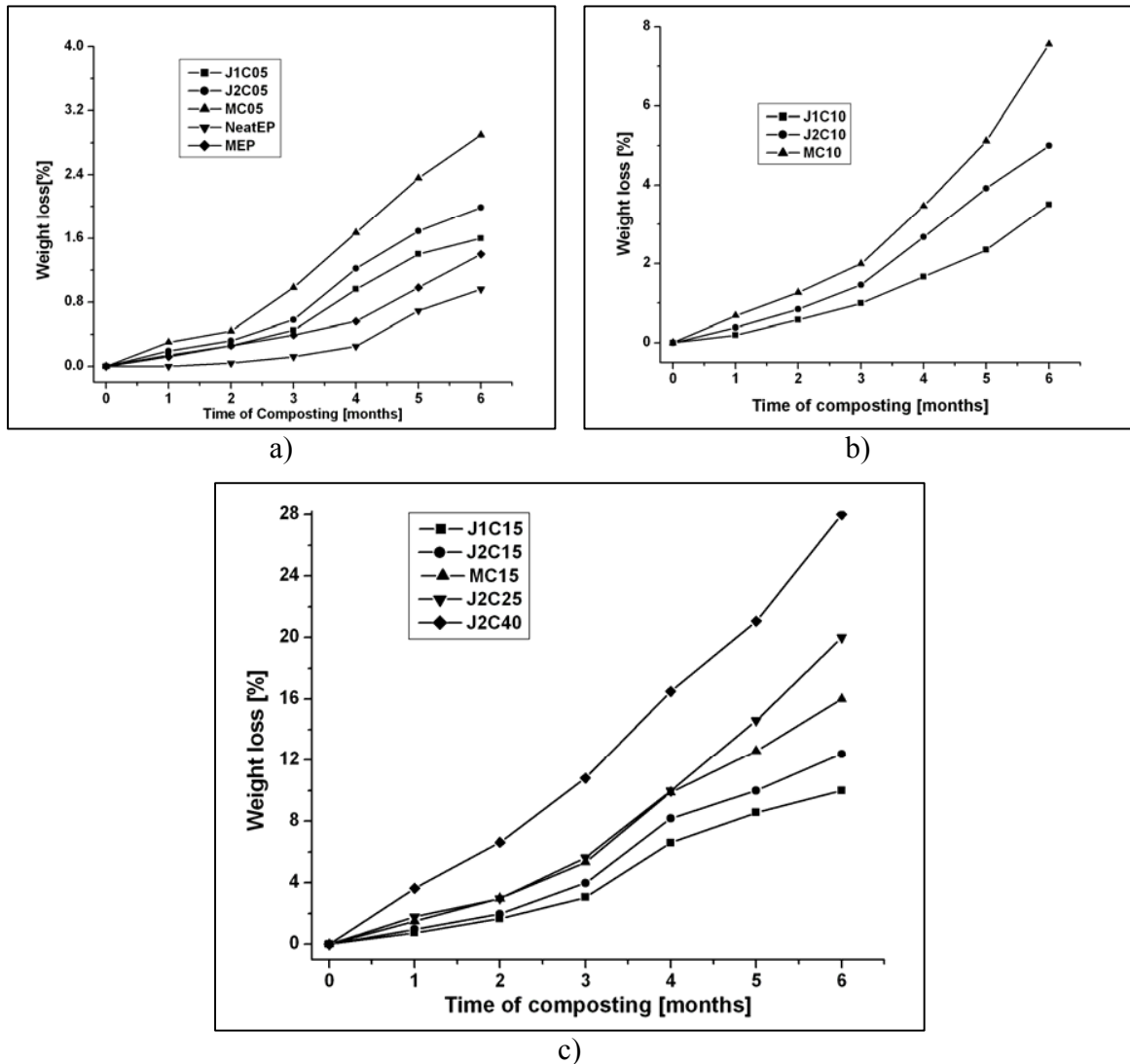


Figure 3.14: Weight loss [%] of the non-irradiated films composites with a) 5% of fibers b) 10% of fibers and c) 15, 25 and 40% of fibers during composting

The non-irradiated films of the composites show higher weight loss than neat polymer and the weight loss was observed to increase with increasing content of the fibers. The

Chapter 3

hydrophilic nature and bio-assimilability of fibers facilitates adhesion of the microorganisms on the surface of the composite films.

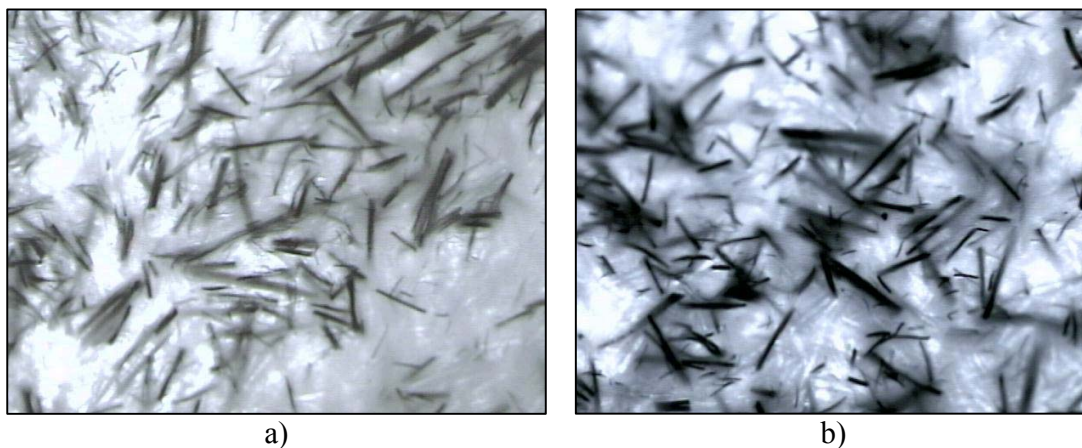


Figure 3.15: Optical micrograph of one month composted samples a) J1C25 and b) J2C25

Figure 3.15 shows the optical micrographs (4x magnification) of the samples after one month of composting, washing and drying, where the microbial colonization can be seen as black spots inside and adjacent to the surface of the films. In earlier time of composting, the weight loss (%) of the composites was found to be low and increased with increasing time. This may be because of initiation time needed for penetration microbes into the matrix. In comparison, the MC composites show relatively higher weight loss than alkali treated fiber composites while the J1 composites show less weight loss. In case of composites where one component degrades faster than other, the weight loss in biotic conditions would mostly be due to degradation of that component. Polymer matrix would remain intact. The loss of fibers from the composites may decrease the mechanical integrity of samples. Therefore, the non-irradiated fiber reinforced composites could not be true biodegradable material, but they can be disintegrated. This disintegration might facilitate the invasion of microorganism but not the complete degradation of the matrix. The difference in results presented here depicted the difference in the bio-accessibility of fibers only. In jute fibers cellulose which is most susceptible to biotic degradation is cross linked (phenolic linkage) with lignin and other extractives. Since the lignin is aromatic based component, it could reduce the bio-accessibility to the cellulose chains⁴³. Therefore, the variation in alkali treatment influences the bio-disintegrability of fibers. According to

Chapter 3

Gharpuray et. al ⁴⁴ and Gossett et al ⁴⁵, the enhancement in bio-accessibility by combined pretreatments in composites of microfibers might be attributed to the enhancement of surface area at which enzymatic hydrolysis would be rapid.

The effect of photo-irradiation on the biodegradation can be seen in *Figure 3.16*, which shows the weight loss (%) values during composting of 50 h photo-irradiated samples.

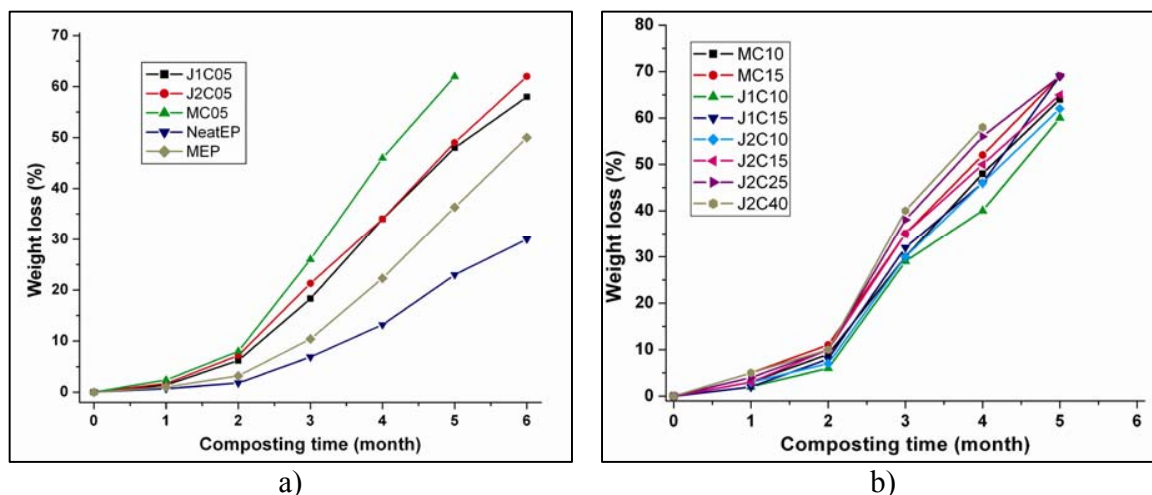


Figure 3.16: Weight loss (%) values during composting of 50 h photo-irradiated samples

It can be observed that the 50h irradiated samples susceptible to microbial degradation than non-irradiated ones. This can be attributed to the functional groups generated on the film surface by photo-oxidative degradation. Similar trend was observed by Pandey et. al. ²⁴⁻²⁶ for the photo-oxidized polyolefin films. As seen as earlier (*Figure 3.12*), the crack formation can also induce the auto-acceleration as well as microbial adhesion on the surface. *Figure 3.17* shows the surface morphology of 50h irradiated and 2 months composted MC05 and J1C05 specimen. The erosion on the surface after microbial attack was found. This can be attributed to bioassimilation of photo-oxidized products on the surface.

Chapter 3

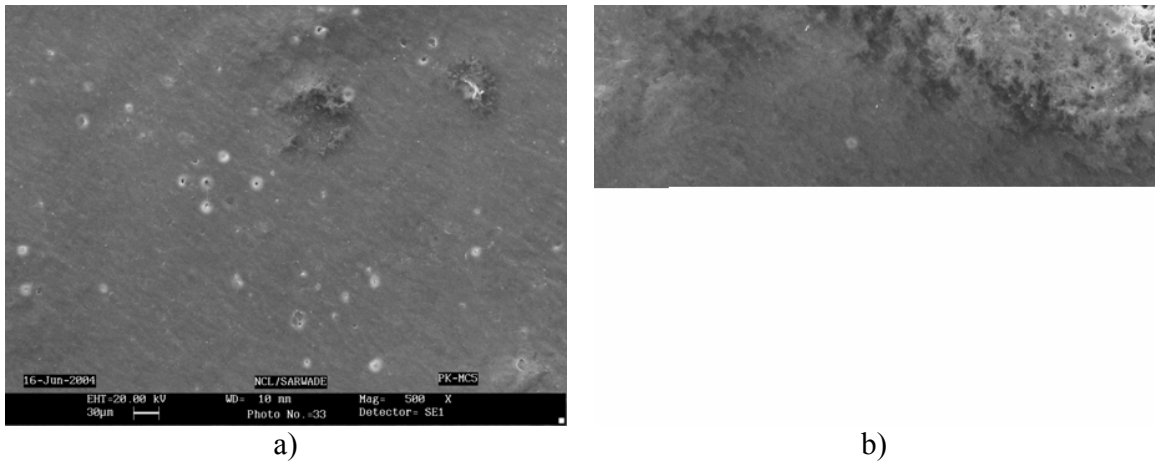


Figure 3.17: SEM images of 50h irradiated and 2 month composted specimen of a)MC05 and b) J1C05

The crack formation on the surface and photo-degraded products in the films facilitate the adhesion and penetration microorganisms into the matrix. In comparison of non-irradiated samples, it can be understood that though the biodegradable additive (like cellulose) present in the system, pre-treatment like photo-oxidation is very important for acceptable level of biodegradation. Therefore, it will become convenient to choose the pathways for disposal of commodities based on the fiber-reinforced composites.

Based on our overall observation of the above results and discussion, the trend in various properties of prepared composites was represented in *Table 3.4*.

Table 3.4: Trends in properties of composites

Property	Order
Mechanical properties -I (Tensile Modulus and strength)	MC > J1C > J2C > NeatEP
Mechanical properties - II (Elongation % at break)	NeatEP > MC > J2C > J1C
Thermal Stability (Maximum decomposition temperature of host matrix)	J1C > J2C > MC > NeatEP
Photo-resistance	NeatEP > MC > J2C > J1C
Bio-accessibility	NeatEP < J1C < J2C < MC

3.4. Conclusion

The material properties such as mechanical and thermal properties, durability/degradability of the fiber-reinforced composites depend on their chemical constituents and preparation methods. The quality of fiber was generally influenced by the kinds of treatments. Based on the present investigation, it is found that the variations in treatments on the natural fibers have influenced the performance and durability of their composites. The composites prepared from the jute fiber which was treated with low concentrated alkaline solution, have shown improved mechanical properties and thermal stability. They also have exhibited lower photo-resistance and bioaccessibility / bio-disintegrability. This may be due to the presence of lignin, which is cross-linked with cellulose chains. The composites based on the jute fiber that was treated with alkaline solution of higher concentration have relatively shown higher photo-resistance and bio-accessibility than earlier composites, but their mechanical properties like modulus and strength have been affected. Microcrystalline cellulose reinforced composites have exhibited much improved mechanical properties due to their better dispersion as being smaller in size than other two fibers. But they have shown lower thermal stability than others. In comparison of composites, microcrystalline cellulose reinforced composites have shown higher photo-resistance as well as bio-accessibility. The weight loss values after photo-irradiation suggest that for the polyolefins - natural fiber composites, pre-treatment like photo-oxidation is very important for acceptable level of biodegradation. Finally, it can be concluded that for various applications of natural fiber reinforced composites, the treatments on the fiber have to be optimized depending on their durability requirement.

References

1. Joly, C.; Kofman, M.; Gauthier, R. *J. Macromol. Sci. Part A Pure Appl. Chem.* **1996**, *A33*, 1981.
2. Zadorecki, P.; Michell, A. J. *Polym. Compos.* **1989**, *10*, 69.
3. Beshay, A.D.; Hoa, S.V. *Sci. Engg. Compos. Mater.* **1992**, *2*, 86.
4. Bledzki, A.K.; Gassan, J. *Prog. Polym. Sci.* **1999**, *24*, 221.
5. Felix, J. M.; Gatenholm, P. *J. Appl. Polym. Sci.* **1991**, *42*, 609.
6. Woodhams, R.T.; Thomas, G.; Rogers, D.K. *Polym. Engg. Sci.* **1984**, *24*, 1160.
7. Bataille, P.; Richard, L.; Sapiha, S. *Polym. Compos.* **1989**, *10*, 103.
8. Joly, C.; Kofman, M.; Gauthier, R. *Comp. Sci. Technol.* **1996**, *56*, 76.
9. Amash, A.; Zugenmaier, P. *Polym. Bulletin.* **1998**, *40*, 25.
10. Rodriguez, C.A.; Medina, J.A.; Reinecke, H. *J. Appl. Polym. Sci.* **2003**, *90*, 3466.
11. Nevell, T.P.; Zeronian, S.H. *Cellulose chemistry and its applications.* **1985.**, Wiley, New York,
12. Safonov, V.V. *Treatment of textile materials.* Legprombitizdat, Moscow, **1991**.
13. Lai, Y. Z.; Sarkanen, K.V. *Cellul. Chem. Technol.* **1967**, *1*, 517.
14. Gentile, V.M.; Schroeder, L. R.; Attalla, R. H. *The structure of Cellulose* in ACS Symp. Ser. No. 340, ed., Attalla, R.H. **1987**, Amer. Chem. Soc., Washington. DC, 272.
15. Fink, H.P.; Ganster, J.; Fraatz, J. Akzo-Nobel viskose chemistry seminar challenges in cellulosic man-made fibres. Stockholm, 30 May–3 June 1994.
16. Hermans, P.H. *Physics and Chemistry of Cellulose fibers*, **1949**, Elsevier, 257.
17. Roy, S.C.; Das, S. *J. Appl. Polym. Sci.* **1965**, *9*, 3437.
18. Roy, S.C. *J. Appl. Polym. Sci.* **1962**, *6*, 541.
19. Rowel, R. M. in *Proceedings of the 3rd international conference on frontiers of polymers and advanced materials: January 16-20, Kuala Lumpur, Malaysia*, eds. Mark P.N.; James E.; Loo F. T., **1995**, Plenum Press, New York, 659.
20. Gassan, J.; Bledzki, A. K. *Die Angew Makromol Chem*, 1996, 236, 129.
21. Belgacem, M. N.; Bataille, P.; Sapiha, S. *J. Appl. Polym. Sci.* **1994**, *53*, 379.
22. TAPPI method T222 om-88, TAPPI press, Atlanta, GA, **1988**
23. Billmeyer, F.W.; Sultzman. *Principles of colour Technol.* Interscience, New York **1966**, 38.
24. Pandey, J.K.; Singh, R.P. *Biomacromol.* **2001**, *2*, 881.
25. Pandey, J.K.; Kumar, A.P.; Singh, R.P. *Macromol. Symp.* **2003**, *197*, 411.
26. Pandey, J.K.; Ahmed, A.; Singh, R.P. *J. Appl. Polym. Sci.* **2003**, *90*, 1009.
27. a) Eldsater C; Karlsson S; Albertsson A C. *Polym. Degrd. Stab.* **1999**, *64*, 177, b) Grima S, Bellon-Maurel V, Feuilloley P, Silvestre F, *J Polym Environ* **2000**, *8*, 183
28. Noorstrom H., *Sven. Papperstidn.*, **1969**, *72*, 25
29. a) Hon D.N.-S., *J. Polym Sci. Polym Chem Ed.*, **1975**, *13*, 1347 b) Bos A.. *J. Appl. Polym. Sci* **1972**, *16*: 2567
30. Fung, K.L.; Li, R. K. Y.; Tjong, S. C. *J. Appl. Polym. Sci.* **2002**, *85*, 169.
31. Kramer, E.J. *Adv. Polym. Sci.* **1983**, *52/53*, 1.
32. Pouteau, C.; Dole, P.; Cathala, B.; Averous, L.; Boquillon, N. *Polym. Degrad. Stab.* **2003**, *81*, 9.

Chapter 3

33. a) Singh, R.P.; Singh, A. *J. Macromol. Sci. – Chem.* **1991**, *A28*, 487., b) Singh, R.P.; Sivaram, S. *Adv. Polym. Sci.* **1991**, *101*, 169.
34. Wiwik, S.; Subowo, M.; Barmawi, Liang, O. B. *J. Polym. Sci. Part A: Polym. Chem.* **1986**, *24*, 1351.
35. Colom, X.; Carrillo, F.; Nogues, F.; Garriga, P. *Polym. Deg. Stab.* **2003**, *80*, 543.
36. Hon, D.N.-S. *J. Macromol. Sci. –Chem.* **1976**, *A10*, 1175.
37. Hon, D.N.-S. *J. Polym.Sci. Polym.Chem. Ed.* **1979**, *17*, 441.
38. Scott, G. *Atmospheric Oxidation and Antioxidants*, 272, 1st edn, Elsevier. **1965**.
39. Pabiot, J.; Verdu, J. *Polym. Eng. Sci.* **1981**, *21*, 32.
40. Naddeo, C.; Guadagno, L.; Luca, S. D.; Vittoria, V.; Camino, G. *Polym. Deg. Stab.* **2001**, *72*, 239.
41. Raab, M.; Kotulak, L.; Kolarik, J.; Pospisil, J. *J. Appl. Polym. Sci.* **1982**, *27*, 2457.
42. Bicerano, J. *Prediction of polymer properties* (3rd edn.) Marcel Dekker Inc. New York. **2002**.
43. Veeken, A. H. M.; Adani, F.; Nierop, K. G. J.; de Pater, P. A.; Hamelers, H. V. M. *J. Environ. Qual.* **2001**, *30*, 1675.
44. Gharpuray, M. M.; Lee, Y. -H.; Fan, L. T. *Biotechnology and Bioengineering.* **1983**, *25*, 157.
45. Gossett, J.M.; Healy, J.B.; Jr Owen, W. F.; Stuckey, D. C.; Young, L. Y.; McCarty, P. L. *Heat Treatment of Refuse for Increasing Anaerobic Biodegradability. Final Report. ERDA/NST/7940-7612.* **1976**. National Technical Information Service, Springfield, VA.

**Effect of Nano-Clay Reinforcement on the Properties and
Durability of Cellulose - Reinforced Composites***

* *J. Appl. Polym. Sci.*, **2007**; 104(4): 2672-2682

4.1. Introduction

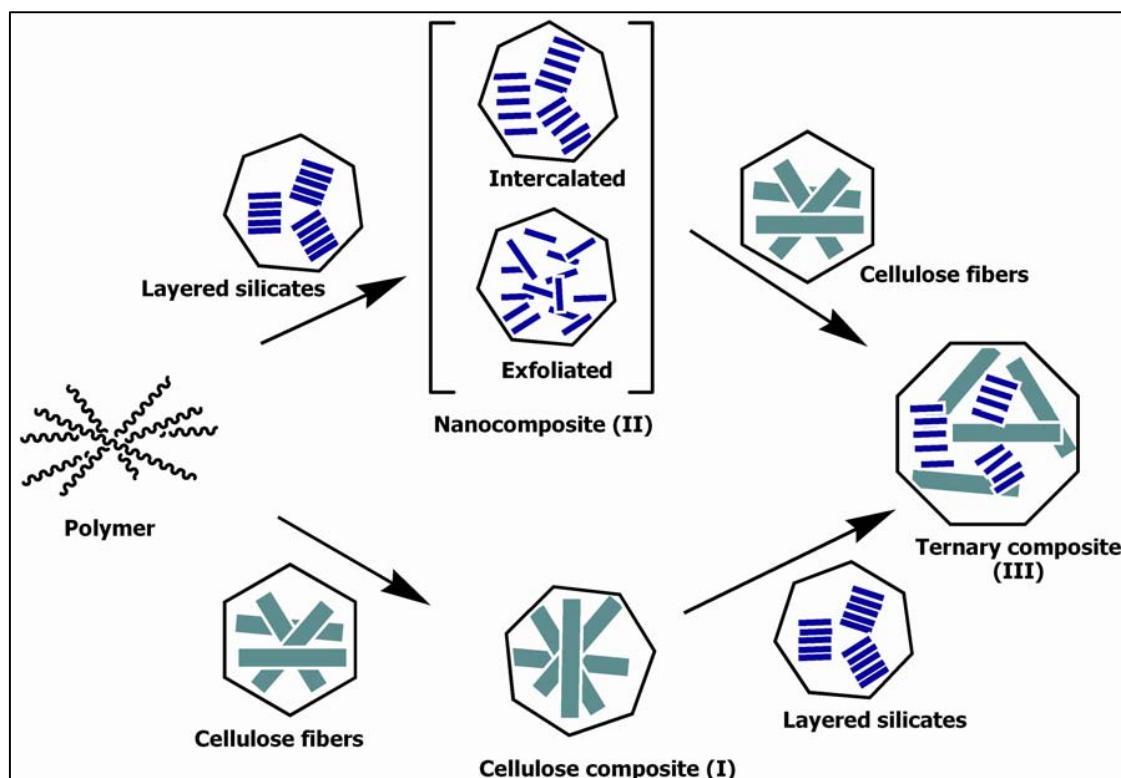
There is currently a wide revival of interest in the use of biopolymers for applications in which synthetic polymers have traditionally been the material of choice. Conventional plastics are persistent in the environment and every plastic material disposed improperly is a significant source of environmental pollution, which potentially harms wild life.¹ Bio-based materials have received considerable attention in the past two decades as eco-friendly materials and natural fiber reinforced composites have been utilized in many applications for last few decades. In natural fibers, cellulose which is a linear condensation polymer consisting of D-anhydroglucopyranose units (AGU) linked together by β 1,4-glycoside bond, is major component and other components are lignin, hemicelluloses and water soluble sugars. Conventionally, the composites are made by incorporating natural fibers during processing of the resin in the case of thermoplastics and during polymerization / curing in the case of thermosets. In general, the short fibers (4-10 mm) are utilized as reinforcement to reduce the difficulties during conventional processing conditions and for uniform dispersion throughout the matrix. In recent years, the consumption of these composites has been skyrocketed not only for environmental concerns but also for yielding a unique combination of high performance, great versatility and processing advantages at favorable cost.²⁻³ The dramatic improvement by fiber (type) reinforcement is found in dimensional stability.⁴⁻⁶ The improvement in material properties of the natural-fiber reinforced composites are mostly influenced by the orientation and dispersion of the fiber through out the matrix, individual quality of the fibers and ultimately the quality of interface.⁷ In comparison to glass-fibres, the lower thermal stability of natural-fibres with up to 230°C, limits the number of thermoplastics to be considered as matrix material for natural fibre thermoplastic composites. Only those thermoplastics are useable for natural fibre reinforced composites, whose processing temperature does not exceed 230°C for example, polyolefins⁸. Thus, in the present study, for preparation of composites polyolefins thermoplastics have been chosen. Over the past 50 years in plastic industry, the success of plastics (esp. polyolefins) based on petroleum resources can be attributed not only to the reliable raw materials basis, but also to their versatile applications (packaging and biomedical devices) and to their melt-processability⁹. For structural applications like construction, automotive industry and aerospace, the

Chapter 4

mechanical and thermal properties of these commodity plastics have to be still improved¹⁰. The specific properties of natural fibers, namely low cost, lightweight, renewable character, high specific strength and modulus, availability in a variety of forms throughout the world, reactive surface and the possibility to generate energy, without residue, after burning at the end of their life-cycle, motivate their association with these polymers to elaborate composite materials¹¹⁻¹³. Since there is an incompatibility between the hydrophilic (polar) polysaccharides and hydrophobic (non polar) polymer matrix, compatibilization is typically done by some physical methods and chemical methods such as change of the surface energy, impregnation, coatings, coupling agents and graft copolymerization^{8, 14}. Among many other additives used for this purpose, grafting of maleic anhydride / maleation of polymer matrix has been found to be very efficient in improving the filler dispersion and the compatibility in polypropylene-cellulose composites.^{2, 7, 8, 15}

On the other hand, in last decade, reinforcement of nano-scale fillers has been found to improve the physical, thermal and mechanical properties of the obtained composites with very low amount of loading. The polymer-layered silicate (PLS) based nanocomposites have received a great deal of interest from researchers from both the scientific and industrial filed. The insertion of polymer chains in the clay platelets which are in the nanometer scale often results in nanocomposites, which exhibit enhanced properties such as improved mechanical properties, heat stability, flame retardancy and gas barrier properties at very low filler content usually less than 5%.¹⁸⁻²¹ The improved properties are presumably due to the synergistic effect of the nano-scale structure (high aspect ratio) and the maximized interactions (unique characteristics such as intercalation / exfoliation) between the filler and polymer molecule. These layered silicates have attracted great attention of researchers because of their low cost, abundance and high aspect ratio, which give greater possibility of energy transfer from one phase to another.²²⁻²⁴ Many attempts are being made to improve the properties of commodity polymers such as polyethylene and polypropylene by nano-clay reinforcement.²⁵⁻²⁹ In this system too, the observed problem is incompatibility between polymer (nonpolar) matrix and clay (polar), and thus compatibilization by modifying clay surface, functionalizing polymers and use of compatibilizers is essentially done.³⁰ Considering the dimensional stability from the fiber

type reinforcement and the toughness, barrier properties, thermal stability, multidirectional stress transfer (as advantage) from the platelet type reinforcement, in the present work, both the strategies for reinforcing the synthetic polymers are combined to reinforce the thermoplastics. Three types of composites can be prepared employing the preparation strategy as represented in *Scheme 4.1*.



Scheme 4.1: Schematic representation of three types of composites

These polyolefin polymers have been found to undergo by photo-oxidation³¹⁻³², photo-induced biodegradation³³ and in natural and accelerated composting³⁴. Then, very few studies were made on the biodegradation of cellulose fiber-reinforced composites in different ways such as in aqueous media³⁵, in terrestrial environment³⁶ and in composting³⁷. Thus it is worthwhile to study the degradability / durability of these three types of composites and to rationalize the effect of nanoclay on the properties and durability of composites in different environmental conditions like accelerated weathering and composting.

4.2. Experimental

4.2.1. Materials

The linear low-density polyethylene (LLDPE) with melt-flow index (MFI) about 2.0 g / 10 min and density (ρ) about 0.91 g/cm³ and polypropylene with MFI~ 2.0 g / 10 min were obtained from M/s. Reliance Industries Ltd, Mumbai, India. The EP copolymer containing ethylene 15.1% molar content with MFI about 3.5 g / 10 min and ρ about 0.9 g/cm³ was obtained from M/s Montell Ferrara, Italia. The polymers were purified by dissolving in xylene, precipitating in cold methanol and drying in vacuum oven at 50 °C for 10 to 12 h to obtain 'additive free' samples. Maleic anhydride and benzoyl peroxide were obtained from M/s. Sd.Fine Chemicals Ltd. Baroda, India. Cloisite® 20A (natural montmorillonite modified with dimethyl dihydrogenatedtallow quaternary ammonium cation) was from M/s. Southern Clay Products, Inc. USA. The solvents were used as obtained from M/s. Sd. Fine Chemicals, India. Microcrystalline cellulose fiber was obtained from M/s. Loba chemicals, India.

4.2.2. Maleation of Polymers

The neat polymers were functionalized by maleic anhydride grafting or maleation method. The vacuum oven dried (at 50°C for 10 h) 'additive free' polymers were melt-mixed in a Brabender (Plasticorder – 487106) with benzoyl peroxide (0.15 wt%) and maleic anhydride (5 wt%) for 3 min. Melt-compounding was done for LLDPE (NeatPE), polypropylene (NeatPP) and ethylene propylene copolymer (NeatEP) at 120 °C, 180 °C and 170 °C, respectively. The obtained crude product was purified by dissolving in xylene, precipitating in cold acetone and

4.2.3. Preparation of Composites

The processing temperature for LLDPE (NeatPE), polypropylene (NeatPP) and ethylene-propylene copolymer (NeatEP) was around 150 °C, 180-190 °C and 170-175 °C, respectively, for all type of composites. The first type of composites [I] have been prepared by melt-mixing of neat polymers and maleated polymer in Brabender chamber with 70 rpm for 1 min and then with cellulose (5 – 15 wt%) for another 3 min. The composition of neat polymer / maleated polymer was maintained at 60/40 in all type of composites. The second

Chapter 4

type of composite [II] was obtained by melt-mixing neat polymer and maleated polymer in the Brabender with 70 rpm for 1 min and then with 5 wt% of the clay (MMT20A) for another 3 min. The third type of composites [III] was prepared by following the same experimental conditions used for II. Subsequently after 2 min. of the addition of clay (MMT20A), cellulose fibers (5 - 15 wt%) were added and allowed to mix for another 3 min. The formulations were given using acronyms in the following order matrix-type of composite-weight percentage of fiber (clay content for NC05). For example, the samples containing 5 wt. % cellulose fiber in polyethylene matrix, is coined as PE-CC05. These composites were molded into films using a hydraulic Carver press by pressing in between two electrically preheated plates (up to 160, 200 and 180 °C for PE, PP and EP samples) covered with aluminium foil for 2 min, keeping the pressure about ~15,000 pounds and quench-cooling to room temperature (27°C) for 1 min under pressure. The obtained films were observed to have thickness about $100 \pm 10 \mu\text{m}$. These films were utilized for further measurements.

4.2.4. Characterization

4.2.4.1. FTIR Spectroscopy

The functional group changes of the samples (as films) were followed using Perkin Elmer 16 PC FTIR spectrophotometer. The samples were scanned in the range of $4000 - 400 \text{ cm}^{-1}$ at a resolution of 4 cm^{-1} . A total of 10 scans were used for signal averaging.

4.2.4.2. Mechanical Properties Measurements

The films were cut according to IS: 2508-1984:A4 for tensile property investigations. The static tensile behavior of these specimens was investigated at room temperature ($27 \pm 2^\circ\text{C}$) and $65 \pm 5 \%$ relative humidity using a Universal Testing Machine (Instron model 4204) at crosshead speed at 10 mm/min.

4.2.4.3. Thermal Analysis

The films were cut and used for thermal analysis. The sample weight was about 5 mg. The melting behavior of the samples was analyzed by using Perkin Elmer DSC-7. The samples were scanned from -30°C to 300°C at the heating rate of $10^\circ\text{C}/\text{min}$ and held for 1 min at

Chapter 4

300°C and then cooled to 25°C with the same rate. For measuring the thermal stability, the samples were heated using Perkin Elmer TGA-7 from 30°C to 900°C with a heating rate of 10 °C/min under nitrogen atmosphere with flow rate of 20 ml/min.

4.2.4.4. X-ray Diffraction Measurements

The wide-angle X-ray diffraction (WAXD) patterns of the film samples were obtained using a Rigaku (Japan) Dmax 2500 X-ray diffractometer with Cu-K α radiation. The system consists of a rotating anode generator with a copper target and a wide-angle powder goniometer having a diffracted beam graphite monochromator. The generator was operated at 40 kV and 150 mA. All the experiments were performed in the reflection mode. The samples were scanned between $2\theta = 2$ to 30° at a scan speed of $2^\circ/\text{min}$. The d spacing was calculated by Bragg's formula where the λ was 0.154 nm.

4.2.4.5. Microscopic Measurements

The dimensions of fibers were determined by using optical microscope (Olympus, Model Bx50 F4, Japan) with $\times 50$ magnification. The diameter of the cellulose fibers was $14.8 \pm 0.2 \mu\text{m}$ and the length was $38.8 \pm 0.2 \mu\text{m}$. Surface morphology of samples were examined by staining the samples with osmium tetroxide, drying under vacuum at 50°C for 24h and scanning under electron microscope (Leica Cambridge Stereoscan 440 model). To clarify the nanoscale structure, transmission electron microscopic (TEM) image was obtained by TEM 2000 EX-II instrument (JEOL, Tokyo, Japan) operated at an accelerating voltage of 100 kV to observe the nanoscale morphology. All the ultrathin sections were microtomed using a Super NOVA instrument (M/s Leica, Switzerland) with a diamond knife and then subjected to TEM without staining.

4.2.4.6. Water Absorption

The test specimens were cut according to ASTM D570, placed in a vacuum oven at 80°C for 24 h and then cooled in a dessicator. Immediately after cooling, the specimens were weighed using Precisa 205 A SCS, Switzerland with 0.0001 g accuracy and this was considered as the initial weight (W_0). All the specimens were submerged in deionized water for 24 h at $25 \pm 0.2^\circ\text{C}$. The specimens were removed after 24 h and immediately

Chapter 4

wiped with dry clean cotton cloth (to remove water on the surface of the films). Their weights were recorded as final weight (W_1).

$$\left. \begin{array}{l} \text{Water} \\ \text{absorption} \end{array} \right\} (\%) = \left[\frac{\text{Weight of sample after immersion } (W_1) - \text{Weight of sample before immersion } (W_0)}{\text{Weight of sample before immersion } (W_0)} \right] \times 100$$

4.2.5. Durability evaluation

4.2.5.1. Photo-degradation

The specimens were irradiated (≥ 290 nm) in a polychromatic irradiation chamber (SEPAP 12/24 M/s. Material Physico Chimique, Neuilly, Marne, France) at 60 °C under air. It consists of four (400W) medium-pressure mercury vapor lamps supplying radiation longer than 290 nm²⁴⁻²⁶. The photo-degradation was monitored by changes in functional groups and mechanical properties.

4.2.5.2. Biodegradation: Composting Method

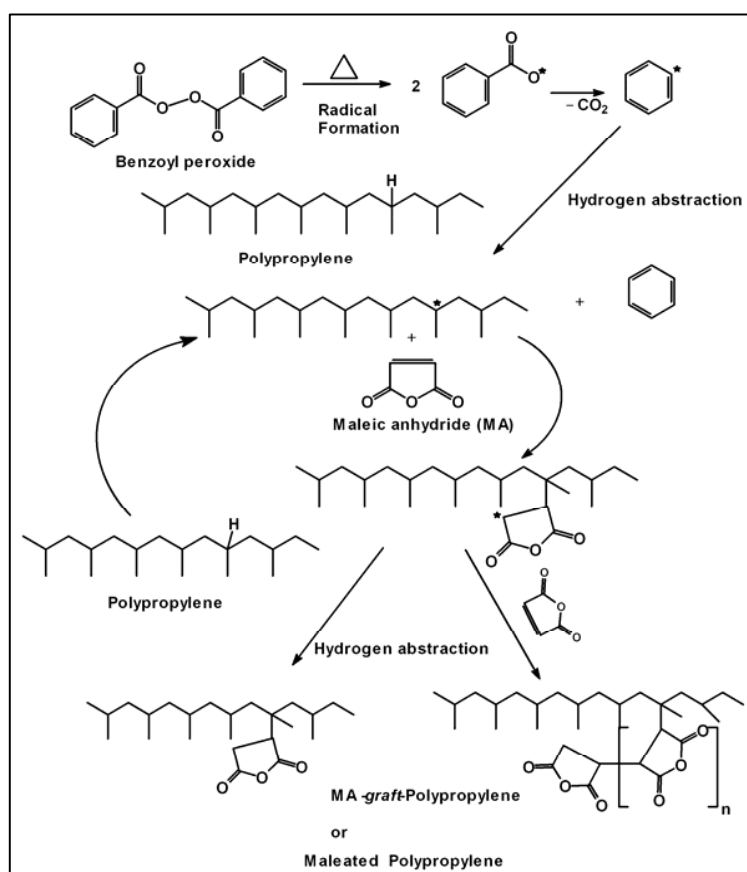
The compostability tests of 4 x 4 cm² specimens were done in a laboratory-scale composting bin. The constitution of solid waste mixture (compost) used for biodegradability testing of samples was as follows (in dry weight): 40.8% shredded leaves, 11.4% cow manure/dung, 15.8% newspaper and computer paper, 2% white bread, 7.8% sawdust, 19.2% food waste (dry milk, potato, carrot, banana, and other vegetables), and 3.0% urea. The total dry solid content of compost was 50-60 %. The compost bin was covered with green grass and moisture content was maintained by spraying water periodically. To avoid anaerobic conditions, the bin was constantly aerated with oxygen through a hollow tube. Through out the study, the carbon/nitrogen (C/N) ratio was measured by elemental microanalysis of dry solid to follow the quality of compost. It was observed to be ~ 10/1 to 30/1. The temperature of compost was observed to be slightly higher (up to 42 ±1 °C) than that of atmosphere (35 ±1) °C. Compostability was measured in terms of weight loss (%), which is calculated using the following formula:

$$\text{Weight Loss } (\%) = [(\text{Initial weight (g)} - \text{Final weight (g)}) / \text{Initial weight (g)}] \times 100$$

4.3. Results and Discussion

4.3.1. Characterization

Maleation of polymers is schematically represented in *Scheme 4.2* using polypropylene as an example, which is in higher content in the sample used for this study. The mechanism which has been represented, involves three steps; i) radical formation from initiator, macromolecular radical formation (by hydrogen abstraction from polymer), ii) addition of maleic anhydride to yield polymer-chain-substituted succinic anhydride radical which leads to further propagation steps and iii) termination via various processes such as radical recombination and / or disproportionation.²⁸ During grafting the polyolefins, the product is the major part.^{38, 39}



Scheme 4.2: General reaction mechanism of maleic anhydride grafting on a polyolefin PP

Thus, it is essential to analyze the changes at carbonyl group region³⁸⁻³⁹.

Chapter 4

Figure 4.1 shows the FTIR spectra of neat polymer matrices, maleated polymer and their composites.

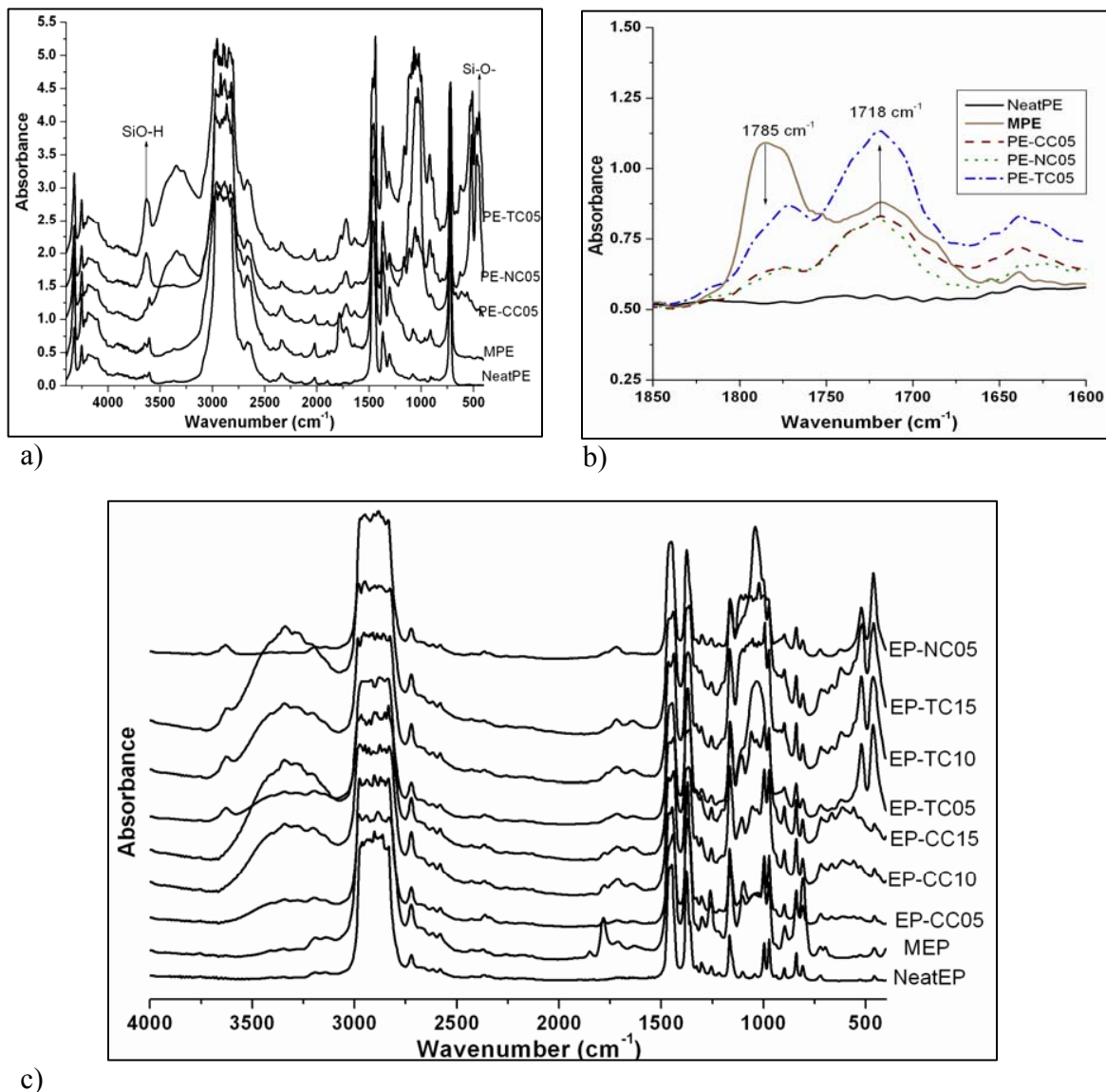


Figure 4.1: FTIR spectra of neat polymer, maleated polymer and composites of a) PE, b) PE samples at carbonyl region, and c) EP copolymer

In Figure 4.1b, the bands at 1780 cm⁻¹ and 1853 cm⁻¹ for cyclic anhydride, and at 1713 cm⁻¹ for carboxylic acid dimer indicate the maleation of PE. It was further confirmed by the decrease in the absorbance of the bands at 1363 cm⁻¹ and 1580 cm⁻¹, which is attributed to the absence of the anionic form of carboxylic acid dimer in MPE. In composites (CC05,

NC05 and TC05) the decrease in the absorbance of the 1780 cm^{-1} band (cyclic anhydride) and the evolution of bands at $1740\text{-}1720\text{ cm}^{-1}$ (stretching of ester C=O) are attributed to the ester formation. This absorption was found to increase with increasing content of cellulose. The ester formation, which is an evidence for improved chemical compatibility⁷, depends on the availability of hydroxyl groups on the surface of the fillers. In *Figure 4.1a and c*, the broad and higher absorbance at hydroxyl region ($3300\text{-}3475\text{ cm}^{-1}$), which is assignable for free and hydrogen bonded hydroxyl groups indicate the presence of cellulose. For clay containing samples (NCs and TCs), the observed bands at 670 cm^{-1} and $1230\text{-}1250\text{ cm}^{-1}$ regions are assigned for the deformation and stretching of the Si–O bond. The absorbance for bending vibrations of the Si–O bond of smectite clays can be observed in the $522\text{-}466\text{ cm}^{-1}$ region. In addition, the band for free hydroxyl groups of the inorganic layered silicate was also seen at 3600 cm^{-1} .

4.3.2. Structure and Morphology

The characteristic of interactions between polymer chains and clay are typically analyzed using XRD and TEM tools. Typically, a shift in peak of 001 basal plane from higher angle ($2\theta = 4\text{-}6^\circ$) to lower angle ($2\theta = 1.5\text{-}3^\circ$) represents the d spacing between the silicate layers. The increase in the d-spacing indicates the crawling of macromolecular chains into the gallery of layered silicates which is generally called as ‘intercalation’, while delamination of these silicate layers from the gallery order can be called as ‘exfoliation’ for which no peaks at lower angles will be observed¹⁸. WAXD patterns of prepared composites are shown in *Figure 4.2 a-d*. In *Figure 4.2c*, the peaks at about 2θ , 16 and 23° are observed for neat cellulose crystalline fibers. These peaks in other samples were hardly detectable which may be due to the destruction of crystalline region of cellulose during processing or by reaction with the compatibilizer used. In *figure 4a-b,d*, the interlayer d-spacing of 001 basal plane in the clay (MMT20A) was observed at about 23.23 \AA ($2\theta = 3.8^\circ$). The intercalation is observed in terms of expansion in this d-spacing for NCs and TCs as represented in *Table 4.1*. This expansion indicates that the melt mixing of neat polymer and compatibilizer with MMT20A resulted in the ‘intercalation’ of the polymer chains into the galleries. The d-spacing values in TCs are higher than that of NCs. This can

be attributed to the extended melt-mixing time (5 min), as the time of dispersion in melt-stage facilitates the crawling of polymer chains in between the silicate layers.

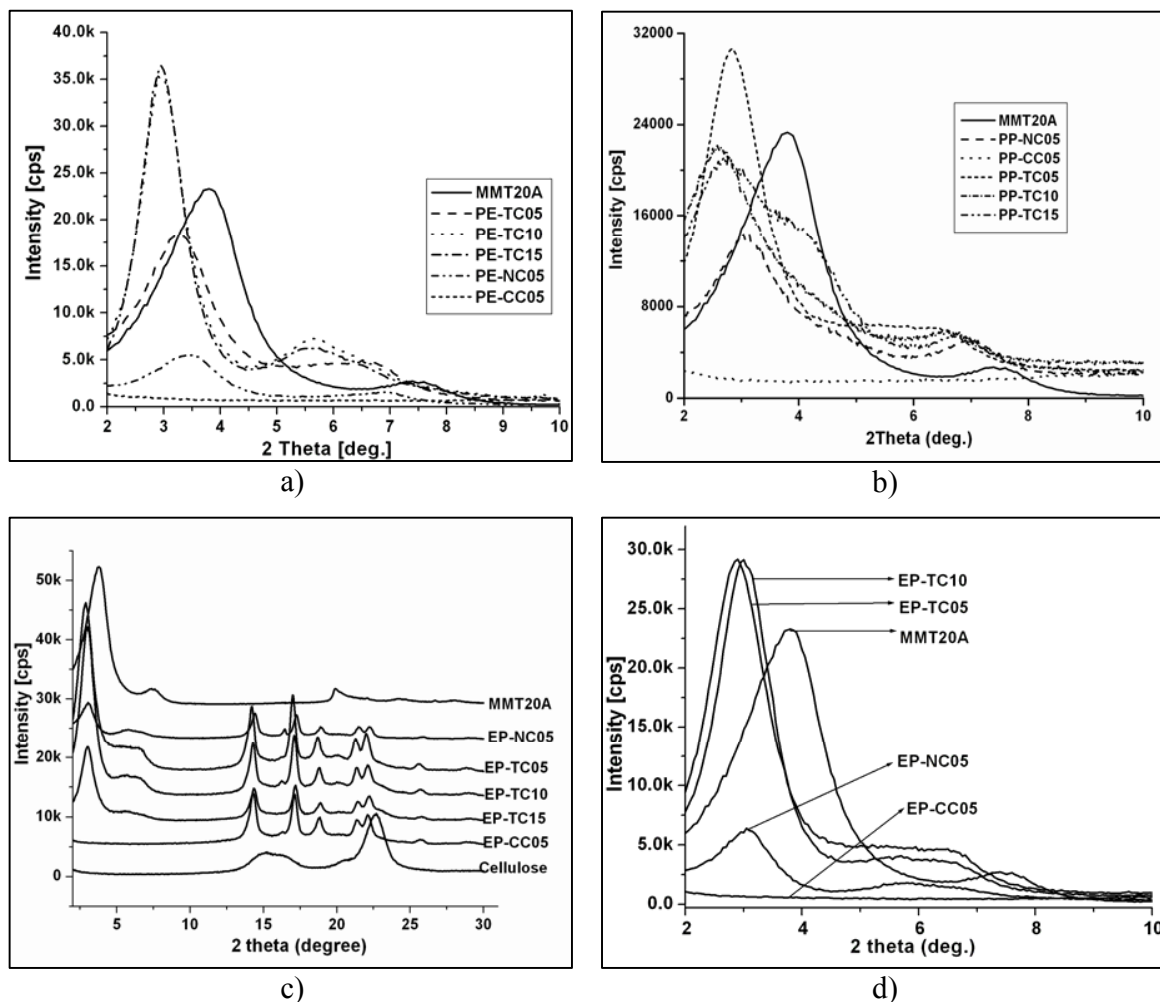


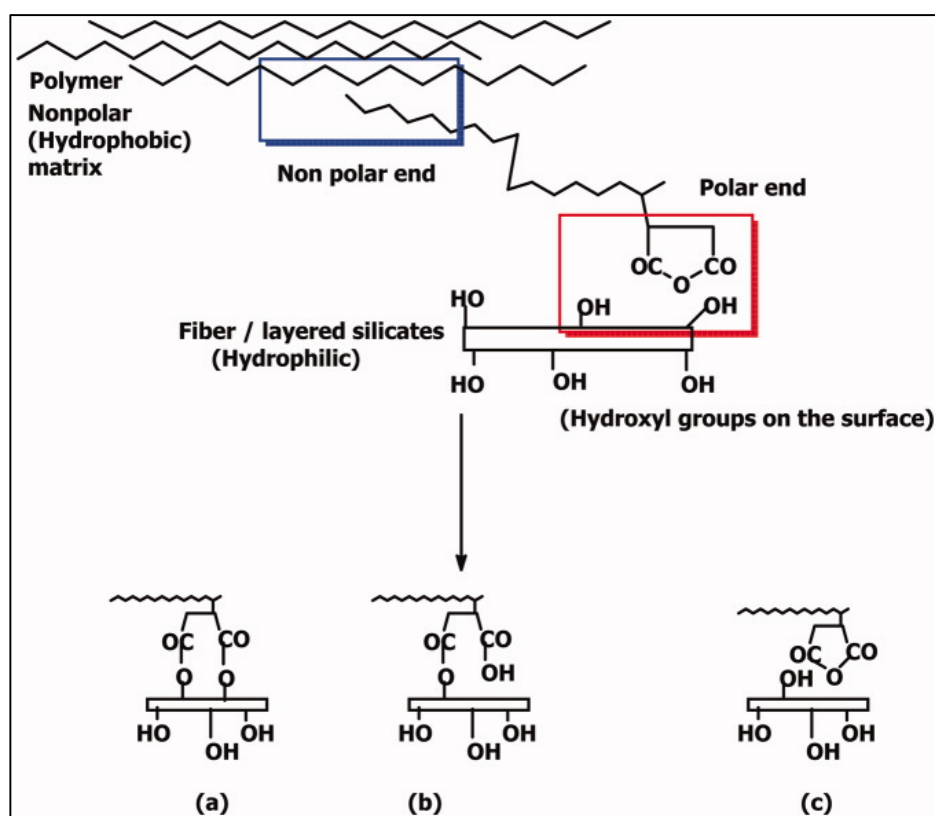
Figure 4.2: WAXD pattern of composites of a) PE, b) PP, c) EP (2-30°) and d) EP (2-10°)

Table 4.1: d-spacing values of 001-basal plane

Polymer matrix	NC (Å)	TC05 (Å)	TC10 (Å)	TC15 (Å)
PE	25.58	27.20	29.92	29.92
EP	28.47	30.44	29.42	29.42
PP	28.84	30.97	33.69	32.45

Unlike the heterophasic copolymer (EP), for both homopolymers (PE and PP), the higher d-spacing was observed for TC10 than TC05. However, further increase in d-spacing was

not observed in comparison of TC10 to TC15. This can be correlated through the possible interactions between fillers, compatibilizer and polymer, and the availability of acid anhydride groups of maleated polymers, which are reactive and interact with both cellulose fiber and clay. According to Hasegawa et.al.²⁵⁻²⁶, on using the maleated polyolefins as compatibilizer for the polyolefin-clay nanocomposites, the acid anhydride content, molecular weight of compatibilizer and composition are the strongly influencing the factors for the formation of nanocomposites. The possible interactions of fillers, compatibilizer and polymer are schematically represented in *Scheme 4.3*.



Scheme 4.3: Schematic representation of possible interactions between polymer, compatibilizer and fillers

The interactions (a) and (b) result in the formation of covalent bond between the compatibilizer and fillers/fibers. The complete ester formation could be predominantly favored by solution-impregnation method while by melt-mixing method, the esterification reaction could occur in lesser extent⁷. Thus, in the prepared composites, just the *polar-*

Chapter 4

polar interactions (c) may also possibly be present.^{7, 40} At higher concentration of cellulose, the reaction of acid anhydride groups with cellulose can lead to increase in mass value, which may result in the decrease in transformations. In other words, the mobility of the macromolecular chains may be reduced, thus, reducing the confinement of the polymer chains into the silicate galleries. In the present study, the ratio between polymer and compatibilizer is kept constant. Thus, it is assumed that in composites with constant ratio of polymer and compatibilizer, the increasing cellulose content may not favor the confinement of polymer chains into silicate galleries.

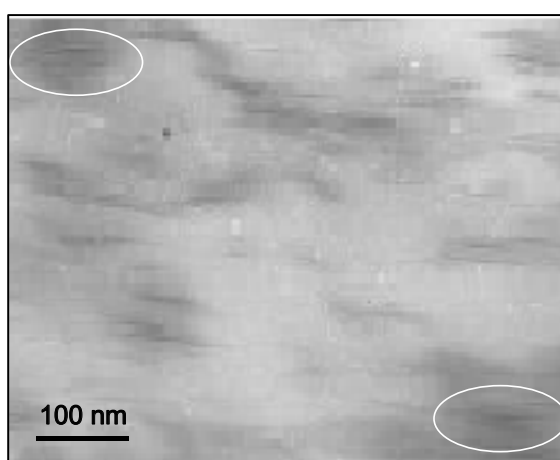


Figure 4.3: Bright field TEM image of EP-TC05

The bright field TEM image of the type [III] composite EP-TC05 is given in *Figure 4.3*. It shows the characteristic platelets of the montmorillonite (MMT) tactoids, in which the dark entities are the cross section of intercalated MMT layers and bright areas represent the polymer matrix.

4.3.3. Thermal Properties

The thermal behavior of these composites, which were analyzed by DSC and TGA, can be seen in *Figure 4.4 a-b*. The melting point for the neat PE, PP, and EP was observed at ~118, 166°C and 165 °C, respectively. In the composites, slight increase in melting point was observed with increasing content of fillers. The melting points of clay containing composites (TC05 – TC15) are higher than that of CCs, which may be attributed to the heat deflection property of layered silicates and the reduction of thermal motion of the macromolecular chain in the silicate layers.⁴¹⁻⁴²

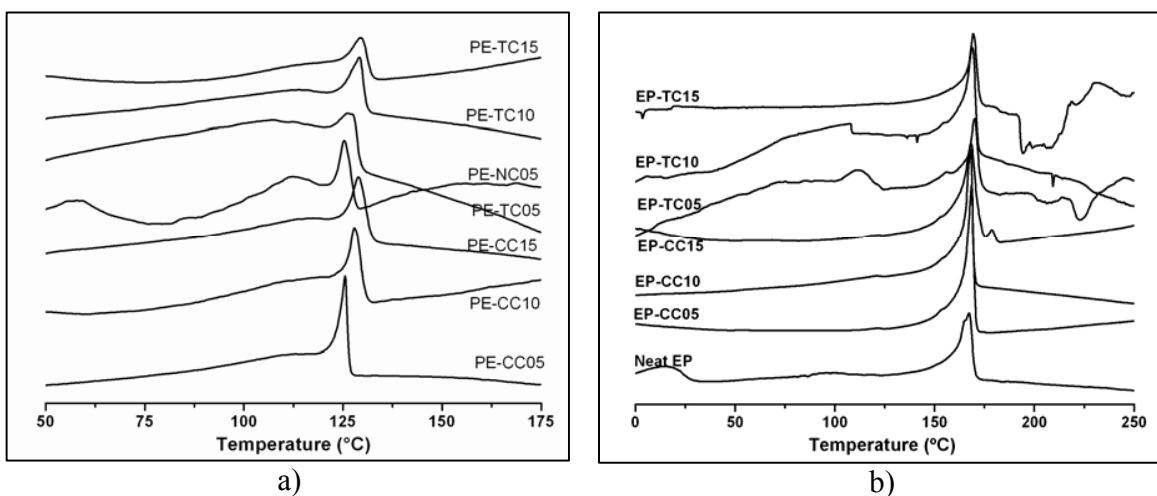


Figure 4.4: DSC thermogram of composites of a) PE and b) EP copolymer

According to Tyan et.al.⁴³ thermal expansion in nanocomposites upon melting is reduced, since the macromolecular chains are sandwiched in between silicate layers and plane (platelet)-oriented, tend to relax in a direction normal to its original direction. This may be because of the silicate layers which are much more rigid in nature than polymer molecules and do not deform and it becomes difficult for polymer molecules to relax. In ternary composites, transitions above the melting point of the matrix may be explained by the assumption that the layered silicates and increasing concentration of cellulose fibers increase the phase separation and apparently accelerate the heterogeneous nucleation to crystallize at higher temperatures by acting as nucleation centers.⁴⁴

In *Figure 4.5 a-b* the maximum decomposition of (host) matrix T_d (°C) can be observed. Among neat polymers, the T_d (°C) of polypropylene matrix is lower than others. This can

Chapter 4

be attributed to the stability of tertiary carbon atoms in the chains during degradation. It is well documented that the susceptibility of polyolefins towards degradation depends on the number of tertiary carbon in the polymer chain⁴⁵⁻⁴⁶

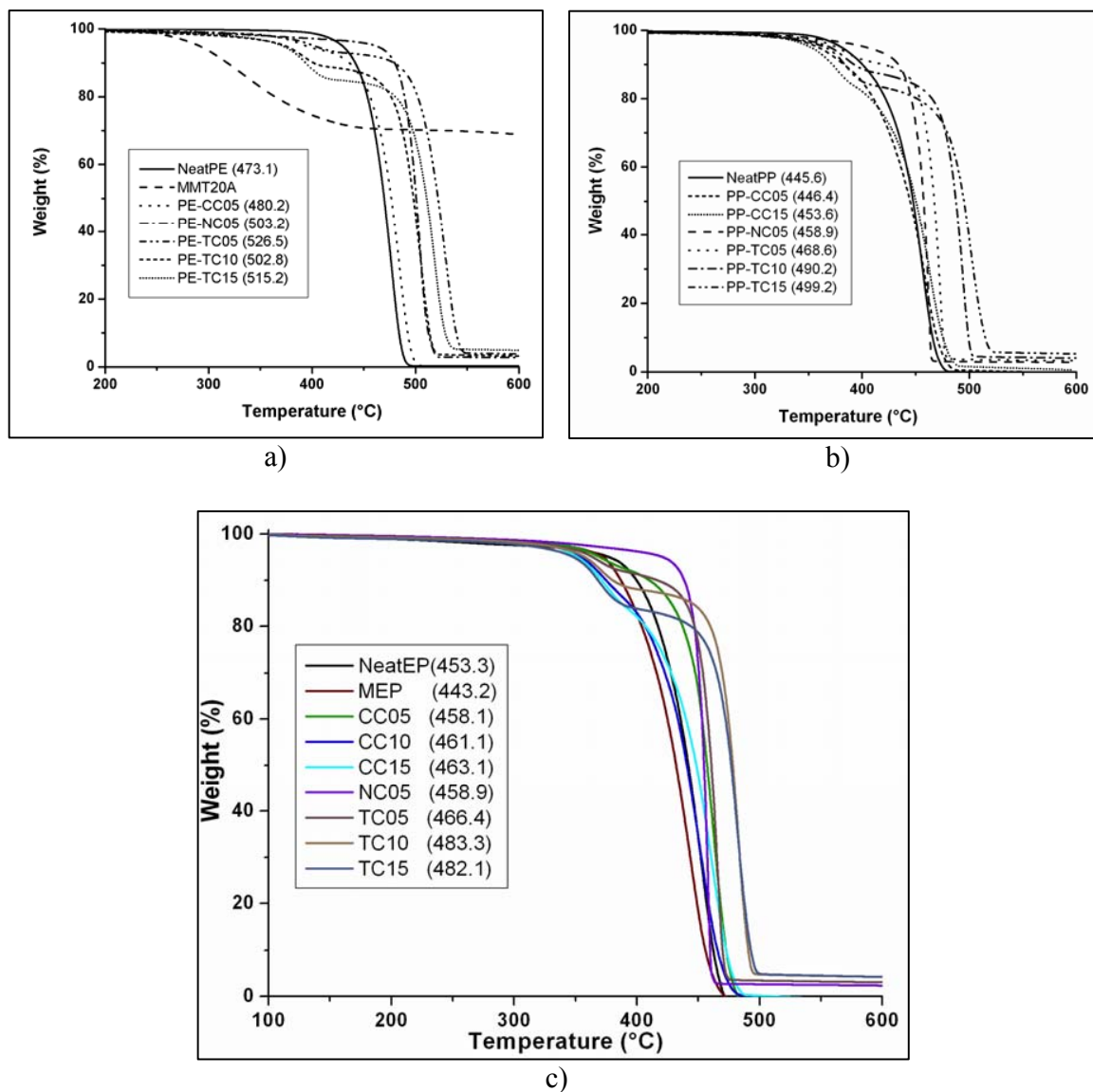


Figure 4.5: TGA thermograms of composites

The T_d of maleated polymers (MPE, MPP and MEP) is lower than their neat polymer, which may be due to the facilitation of degradation by the functional moieties such as acid anhydride. The composites show higher thermal stability than neat polymer matrix. In case

of composites, the Td is higher for clay containing (especially TCs) samples. This can be attributed to the barrier property of silicate layers and the char formation during thermal degradation⁴⁷⁻⁴⁸. As we know that the montmorillonite clay is typically modified with a surfactant in order to make the gallery space sufficiently organophilic to permit it to interact with the polymer. However, the molecular structure (length and number of alkyl chains and unsaturation) is also a determining factor of the thermal stability of the polymer / MMT nanocomposites⁴⁹⁻⁵¹. As it can be seen in *Figure 4.5a*, the weight loss for clay (MMT20A) is at lower temperature region 250-400 °C. During decomposition, first the lower molecular weight organic chains are degraded and released, while the high molecular weight organic species are still trapped layered silicates in the matrix. The high molecular organic polymer chains may still exist between the inter-layers until the temperature is high enough to lead to their further decomposition. In addition, the silicate layers have an excellent barrier property that prevents / reduces the permeation of various gaseous products. In case of nanocomposites, these charred materials might be absorbed on clay surface. Owing to their high aspect ratio, the charred materials on the clay surface can act as carbonaceous insulators. Thus, the addition of clay enhanced the overall thermal stability by acting as a superior insulator and mass transport barrier to the volatile products generated during decomposition.

4.3.4. Mechanical Properties

Figure 4.6 and *4.7* depict the improvement in mechanical properties due to the reinforcement of microcrystalline cellulose and layered silicates. In *Figure 4.6a* and *4.7a*, the modulus, expressing the stiffness of materials, was observed to increase linearly with cellulose content. With the same amount of loading of fillers (5 wt%), NC05 has shown higher modulus value than CC05, indicating that, the nanoscale silicate layers are better reinforcer than microcrystalline cellulose due to higher aspect ratio of nano-sized platelets. It has been well explained⁵²⁻⁵³ that the higher surface area [$\sim 760\text{m}^2/\text{g}$] of layered silicates enhances interfacial region and more ‘polymer – filler’ interactions, which facilitate the stress-transfer to the silicate layers.

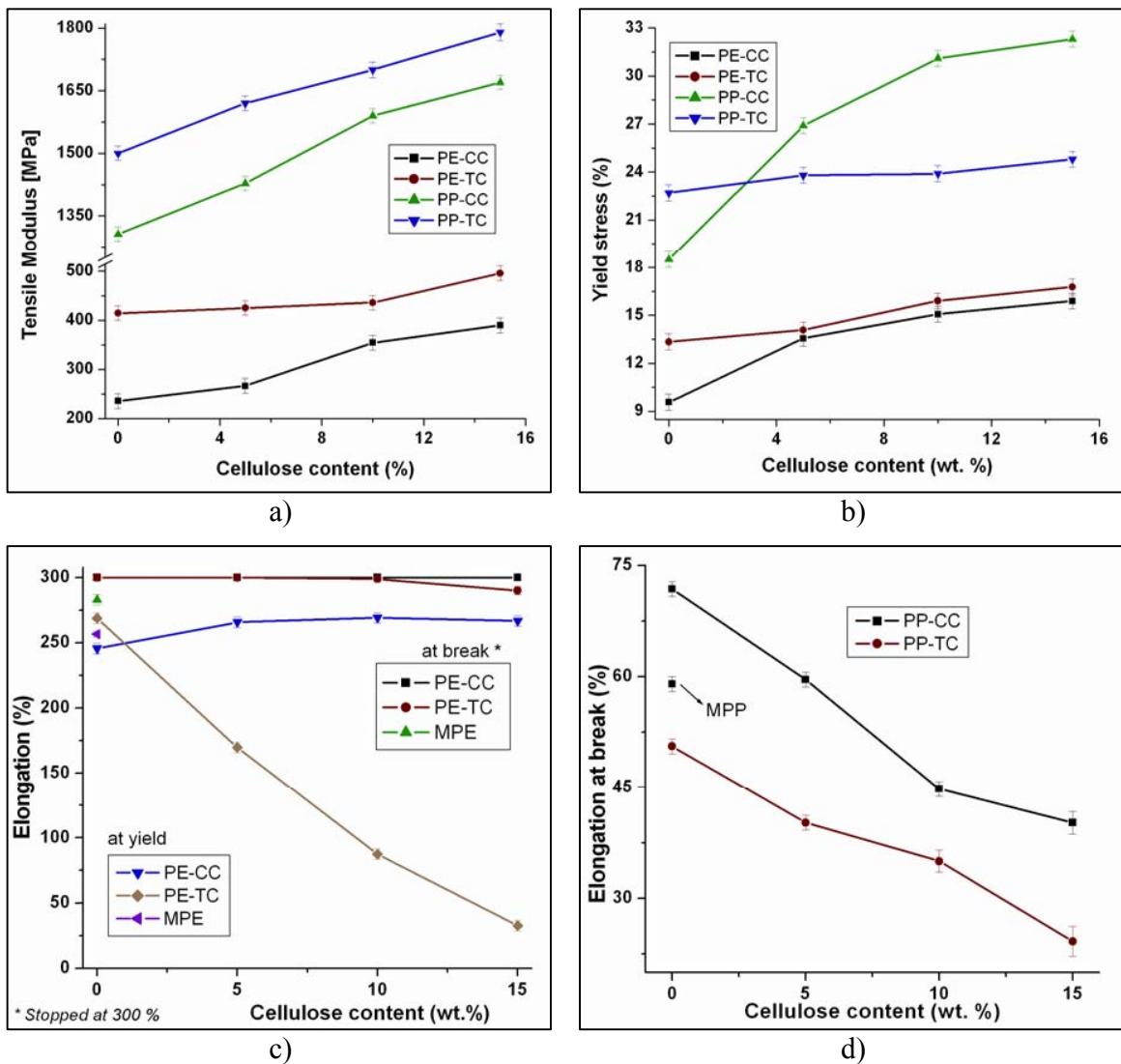


Figure 4.6: Tensile properties of PE and PP samples a) Tensile modulus, b) Yield stress c) Elongation (%) of PE samples and d) Elongation (%) at break for PP samples

The yield stress, which denotes the hardness of the material, was also found to increase linearly with cellulose content. (Figure. 4.6 b, and 4.7 b), indicating the stress resistance improved by cellulose fibers. The incorporation of layered silicates in polymer exhibited improved yield stress (NC05s). However, when the clay is incorporated in cellulose composites, the significant improvement in yield stress was not observed for PE-TCs. Even lower values were observed for PP-TCs and EP-TCs than their counter parts of PP-CC and EP-CC compositions.

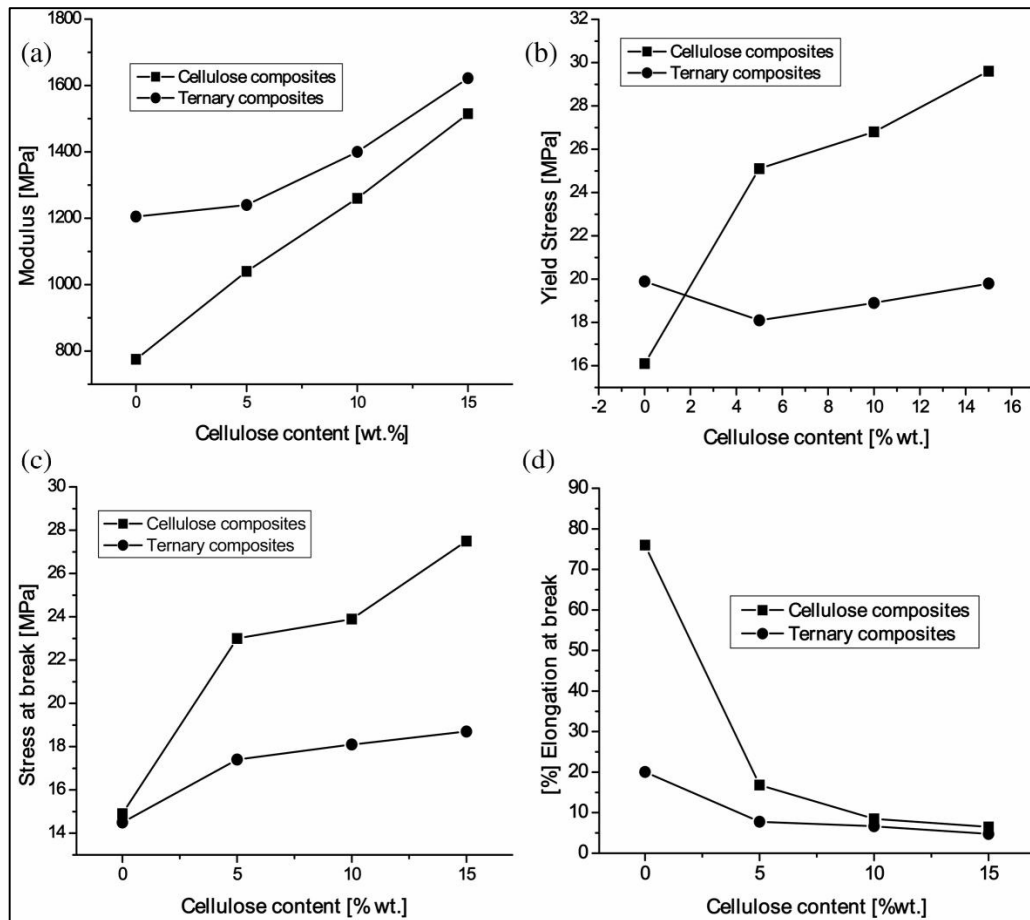


Figure 4.7: Influence of clay on the tensile properties of cellulose composites of EP

In other words, the incorporation of clay in cellulose composites decreases the yield stress of the samples, indicating that the applied stress is not efficiently transferred to the fillers in the case of ternary composites. Obviously, it is contrary to our expectation. This peculiar behavior can be attributed to the reduced compatibility arisen by the increasing content of various fillers (phases). With the constant ratio of polymer and compatibilizer, increasing content of the cellulose fibers in ternary composites, acid anhydride groups of compatibilizer may mostly interact with organic hydroxyl groups from the cellulose fibers. This may reduce the interaction (i.e. compatibilization) with inorganic silicate layers, which may also be the reason for non-expanding behavior of silicate layers as it was observed in WAXD patterns of TC10 and TC15. Thus, the reduced interaction between clay and macromolecular chains may result in agglomeration of layered silicates. Even for TC05 (5 wt.% cellulose), as it can be seen in TEM image, some part of the silicate layers

Chapter 4

(dark entities) seem to be continuous indicating the agglomeration of silicate layers. This agglomeration is believed to cause the phase separation and ultimately decrease in yield stress. Kazayawoko et. al.⁵⁴ demonstrated that only the chemical compatibility such as ester bond formation between hydroxyl group of fibers and anhydride group of compatibilizer is not only the key determining factor for enhancing the mechanical properties. The other factors, which improve the mechanical properties, are be reduction in surface energy, polarity and mechanical interlocking of compatibilizer and filler.^{54, 55} The detrimental effect of incompatibility can be found in decrease in stress at break which is the ultimate strength of the material (Figure 4.7c). With increasing cellulose content (CC05-CC15) the ultimate strength values increased linearly in the cellulose composites. The lower stress at break was found for polymer-clay nanocomposite (NC05) than cellulose composite (CC05). Hasegawa et. al.²⁵⁻²⁶ have also observed the reduction in stress values after incorporation of layered silicates into polypropylene matrix with oligomeric maleated PP. Ternary composites (TC05-TC15) exhibited lower ultimate strength values than their counter parts of cellulose composites. The elongation (%) at break, which denotes the ductility of samples, can be seen in *Figure 4.6c-d* and *4.7d*. For both CCs and TCs, it decreases with increasing content of cellulose and the decrease was adverse for PP-TCs. The decrease in elongation for clay-containing composites may be due to the restriction in momental velocity of polymer chains, as the chains are in sandwiched form in the silicate galleries. It appears that during the tensile test under applied stress the macromolecular chains may undergo three steps which are uncoiling, stretching and slippage⁵⁶. These are restricted in the nanocomposites due to the stretching and confinement of polymer chains into the silicate galleries. Under applied stress, the ‘incompatible centers,’ created due to incorporation of different fillers, initiate failure mechanism by causing the local stress in their vicinity to exceed the strength of the material at early stages of the tensile tests. Predominantly, the mechanical properties (other than elongation (%)) of the cellulose composites were found to be higher than neat matrices. The clay incorporated cellulose composites (i.e. TCs) have shown increased tensile modulus. However, the usefulness of the polymeric material in many applications is largely determined by its predominant failure mechanism under the conditions of applications. In the tensile test, the neat polymer films were believed to follow the craze

failure mechanism which require the mobility of molecular chains to absorb more energy while the reinforced composites could be considered to follow the crack mechanism.⁵⁷

4.3.5. Water Absorption Behavior

The water absorption behavior is an important parameter to be examined, when we deal with hydrophilic cellulose fiber reinforced thermoplastic composites. Higher water uptake of the composite worsens the mechanical properties and changes the dimensional stability of articles by swelling.⁵⁸ Figure 4.8 shows the water absorption (%) for all the samples. It can be seen that water absorption of composites is higher than that of corresponding neat polymers. With increasing content of cellulose, the resistance towards water absorption decreases. This may be due to the increased water uptake by cellulose fibers that are typically hydrophilic in nature and have voids in it (ref).

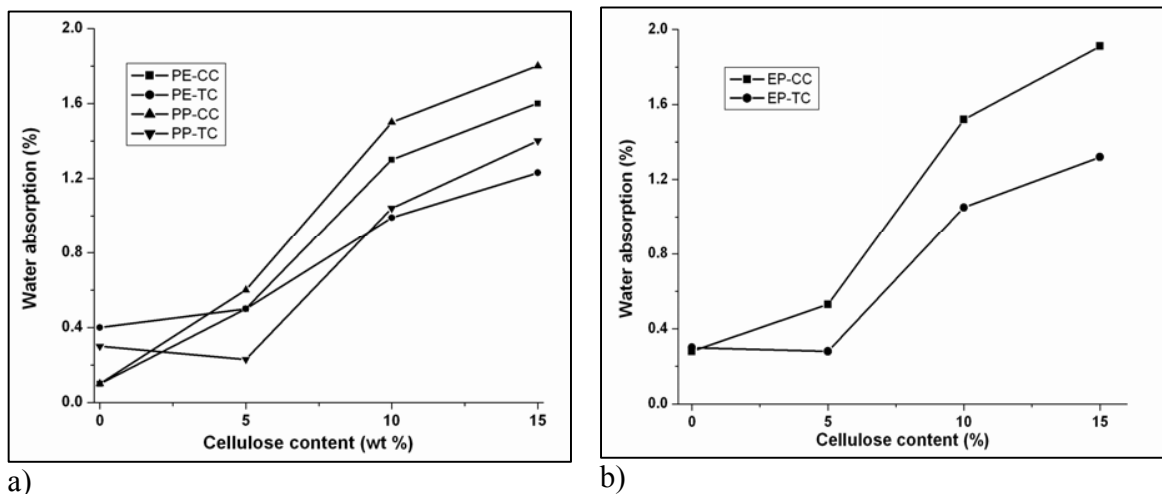


Figure 4.8: Water absorption behavior of composite samples

It can also be seen that the incorporation of layered silicates decreases the water uptake into the composites. Generally, the layered silicates are rich in water content. The clay used in this work was hydrophobically modified. The reduction in absorption may be due to the presence of completely immobilized clay and partially immobilized polymer chains on the amorphous region. According to Tsgaropoulos et. al⁵⁹, when the polymers are filled with very fine particles, the interaction between polymer and fine particle with higher surface area restricts the mobility of polymer chains and leads to the formation of tightly

bound polymer phase on the surface of filler and loosely polymer phase in the matrix. In the present study, the polymer chains are believed to be sandwiched in between silicate galleries. This phase can act as immobilized phase so that the water inclusion in this phase is difficult / reduced. With increasing filler content, these immobilized phases could also increase. This may be the cause for reduction in water absorption for clay containing composites (NC and TCs). From the results, it appears that the incorporation of layered silicates can improve the water resistance of cellulose composites.

4.3.6. Durability Evaluation

4.3.6.1 Photo-irradiation

4.3.6.1.1. FTIR Spectral Changes

The mechanisms of photo-degradation by changes in functional groups and surface morphology upon UV exposure of polyolefins and their copolymers have been well studied^{32-34, 60-61} where the evolution of peaks for hydroxyl ($3700-3200\text{ cm}^{-1}$), hydrogen bonded hydroxyl (3400 cm^{-1}), hydroperoxide (3420 cm^{-1}), associated alcohols (3380 cm^{-1}) and carbonyl compounds ($1850-1600\text{ cm}^{-1}$) has been assigned for oxidation of polyolefins. In carbonyl region, the absorption at 1712 , 1722 , 1740 and 1785 cm^{-1} have been assigned to carboxylic acid, ketone, ester and lactones, respectively. Thus, it is conventional method to study the photo-oxidation by focusing at carbonyl ($1600-1800\text{ cm}^{-1}$) and hydroxyl ($3000-3600\text{ cm}^{-1}$) regions in infrared spectroscopy. Though these functional groups were already present in the case of cellulose composites, the increase in absorbance of these regions in IR spectra were observed to increase upon UV irradiation. *Figure 4.9* shows the FTIR spectral changes in carbonyl and hydroxyl regions during photo-irradiation of PE and maleated PE. The evolution of peaks at carbonyl region ($1800-1600\text{ cm}^{-1}$) with maximum centered sharp increase at 1713 cm^{-1} , which is assignable for ester group, can be found for neat PE. It can also be observed that after 25h of photo-irradiation, the peak for anhydride at 1780 cm^{-1} disappeared in MPE sample. In comparison, the MPE sample shows a rapid increase in absorbance at carbonyl region as well as hydroxyl region. This can be attributed to the functional (acid anhydride) groups present in the compatibilizer. Upon UV irradiation the acid anhydride groups of compatibilizers were transformed in to esters and

other carbonyl compounds. These carbonyl compounds still can accelerate the oxidation rate owing to their photosensitivity.

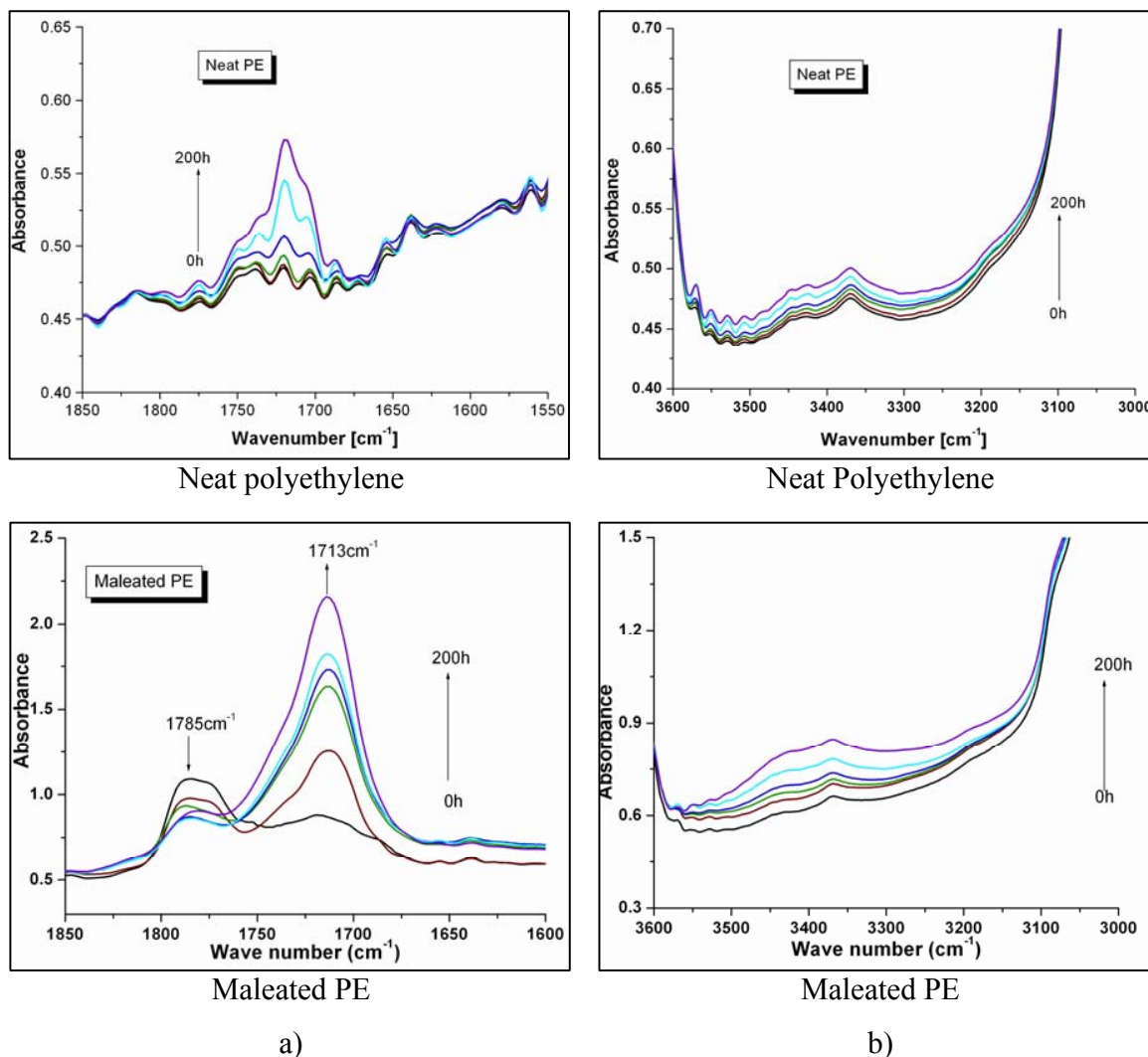


Figure 4.9: FTIR spectral changes at a) carbonyl region and b) hydroxyl region of PE and maleated PE samples upon photo-irradiation

Figure 4.10 and 4.11 show the FTIR spectral changes in carbonyl and hydroxyl regions during photo-irradiation of composite samples of EP and PE, respectively.

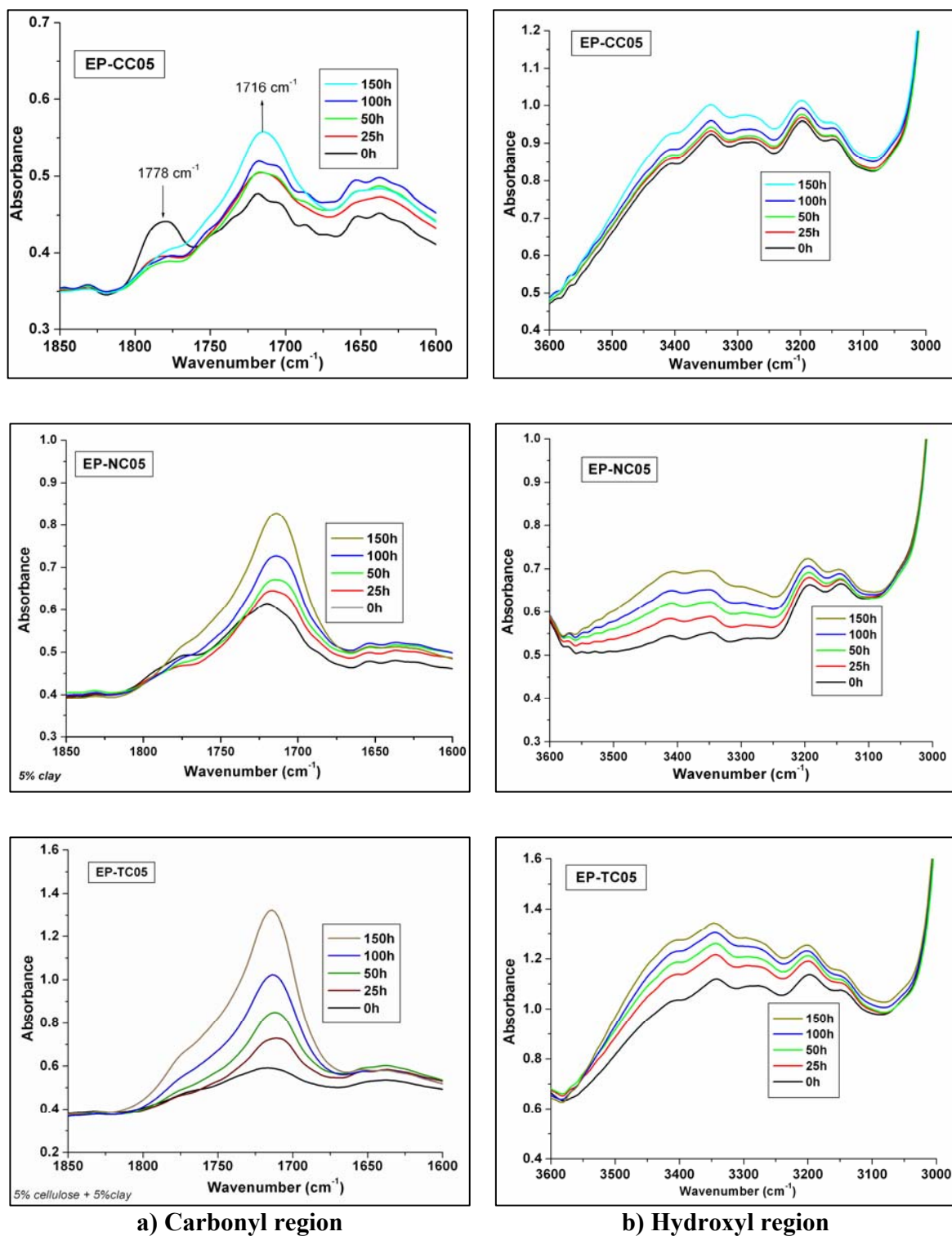


Figure 4.10: FTIR spectra of EP-composite samples upon photo-irradiation at a) carbonyl region and b) hydroxyl region

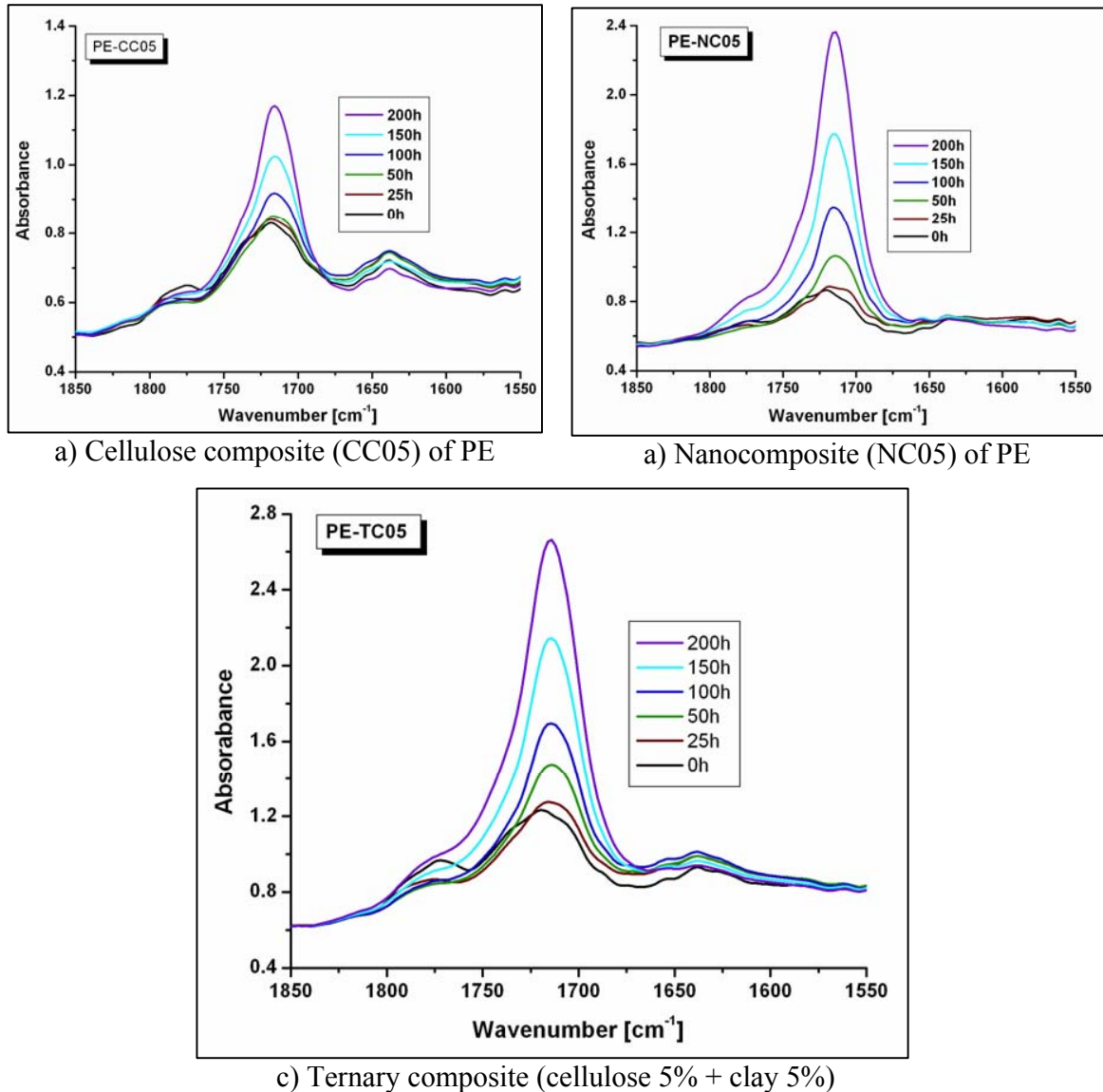


Figure 4.11: FTIR spectra at carbonyl region of PE samples upon photo-irradiation

The increase in absorbance for carbonyl region can be attributed to the formation of oxidized products that include several carbonyl species, such as lactones, ester, ketone and carboxylic acids. Evolution of carbonyl peak is higher for composites than that for neat polymer matrices. In comparison of neat polymer matrix and clay containing composites, during photo-oxidation, the increase in carbonyl region is observed indicating that the pathways or patterns of polyolefin degradation are not altered due to clay. Similar trend was observed in hydroxyl region ($3500\text{-}3100\text{ cm}^{-1}$) also. A very broad band can be seen for

Chapter 4

composite samples with higher increasing rate at 3400 cm^{-1} and 3380 cm^{-1} , which are assigned for hydrogen-bonded hydroxyl and associated alcohol groups, respectively. In cellulose composites, as the cellulose chains are packed by inter and intra molecular-hydrogen bonding, after 25h irradiation they can be esterified with anhydrides of the compatibilizer. The presence of carbonyl groups enhances the photo-oxidation.

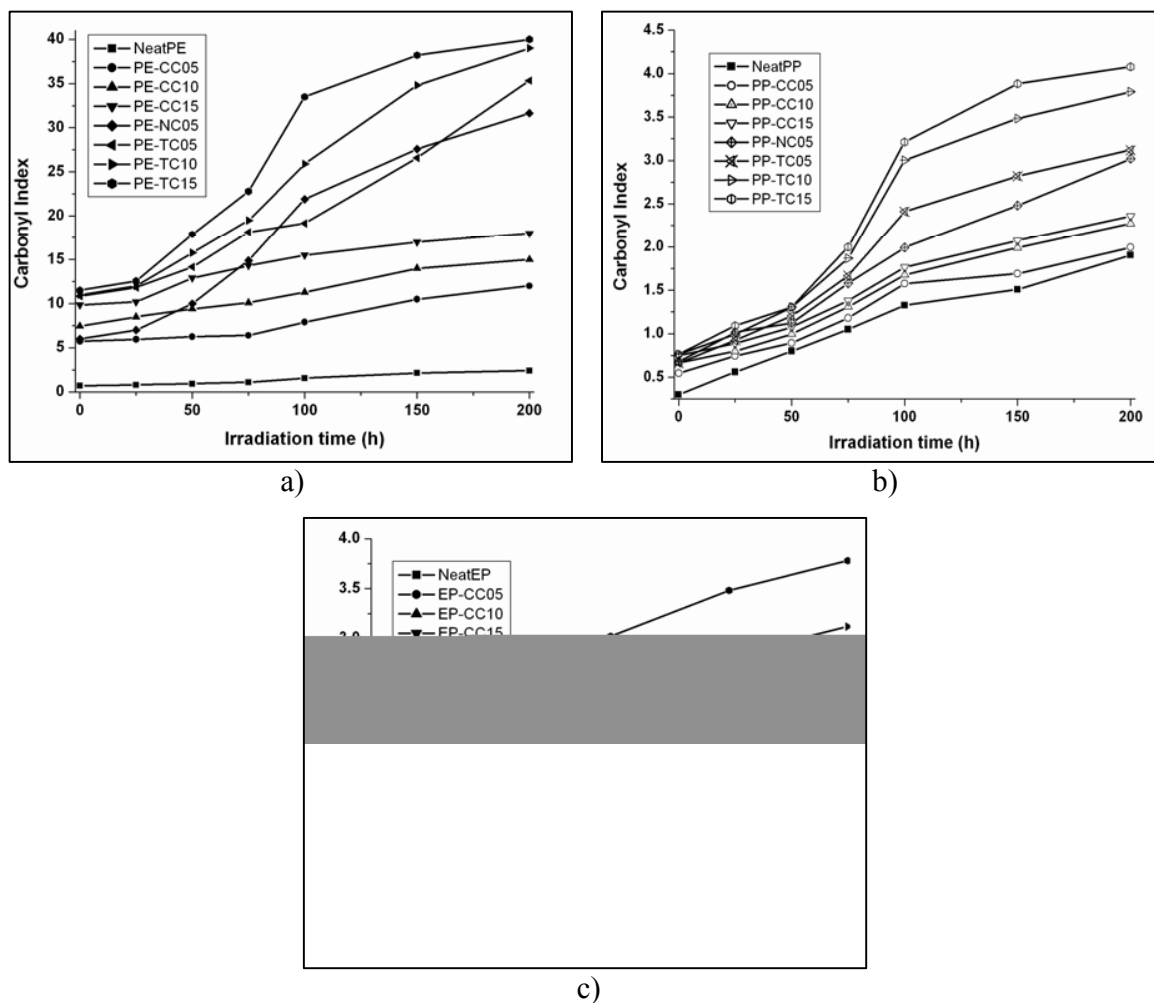


Figure 4.12: Effect of photo-irradiation on samples as carbonyl index in FTIR spectra of a) PE, b) PP and c) EP samples⁶¹

Since the heteroatom functional groups are already present in the system, in order to follow the rate of photo-oxidation it is essential to calculate carbonyl index from FTIR spectra. This conventional method is based on the increase in the absorbance of the carbonyl region

Chapter 4

due to carbonyl formation in the polymer to that of a fixed deformation band⁶¹. It was calculated as follows:

$$\text{For polyethylene samples; carbonyl index} = \frac{A(1713 \text{ cm}^{-1})}{A(1890 \text{ cm}^{-1})}$$

For polypropylene and ethylene-propylene copolymer samples;

$$\text{Carbonyl index} = \frac{A(1713 \text{ cm}^{-1})}{A(905 \text{ cm}^{-1})}$$

Figure 4.12 shows the carbonyl index at various time intervals of photo-irradiation. It can be observed that the photo-oxidation of composites is faster in composites than that of neat polymer matrices. The carbonyl index values for CCs and TCs increase with the increasing content of cellulose. Among all composites, TCs show more susceptibility towards photo-oxidation. The rate of photo-oxidation for samples can be represented in the following order neat polymer < CCs < NCs < TCs. The enhanced rate of photo-oxidation for montmorillonite clay-nanocomposites of polypropylene⁶², polyethylene⁶³ and EPDM⁶⁴ was earlier also reported in literature. This can be attributed to the degradation of the alkyl-ammonium cation exchanged in MMT during melt processing and upon photo-irradiation and the catalytic effect of iron impurities present in the organo-montmorillonite. Iron could catalyze the decomposition of the primary hydro-peroxide formed by photo-oxidation of polymers⁶⁴⁻⁶⁶.

In addition, the reduced gas permeability of nanocomposite may also assist in enhancing photo-oxidation. It is well known that the degradation would start at amorphous region; Oxygen present in atmosphere might diffuse through amorphous region and spread into whole matrix^{45, 67}. If oxygen gas molecules enter through the nanocomposite films, the oxygen molecules can be trapped in between the silicate layers and ultimately become oxygen rich environment. The oxidation of polymers in between silicate layers has been reported to result in low molecular weight polymer chains⁶⁸. The combined effect of iron impurities degradation of organic modifiers, and reduced gas permeability can increase the photo-oxidation in NCs and TCs.

4.3.6.1.2. Morphological Aspects

The changes on the surface morphology have also been important to characterize the photo-induced oxidation, because the factors that are morphology, humidity and wetness have also significant effect on free radical formation and degradation rate. *Figures 4.13–4.15* show scanning electron microscopic images of samples at various time intervals of photo-irradiation.

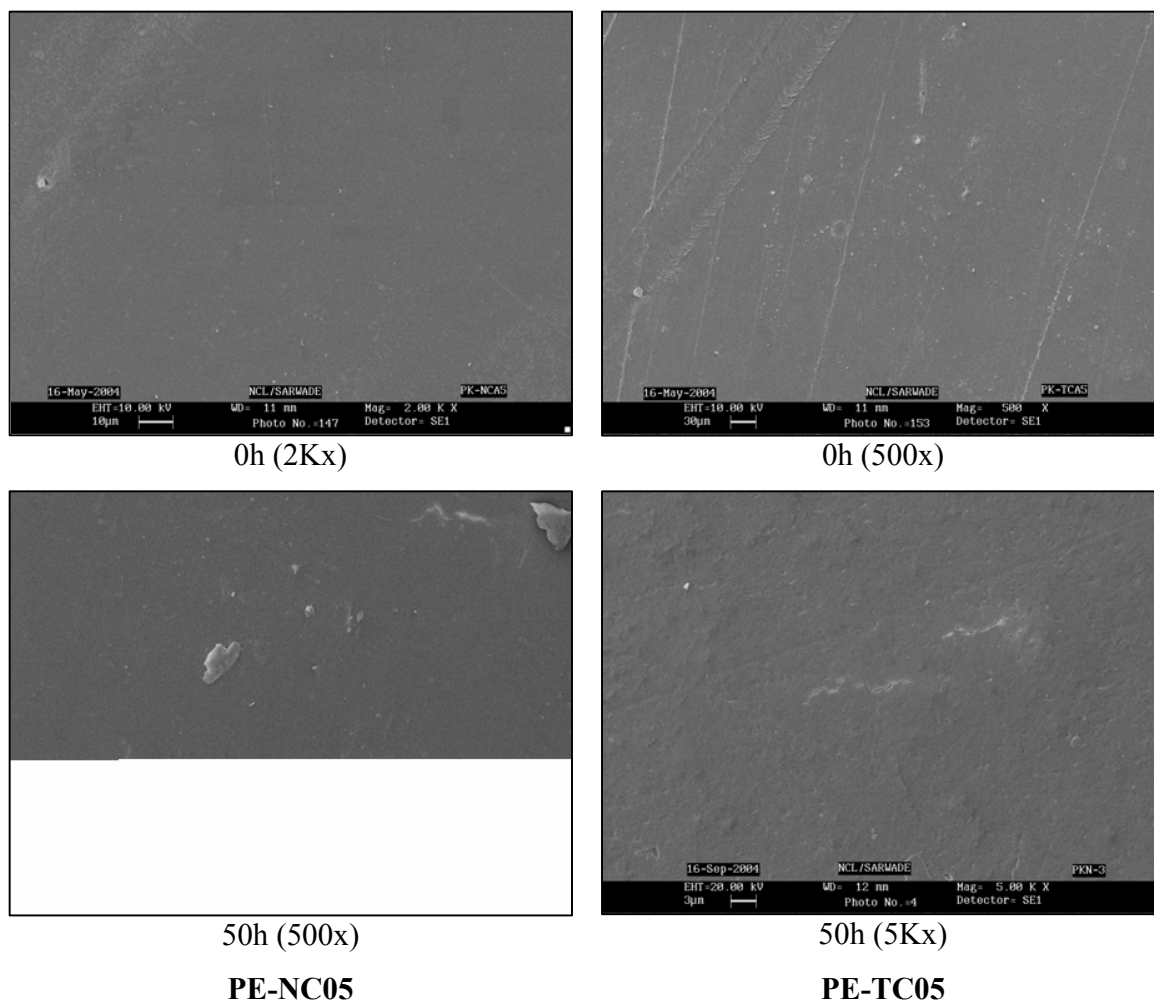
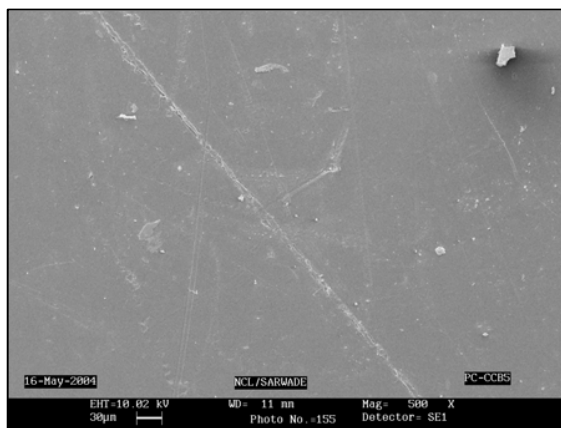


Figure 4.13: Scanning electron micrographs of 0h and 50h photo-irradiated samples of PE

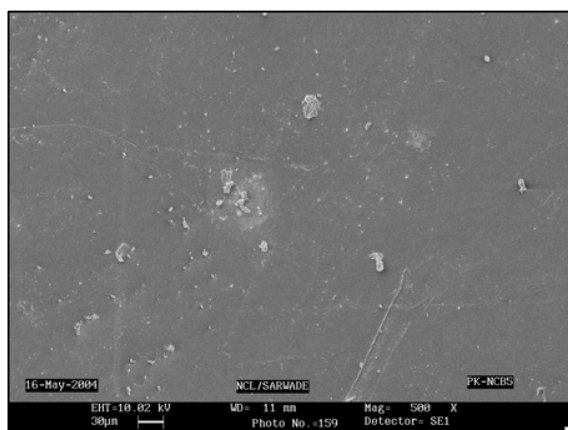
With increasing time of photo-irradiation, the crack formation can be observed on the surface of samples. It is obvious that crack formation (amorphous) on the surface may accelerate considerably and the further rate of auto-photo-oxidation, since any kind of

Chapter 4

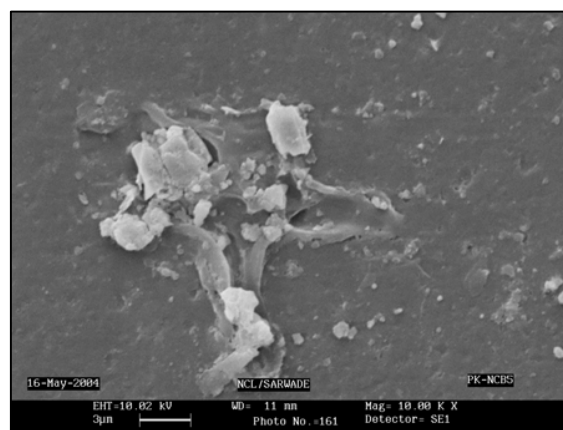
degradation (hydrolysis or oxidation) is initiated at amorphous surface of the polymer samples^{45,67}.



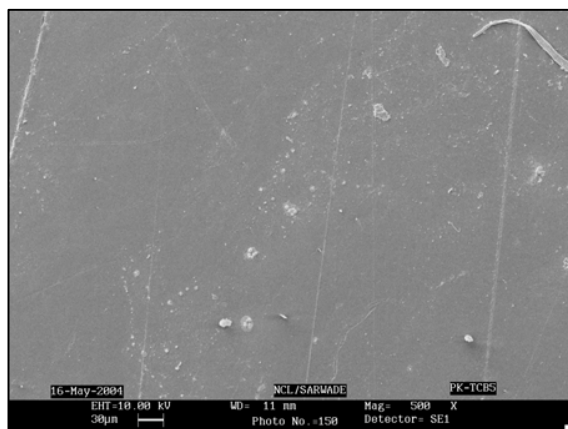
EP-CC05 (500x)



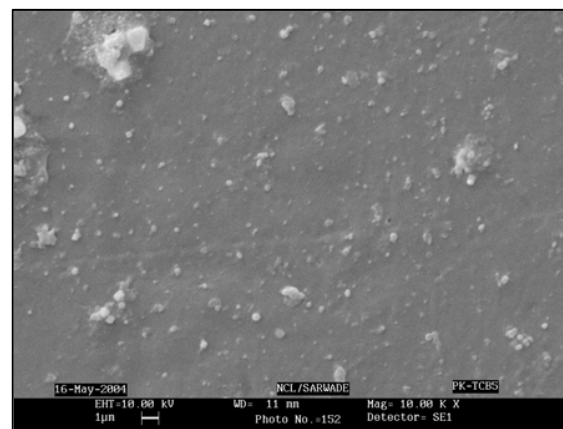
EP-NC05 (500x)



EP-NC05 (10Kx)



EP-TC05 (500x)



EP-TC05 (10Kx)

Figure 4.14: Scanning electron micrographs of 50 h photo-irradiated samples of EP

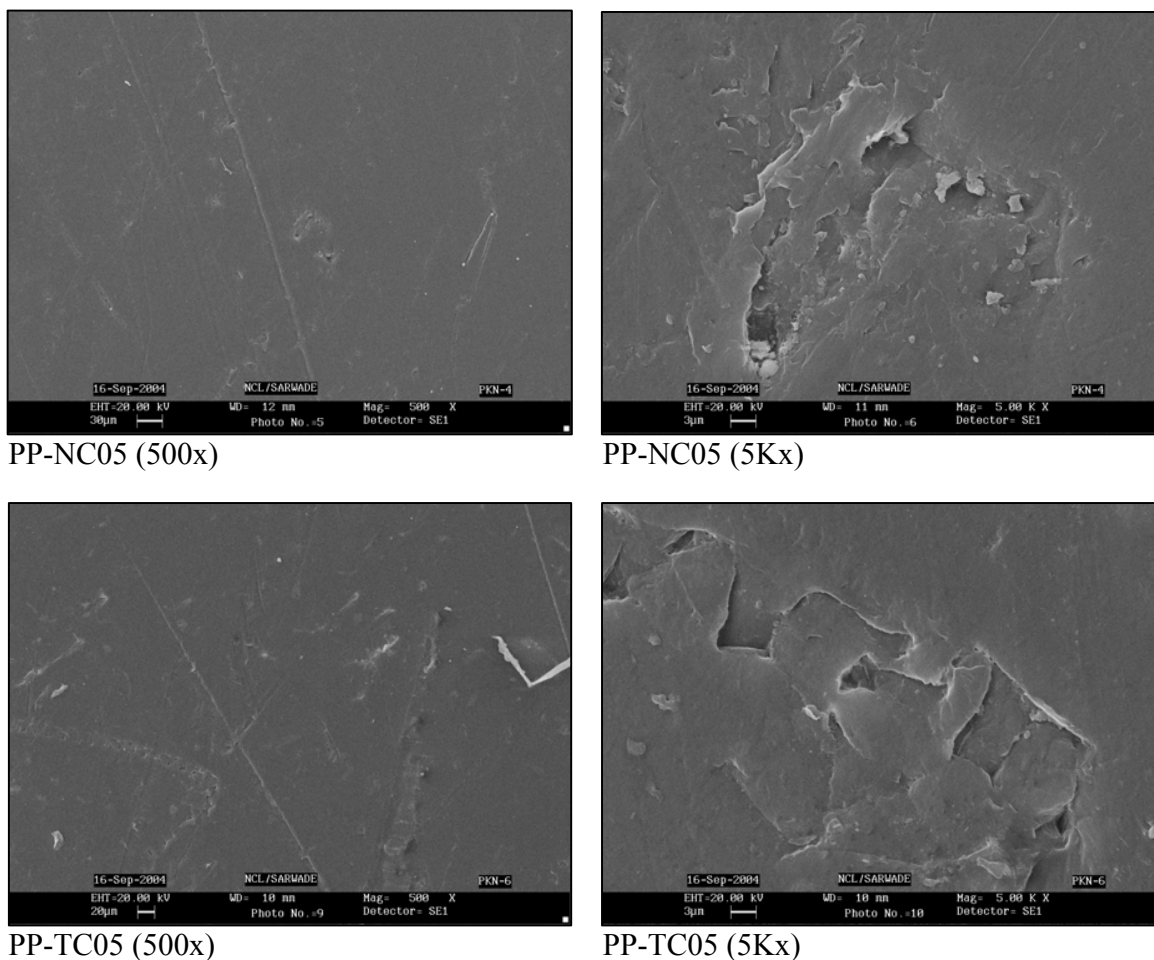


Figure 4.15: Scanning electron micrographs of 50 h photo-irradiated samples of PP

4.3.6.1.3. Changes in Mechanical Properties

The detrimental effect of photo-irradiation can also be observed on mechanical properties in the *Figures 4.16*. *Figure 4.16a-c* shows the increase in tensile modulus. It can be seen that the tensile modulus shows wide deviations because of their brittle nature and during photo-irradiation, handling of photo-irradiated films was little difficult. According to earlier reports^{69, 70}, the changes in tensile modulus had not been a vital determinant parameter of mechanical properties due to its inconsistency for polyolefin matrices.

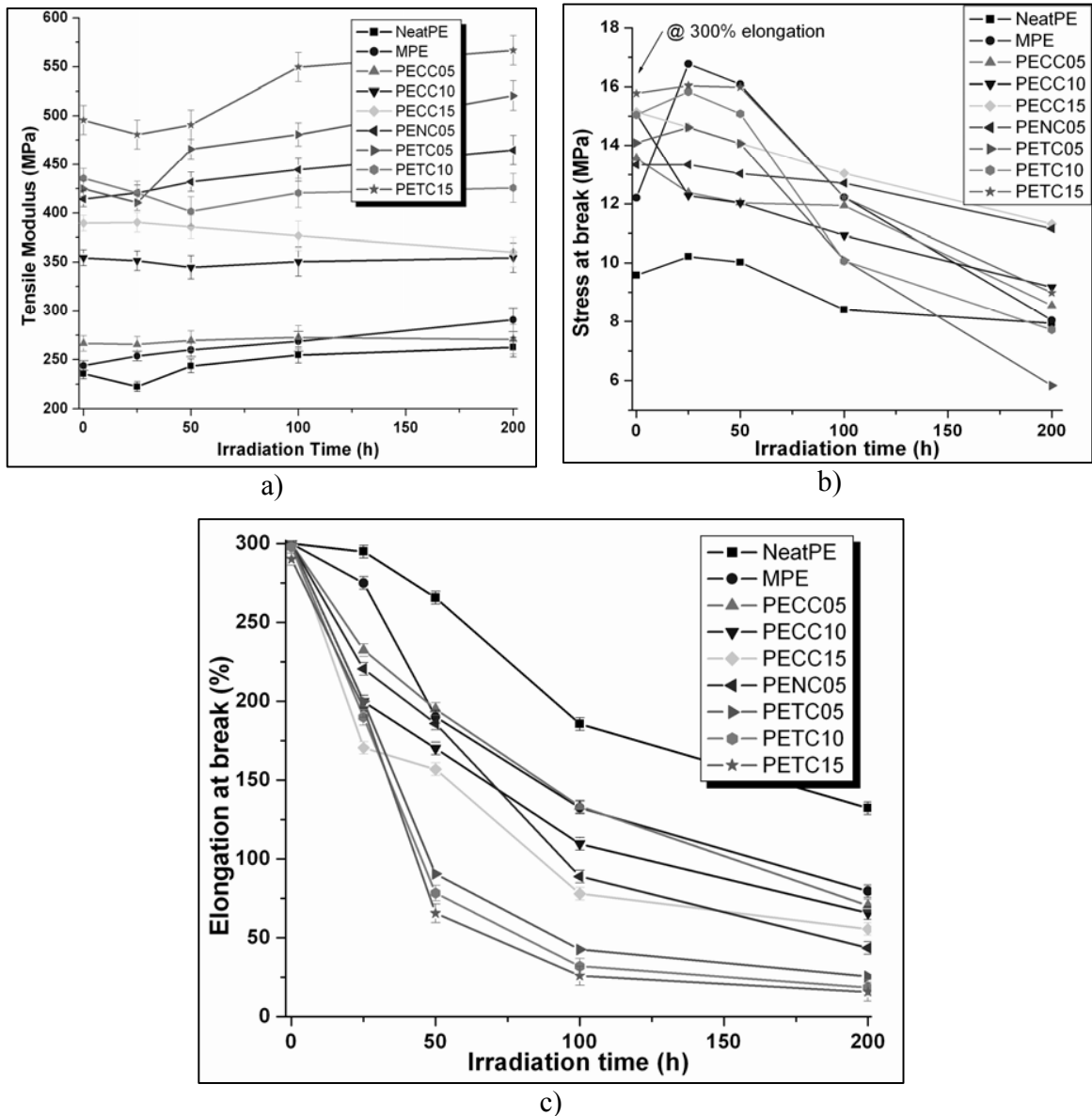


Figure 4.16: Effect of photo-irradiation on the mechanical properties a) Tensile modulus, b) Stress at break and c) elongation at break of PE samples

It could be observed in the *Figure 4.16 b-c* that the strength and elongation values of the composites were adversely affected, indicating the brittle nature of photo-irradiated specimen. Similar trend was also observed for the composite samples of EP and PP. The increase in tensile modulus and decrease in strength values are somewhat peculiar behavior of photo-irradiated films. The changes in the mechanical properties can be explained by two possible structural modes, viz., crosslinking and additional crystallization. Under UV

irradiation, the formation of radicals, leads to oxidation products, breaking chain but / and also crosslinking reactions due to radical recombination. It should be noted that photodegradation proceeds preferentially in a comparatively localized region near the initiation site (such as photosensitive carbonyl groups of compatibilizer, cellulose, and clay surface). Such a localization of the process is a consequence of the low molecular mobility of both the polymer and of the photoactive site in the solid state⁷⁰. This will disfavor the entanglement of polymer chains under applied stress and ultimately reduce the elongation (%) at break. Chemical reasons are also involved here, e.g., the zip-mechanism of degradation along the polymer chain. The probability of the occurrence of such degradation sites is higher in the surface layer of the specimen, in particular in the case of polyolefins⁷¹, but such sites may also lie inside the bulk of the material. Thus, when the photo-irradiated specimen is subjected to mechanical stress, not only the incompatible centers created by fillers and also the degraded weak sites act as stress concentrators and crack nuclei. This may be due to the crosslinking throughout polymer matrix with fillers because of free radical formation upon photo-irradiation. As seen earlier, upon photo-irradiation, the smooth surfaces of specimen are also cracked. The crack formation is believed to accelerate further degradation. The overall embrittlement of the material is a result of the formation of cracks that act qualitatively similarly to macroscopic incisions introduced into the test piece. In addition, the surface morphological changes i.e. crack formation and chain scission, also observed to lead to deterioration in elongation (%) at break.

4.3.6.2. Biodegradation: Composting

4.3.6.2.1. Weight loss During Composting

Figure 4.17 shows the compostability / bio-disintegrability of non-photo-irradiated films under composting environment after particular time intervals in terms of percentage weight loss. The weight loss in neat polymer is hardly detectable even after 3 months of incubation. The maleated polymer (separately) has shown the higher weight loss than neat polymer matrices. This can be attributed to the polarity (due to carboxylic acid and acid anhydride groups) induced in the specimen by grafting of maleic anhydride on the polymer.

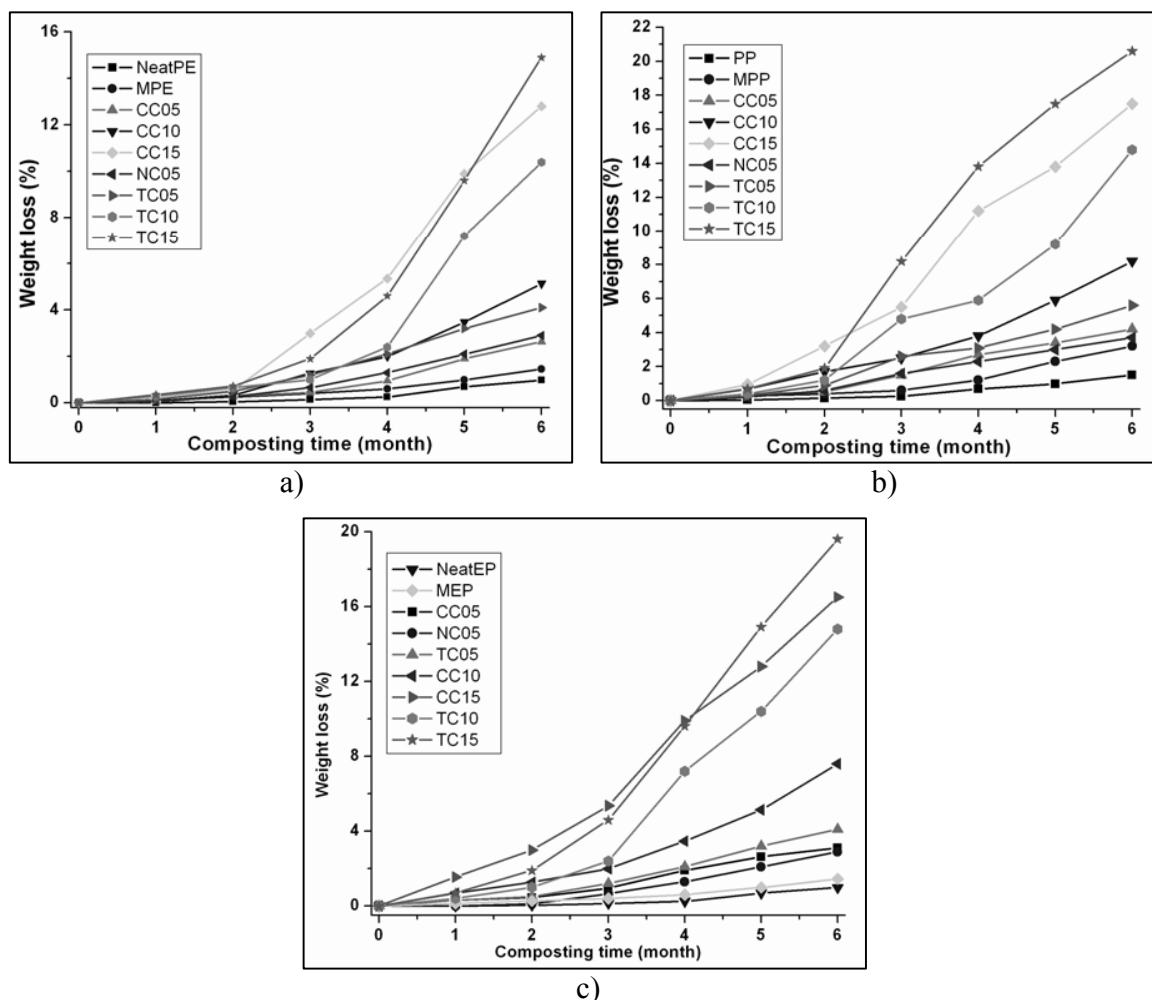


Figure 4.17: Weight loss (%) of non-irradiated samples upon incubation in compost

The composite samples have also shown higher weight loss than their corresponding neat polymer matrices. With increasing content of cellulose content, the weight loss was also observed to increase. This can be attributed to the hydrophilic nature and bio-assimilability of cellulose fibers, which can facilitate the adhesion of microorganisms on the surface of the composite films. The weight loss (%) of samples can also be observed with increasing time of composting. In earlier time of composting, the weight loss (%) of the composites was found to be low and increased with increasing time. This may be because of initiation time needed for microbes to penetrate into the matrix. Among composites, the increase in biodegradability can either be due to the hydrophilic nature of cellulose or due to the phase separation in composites. In comparison, ternary composites show more weight loss

than the cellulose composites and neat polymer. This higher can be attributed to the phase separation which facilitate the microbial penetration into the matrix.

Table 4.2 shows the effect of photo-irradiation on the biodegradation in composting of samples. In comparison of non-irradiated samples, 50-h irradiated samples show higher weight loss indicating the susceptibility of photo-oxidized samples for microbial degradation. It can be observed that with increasing time of incubation, the weight loss has also increased.

Table 4.2: Weight loss (%) of 50-h photo-irradiated samples during composting

Sample	1 month	2 month	3 month	4 month	5 month	6 month
NeatPE	0.7	2.9	4.7	9.0	15.7	20.8
MPE	0.8	3.6	10.4	17.9	25.6	32.4
PE-CC05	1.2	5.4	14.7	24.6	38.7	56
PE-NC05	0.6	2.2	10.3	28.9	39.6	56
PE-TC05	1	4.5	19.5	32.6	45.6	63
NeatPP	1.0	4.8	12.1	20.4	27.5	32.6
MPP	1.6	5.2	18.6	29.4	42.6	56.7
PP-CC05	1.8	9.0	23.5	36.6	48.9	64.3
PP-NC05	1.2	3.2	14.0	29.6	49.7	64.5
PP-TC05	1.6	5.3	23.5	42.6	68.8	-
NeatEP	0.9	3.4	10.2	17.5	26.6	30.7
MEP	1.5	4.5	13.7	25.7	38.7	50.8
EP-CC05	2.3	8	26	45	56	63.9
EP-NC05	1.3	3.6	14.0	27.6	40.6	56.3
EP-TC05	1.8	6.0	22.7	40.3	68.5	-

Among composites, the clay containing composites show lower weight loss than CCs. However, after 3 months of composting, NCs and TCs precede to show higher weight loss. This can be attributed to microbial adhesion favored by photo-oxidized products, eroded surface or crack formation during photo-irradiation^{72, 73}.

4.3.6.2.2. Surface Morphological Aspects

The surface erosion and / or hole formation on surface due to microbial consumption of biopolymer (cellulose) and functional compounds in the composites can be seen in *Figure 4.18*.

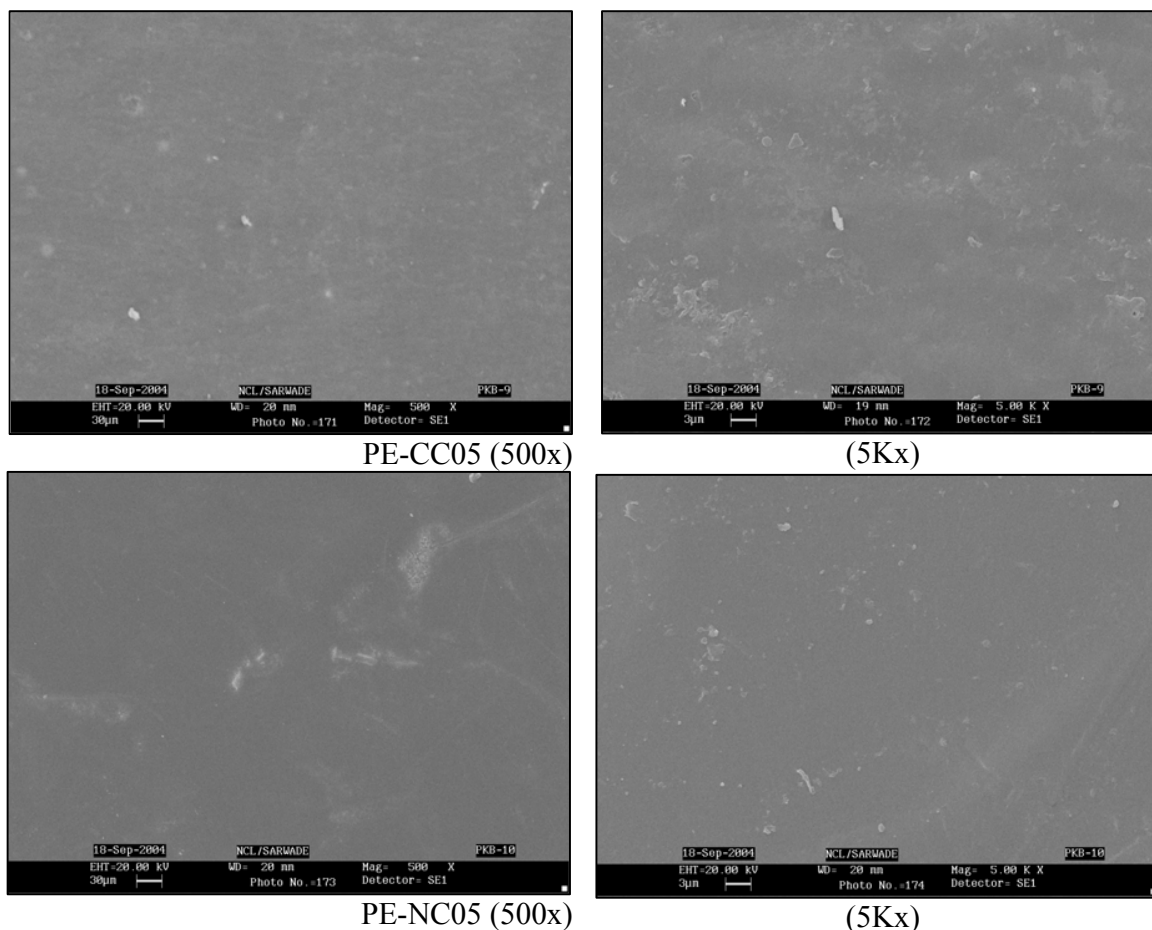


Figure 4.18: Scanning electron micrographs of non-irradiated samples of PE after 1 month of composting

The susceptibility of 50 h photo-irradiated samples can be found in *Figure 4.19* as more erosion on the surface of specimen after 1 month of composting. The increased surface erosion also confirms the enhanced susceptibility of photo-irradiated samples towards microbial bio-disintegrability and bio-assimilation. Thus it can be anticipated that the photo-irradiated samples can be disposed in biosphere directly rather than non-irradiated materials.

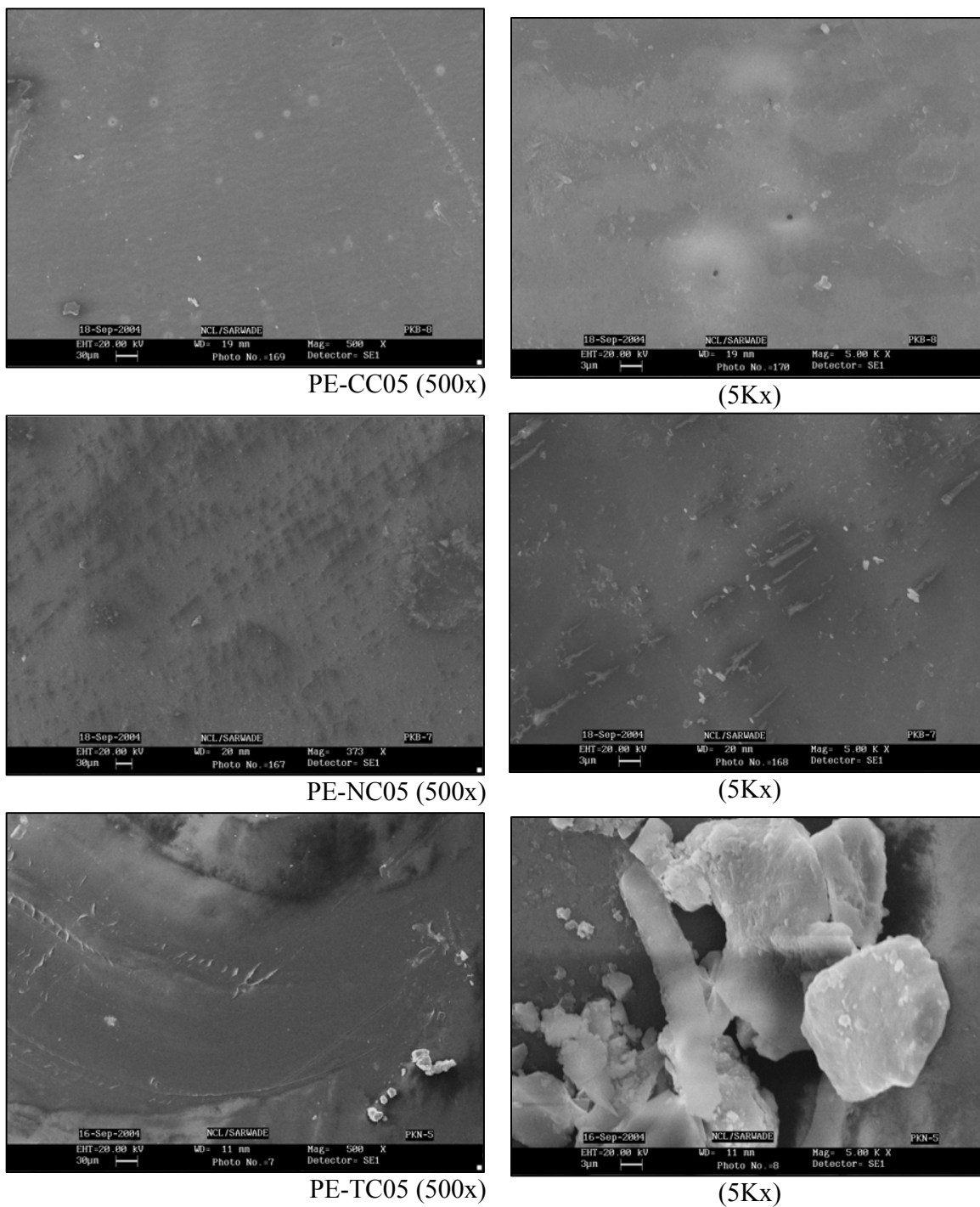


Figure 4.19: scanning electron micrographs of 50h-irradiated composite samples of PE after 1 month of composting

4.4. Conclusion

The present study discussed the effect of nano-clay reinforcement on the material properties and durability of the cellulose-reinforced composites.

- The incorporation of microcrystalline cellulose has improved the mechanical properties (tensile strength and modulus) linearly with its loading amount. It increased the water absorption also. Thermal transitions have shown marginal change after cellulose reinforcement.
- The incorporation of layered silicates in neat polymer matrices and cellulose composites has resulted in intercalated nanocomposites. It enormously improved the mechanical properties (esp. tensile modulus) significantly. The NCs and TCs were observed to be more stiffer and than cellulose composites.
- Thermal stability of composites was also improved particularly the intercalated nanocomposites.
- The nano-clay incorporation has increased the resistance towards water absorption of cellulose composites. In the absence of clay, CCs show higher water absorption behavior.
- As far as durability is concerned, neat polymer and cellulose composites show more resistance towards photo-induced oxidation. In other words, the clay-incorporated samples are more susceptible towards photo-oxidation (weathering).
- Biodisintegrability of cellulose composites are higher than neat polymer matrices owing to the hydrophilicity of cellulose fibers. The incorporation of clay has no significant effect on earlier stage of composting. The biodegradability of photo-irradiated samples is higher than that of non-irradiated ones, which suggest that for the polyolefins – cellulose composites and polyolefin-clay composites, pre-treatment like photo-oxidation is very important for acceptable level of biodegradation.

Chapter 4

References

1. Scott G. In *Degradable Polymers Principles and Applications* Scott G, Gillead D. Editors, **1995**, Chapter
2. Joly C; Kofman M; Gauthier R., *J Macromol Sci A33*, **1996**,12, 1981.
3. Zadorecki P; Michell A.J. *Polym Compos*, **1989**, 10, 69.
4. Elvy S.B; Dennis G.R; Ng L.T, *J Mater Process Technol*, **1995**, 48, 365
5. Gauthier R.; Joly C.; Coupas A.C; Gauthier H; Escoubes M., *Polym. Compos*, 1998, 19, 287,
6. Maldas D; Kokta B.V. *J. Appl Polym Sci* **1991**, 42, 1443
7. Felix J.M.; Gatenhom P, *J. Appl Polym Sci* **1991**; 42: 609
8. Bledzki A.K.; Gassan J. *Prog Polym Sci* **1999**; 24: 221
9. Mecking S, *Angew. Chem., Int. Ed.* **2004**, 43, 1078
10. Powers, W. F., *Adv. Mater. Process*, **2000**, May, 38
11. Gassan J.; Bledzki A.K, *Die Angew Makromol Chem* **1996**, 236, 129.
12. Mohanty, A.K; Misra, M.; Hinrichsen, G. *Macromol. Mater. Eng.* **2000**, 276-277, 1
13. Azizi Samir, M.A.S.; Alloin, F.; Dufresne, A. *Biomacromolecules*, **2005**, 6, 612.
14. John M.J.; Anandjiwala R.D., *Polym Compos*, **2008**, 29, 119
15. Amash A.; Zugenmaier P, *Polym Bull* **1998**, 40, 25.
16. US Patent 4,739,007, 19 Apr 1988
17. Kojima Y.; Usuki A.; Kawasumi M.; Okada A.; Fukushima Y.; Kurauchi T.; Kamigaito O, *J Mater Res* **1993**, 8, 1185
18. Alexandre M.; Dubois P, *Mater Sci Engg: R: Report*, **2000**, 28, 1
19. Ray S.S.; Okamoto M. *Prog Polym Sci* **2003**, 28, 1539
20. LeBaron P.C.; Wang Z.; Pinnavaia T.J., *Appl Clay Sci* **1999**, 15, 11
21. Kojima Y, Usuki A, Kawasumi M, Okada A, Fukushima Y, Kurauchi T, Kamigaito O. *J Mater Res* **1993**, 8, 1179.
22. Lan T.; Pinnavaia T.J. *Chem Mater* **1994**, 6, 2216
23. Krishnamoorti R; Vaia R.A.; Giannelis E.P, *Chem Mater* **1996**, 8, 1728
24. Solomon M.J.; Almusallam A.S.; Seefeldt K.F.; Somwangthanaroj A.; Varadan P, *Macromolecules*, **2001**, 34, 1864
25. Hasegawa N.; Kawasumi M.; Kato M.; Usuki A; Okada A, *J Appl Polym Sci* **1998**, 67, 87
26. Kawasumi M.; Hasegawa N.; Kato M.; Usuki A.; Okada A, *Macromolecules* **1997**, 30, 6333
27. Manias E.; Touny A.; Wu L.; Strawhecker K.; Lu B.; Chung T.C, *Chem Mater* **2001**, 13, 3516.
28. Wang K.H; Choi M.H; Koo C.M; Choi Y.S; Chung I.J *Polymer* **2001**, 42, 9819
29. Liu X; Wu Q, *Polymer*, **2001**, 42, 10013
30. Mishra J.K; Hwang K.J; Ha C.S, *Polymer* **2005**, 46, 1995.
31. Singh R.P.; Singh A. *J Macromol Sci – Chem* **1991**, A28, 487
32. Singh R.P.; Sivaram S. *Adv Polym Sci* **1991**, 101, 169
33. Pandey J.K.; Singh R.P. *Biomacromol* **2001**, 2, 881.
34. Pandey J.K.; Kumar A.P, Singh R.P. *Macromol Symp* **2003**, 197, 411.
35. Prian L.; Barkatt A. *J Mater Sci* **1999**, 34, 3977.
36. Wool R.P.; in *Degradable Polymers: Principles and Applications* Ed. Scott G.; Gillead D, Chapman & Hall, London, **1995**, 138

Chapter 4

37. Pandey J.K.; Ahmed A.; Singh R.P, *J Appl Polym Sci* **2003**, *90*, 1009
38. Moad G. *Prog. Polym. Sci.* **1999**, *24*, 81
39. Roover B.D; Sclavons M.; Carlier V.; Devaux J.; Legras R.; Momtaz A, *J Polym Sci Part A: Polym Chem*, *33*, 829
40. Kumar. A.P, Depan. D, Singh. R.P, *J. Themoplas. Compos. Mater.* **2005**, *18*., 489
41. Blumstein A. *J Polym Sci A3*, **1965**, 2665.
42. Burnside S.D; Giannelis E.P. *Chem Mater* **1995**, *7*, 1597.
43. Tyan H.-L; Liu Y-C; Wei K.-H. *Chem Mater* **1999**, *11*, 1942
44. Amash A; Zugenmaier P. *Polymer* **2000**, *41*, 1589
45. Scott G.; in *Atmospheric Oxidation and Antioxidants*, 1st edn, Elsevier, **1965**, 272
46. Scott G.; in *Degradable Polymers, Principles and Applications* Ed. Scott G.; Gillead D, Chapman & Hall, London, **1995**, 3
47. Bharadwaj R.K; Mehrabi A.R; Hamilton C; Trujillo C; Murga M; Fan R; Chavira A; Thompson A.K. *Polymer* **2002**, *43*, 3699
48. Tidjani A; Wald O; Pohl MM; Hentschel MP; Schartel B., *Polym Degrad Stab* **2003**, *82*, 133
49. Leszczyńska A.; Njuguna J.; Pieliowski K.; Banerjee J.R, *Thermochimi Act* **2007**, *453*, 75
50. Xie W.; Gao Z.M.; Pan W.P.; Hunter D.; Singh A.; Vaia R.A., *Chem. Mater* **2001**, *13*, 2979
51. Zheng X.; Wilkie C.A.; *Polym Degrad Stab* **2003**, *82*, 441
52. Messersmith P.B; Giannelis E.P. *Chem Mater* **1994**, *6*, 1719
53. Messersmith P.B; Giannelis E.P. *J Polym Sci, Part A: Polym Chem* **1995**, *33*, 1047
54. Kazayawoko M; Balatinez J.J; Matuana L.M; *J Mater Sci* **1999**, *34*, 6189
55. Keener T.J; Stuart R.K; Brown T.K. *Compos Part A: Appl Sci Manuf*, 2004, *35*, 357
56. Bicerano J, *Prediction of Polymer Properties (III ed.)*, Marcel Dekker Inc., New York **2002**, 403
57. Kramer E.J, *Adv Polym Sci* **1983**, *52–53*, 1
58. Qiu W; Zhang F; Endo T; Hirotsu T. *J Appl Polym Sci* **2003**, *87*, 337
59. Tsagaropoulos G; Eisenberg A. *Macromolecules* 1995, *28*, 6067
60. Cicchetti O, *Adv Polym Sci, Fortschr Hochpolym-Forsch* **1970**, *7*, 70
61. Mellor, D.C.; Moir A.B.; Scott G., *Europ. Polym. J*, **1973**, *9*, 219
62. Morlat S.T.; Mailhot B.; Gonzalez D.; Gardette J-L, *Chem Mater.* **2005**, *17*, 1072
63. Qin H.; Zhao C.; Zhang S.; Chen G.; Yang M. *Polym. Degrad. Stab.* **2003**, *81*, 497
64. Morlat S.T.; Mailhot B.; Gardette J-L.; DaSilva C.; Haidar B.; Vidal A., *Polym. Degrad. Stab.* **2005**, *90*, 78
65. Osawa Z. *Polym. Degrad. Stab.* **1988**, *20*: 203
66. Morlat, S.; Mailhot, B.; Gonzalez, D.; Gardette, J.-L. *Chem. Mater.* **2004**, *16*, 377
67. Billingham N.C, in *Atmospheric Oxidation and Antioxidants*, Ed. Scott, G. 2st edn, II, Elsevier Science Publishers, Amsterdam. **1965**, Chapter 4
68. Lewin, M.; Tang, Y. *Macromolecules*, **2008**, *41*, 13
69. Pabiot, J.; Verdu, J. *Polym. Eng. Sci.* **1981**, *21*, 32.
70. Naddeo, C.; Guadagno, L.; Luca, S. D.; Vittoria, V.; Camino, G. *Polym. Deg. Stab.* **2001**, *72*, 239.
71. Raab, M.; Kotulak, L.; Kolarik, J.; Pospisil, J. *J. Appl. Polym. Sci.* **1982**, *27*, 2457.
72. Albertsson A.C.; Andersson S.O.; Karlsson S, *Polym Degrad Stab*, **1987**, *18*, 73

**Improvement of properties of cellulose reinforced starch
composites by photo-induced crosslinking***

* Bioresource Technology, **2008**, (DOI No: 10.1016/j.biortech.2008.04.045)

5.1.Introduction

Starch, which consists of amylose (linear) and amylopectin (branched), contains repeated units of α -1-4 linked D-glucose. Starch is not truly a thermoplastic like most synthetic polymers, but it can be melted / processed using conventional plastic processing equipments with the addition of water and / or other plasticizers (e.g. polyols) and made to flow at high temperatures under pressure and shear^{1, 2}. If the mechanical shear becomes too high, then starch will degrade to form low molecular weight products. This results from the glass transition temperature (T_g) and melting temperature (T_m) of pure dry starch, which have been estimated to be 230 °C and 220-240 °C, respectively³⁻⁵. In order to extrude or mold an object from starch, it should be converted into thermoplastic starch (TPS) by the addition of plasticizers. Considering the performance of these materials, starch is still poor thermoplastic because of its water absorption, brittleness (in absence of plasticizer), and dependence of mechanical properties on environmental conditions esp. relative humidity⁶. The aging of hydrophilic polymers is caused by sorbed water molecules, which enhance the molecular motions. Blending and / or reinforcing with some synthetic polymers are, few ways to improve material properties⁷⁻¹¹. However, still, mechanical properties and inherent biodegradability were dramatically affected^{12,13}.

The chemical modifications such as esterification, etherification, grafting and crosslinking are able to limit the excessive water uptake and macromolecular reorganizations (aging)¹⁴⁻¹⁵. Radiative grafting processes using high-energy sources such as gamma irradiation¹⁶ and electron beam^{17, 18} have been restricted with vinyl monomers. Classical crosslinking treatments have been performed by treating crosslinking agents (epichlorohydrin, sodium trimetaphosphate, phosphoryl chloride) with granular starch in dry / semi-dry media¹⁹⁻²¹. The photosensitized crosslinking of polyethylene oxide, polyphosphazene (using benzophenone) and polyvinyl alcohol (using benzoic acid derivatives) resulted insoluble materials in the solvents in which they were originally soluble²²⁻²⁴. Recently, Delville et al.²⁵ have successfully prepared the homogeneously cross-linked starch material using sodium benzoate as photo-sensitizer.

On the other hand, Dufresne et. al.^{1, 2, 6, 26,27} demonstrated that an alternative way to improve the thermo-mechanical properties and to decrease the water sensitivity of starch-based systems with retained biodegradability, is the use of cellulose fibers as natural and

biodegradable filler. As it is seen earlier in Chapter 1, the inter- / intra-molecular hydrogen bonds result the linearity, the stiffness, the rigidity, strength and ultimately to form thread like material called micro-fibrils that are apparently bound to form natural fibers. Recently, the consumption of natural fiber-reinforced composites has been skyrocketed not only for environmental concerns but also for yielding a unique combination of high performance, reactive surface, great versatility and processing advantages at relatively favorable cost. However, such fibers are used only to a limited extent in industrial practice, which may be due to the difficulties in achieving acceptable dispersion levels. For water-soluble polymers like starch, PVA and latex, the aqueous suspension of cellulose is reported to be better choice of reinforcement for achieving higher level of dispersion^{1,6, 26-29}. In the present study, we have combined both the approaches of reinforcing starch with aqueous suspension of microcrystalline cellulose and photo-crosslinking of matrix. The effect of photo-irradiation on sorption behavior, physical, thermal and mechanical properties is focused.

5.2. Experimental

5.2.1. Materials

The sodium benzoate (photo-sensitizer) and the maize starch (amylopectin / amylose ratio: 76 / 24 and moisture content: ~ 15%) were purchased from M/s SD Fine Chemicals, Mumbai, India. Microcrystalline cellulose powder was obtained from M/s LOBA Chemie, Mumbai, India.

5.2.2. Preparation and Photo-Irradiation of Composite Films

Keeping the starch/cellulose ratios as 100/0, 95/05, 90/10, and 85/15 (relative to dry starch, with a total mass of 2g) the weighed amount of starch and microcrystalline cellulose were separately dispersed in 20 ml and 10ml of deionized water, respectively, for 24 hr (Table 5.1). The dispersed starch heated up to 75-80 °C for 15-20 min and glycerol was added and heated up to 100-105 °C under pressure for 1.5 h to plasticize starch. The dispersed cellulose was slightly heated and transferred into plasticized starch and heated up to 100-105 °C under pressure for another 1 hr with rigorous stirring. Sodium benzoate (0.15%) was added as photo-initiator.

Table 5.1: Formulations of the composites prepared*

S.No	Starch (wt. %)	Cellulose (wt. %)	Glycerol (wt. %)	Glycerol / Starch+ Glycerol	Sample code
1.	100	-	30	0.23	NeatSt
2.	95	5	30	0.24	StCell5
3.	90	10	30	0.25	StCell10
4.	85	15	30	0.26	StCell15

* Where sodium benzoate 0.15 wt. % (of 2g)

Prior to casting the films, the suspension was cooled down to 85-90°C and degassed with stirring by vacuum. The composite films were prepared from starch-cellulose aqueous suspensions by casting on glass plates, drying at 50-60 °C (to avoid retrogradation). The slower drying (below 40 °C) resulted in hazy films, which may be due to reorganization of starch molecules and agglomeration of cellulose micro-fibers. The casted films were irradiated under medium-pressure mercury vapor lamps (400W) supplying radiation longer wavelength than 290 nm for relevant time. The atmospheric temperature was maintained by water circulation about 60 °C. After irradiation, they were stored in a desiccator with relative humidity 43 ± 0.5 % using (ASTM E 104-1985) saturated solution of potassium carbonate (K_2CO_3) for 2-3 weeks.

5.2.3. Characterization

5.2.3.1. Water Absorption

Water absorption was measured by storing under 100 % relative humidity. Weights are measured using *Prescisa 205 A* SCS, Switzerland, with 0.0001 g accuracy. The specimens of irradiated films were dried at 110°C in vacuum oven for 12 hr till their constant weight (W_1). Then, they were conditioned at 100% relative humidity at 25 ± 2 °C using a closed vessel containing water in its interior for 2-3 days till the specimen reach constant weight (W_2). The water absorption (%) at 100% RH was calculated using the formula $(W_2 - W_1 / W_1) \times 100$.

5.2.3.2. Swelling Degree and Gel Fraction Measurement

Photo-crosslinking was characterized by swelling behavior in dimethylsulphoxide (DMSO) in which neat starch is completely soluble. The conditioned films were weighed (W_i) and immersed in 20-25ml of DMSO at room temperature ($25 \pm 2^\circ\text{C}$) for 24 h. The swollen films were carefully wiped with clean cloth and weighed (W_s). For the extraction of DMSO, the swollen films were immersed in water and then in ethanol (for 2-3 times). This fraction was dried in vacuum oven till it reached constant weight (W_d). The degree of swelling (as ratio) was calculated using following formula: $(W_s - W_d) / W_d$

Then, gel fraction (%) was calculated using following formula: $(W_d / W_c) \times 100$

Where W_c represents dry weight of starch and cellulose and is calculated by subtracting the water, glycerol content (%) from W_i (considering the weight % of sensitizer is to be negligible). Average value out of four measurements is reported here for each composition.

5.2.3.3. Thermal Analysis

Differential scanning calorimetric (DSC) analysis of conditioned specimen was performed using TA Instruments-DSC-Q100 in temperature range from -50 to 200°C with a heating rate of $10^\circ\text{C min}^{-1}$ under nitrogen flow (25ml min^{-1}). Thermal gravimetric analysis (TGA) was done using Perkin-Elmer TGA-7 by heating from 50°C upto 600°C with a heating rate of $10^\circ\text{C min}^{-1}$ under nitrogen flow rate of 20ml min^{-1} .

5.2.3.4. Mechanical Properties Measurement

For tensile properties testing, specimens were cut according to IS: 2508-1984:A4 and their static tensile behavior was investigated at room temperature ($27 \pm 2^\circ\text{C}$) and $57 \pm 5\%$ relative humidity using a Universal Testing Machine (Instron model 4204) at crosshead speed at 10 mm/min . Average value out of six measurements is reported here for each composition.

5.2.3.5. Microscopic Analysis

The dimensions of fibers were measured using optical microscope (Olimpus, Model Bx50 F4, Japan) with x50 magnification.

5.3. Results and Discussion

5.3.1. Characterization

Figure 5.1a shows the polarized optical micrograph of microcrystalline powder. The dimensions of microcrystalline cellulose fiber are $14 \pm 2 \mu\text{m}$ in diameter and $40 \pm 2 \mu\text{m}$ in length.

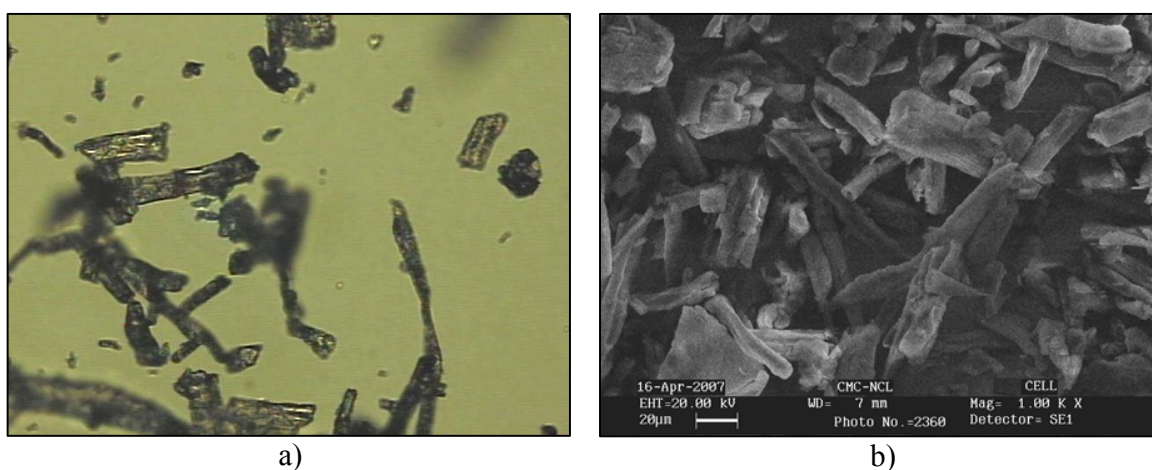


Figure 5.1: a) Polarized optical micrograph (x50 magnification) and b) scanning electron micrograph of microcrystalline cellulose powder

Figure 5.1b shows the scanning electron micrograph of cellulose fibers which are dispersed in water for 24h where slightly swelled and defibrillated fibers are seen after water dispersion.

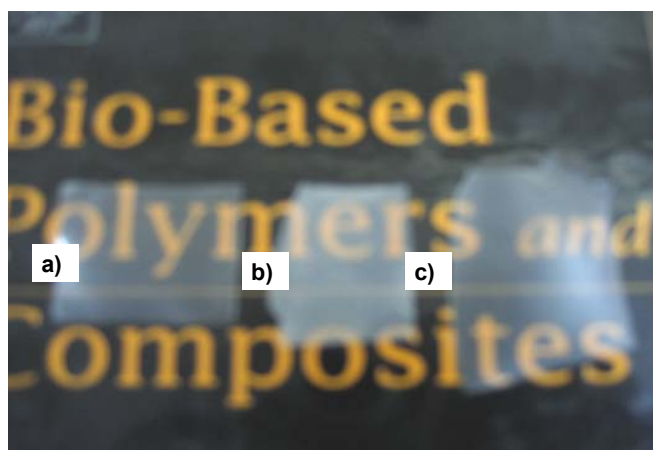


Figure 5.2: Picture of a) NeatSt (faster) dried at 50-60 °C and 20 min irradiated, b) StCell5 (slowly) dried at 30 °C and 20 min irradiated, and c) StCell5 (faster) dried at 50-60 °C and 20 min irradiated

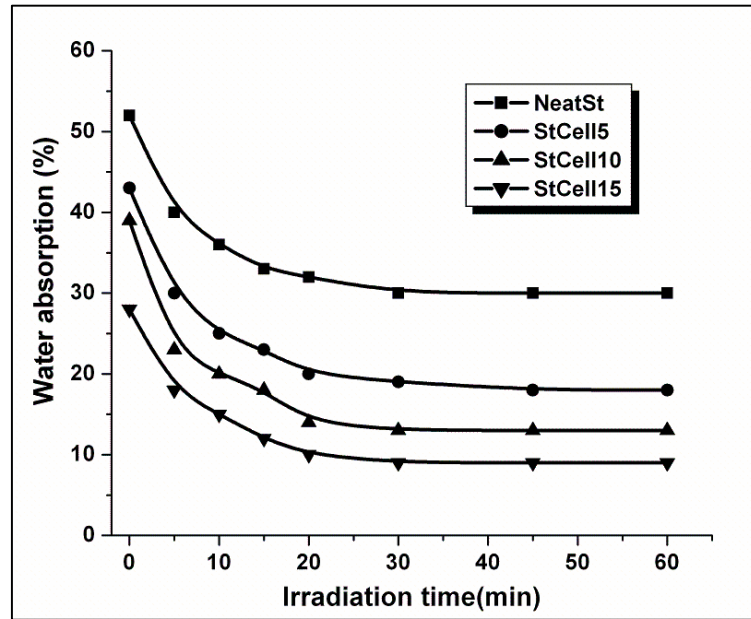
Chapter 5

Figure 5.2 shows the photograph of irradiated specimen of 'NeatSt' and 'StCell5'. The specimen a) shows the photograph of irradiated specimen of 'NeatSt'. The specimen b) is the slowly dried (at 30 °C) and 20 min UV irradiated one of 'Stcell5' whereas c) shows the rapidly dried (at 50-60 °C) and 20 min UV irradiated specimen of 'Stcell5'. It can be observed that the slowly dried and irradiated specimen is more opaque than others. This can be attributed to retro-gradation or macromolecular reorganization because of slow evaporation of solvent (water) at low temperature for long period of time.

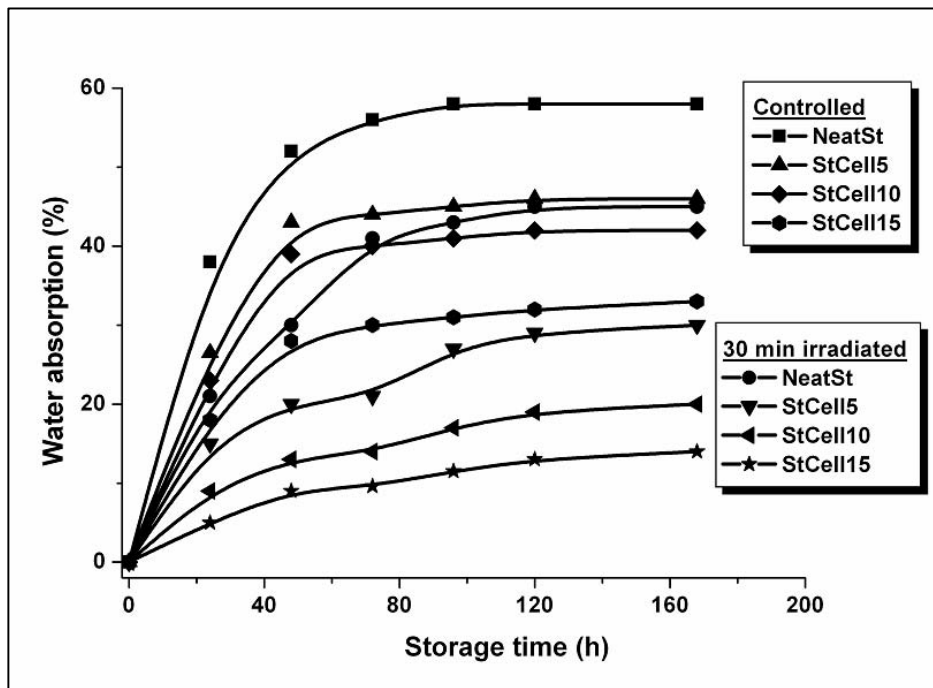
5.3.2. Sorption Behavior

5.3.2.1. Water Absorption Behavior

Figure 5.3 shows the water absorption behavior at 100% relative humidity of prepared composite films. Figure 5.3a depicts the water absorption of samples which are irradiated for different period of time after 48 h of storage under 100% relative humidity. By incorporation of microcrystalline cellulose fibers, the reduction in water uptake can be observed and the reduction was linear with increasing content of cellulose. This reduction may be due to insolubility and poor swellability of cellulose (*though it is hydrophilic*) in water in comparison of starch matrix. In the other words, the presence of completely immobilized cellulose fibers and partially immobilized amylopectin chains at the interface (explained below in DSC section) can also be attributed to the reduction in water absorption. In such a system, according to Tsagaroulos et. al.³⁰, with increasing content of fillers, the immobilized phases will also increase and the inclusion of water into these phases, will be very difficult. The effect of photo-irradiation can also be found as decrease in water absorption increasing time of UV irradiation. The plasticized starch (NeatSt) reaches its plateau level after 15 min of irradiation whereas composites reach after 20 min. Figure 5.3 b shows water absorption of samples as a function of storage time. It can be seen that after 1 week of storage, the water uptake of controlled and 30 min irradiated 'NeatSt' was about 58% and 45 %, respectively. The water absorption of controlled composite samples is lower than that of 'NeatSt' even after 1 week of storage. The plateau level of water absorption of controlled 'NeatSt' specimen was observed after 72 h, whereas, for 30 min irradiated specimen of 'NeatSt', it was shifted to higher storage time.



a)



b)

Figure 5.3: Water absorption % of samples a) after 48 h of storage as a function of UV irradiation time and b) as a function of storage time, under 100 % relative humidity

The irradiated composite samples have also shown the shift in time for reaching plateau level from that of controlled specimen. It can also be seen from the curves that rate of

water absorption of 30 min irradiated samples is slower than that of controlled ones. This may be due to the reduced functionality and increased integrity after photo-crosslinking.

5.3.2.2. Swelling Degree and Gel Fraction in Dimethylsulphoxide (DMSO)

Figure 5.4 shows the photograph of samples after 24 h soaking in DMSO. Figure 5.4a and 4b show the controlled specimen of ‘NeatSt’ and ‘Stcell5’ which are soluble in solvent. In Figure 5.4c, 30 min-irradiated specimen of ‘Stcell5’ was observed as insoluble film. Figure 4d shows the swollen gel of ‘Stcell5’, which is used further for calculating gel fraction before the extraction of DMSO and glycerol and drying.

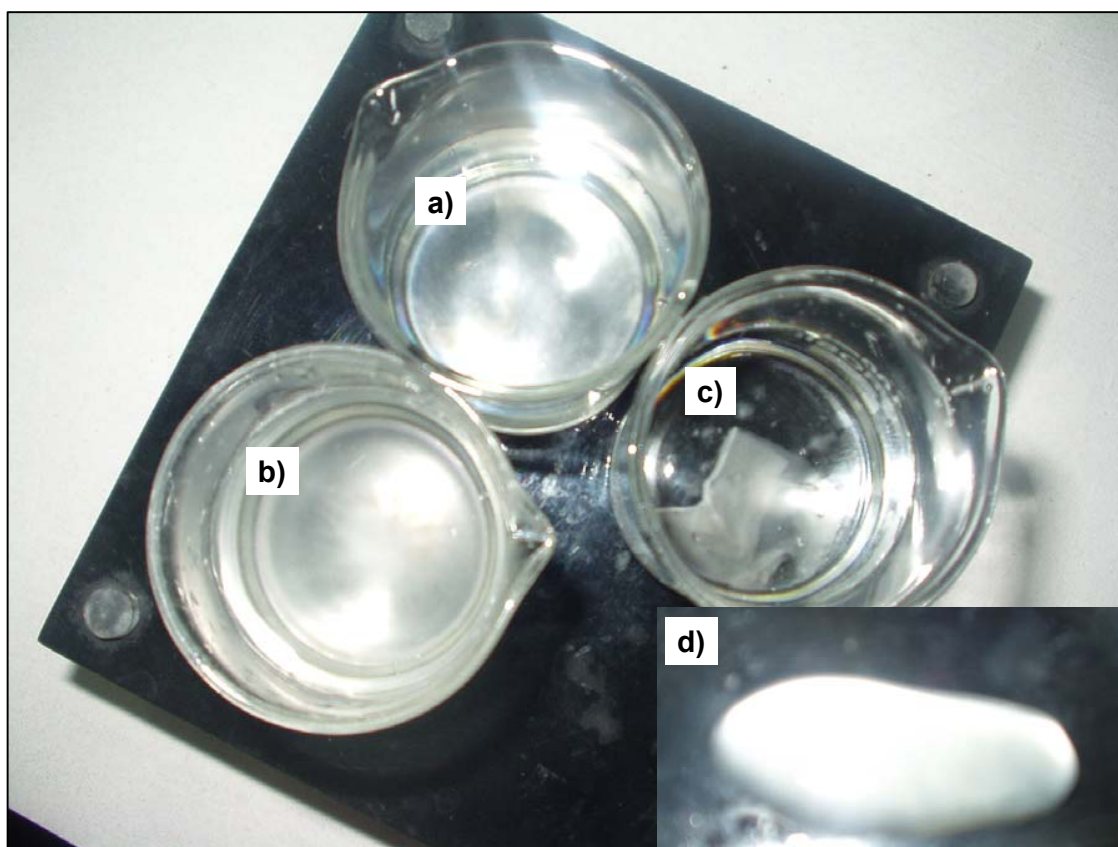


Figure 5.4: Picture of specimens of a) controlled ‘NeatSt’, b) controlled ‘Stcell5’, c) 30-min irradiated ‘Stcell5’ and d) swollen gel of c, after 24 h soaking in DMSO

Photo-crosslinking was characterized by calculating swelling degree and gel fraction. *Figure 5.5* shows the swelling degree (ratio) values of the samples after 24 h of immersion as a function of photo-irradiation time.

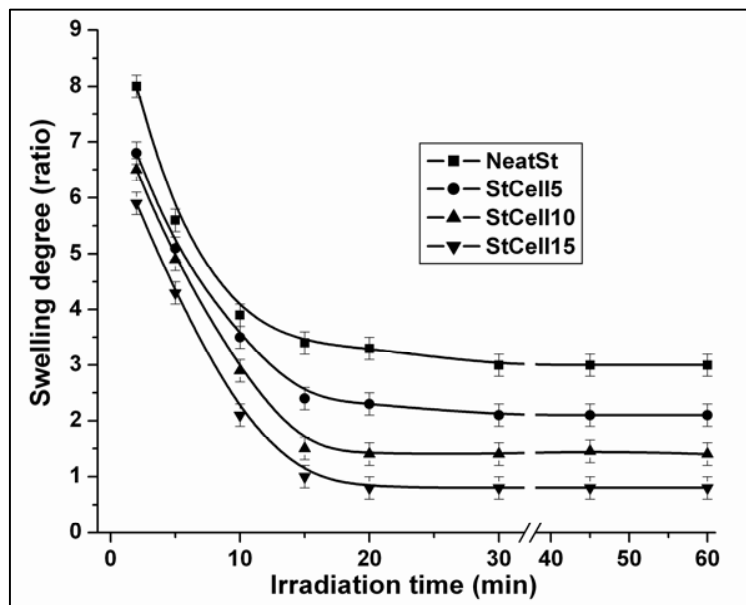


Figure 5.5: Swelling degree of prepared composite films as a function of irradiation time

The controlled samples were observed as soluble and their swelling degree was considered to be infinite. It can be observed that with increasing time of photo-irradiation, the swelling degree decreases and it reaches plateau level after 20 min of irradiation. The effect of cellulose reinforcement can also be seen as the reduction in the degree of swelling. *Figure 5.6* shows the effect of photo-irradiation on the gel fraction of irradiated films. Because of solubility of controlled films, the gel fraction values are not measured and considered to be zero. The photo-irradiation and cellulose reinforcement have been observed to increase the mass of gel fraction. It is well established that dispersion of cellulose fiber is better in plasticized starch matrix even up to 50% of cellulose loading ^{6, 26}, because of their chemical compatibility. The exact cause for decreased swelling degree and increased gel fraction of reinforced and irradiated samples is unclear. However, as mentioned above, the interactions between completely immobilized and partially immobilized phases can support the reduced swelling degree.

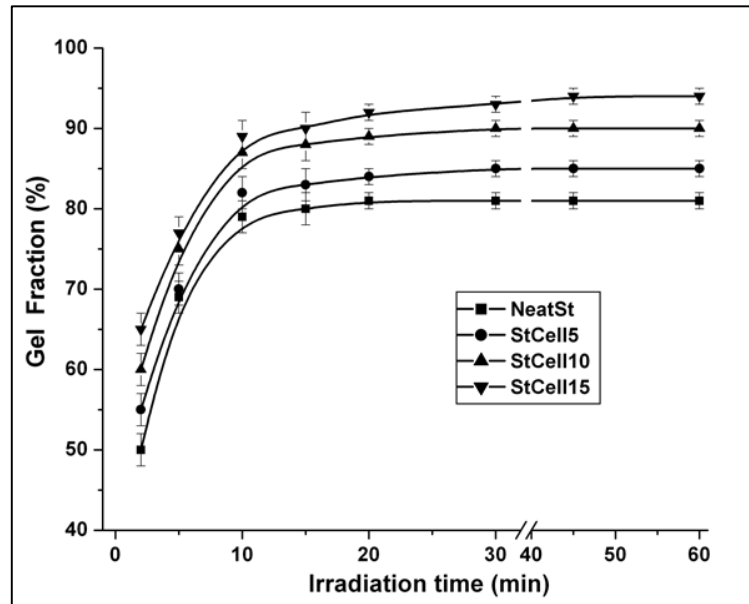


Figure 5.6: Effect of photo-irradiation on the gel fraction (%)

In such a photo-crosslinked system, insoluble cellulose fiber may either be trapped in between crosslinked starch matrix or cellulose itself participate in cross-linking with amylopectin or plasticizer through hydroxyl groups on fiber surface.

5.3.3. Thermal Properties

Figure 5.7 shows the thermogravimetric thermograms of composite samples.

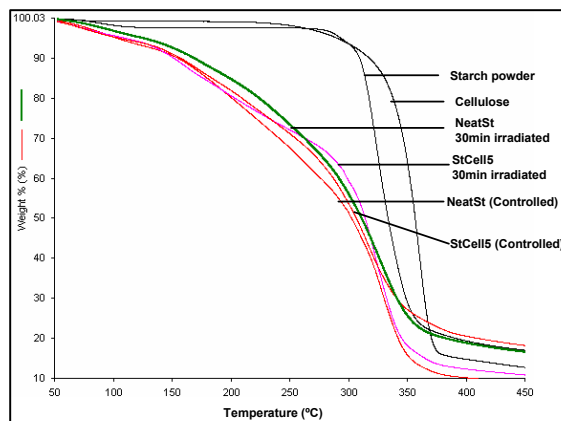


Figure 5.7: Thermal gravimetric (TGA) thermograms of controlled and 30min irradiated specimen of plasticized starch and composite films

It revealed that the thermal stability (maximum decomposition temperature of host matrix) was not significantly affected by both cellulose fiber reinforcement and photo-irradiation. The weight loss was observed from 95 to 360 °C, for all the samples.

5.3.3.1. Anti-Plasticization Effect

The differential scanning calorimetric (DSC) thermograms of composite films are shown in *Figure 5.8*.

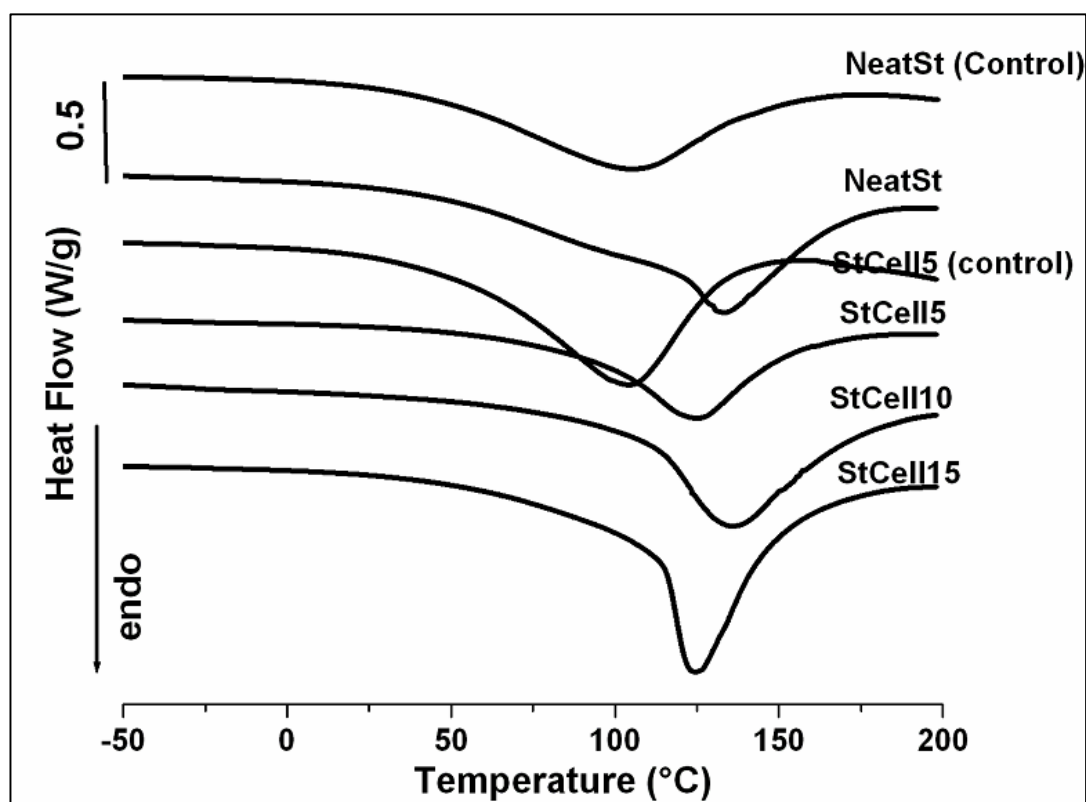


Figure 5.8: Differential scanning calorimetric (DSC) thermograms of controlled and 30min irradiated specimen of plasticized starch and composite films

A wide temperature range (from 9 to 168 °C) of melting endotherm can be observed for controlled NeatSt specimen with melting peak at 102.1 °C. According to Silverio et. al.³¹, starch could undergo two endothermal events which are melting of amylopectin between 50 and 120 °C and that of amylose between 120 and 170 °C. As reported elsewhere³², after 48 h of crystallization at 60 °C, plasticized starch exhibited the bimodal (at 70 and 110 °C) endotherm. In the present study, the obtained endotherm for controlled plasticized starch is

wide (9-168 °C), after 2 weeks of storage under 43 % relative humidity at room temperature which indicates that the moisture content tends to stabilize because of water-induced crystallization of amylopectin domains. The effect of incorporation of microcrystalline cellulose into plasticized starch matrix (StCell5 (control)) can be seen as shift in the melting endotherm range to 25-145 °C with peak at 105.3 °C. The increase in peak temperature can be attributed to anti-plasticization of amylopectin-rich domains by incorporating the cellulose microfibrils. According to Angles et. al.²⁷, the strong affinity of amylopectin molecules towards surface of cellulose fiber through high density of hydroxyl groups could reduce the global mobility of amylopectin domains. Earlier, it was demonstrated³³ that in the blends of poly(vinyl alcohol) (PVA) and hydroxypropylmethylcellulose (HPMC), glycerol showed selective partitioning into HPMC-rich phase in the system of 80% PVA / 20% HPMC. Thus, it can be understood that in the starch-cellulose composites, the migration of glycerol molecules towards surface of cellulose will be higher (than starch matrix). In such a system, at the interface, crystalline (ordered) coating of glycerol and amylopectin could result in restricted mobility on surface of cellulose fiber. This can be later confirmed in the tensile properties as increase in yield stress and decrease in elongation (%).

5.3.3.2.Reduction in Anti-Plasticization by Photo-Irradiation

It can also be observed that photo-irradiation (30 min irradiated NeatSt) has shifted the melting ending range (from 32 to 175 °C) with peak at 133 °C. These endothermic events were observed as bimodal events at 96°C and 133 °C. This observation is in concordance with earlier observation of Delville et al.³⁴, where the plasticized wheat starch film showed bimodal events after photo-irradiation and storage at higher relative humidity. For photo-irradiated 'NeatSt', the decrease in first melting peak from 102.1 °C to 96°C is due to reduced retrogradation of crosslinked amylopectin chains. The second melting peak has shown 30 % increase, which may be due to partial retrogradation of amylopectin. Thus, one can expect very high shifting for photo-irradiated samples cellulose-reinforced starch composites. However, only 18 % increase in the melting peak (124.33°C) endotherm with range 64-165 °C was observed for 30min irradiated StCell5 specimen. This can be

attributed to reduced retro-gradation of amylopectin chains³⁴. The reduced retro-gradation mechanism has been schematically represented in *Figure 5.9*.

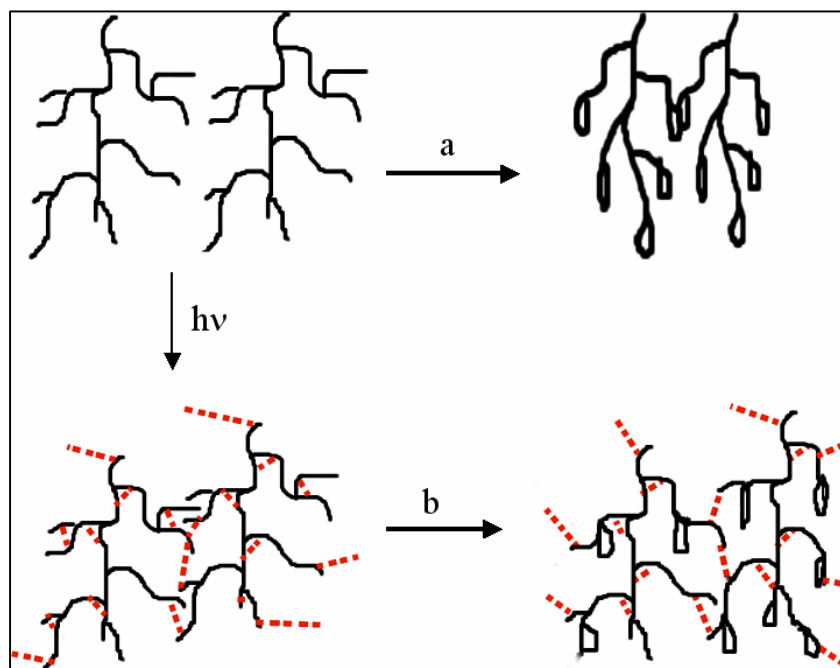


Figure 5.9: Schematic representation of reduced retrogradation a) plasticized amylopectin and b) photoirradiated amylopectin. Ovals / coils are to symbolize retrogradation and dotted lines represent inter-/ intra-molecular crosslinking

The uncrosslinked (a) plasticized amylopectin (in starch) undergoes macromolecular reorganization, because of plasticizer-induced mobility. The network formation by photo-induced crosslinking has been shown as dotted lines. It can be seen in b) that the retrogradation of amylopectin chains is lower / at slower rate.

5.3.4. Mechanical Properties

Figure 5.10 shows the effect of cellulose reinforcement and photo-irradiation and on tensile modulus that denotes the stiffness of the films. By comparing the controlled samples, it can be observed that the incorporation of microcrystalline cellulose has improved the tensile modulus linearly with increasing content. The effect of photo-

irradiation can be witnessed by comparing the modulus values of controlled and irradiated samples.

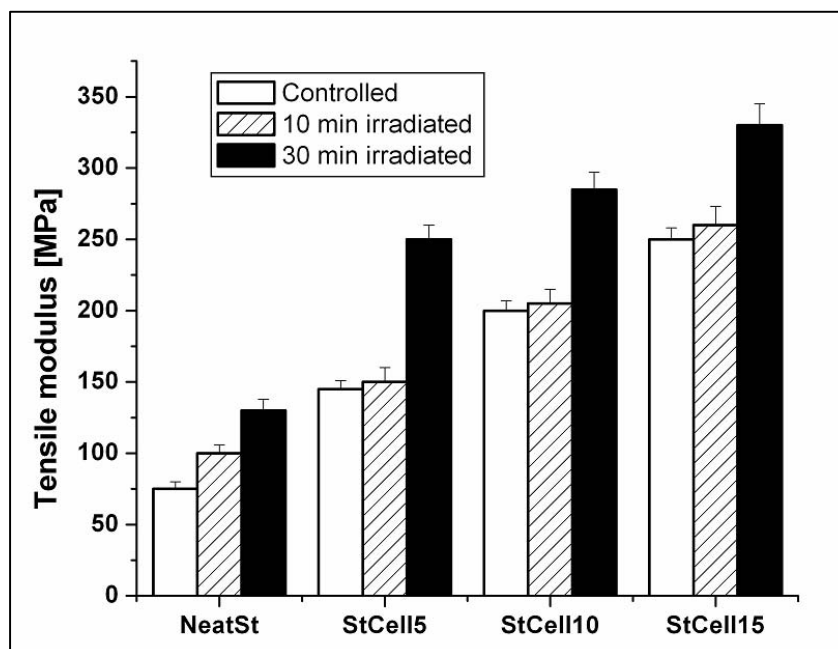


Figure 5.10: Effect of photo-irradiation on tensile modulus of composite films

In comparison of the controlled ‘NeatSt’, the improvement in modulus was observed to be about 33.33% and 73.33% for 10 and 30 min irradiated samples, respectively. For composite samples, The increase in modulus of 5, 10 and 15 wt. % cellulose reinforced samples which are irradiated for 30 min was found to be about 72.41%, 42.5% and 32%, respectively, in comparison of their corresponding controlled ones.

Figure 5.11 shows the effect of photo-irradiation on stress at break and yield stress. The stress at break (*Figure 5.11a*), which represents the ultimate tensile strength, can be observed to increase with increasing content of cellulose and time of photo-irradiation. The 10 min of irradiation on ‘NeatSt’ does not affect the value of stress at break significantly. Among all the samples, 30 min photo-irradiated samples have shown improved ultimate tensile strength. The same trend can also be found for the yield stress (*Figure 5.11b*), which is measure of hardness of materials. It has been improved by incorporation of cellulose as well as increasing time of photo-irradiation.

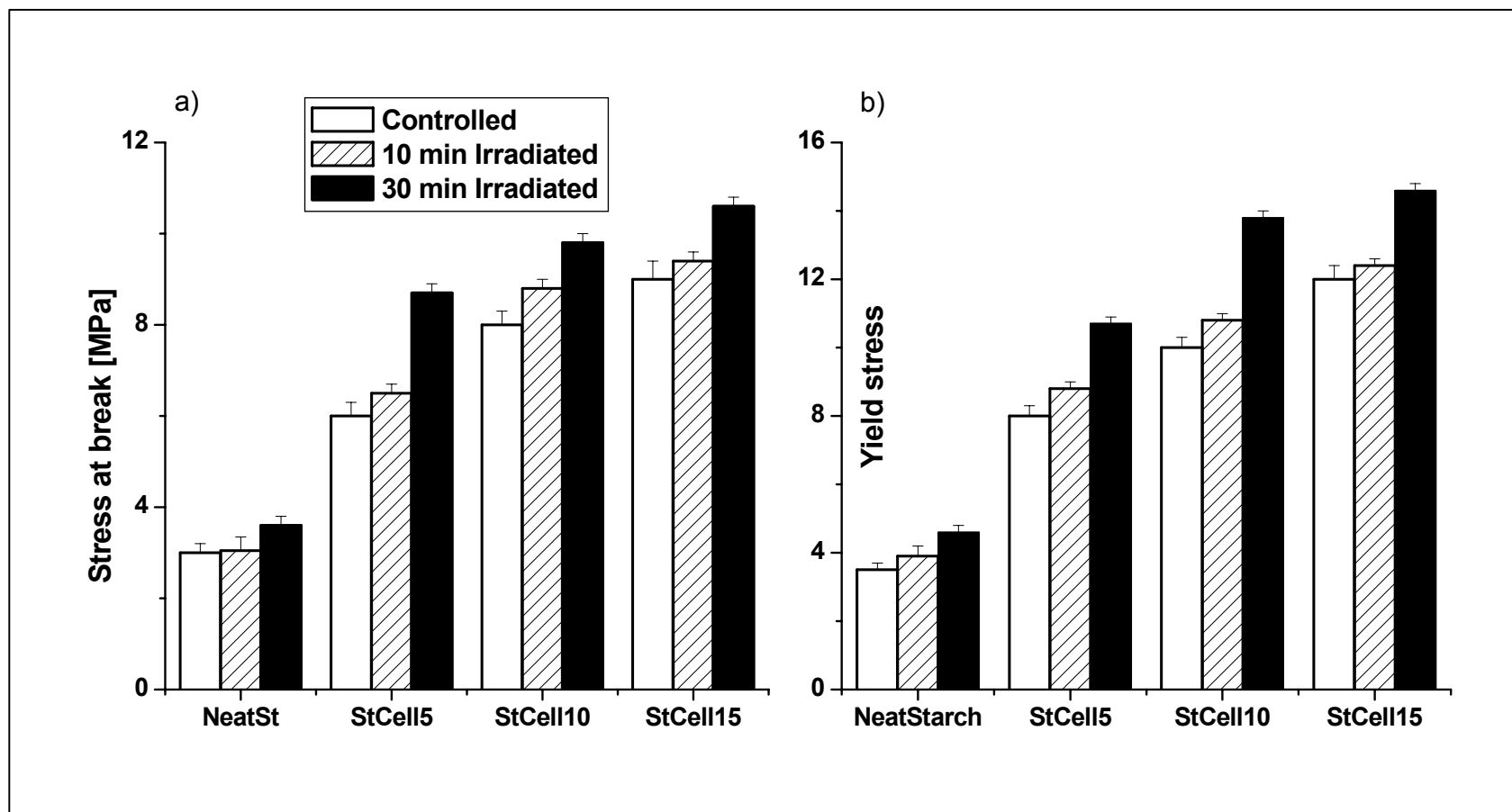


Figure 5.11: Effect of photo-irradiation on a) stress at break and b) yield stress

Figure 5.12a and b represent the elongation (%) of samples at break and yield point, respectively. The elongation (%) at break, which is directly related to toughness of the material, represents the deformation for complete breakage / failure of material whereas that at yield point represents the maximum deformation up to which the sample can withstand.

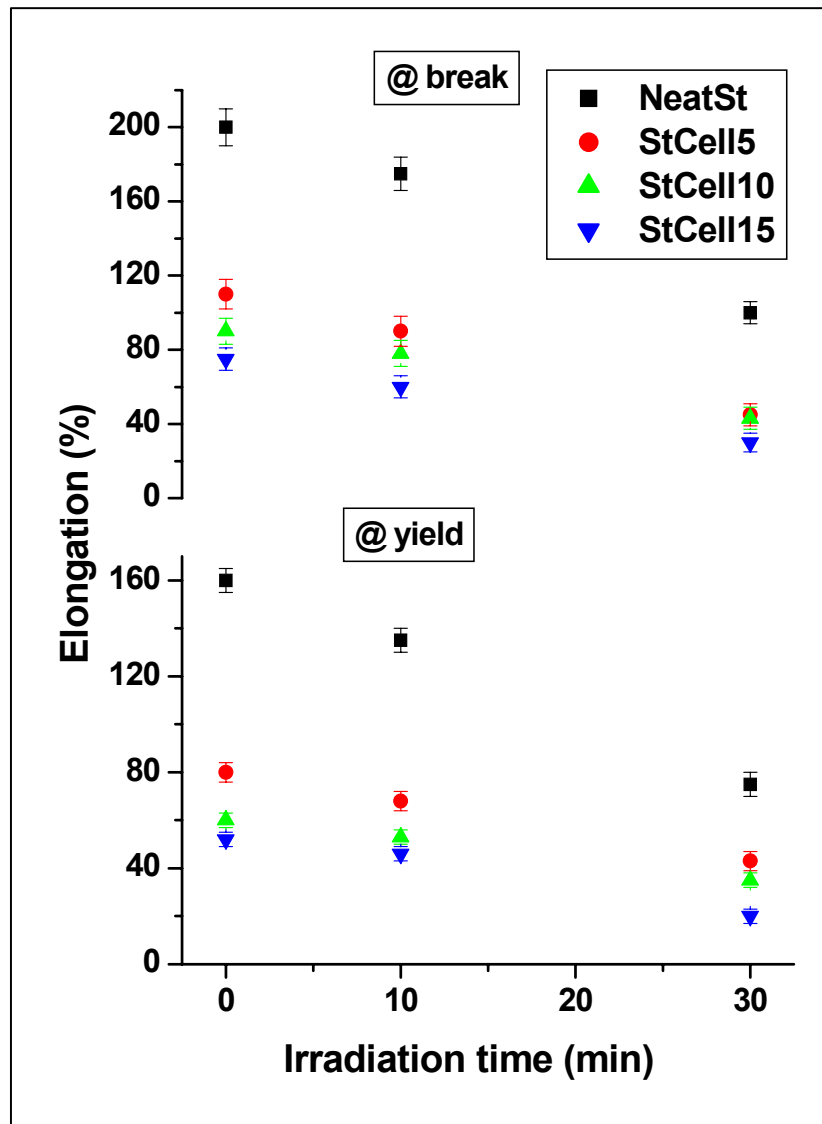


Figure 5.12: Elongation (%) a) at break and b) yield of controlled and (10, 30 min) irradiated composite films

Chapter 5

The elongation (%) values are found to decrease with increasing content of cellulose fiber and time of photo-irradiation. The gap between elongation (%) yield and break points was about 50 % for controlled plasticized starch. A well-defined yield point before the break point indicate the induced ductility by plasticizer i.e. glycerol. This gap is being reduced in case of photo-irradiated specimen as well as composite films. The controlled 'NeatSt' shows higher elongation (%) than others. It appears that during the tensile test under applied stress, the linear macromolecular chains may undergo three steps which are uncoiling, stretching and slippage. It is well known that starch consists of linear amylose and branched amylopectin. After plasticization with 30 % glycerol, the plasticizer molecules may allow these macromolecular chains to undergo stretching and slippage stages under stress. In case of composites, these stages might be reduced due to the transfer of applied stress to the fibers. The stress transfer, which can reduce the deformation of the host matrix, mainly depends on the interfacial interactions. The interfacial interaction between hydrophilic cellulose and plasticized starch is expected to be better²⁶⁻²⁷. The effect of photo-crosslinking has also been found to reduce the elongation (%) values. This reduction can obviously be attributed to the reduced mobility of macromolecular chains by inter- and intra-molecular hydrogen bonding and crosslinking. In other words, the applied stress is expected to be effectively transferred throughout the specimen because of network formation after photo-crosslinking. This phenomenon can be witnessed by the higher stress values at both yield and break points. However, the usefulness of the polymeric material in many applications is largely determined by its predominant failure mechanism under the conditions of applications. In the tensile test, the linear polymer films were believed to follow the craze failure mechanism which requires the mobility of molecular chains to absorb more energy while the fiber-reinforced composites could be considered to follow the crack mechanism³⁵. In this study, significant crazing / necking above the yield point was not observed. In case of composites, at higher deformation, the interface may become weak and act as 'stress concentrators' where failure mechanism initiated by causing the local stress in their vicinity to exceed the strength of the sample and ultimately the samples break. In case of photo-irradiated samples, the crosslinked 'net-points' may also act as 'stress concentrators'. These net points may be higher as it was observed by Delville et al.²⁵ in neat plasticized starch matrix containing 0.1 to 3 wt% of sodium benzoate with

Chapter 5

faster kinetics and lower degree of swelling. In general, the photo-irradiation was found to improve the mechanical properties of both the plasticized starch as well as composite films.

5.4. Conclusion

The microcrystalline cellulose-starch composites have been prepared by casting method using glycerol as plasticizer and photo-irradiated them using sodium benzoate as photosensitizer. Water absorption of the plasticized starch matrix was found to decrease after incorporation of microcrystalline cellulose as well as photo-irradiation. The controlled samples were soluble and photo-crosslinked samples were insoluble in dimethylsulphoxide. The swelling degree was found to reduce with increasing time of photo-irradiation and cellulose content. The increase in gel fraction was also observed for irradiated samples. The thermal transitions of photo-irradiated samples suggest the reduction in anti-plasticization. Improvement in tensile properties was observed drastically with increasing photo-irradiation time and cellulose content. Finally, it can be summarized that combination reinforcement with microcrystalline cellulose and photo-crosslinking of starch matrix has improved the physical and mechanical properties of plasticized starch. Since both the polymer matrix and fillers are biodegradable and derived from renewable resources, the prepared composite materials can be coined as '*green composites*'.

References

1. Dufresne A., Vignon M.R., *Macromolecules*, **1998**, 31, 2693
2. Mathew, A.P., Dufresne A., *Biomacromolecules*, **2002**, 3, 1101.
3. Orford P.D. Parker R., Ring S.G., Smith A.C., *Int J Biol Macromol* **1989**, 11, 91.
4. Russel P.L., *J Cereal Sci* **1987**, 6, 133.
5. Shogren R.L., *Carbohyd Polym* **1992**, 19, 83.
6. Dufresne A., Dupeyre, D., Vignon, M.R. *J Appl Polym Sci*, **2000**, 76, 2080
7. Westhoff, R.P., Otey, F.H., Mehlretter, C.L., Russell, C.R., *Ind. Eng. Chem. Prod. Res. Dev.* **1974**, 13, 123.
8. Griffin G.J.L., *Brit. Pat.* 1485833. **1972**.
9. Lenz R.W., *Adv. Polym. Sci.*, **1993**, 107, 1
10. Otey, F.H., Westhoff, R.P., Doane, W.M., *Ind. Eng. Chem. Prod. Res. Dev.*, **1980**, 19, 592.
11. Sen A., Bhattacharya M., *Polymer* **2000**, 41, 9177.
12. Ollett, A.L., Parker, R., Smith, A.C., *J. Mater. Sci.* **1991**, 26, 1351
13. Arvanitoyannis, I., Biliaderis, C.G., Ogawa, H., Kawasaki, N., *Carbohyd Polym*, **1998**, 36, 89
14. Fringant, C., Debrieres, J., Rinaudo, M., *Polymer*, **1996**, 37, 2663
15. Laignel B., Bliard, C. Massiot G., Nuzillard J.M., *Carbohyd Polym* **1997**, 298, 251.
16. Fanta, G.F., Burr, R.C., Doane, W.M. Russell, C.R., *J. Polym. Sci.: Symposia*, **1974**, 45, 89
17. Olivier A., Cazaux F., Gors C., Coqueret X., *Biomacromolecules*, **2000**, 1, 282
18. Zhai, M., Yoshii, K., Kume, T., *Carbohyd. Polym.*, **2003**, 52, 311
19. Kuniak. L, Marchessault R.H, *Die Stärke*, **1973**, 24, 110.
20. Woo K.; Seib P.A, *Carbohyd. Polym.* **1997**, 33, 263
21. Yook, C., Pek, U-A., Park, K-H., *J. Food Sci.* **1993**, 58, 405.
22. Doytcheva, M. Stamenova R., Zuetkov V., Tsevetanov, C.B. *Polymer* **1998**, 69, 6715.
23. Graves, R.; Pintauro P.N., *J Appl Polym Sci*, **1998**, 68, 827.
24. Takakura K.; Takayama G.; Ukida J, *J Appl Polym Sci* **1965**, 9, 3217.
25. Delville. J, Joly C., Dole P., Bliard C., *Carbohyd. Polym.* **2002**, 49, 71.
26. Mathew, A.P., Dufresne, A, *Biomacromolecules*, **2002**, 3, 609.
27. Angles, M.N., Dufresne, A., *Macromolecules* **2000**, 33 (22), 8344.
28. Averous L., Fringant C., Moro, L. *Polymer* **2001**, 42, 6565.
29. Averous, L., Boquillon, N., *Carbohyd. Polym.* **2004**, 56(2), 111.
30. Tsagaroulos, G., Eisenberg, A., *Macromolecules*, **1995**, 28, 6067.
31. Silverio, J., Svensson, E., Eliasson., A.C., Olofsson, G., *J. Therm. Anal.* **1996**, 47(5), 1179.
32. De-Meuter, P., Amelrijckx, J., Rahier, H., Van-Mele, B., *J. Polym. Sc. Part B: Polymer Physics*, **1999**, 37(20), 2881.
33. Sakellariou, P., Hassan, A., Rowe, R.C., *Colloid. Polym. Sci.*, **1994**, 272, 48.
34. Delville, J., Joly, C., Dole, P., Bliard, C., *Cabohyd. Polym.*, **2003**, 53, 373.
35. Kramer, E.J., *Adv. Polym. Sci.*, **1983**, 52/53, 1.

**Preparation and Characterization of Bionanocomposites based
on Cellulose esters and Clay**

6.1. Introduction

Biopolymers currently achieve high interest in materials science since they offer reductions of landfill space during waste management as well as new end-user benefits in various fields of applications¹⁻². Among these materials, those from renewable resources such as polysaccharides additionally offer CO₂-neutrality, partial independence from petrochemistry-based products and the exploitation of nature's synthesis capabilities via photosynthesis³⁻⁴. Cellulose, being a constituent of wood, is regenerated in much larger quantities than starch by natural photosynthesis from CO₂ and water⁵. The very substantial, but so far little exploited category of cellulose-based materials, which has led to some of the very first industrial polymer-products such as celluloid and cellophane still offers numerous new possibilities for polymeric materials⁶⁻⁷. Basically two main groups of cellulose-materials can be distinguished: regenerated celluloses are suitable only for fibre and film production from conventional and new processes. Secondly, melt-processable cellulose derivatives such as esters can be used for extrusion and molding⁸. Cellulose ester plastics have, however, continued to satisfy significant marketplace needs and their properties have continued to attract interest⁹. In fact, cellulose derivatives were the basis of the original synthetic plastics. Nitrocellulose was first employed in film and cast applications in middle of the 19th century¹⁰. Cellulose acetate (CA) began to be used as a coating lacquer for airplane wings in World War I, and then as a spun fiber for clothing applications¹¹. It could readily be used to form many useful articles, including film, sheet, and molded objects. The mixed esters cellulose acetate propionate (CAP) and cellulose acetate butyrate (CAB), were introduced in the 1930s and 1940s as tougher versions of CA, that could be thermally processed at lower temperatures or with lower amounts of plasticizers¹²⁻¹³. The general characteristics of cellulose organic esters that are valuable in plastics applications include stiffness, moderate heat resistance, high moisture vapor transmission, grease resistance, clarity and appearance, and moderate impact resistance¹¹. They are very easy materials to extrude and injection mold, and so are appreciated by end users¹⁴. Some of the detrimental properties include a relatively narrow window between the melt flow temperature and the decomposition temperature, because of the relative lability of the polysaccharide backbone at high temperatures.

Chapter 6

In addition, there are some drawbacks in using external plasticizers while processing and usage such as leaching out of plasticizer apparently harms the environment¹⁵. This problem can be avoided in case of internal plasticizers. Thus, it will be worthwhile to graft low molecular weight polymer chains that can act as plasticizers and are also biodegradable¹⁶. On the other hand, in last decade, the reinforcement of nano-scale fillers has been found to improve the physical, thermal and mechanical properties with very low amount of loading. Among them, the polymer-layered silicate (PLS) based nanocomposites have received a great deal of interest from researchers and industrialists because of their low cost, abundance and high aspect ratio, which give greater possibility of energy transfer from one phase to another.¹⁷⁻¹⁸. Presumably owing to the synergistic effect of the nano-scale structure (high aspect ratio) and the maximized interactions (unique characteristics such as intercalation / exfoliation) between the filler and polymer molecule, these nanocomposites exhibit enhanced properties such as improved mechanical properties, heat stability, flame retardancy and gas barrier properties at very low level loading (5%).¹⁹⁻²⁰ The nanoscale fillers can be mixed with these thermoplastic cellulose derivatives with aid of plasticizers. Recently, Park et al.²¹ successfully used melt intercalation technique for the fabrication of cellulose nanocomposites from cellulose acetate (CA), triethyl citrate (TEC, as plasticizers) and organically modified clay.

In the present study both the approaches of grafting the biodegradable polymer chains on cellulose ester and reinforcing with nano-scale fillers have been combined to prepare bionanocomposites of cellulose esters. It has been portrayed in two parts.

6.2. Bionanocomposites from Polyethylene Glycolated Cellulose Esters and Organically Modified Montmorillonite

In the first study, the cellulose esters cellulose acetate (CA) and cellulose acetate butyrate (CAB) were grafted by polyethylene glycol (PEG) via urethane linkage. For this purpose, cellulose esters were reacted with isocyanate-terminated PEG prepolymer as shown in *Scheme 6.1*. The grafted copolymer was incorporated with organically modified montmorillonite to prepare nanocomposites. The preparation of nanocomposites was also performed by varying the sequence of addition of clay and prepolymer.

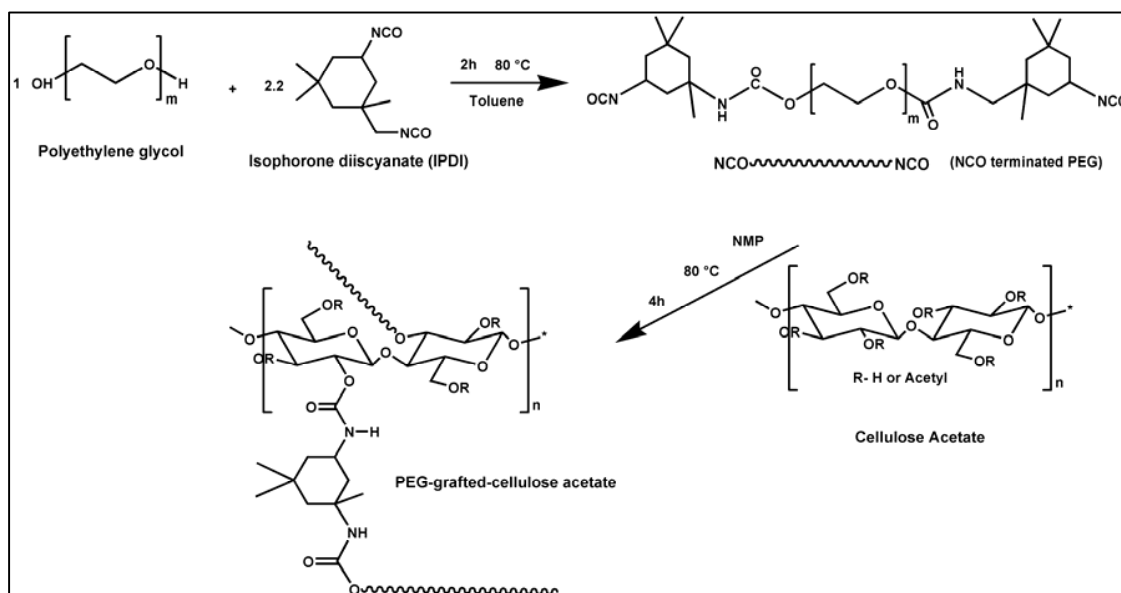
6.2.1. Experimental

6.2.1.1. Materials

Cellulose acetate (M_n : 30000; acetyl content; 39 wt. %), Cellulose acetate and butyrate (M_n : 30000; acetyl 12 wt. %, butyryl wt. 36%) were purchased from M/s Sigma-Aldrich, USA. Glycerol triacetate (Triacetin), was obtained from LOBA Chemie, India Polyethylene glycol – 600 (M_n 600), the solvents, N-methyl pyrrolidone (NMP), toluene, methanol, acetone and ethanol were obtained from M/s Merck (India) Ltd, Mumbai. Cloisite 30B, (C30B) a natural montmorillonite modified with hydrogenated tallow bishydroxyethyl quaternary ammonium salt, was purchased from Southern Clay Products. Inc., USA.

6.2.1.2. Preparation of Isocyanate-terminated Polyethylene glycol (PEG) Prepolymer

In a four necked round bottom flask equipped with nitrogen inlet, over-head stirrer and thermo-well, 2.2 part of isophorone diisocyanate (IPDI) was dissolved in toluene and heated up to 80 °C with continuous purging of nitrogen gas. The addition of polyethylene glycol (PEG) (1 part) was done drop-wise to this solution. The reaction was carried out for 2 h at 80 °C. The course of reaction was characterized by FTIR spectroscopy.



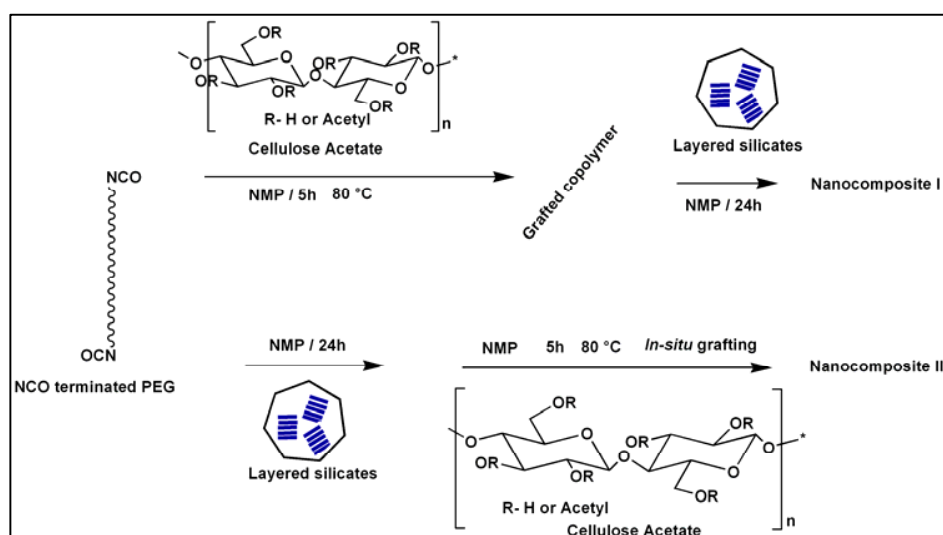
Scheme 6.1: Grafting reaction of polyethylene glycol on cellulose acetate via urethane linkage

6.2.1.3. Grafting of PEG on Cellulose Acetate:

To the dissolved cellulose acetate in N-methyl pyrrolidone (NMP), the isocyanate-terminated polyethylene glycol prepolymer was added. Keeping the solid: liquid ratio as 1:10, the reaction was performed at 80 °C for 4-5 h. The reaction was quenched and washed with methanol. This grafted copolymer was dissolved in NMP. For casting film, the mixture was poured on polypropylene (PP) petri dish and dried in vacuum oven at 60 °C for 12 h.

6.2.1.4. Preparation of nanocomposites

Two types of nanocomposites were prepared by changing the sequence of polymer addition as shown in *Scheme 6.2*. First type nanocomposites, the grafted copolymer was dissolved in NMP and C30B was dispersed in NMP for 24 h separately. Then both were mixed and casted. Second type of composites was prepared by, first dispersing C30B in isocyanate-terminated PEG for 24h, adding to dissolved cellulose acetate in NMP and heating at 80 °C for 3 h. After 5 h of reaction, the mixture was poured on petri dish and casted as films by drying in vacuum oven at 60 °C for 12 h. For comparison, using triacetin as plasticizer (25 wt%), the nanocomposite samples were prepared by solution casting method.



Scheme 6.2: Pathways for preparation of nanocomposites based on polyethylene glycolated cellulose acetate and clay

6.2.1.5. Characterization

6.2.1.5.1. FTIR Spectroscopy

The functional group analysis was done using FTIR Spectrum GX Perkin Elmer spectrophotometer. Infrared spectra of the samples were recorded in the range of 4000-400 cm^{-1} at a resolution of 4 cm^{-1} . A total of 15 scans were used for signal averaging.

6.2.1.5.2. NMR Spectroscopy

^1H and ^{13}C -NMR spectra of samples were recorded on a Bruker 200 MHz instrument with CDCl_3 for cellulose esters and grafted copolymer, acetone- d_6 for isocyanate-terminated prepolymer, respectively with tetramethylsilane as internal standard. For grafted copolymer, 1-2 drops of acetone- d_6 were additionally added for better solubility.

6.2.1.5.3. Wide Angle X-ray Diffraction

The wide angle X-ray diffraction (WAXD) pattern of sample was obtained using a Rigaku (Japan) Dmax 2500 X-ray diffractometer (Cu $\text{K}\alpha$ radiation with $\lambda = 0.154 \text{ nm}$, 40kV, 80 Am) at room temperature. The samples were scanned between $2\theta = 2$ to 30° at a scan speed of 2 $^\circ/\text{min}$.

6.2.1.5.4. Thermal Properties

Differential scanning calorimetric (DSC) analysis of prepared films was performed using TA Instruments-DSC-Q100 in temperature range from -50 to $200 \text{ }^\circ\text{C}$ with a heating rate of $10^\circ\text{C min}^{-1}$ under nitrogen flow (25ml min^{-1}). Thermal gravimetric analysis (TGA) was done using Perkin-Elmer TGA-7 by heating from 50°C up to 900°C with a heating rate of $10^\circ\text{C min}^{-1}$ under nitrogen flow rate of 20ml min^{-1} .

6.2.1.5.5. Dynamic Mechanical Properties

Dynamic mechanical properties of the samples were studied on casted films using a Rheometrics Dynamic Mechanical Analyzer model DMTA IIIIE, in the tensile mode. The samples were tested in a temperature range from -50 to 150°C at a heating rate of 5°C / min and frequency of 10 rads/sec.

6.2.1.5.6. Tensile Properties

Tensile specimens were cut according to ASTM D 412 and their static tensile behavior was analyzed at room temperature (27 ± 2 °C) and 57 ± 5 % relative humidity using a Universal Testing Machine (Instron model 4204) at crosshead speed at 10 mm min^{-1} . Average value out of six measurements is reported for each composition.

6.2.1.5.7. Biodegradation: Composting

The compostability of specimens ($3 \times 3 \text{ cm}^2$) was measured by incubating them in a laboratory-scale composting bin as described in Section 3.2.5.2, and by monitoring the change in weight of specimen periodically. The compostability was measured in terms of weight loss (%), which is calculated using the following formula:

$$\text{Weight Loss (\%)} = [(\text{Initial weight (g)} - \text{Final weight (g)}) / \text{Initial weight (g)}] \times 100$$

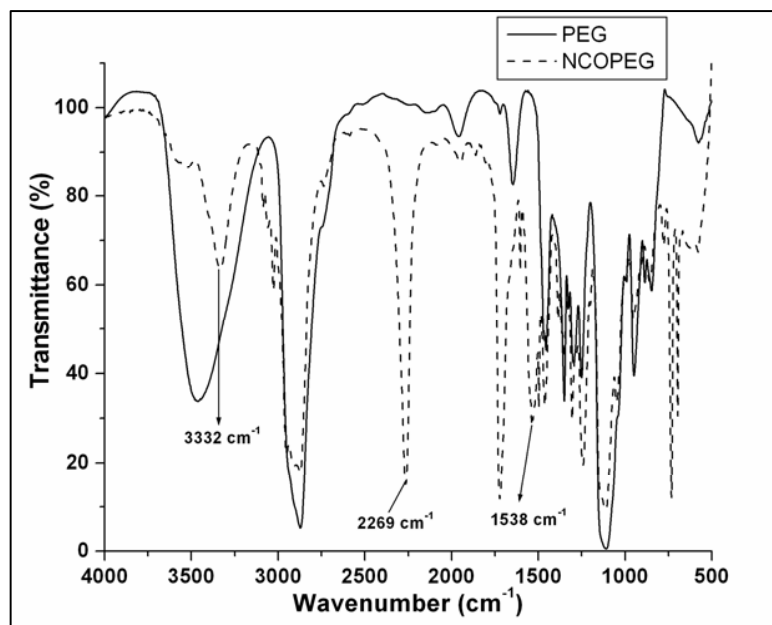
6.2.2. Results and Discussion

6.2.2.1. Synthesis of Isocyanate-terminated Prepolymer

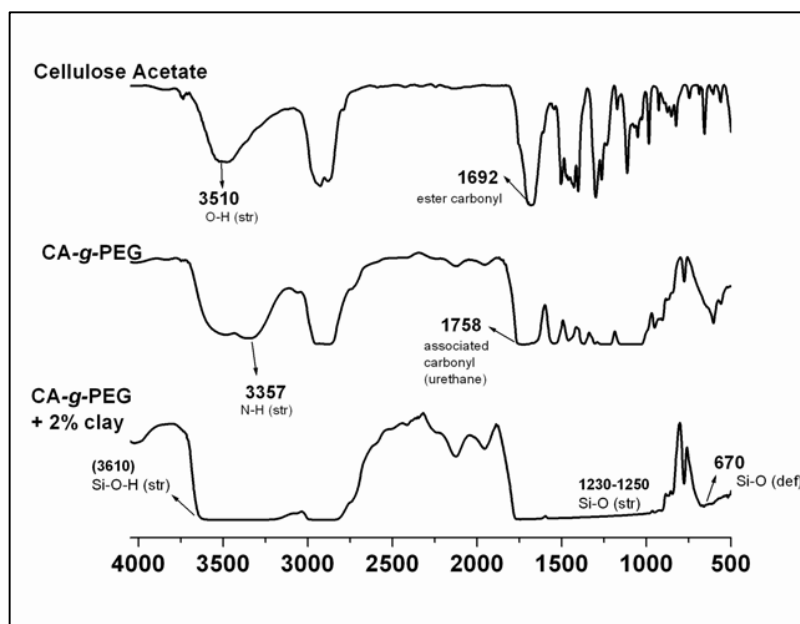
Keeping the composition of polyethylene glycol and IPDI as 1:2.2, the reaction was performed without any catalyst at 80 °C. The addition of PEG solution was done dropwise to prevent chain propagation and / or crosslinking. The FTIR and $^1\text{H-NMR}$ spectra of samples are shown in *Figure 6.1*, and *6.2*, respectively. The evolution of peak (in *Figure 6.1a*) at 3332 cm^{-1} and disappearance of peak at 3503 cm^{-1} which is for hydroxyl groups of PEG indicate the formation of urethane linkage. The peak at 2229 cm^{-1} is characteristic absorption for NCO groups, which are at terminal of the chains. $^1\text{H-NMR}$ spectra also confirm the reaction of NCO and OH of PEG and the presence of terminal NCO groups (*Figure 6.2a*). Owing to the difference in reactivity of primary and secondary isocyanates, IPDI is generally used for synthesizing polyurethanes with controlled structure. In presence of non-polar solvent like toluene the primary isocyanate will be more reactive than cycloaliphatic secondary isocyanate²². This reactivity difference can be reduced at higher temperature in presence Lewis acid catalyst²³.

6.2.2.1. Grafting of Isocyanate-terminated PEG with Cellulose Ester

Figure 6.1b shows the FTIR spectra of cellulose and cellulose acetate-g-polyethylene glycol.



a)

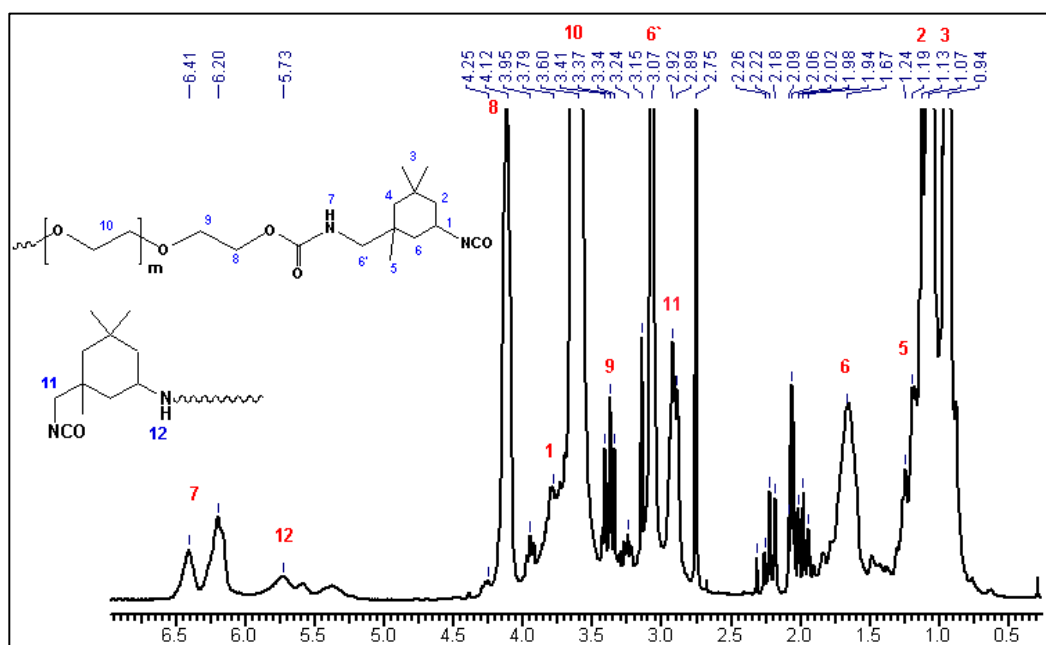


b)

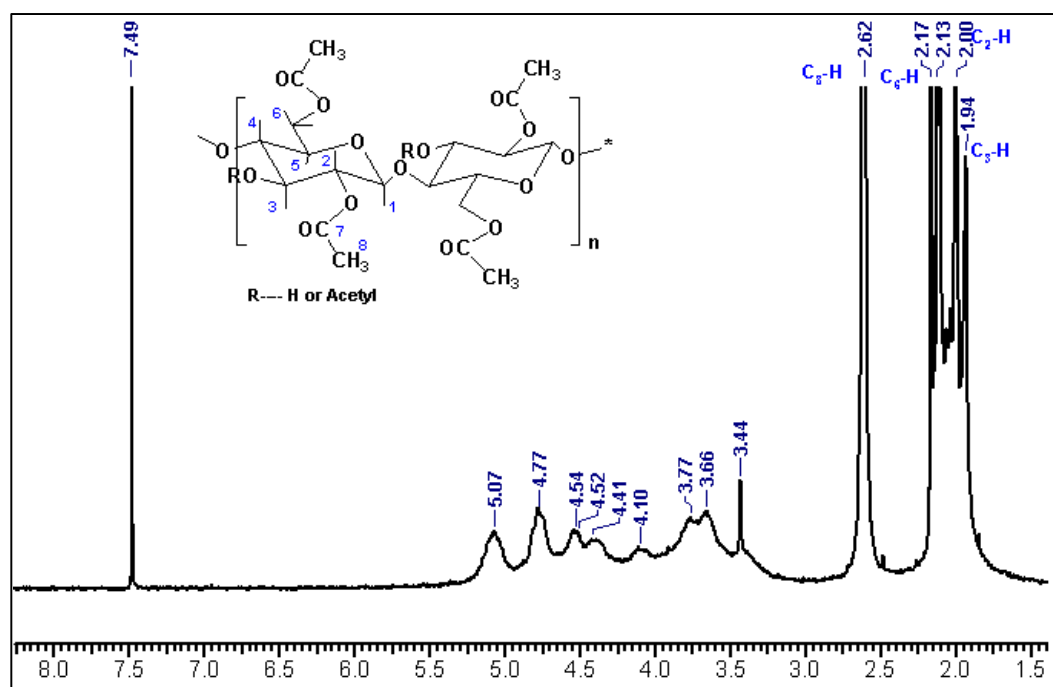
Figure 6.1: FTIR spectra of a) isocyanate terminated polyethylene glycol, and b) cellulose acetate and grafted copolymer

Chapter 6

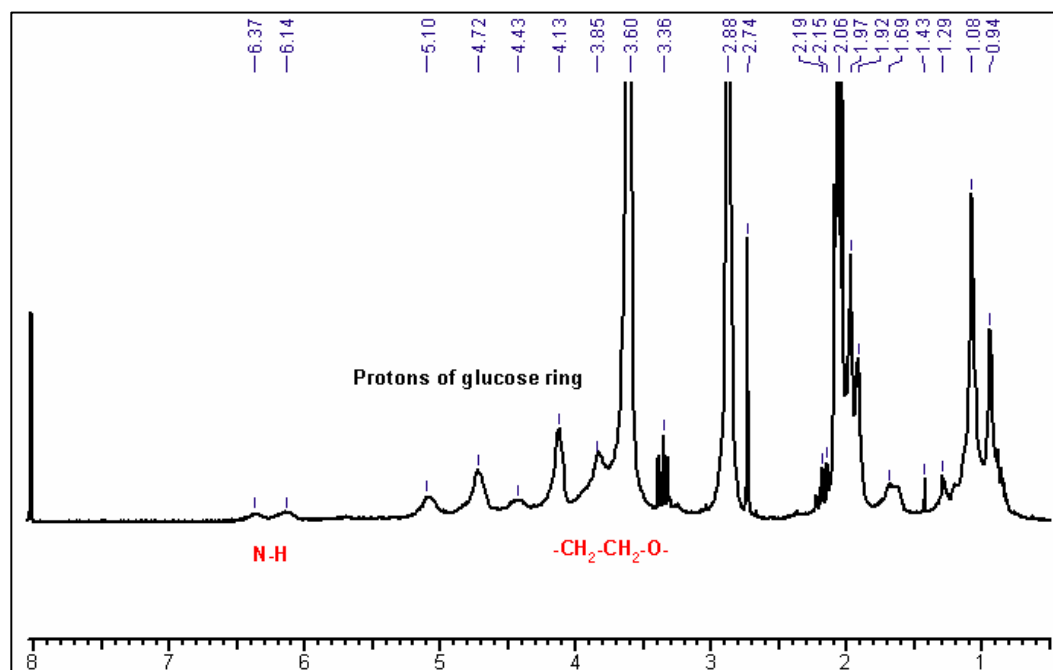
After the reaction between isocyanate-terminated PEG and cellulose acetate, the characteristic peak for isocyanate at 2230 cm^{-1} was diminished. The absorption bands at 3357 cm^{-1} and 1758 cm^{-1} which are assignable for NH of urethane and associated carbonyl groups of urethane, respectively, are also observed. The quantitative measurement showed the decrease in absorbance at 3510 cm^{-1} (assigned for hydroxyl group) indicating the reaction between NCO of isocyanate-terminated prepolymer and hydroxyl group of cellulose ester. This is also confirmed by $^1\text{H-NMR}$ spectra of grafted copolymer. In comparison of *Figure 6.2 a, b and c*, the formation urethane linkage in grafted copolymer can be observed.



a) Isocyanate terminated polyethylene glycol prepolymer



b) Cellulose acetate

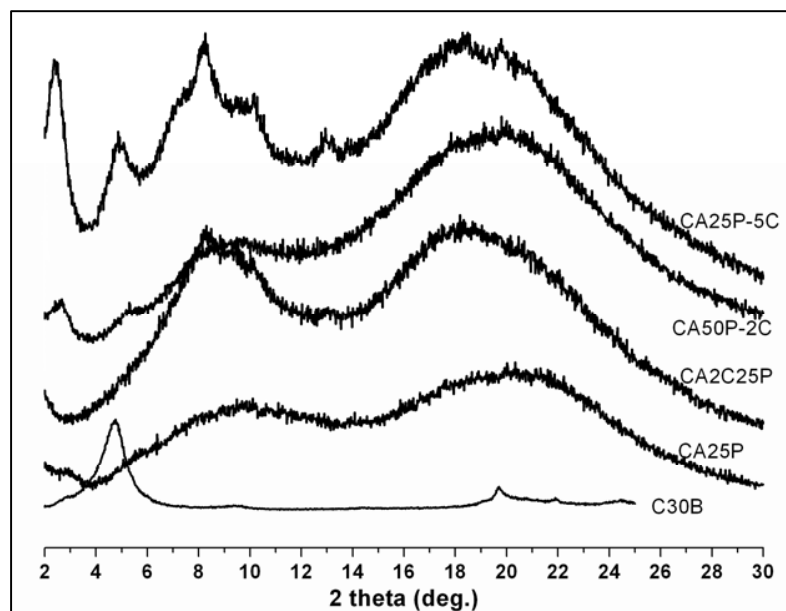


c) Grafted Copolymer

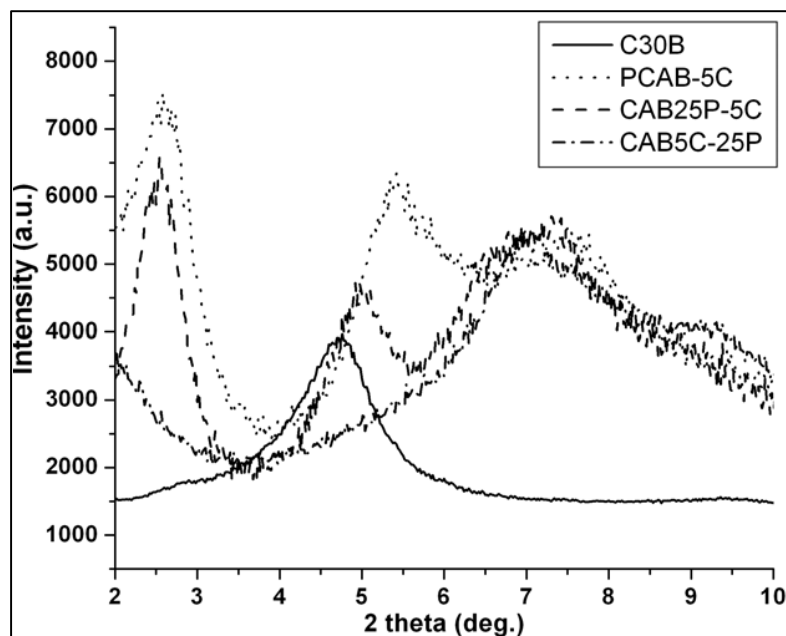
Figure 6.2: ¹H-NMR spectra of a) isocyanate terminated polyethylene glycol, b) cellulose acetate and c) grafted copolymer

6.2.2.3. Wide Angle X-ray Diffraction Pattern

The crystallographic interaction between clay and grafted copolymer can be seen as wide-angle X-ray diffraction (WAXD) patterns in *Figure 6.3*.



a)



b)

Figure 6.3: Wide angle X-ray Diffraction pattern of prepared samples of a) CA and b) CAB

Chapter 6

Typically, a shift in peak of 001 basal plane from higher angle ($2\theta = 4-6^\circ$) to lower angle ($2\theta = 1.5-3^\circ$) represents the d spacing between the silicate layers. The increase in the d-spacing indicates the crawling of macromolecular chains into the gallery of layered silicates which is generally called as 'intercalation', while delamination of these silicate layers from the gallery order can be called as 'exfoliation' for which no peaks at lower angles will be observed¹⁷. The interlayer d-spacing of 001 basal plane in the clay (C30B) was observed at $2\theta = 4.8^\circ$. In Figure 6.3a, the intercalation is observed in terms of expansion in this d-spacing for CA25P-5C and CA50P-2C in which clay (C30B) is incorporated after grafting. Similar intercalative interaction was observed for CAB25P2C, which is first grafted and later reinforced with C30B. However, the in situ grafted samples, CA2C25P and CAB2C25P have shown no peak or shifting of peak for 001 basal plane in the range from 2 to 5° . This can be either exfoliation or semi-exfoliation of layered silicates in nanocomposites.

6.2.2.4. Thermal Properties

Figure 6.4 shows the derivative thermogram of samples under nitrogen atmosphere. It can be seen that the onset degradation of plasticized sample starts at 100 °C. From plasticized sample (PCA) the externally added plasticizer (glycerol triacetate) decomposes around 150 °C. For the grafted copolymer the maximum degradation temperature was observed in the range from 367 to 376 °C.

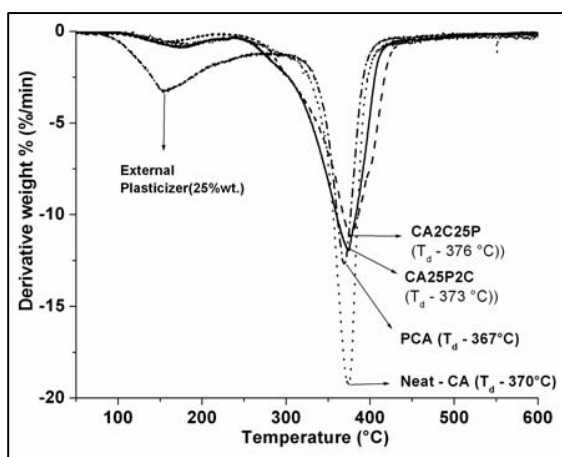
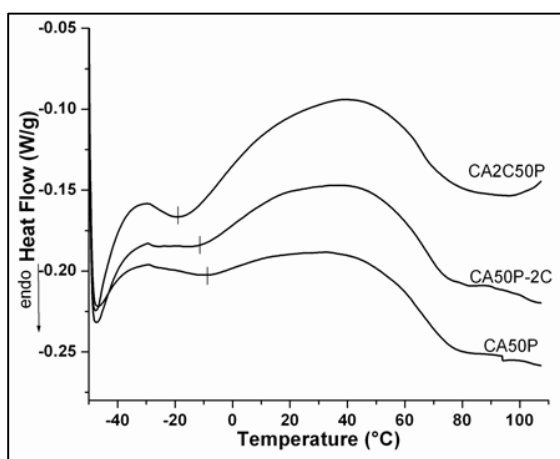


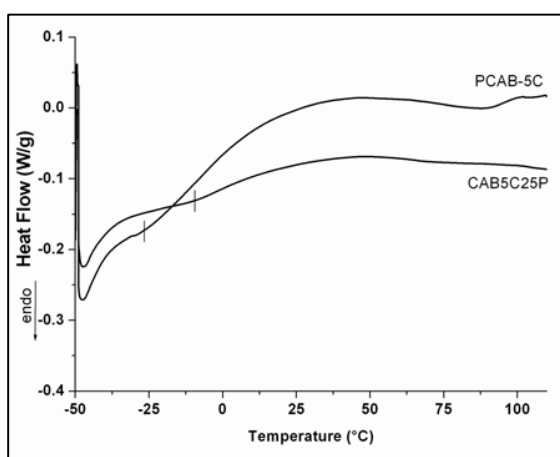
Figure 6.4: Derivative thermogram of samples

Chapter 6

All the prepared samples are flexible at room temperature and transparent. *Figure 6.5* shows the DSC thermogram (-50 to 110 °C) of the prepared films based on a) cellulose acetate and b) cellulose acetate butyrate esters. The first glass transition temperature for grafted copolymer was observed -9 °C without clay incorporation. The transitions for sample CA50P-2C, (first grafted then clay incorporated), CA2C50P (*in-situ* grafted) was observed at -12 °C and -21 °C. It can also be seen (in *Figure 6.5b*) that externally plasticized samples show lower transition than grafted copolymer. This can be attributed to the rigid linkage of urethane in the matrix.



a)

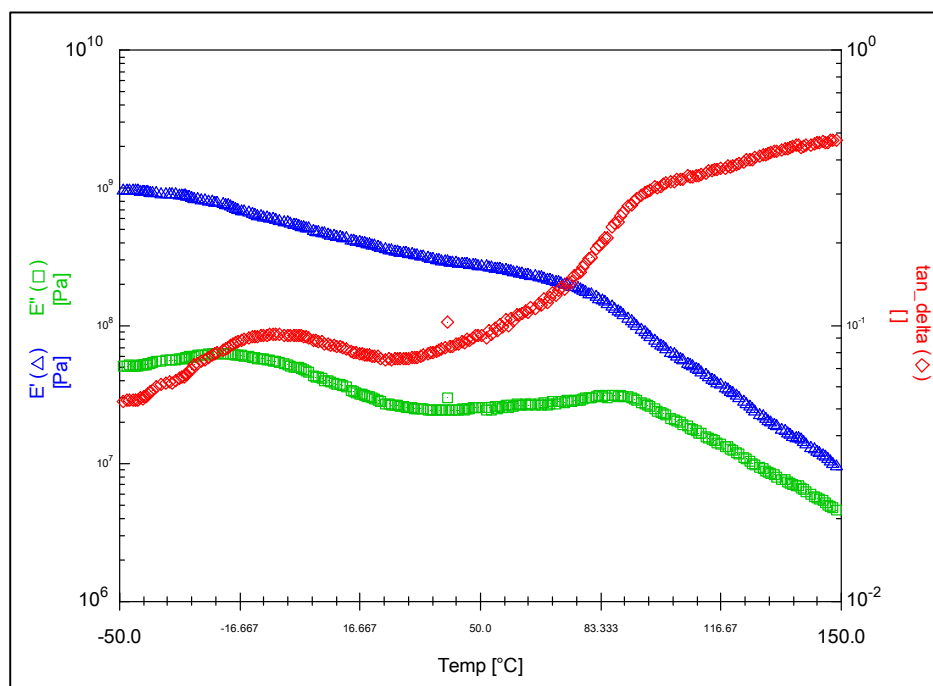


b)

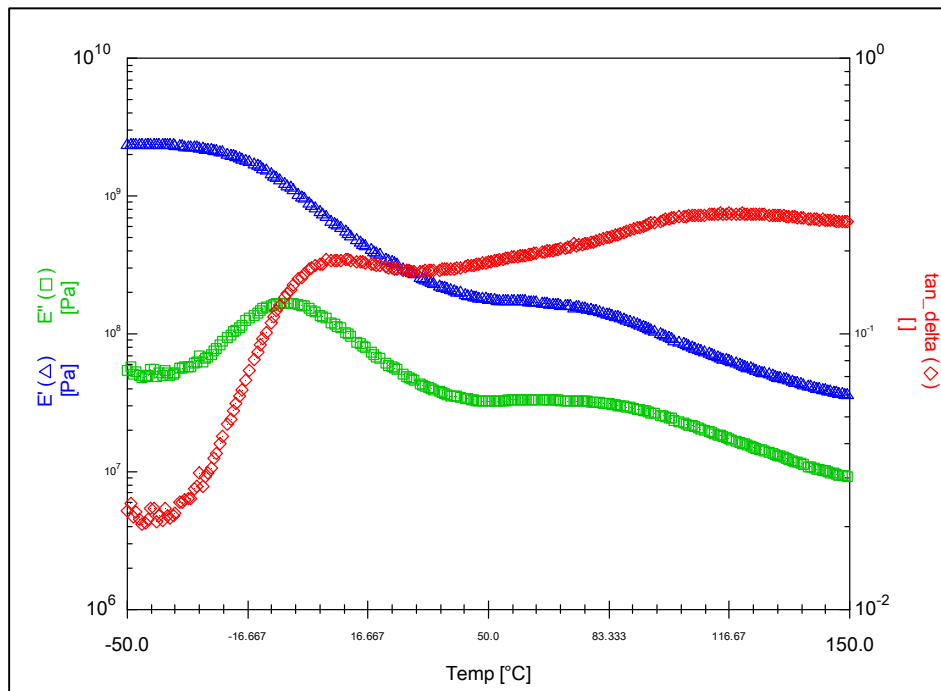
Figure 6.5: DSC thermograms of samples based on a) cellulose acetate and b) cellulose acetate butyrate esters

6.2.2.5. Dynamic Mechanical Analysis

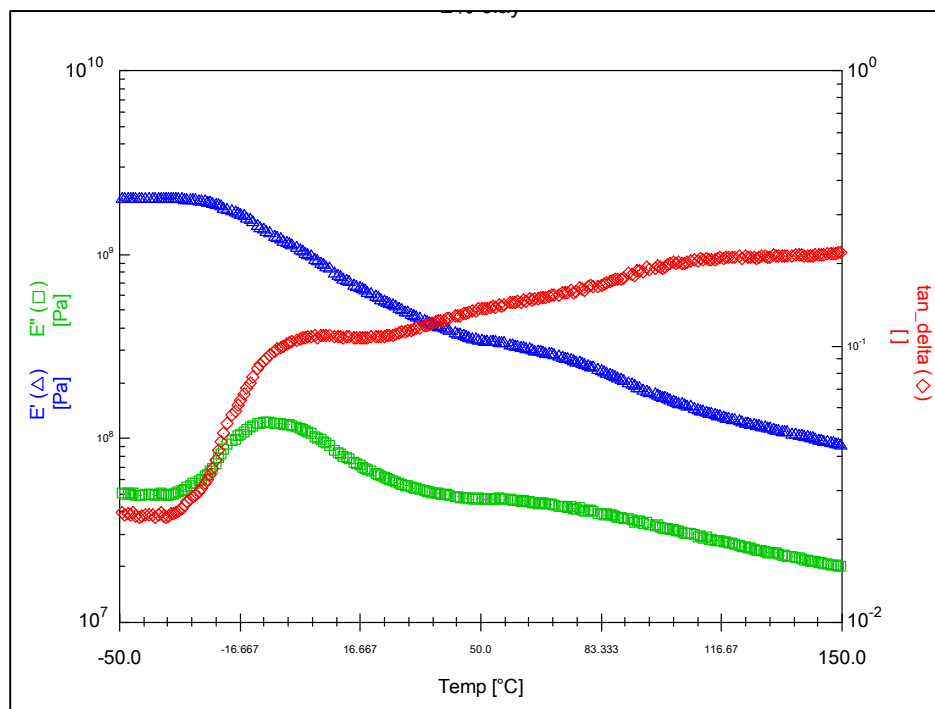
Figure 6.6 shows the temperature dependency of dynamic mechanical properties of prepared samples. It can be seen that the storage modulus of externally plasticized nanocomposite specimen PCA2C decreases with increasing temperature in the temperature range from -25 to 100 °C indicating the temperature dependency of the tensile properties. The internally plasticized or grafted copolymer and its nanocomposite show the transition at -16 and -18 °C, respectively. This is in accordance with transition observed by DSC. Below these transitions, the storage modulus of internally plasticized samples is higher than that of externally plasticized counterparts.



a) Externally plasticized nanocomposite sample: PCA 2C



b) Internally plasticized sample: CA25P



c) Internally plasticized nanocomposite sample: CA2C25P

Figure 6.6: Dynamic mechanical properties (storage modulus (Δ), loss modulus (\square) and tan delta (\diamond))

6.2.2.6. Tensile Properties

The effect of internal plasticization and incorporation of nano-clay on the tensile properties can be seen in *Table 6.1*.

Table 6.1: Tensile properties of externally plasticized and polyethylene glycolated cellulose esters (copolymer) and their nanocomposites

Sample	Tensile Modulus (MPa)	Yield Stress (MPa)	Yield Strain (%)	Stress at Break (MPa)	Strain at Break (%)	Toughness (MPa)
PCA	78 ± 10	1.2 ± 0.2	25 ± 1	0.6 ± 0.2	30 ± 2	-
PCA-2C	125 ± 10	1.4 ± 0.2	20 ± 1	0.6 ± 0.2	25 ± 2	0.5 ± 0.2
PCA-5C	145 ± 10	1.6 ± 0.2	20 ± 1	0.6 ± 0.2	23 ± 2	0.6 ± 0.2
CA25P	104 ± 8	3.4 ± 0.3	30 ± 1	1.6 ± 0.2	48 ± 2	1.2 ± 0.2
CA25P-2C	145 ± 10	3.3 ± 0.3	25 ± 1	1.4 ± 0.2	23 ± 2	0.7 ± 0.2
CA2C25P	245 ± 10	7.9 ± 0.3	23 ± 2	2.4 ± 0.2	46 ± 2	3.5 ± 0.3
CA5C25P	280 ± 10	8.4 ± 0.4	20 ± 2	3.5 ± 0.2	40 ± 2	3.6 ± 0.3
CA50P	78 ± 8	3.2 ± 0.3	40 ± 2	1.5 ± 0.2	73 ± 3	1.2 ± 0.2
CA50P-2C	123 ± 8	2.6 ± 0.4	35 ± 2	1.2 ± 0.2	68 ± 3	0.7 ± 0.2
CA2C50P	156 ± 8	4.2 ± 0.4	33 ± 2	2.4 ± 0.2	56 ± 3	3.5 ± 0.2
CA5C50P	238 ± 8	5.6 ± 0.4	25 ± 2	3.6 ± 0.2	50 ± 3	3.6 ± 0.2
PCAB	84 ± 8	2.4 ± 0.3	34 ± 1	1.3 ± 0.2	48 ± 2	1.4 ± 0.2
PCAB-5C	156 ± 10	4.3 ± 0.3	30 ± 1	1.2 ± 0.2	23 ± 2	1 ± 0.2
CAB2C25P	280 ± 10	8.4 ± 0.3	33 ± 2	2.5 ± 0.2	46 ± 2	3.7 ± 0.3
CAB5C25P	330 ± 10	9.2 ± 0.4	30 ± 2	3.2 ± 0.2	40 ± 2	4.3 ± 0.3

First, the effect of external plasticization on tensile properties can be seen in PCA, PCA-2C and PCA-5C. These films were casted using glycerol triacetate, keeping the plasticizer / cellulose ester ratio constant and varying clay content. The tensile modulus, which denotes the stiffness of the materials, was found to increase with increasing clay content. The

Chapter 6

samples based on CAB, exhibited higher modulus than their counter parts of CA. The yield stress representing the hardness of the material can be found to increase after grafting of isocyanate terminated PEG and clay incorporation. Among nanocomposites with same amount of clay and prepolymer, CA2C25P shows higher yield stress than CA25P-2C indicating the influence of preparation method. This increase for *in-situ* grafted sample (CA25P-2C) can be attributed to the morphology obtained. The similar result was observed with CAB matrix too. The stress at break, which is ultimate tensile strength of film, was found to be lower than that of yield stress and also to increase after grafting and clay reinforcement.

The break strain (%), which is directly related to the toughness, represents the deformation for complete breakage / failure of material whereas that at yield point represents the maximum deformation up to which the sample can withstand. It can be found to increase with increasing prepolymer content and to decrease with increasing clay content. A well-defined yield point before the break point indicates the induced ductility. The gap between yield and break strain points is lower for externally plasticized cellulose esters than that for grafted copolymer. This also confirms the internal plasticization by grafting of polyethylene glycol via urethane linkage. Under deformation, the crazing failure mechanism requires the mobility of molecular chains to absorb more energy. It appears that under applied stress, the coiled macromolecular chains can undergo three steps which are uncoiling, stretching and slippage. In the present study, both internal plasticizer and external plasticizer can induce the flow of polymer chains to undergo the above-mentioned steps to increase the ductility. In *Table 6.1*, the increase in toughness can be found. The higher toughness was observed for *in situ* grafted nanocomposites.

6.2.2.7. Biodegradation: Compostability

Figure 6.7 shows the biodisintegrability of films in terms of weight loss (%) upon composting. It can be observed that with increasing time of composting, the weight loss (%) increases. This can be attributed to the time needed for microbial adhesion and penetration into the specimen. The maximum weight loss was observed during 2-4 months of incubation. These incubated samples become dark brown (1month) and later (after 3months) black in color indicating the microbial penetration and bioassimilation. With

Chapter 6

increasing time of incubation, the brittleness of specimen also increases for all the plasticized samples. This indicates the weight loss of low molecular chains (esp. plasticizers) in the initial stages of composting. In externally plasticized samples, the plasticizer might be first consumed, later cellulose esters depolymerized through hydrolysis mechanism. On the other hand, owing to its hydrophilicity, polyethylene glycol chains might be hydrolyzed and consumed first. The higher weight loss observed for the samples containing higher prepolymer is in accordance. After 4-5 months, the handling of 50 % prepolymer containing samples become difficult, suggesting the biodisintegrability induced by plasticizer. However, to understand the effect of internal plasticization on the hydrolysis and its mechanism, the enzymatic hydrolysis can be investigated using cellulases enzymes. The clay incorporation, by comparing weight loss values of CA25P with that of CA25P-2C and CA2C25P, can be observed to increase the bio-accessibility after 2 months of composting.

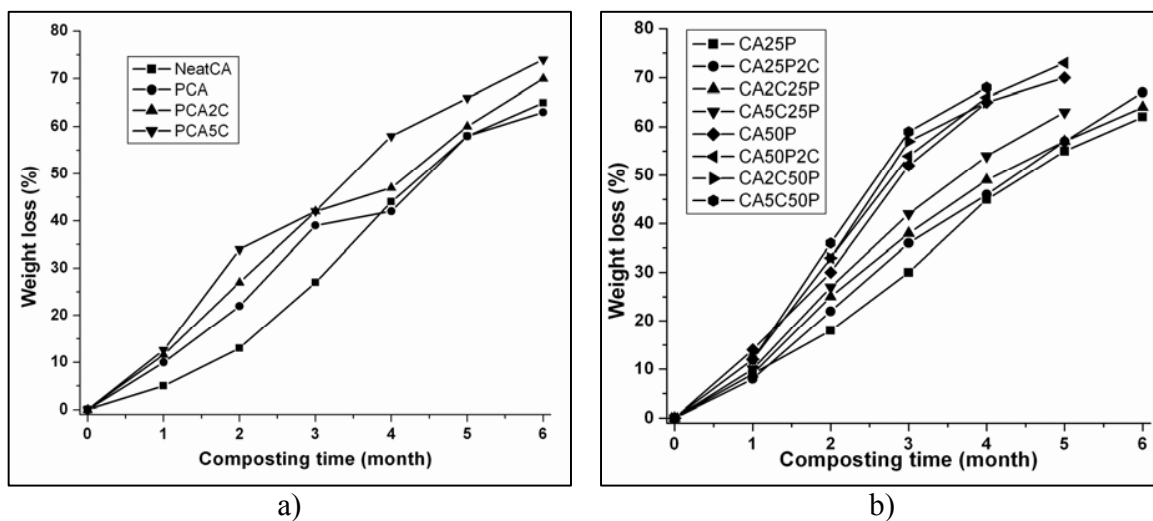


Figure 6.7: Weight loss (%) of the samples upon composting

Thus, it can be summarized from results, of thermal and mechanical properties and compostability, that the grafting of low molecular biodegradable and hydrophilic polymer chains like polyethylene glycol and incorporation of nano-clay can improve the materials properties with retained biodegradability.

6.3. Bionanocomposites from Poly(lactic acid) grafted Cellulose Esters and Organically Modified Montmorillonite

The second part is on grafting of poly(lactide), which is also biodegradable and biobased polymers, on cellulose esters. It is well known that the lactide monomer can be derived from renewable resource by classical chemical reactions and biotechnological processes²⁴⁻²⁵. The ring opening polymerization of cyclic esters has been proposed to under coordination-insertion mechanism in presence of alcoholic hydroxyl groups²⁶. This strategy has been widely exploited for synthesizing copolymers, grafting cyclic esters on hydroxyl group containing polymers. Dubois et. al.²⁷ have grafted lactones on starch for internal plasticization. Yoshioka et.al.¹⁶ have grafted comonomers of lactide and lactones on cellulose diacetate. In the present study, similar methodology has been adopted to graft lactide on cellulose esters. The preparation of nanocomposites has been performed by reactive melt compounding in presence of lactide monomer, clay and cellulose esters.

6.3.1. Experimental

6.3.1.1. Materials

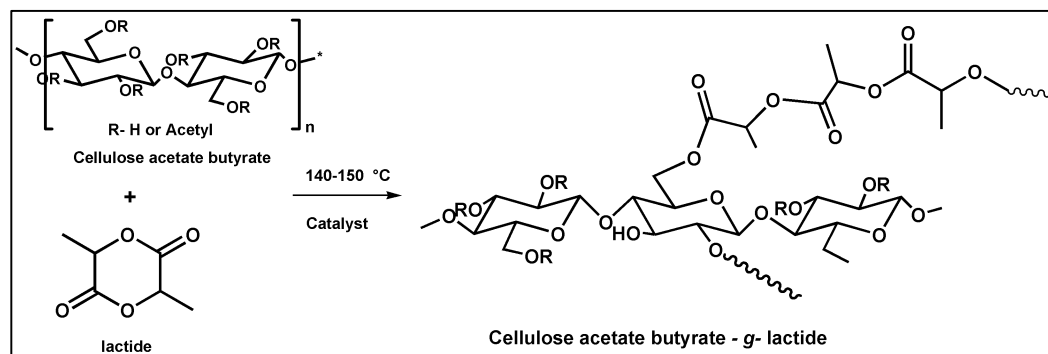
The monomer lactide and catalyst stannous octanoate ($\text{Sn}(\text{Oct})_2$) were purchased from Sigma Aldrich, USA. The clays Cloisite Na (CNa), sodium montmorillonite and Cloisite 30B (C30B), a natural montmorillonite modified with hydrogenated tallow bishydroxyethyl quaternary ammonium salt, were purchased from Southern Clay Products, Inc., USA. The monomer was purified by recrystallization using dry chloroform under inert atmosphere.

6.3.1.2. Grafting of Lactide on Cellulose Acetate and Cellulose Acetate Butyrate

The grafting of lactide on cellulose ester was done by reactive melt-compounding method show in *Scheme 6.3*. Keeping the ratio of cellulose acetate / lactide as 1/5, the weight amount of monomer and cellulose were first dissolved in chloroform for 1h. To this solution, the catalyst stannous octanoate, (0.05 wt. % of monomer), was added. After 15-20 min of stirring, the solvent was evaporated under reduced pressure with nitrogen purge. This mixture was further dried for 12 – 15 h in a vacuum oven at 60 °C. The reactive melt

Chapter 6

compounding was performed in twin-screw microcompounder (5cm³, DSM Research, The Netherlands) at 140-150 °C for 30-40 min with continuous purging of nitrogen.



Scheme 6.3: Pathways for preparation of nanocomposites based on polyethylene glycolated cellulose acetate and clay

The extruded material was purified by dissolving in acetone and precipitating in cold methanol contain 1-5 ml of 0.1 N HCl. The precipitate was centrifuged, washed with methanol and dried in vacuum oven for 12 h at 60 °C. The samples were molded to obtain films (thickness \approx 100 μ m) in electrically heated hydraulic Carver press at 150 °C for 1.5 min and quench-cooled to room temperature (27 °C).

6.3.1.3. Preparation of Nanocomposites

The nanocomposites were prepared by in situ melt graft copolymerization following above-mentioned procedure. The pre-weighted amount of clay (2 %, 5 % wt.) was first dispersed in chloroform after 12 h, it was added to the solution of cellulose ester, monomer and catalyst. After 5 h of stirring, the solvent was evaporated under reduced pressure with nitrogen purge. This mixture was further dried for 12 – 15 h in a vacuum oven at 60 °C. Then reactive melt compounding was done under same conditions. Similar compositions based on cellulose acetate butyrate were also prepared. For comparison, the celluloses esters were also melt mixed with 25 % of plasticizer glycerol triacetate at 140 °C for 30 min. The samples were molded to obtain films (thickness \approx 100 μ m) in electrically heated hydraulic Carver press at 150 °C for 1.5 min and quench-cooled to room temperature (27 °C).

6.3.1.4. Characterization

The above-mentioned characterizations (DSC, TGA, WAXD, DMA, Tensile properties, measurements and composting) were done using molded films.

6.3.2. Results and Discussion

6.3.2.1. FTIR Spectroscopy

Figure 6.8 shows the FTIR spectra of cellulose acetate butyrate and purified grafted copolymer. In comparison of the absorption bands for both, the increased absorption around 1730 cm^{-1} which is assignable for ester bond in the lactide copolymer chains, is observed. The slight decrease in the absorption at hydroxyl group region can also be seen. These suggest the copolymerization initiated at hydroxyl group of cellulose ester. This can be further confirmed by ^{13}C NMR spectroscopy (in CDCl_3).

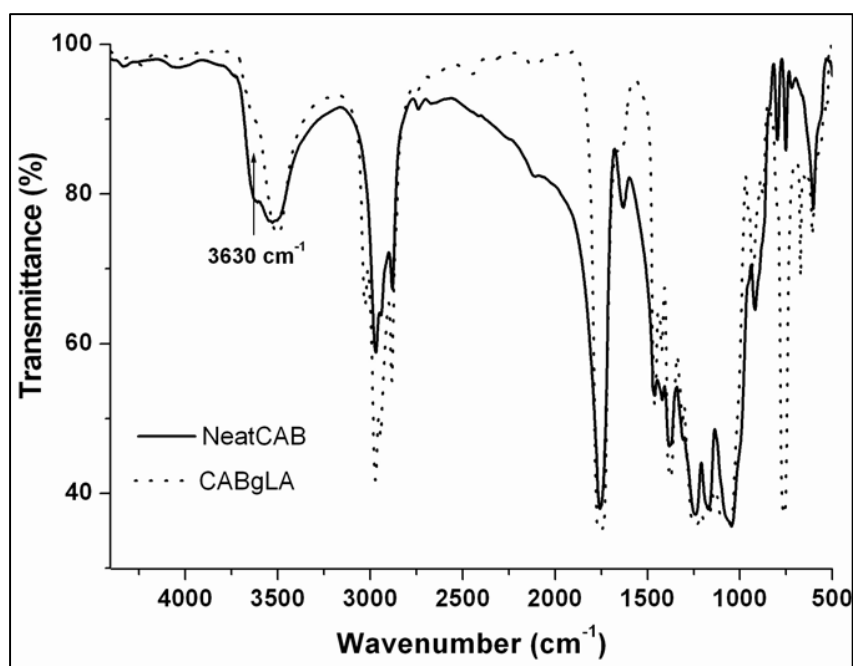


Figure 6.8: FTIR Spectra of neat cellulose acetate butyrate and grafted copolymer

6.3.2.2. ^{13}C NMR-Spectroscopy

Figure 6.9 shows the ^{13}C spectrum of lactide grafted cellulose acetate butyrate. The assignments of chemical shifts of the lactic acid polymer chain and glucose units of

cellulose acetate butyrate are represented. The chemical shift values observed for grafted copolymer confirm the ring opening grafting of lactide monomers on the hydroxyl groups of cellulose ester (CAB).

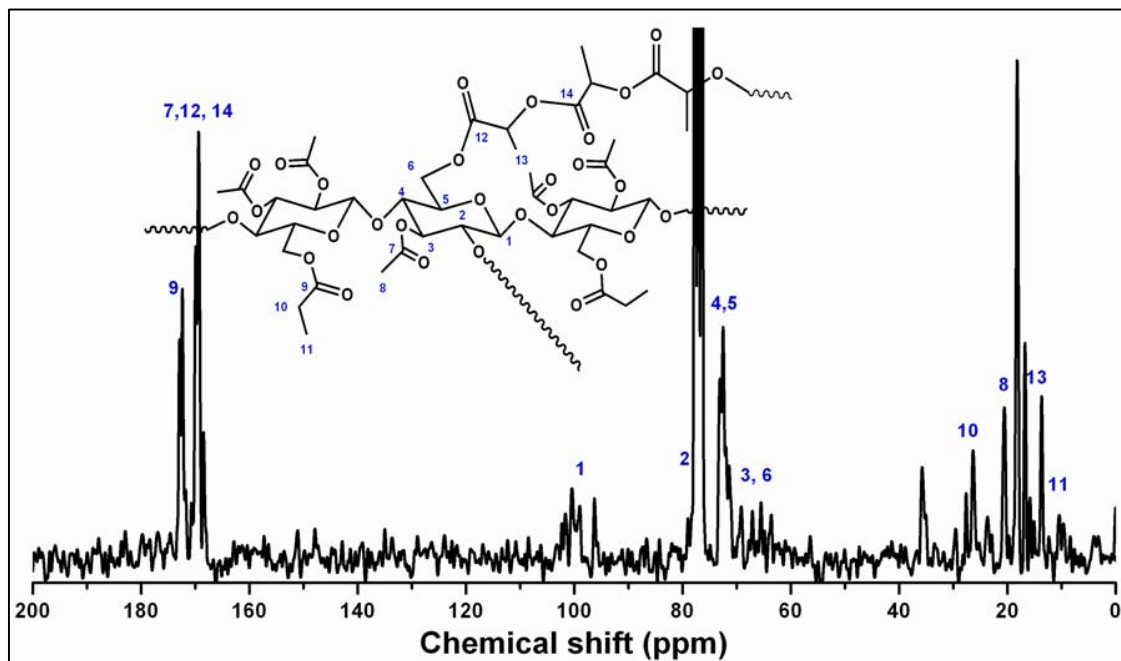


Figure 6.9: ^{13}C -NMR Spectrum of lactide grafted copolymer of cellulose acetate butyrate

6.3.2.3. Wide Angle X-ray Diffraction Pattern

Figure 6.10 shows the WAXD patterns of polylactide grafted cellulose acetate and Cloisite 30B. The expanded d spacing for all the samples can be observed to be higher than that of C30B. Unlike polyethylene glycol grafted copolymer-nanocomposites, these polylactide grafted copolymer-nanocomposites exhibited intercalated morphology in all the compositions.

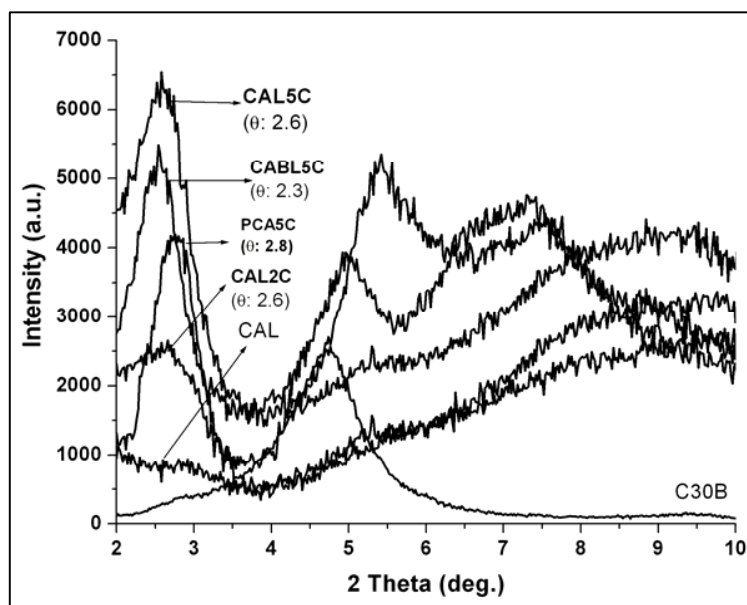
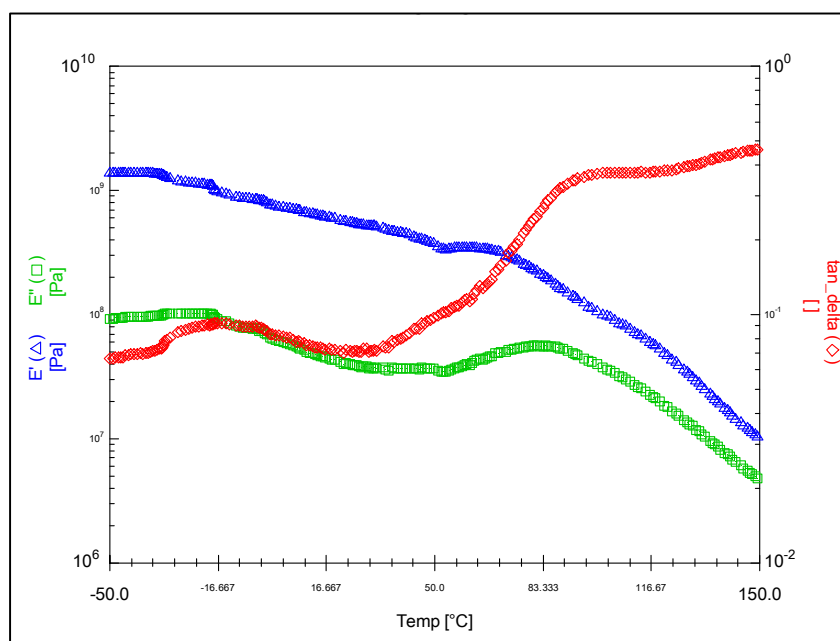


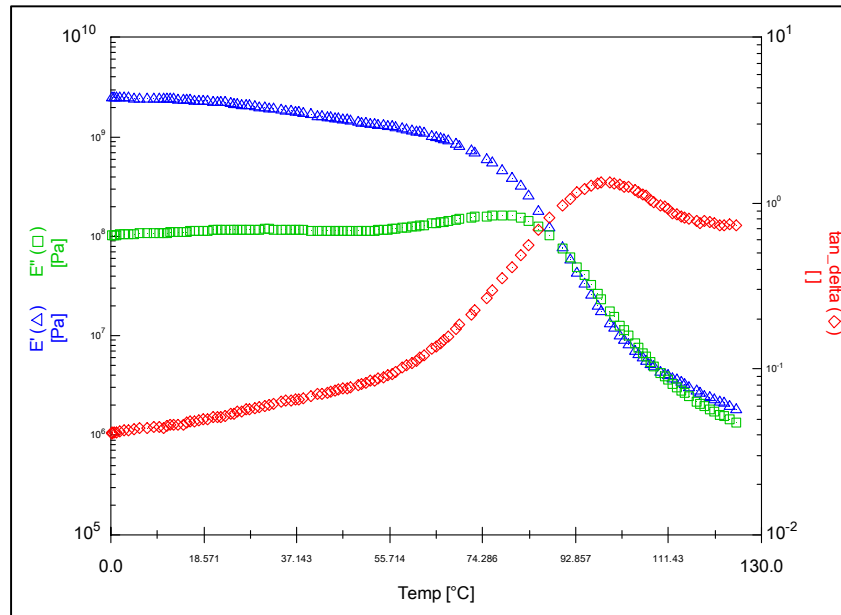
Figure 6.10: WAXD pattern of nanocomposite polylactide grafted copolymer and C30B

6.3.2.4. Dynamic Mechanical Properties

Figure 6.11 shows the temperature dependency of dynamic mechanical properties of grafted copolymer and nanocomposite of externally plasticized cellulose acetate.



a) Nanocomposite (PCA2C) plasticized by 25 % of glycerol triacetate



b) Poly lactide grafted copolymer (CAL)

Figure 6.11: Dynamic mechanical properties (storage modulus (Δ), loss modulus (\square) and tan delta (\diamond))

The storage modulus of PCA2C plasticized by melt compounding is higher than that of casted counter part (Figure 6.6a). The peaks of $\tan \delta$ were observed at $-25\text{ }^{\circ}\text{C}$ and $83.5\text{ }^{\circ}\text{C}$ indicating the transitions. The transition for grafted copolymer (CAL) starts $\sim 62\text{ }^{\circ}\text{C}$ (assignable for the transition of grafted polylactide chains) shows the maximum peak $\sim 93\text{ }^{\circ}\text{C}$. This broad range of transition can be attributed to the internal plasticization.

6.3.2.5. Mechanical Properties

Table 6.2 represents the tensile properties of polylactide grafted and externally plasticized (by melt compounding method) samples. The increase in tensile modulus was observed for nano-clay reinforced cellulose esters. The yield stress and stress at break values show the significant improvement after grafting of lactide. It was observed to decrease with increasing content of layered silicates. The effect of organic modifier can be seen in variation in yield stress and stress at break values. The grafting of polylactide has slightly improved elongation (%) at break, which was observed to decrease after incorporation of clay.

Table 6.2: Tensile properties of externally plasticized and polylactide grafted cellulose esters (copolymer) and their nanocomposites

Sample	Tensile Modulus (MPa)	Yield Stress (MPa)	Elongation at Yield (%)	Stress at Break (MPa)	Elongation at Break (%)
PCA	100 ± 8	3.5 ± 0.9	23 ± 2	1.5 ± 0.9	28 ± 2
PCA2CNa	156 ± 8	4.5 ± 0.5	17 ± 2	2.5 ± 0.5	20 ± 2
PCA5CNa	180 ± 8	6.6 ± 0.4	17 ± 2	2.6 ± 0.4	18 ± 1
PCA5C30B	200 ± 8	8.0 ± 0.6	19 ± 2	3.0 ± 0.6	23 ± 2
CAL	500 ± 10	13.2 ± 0.9	28 ± 1	5.2 ± 0.9	42 ± 3
CAL2CNa	720 ± 10	16.3 ± 0.5	24 ± 2	4.3 ± 0.5	30 ± 2
CAL2C30B	680 ± 10	17.2 ± 0.6	26 ± 2	5.2 ± 0.6	34 ± 2
CAL5CNa	810 ± 10	20.2 ± 0.6	20 ± 1	4.0 ± 0.6	25 ± 2
CAL5C30B	840 ± 10	23.6 ± 0.9	22 ± 1	5.6 ± 0.9	28 ± 2
PCAB	150 ± 10	4.5 ± 0.5	25 ± 2	3.5 ± 0.5	30 ± 2
PCAB2C30B	220 ± 15	7.0 ± 0.6	22 ± 2	3.0 ± 0.6	26 ± 2
CABL	570 ± 10	18.0 ± 0.6	26 ± 2	10.0 ± 0.6	38 ± 2
CABL2C30B	820 ± 20	23.3 ± 0.6	23 ± 2	9.3 ± 0.6	33 ± 2
CAL5CNa	850 ± 20	24.6 ± 0.6	17 ± 2	8.6 ± 0.6	23 ± 2
CAL5C30B	960 ± 20	28.0 ± 0.6	19 ± 2	9.0 ± 0.6	25 ± 2

The trend observed for externally plasticized samples is in reasonable agreement with the results reported elsewhere²⁸.

6.3.2.6. Biodegradation: Compostability

Figure 6.12 shows the biodisintegrability of externally and internally plasticized (polylactide grafted) and molded film specimen in terms of weight loss (%) upon composting time.

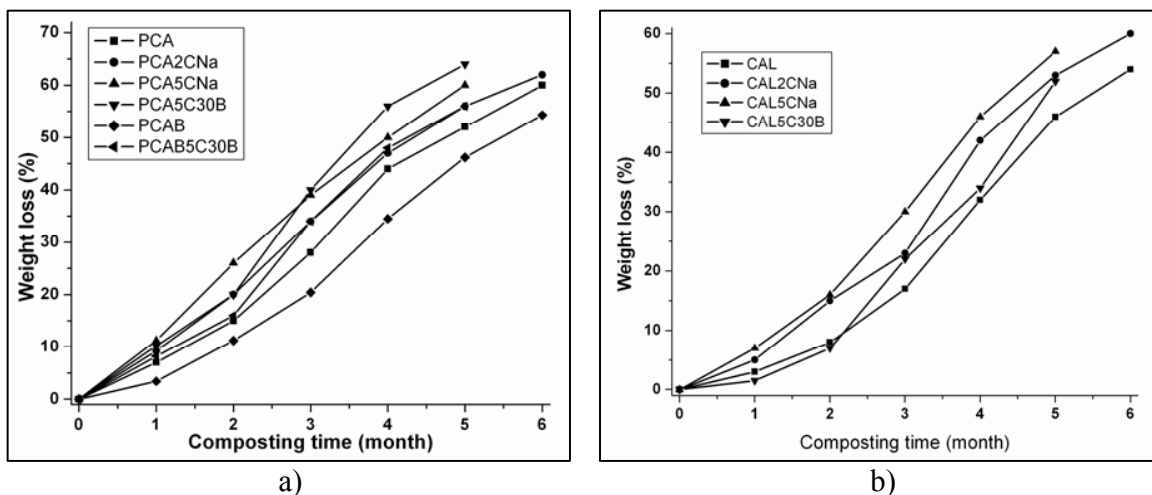


Figure 6.12: Weight loss (%) of samples upon composting

With increasing time of incubation in compost bin, the weight loss (%) of specimen increases. It can be attributed to microbial adhesion and penetration into specimen. The initial weight loss can be due to added and grafted plasticizers. In comparison of Figure 6.6a and 6.10a, among externally plasticized samples, the melt-extruded and molded specimen show lower susceptibility towards microbial degradation than the casted films. This difference can be attributed to the morphology obtained by molding. In comparison of 6.6b and 6.10b, it can be observed that the weight loss (%) values of polylactide grafted cellulose esters and their nanocomposites are significantly lower than polyethylene glycol grafted ones. However, after 5 months of composting, the handling of 5 wt. % clay containing specimen, has become difficult because of brittle nature. Thus, the observed values show the biodegradability under composting conditions.

The exact biodegradation by hydrolysis / depolymerization can be studied by enzymatic degradation, which can reveal the effect of grafting of polymer chains on the cellulose esters. In comparison of neat cellulose esters, the biodegradability of polylactide-grafted samples is significantly affected.

6.4. Conclusion

In the present study, the plasticization of cellulose esters, by grafting biodegradable polymer chains such as polyethylene glycol and polylactide was performed by solvent reaction and reactive melt-compounding methods, respectively. ¹H-NMR, ¹³C-NMR and FTIR spectral analysis show the grafting of polyethylene glycol and polylactide on cellulose esters. Formation of exfoliated nanocomposites in case of polyethylene glycol grafted samples, intercalated nanocomposites in case of polylactide grafted ones is evidenced from WAXD patterns. The internal plasticization was witness from the DSC thermograms and the data obtained from dynamic mechanical analysis. In comparison of externally plasticized samples, grafted copolymers and their nanocomposites have shown drastically improved tensile properties (esp. tensile modulus, yield strength and toughness) of the materials. The sequence of incorporating clay has shown significant effect on the modulus, strength, elongation and ultimately the toughness in case of PEG grafting. The compostability investigation suggests that grafting of polyethylene glycol has no significant on the biodisintegrability of cellulose esters. However, polylactide grafted samples show significant resistance towards disintegration in composting. The further study can be extended to examine the effect of grafting efficiency and degree of substitution and the length of grafted chain on the mechanical, thermal and physical properties and biodegradability.

Chapter 6

References

1. Powers, W. F., *Adv. Mater. Process*, **2000**, May, 38
2. Mohanty, A.K.; Drzal, L.T.; Misra, M., *Polym. Mater. Sci. Engineering*. **2003**, 88, 60
3. Klemm, D; Schmauder H.-P.; Heinze T. in *Biopolymers*, Vandamme E.; De Beats S.; Steinbchel A., Wiley-VCH, Weinheim, **2002**, 6, 290
4. Kaplan D.L. in *Biopolymers from Renewable Resources*, Kaplan D.L Ed., Springer, Berlin, **1998**, 1
5. Marchessault R.H.; Morehandi, F.F.; Walter, N.M., *Nature*, **1959**, 184, 632
6. McNally J. G, Sheppard S. E, *J. Phys. Chem.* **1930**, 34, 165.
7. Hornig, S.; Heinze, T. *Biomacromolecules*, **2008**, 9, 1487
8. Simon J.; Müller H. P.; Koch R. Müller V. *Polym. Degradn Stab*, **1998**, 59, 107
9. Edgar K.J.; Buchanan C.M.; Debenham J.S.; Rundquist P.A.; Seiler B.D.; Shelton M.C; Tindall D., *Prog. Polym. Sci.*, **2001**, 26: 1605
10. Yarsley V.E.; Flavell W; Adamson P.S.; Perkins N.G., *Cellulosic plastics*, Iliffe Books, London, **1964**
11. a) Mork H.S., *Ind. Eng. Chem.* **1919**, 11, 474 b) Drinker P, *Ind. Eng. Chem.*, **1921**, 13, 831
12. Partridge E.P., *Ind. Eng. Chem.* **1931**, 23, 482
13. Fordyce C.R.; Meyer I.W.A., *Ind. Eng. Chem.* **1940**, 32, 1053
14. Malm C.J.; Mench J.W.; Kendall D.L.; Hiatt G.D., *Ind Engg Chem* **1951**, 43, 688
15. Maramorosch K., *Sceince* **1952**, 115, 236
16. Yoshika M.; Hagiwara N.; Shiraishi N. *Cellulose* **1999**, 6, 193
17. a) Alexander M.; Dubois P. *Matr. Sci. Eng.* **2000**, 28, 2023, b) LeBaron P.C.; Pinnavaia T.J.; Wang Z. *Appl. Clay Sci.* **1999**, 15, 11
18. a) Okada A.; Usuki A., *Mater Sci Eng* **1995**, 3, 109, b) Giannelis E.P. *Adv Mater.* **1996**, 8, 29
19. a) Krishnamoorti R; Vaia R.A.; Giannelis E.P, *Chem Mater* **1996**, 8, 1728, b) Ray S.S.; Okamoto M. *Prog Polym Sci* **2003**, 28, 1539
20. Solomon M.J.; Almusallam A.S.; Seefeldt K.F.; Somwangthanaroj A.; Varadan P, *Macromolecules*, **2001**, 34, 1864
21. a) Park, H.-M.; Misra, M.; Drzal, L. T.; Mohanty, A. K. *Biomacromolecules*; **2004**, 5, 2281 b) Park H.-M., Liang X., Mohanty A.K., Misra M. Drzal L.T., *Macromolecules*, **2004**, 37, 9076
22. Lorenz O., Decker H., Rose G., *Angew. Makromol. Chem.* **1984**, 122, 83
23. Lomölder R., Plogmann F., Speier P, *J Coat Technol.* **1997**, 69, 51
24. a) Wood, B.J.B.; Holzappel, W.H., *The Genera of Lactic Acid Bacteria*, 1st edition, Glasgow, UK, Blackie Academic and Professional, **1995**. b) Lindblad, M.S.; Liu, Y.; Albertsson, A.-C.; Ranucci, E.; Karlsson, S., *Adv. Polym. Sci.* **2002**, 157, 139
25. a) *Chem. Eng. News* **2002**, 80, 13; b) S.K. Ritter, *Chem. Eng. News* **2002**, 80, 19. c) *Chem. Eng. News* **2003**, 81, 11. b) Drumright R.E.; Gruber P.R.; Henton D.E., *Adv. Mater.* **2000**, 12, 1841
26. Kricheldorf H.R.; Kreiser-Saunders I.; Boettcher C, *Polymer*, **1995**, 36, 1253, b) Kricheldorf, H. R.; Kreiser-Saunders, I.; Stricker, A. *Macromolecules*; **2000**, 33, 702
27. Dubois P.; Krishnan M.; Narayan R, *Polymer*, **1999**, 40, 3091
28. Park, H.-M.; Mohanty, A.K.; Drzal, L.T.; Lee, E.; Mielewski, D.F.; Misra, M., *J. Polym. Environ.*, **2006**, 14, 27

**Biomimetic Synthesis of Nanohybrids based on Calcium
Hydroxyapatite and Carboxymethyl Cellulose***

* Mater. Sci. Engg. C., 2008 (Communicated)

7.1.Introduction

Over the past decade, the main goal of bone tissue engineering has been to develop biodegradable materials as bone graft substitutes for filling large bone defects. Bone and teeth consist of a small amount of organic matrix, which manipulates the formation of apatite into distinct microstructures suitable for the mechanical forces which they encounter *in-vivo*^{1,2}. There has been widespread use of calcium phosphate bioceramics, as shown in *Table 7.1* for bone regeneration applications

Table 7.1: Calcium phosphates (CaPs) of biomedical significance³

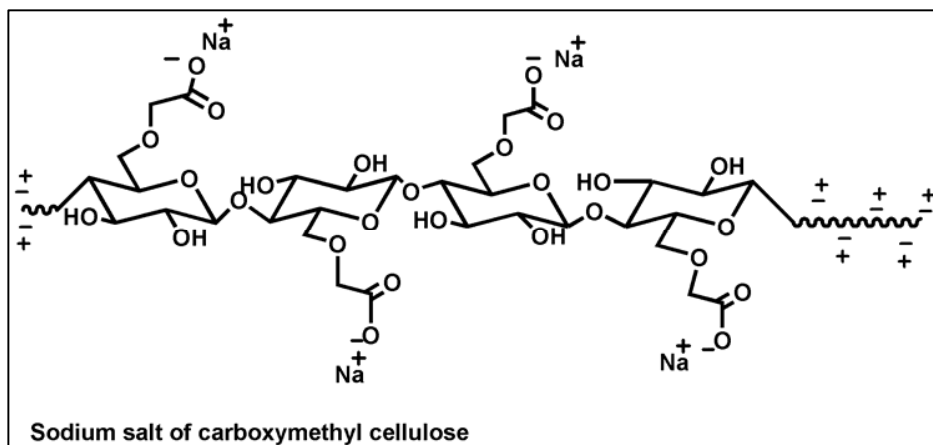
CaP	Compositional Formula	General Acronym
Amorphous calcium phosphate	$\text{Ca}_3(\text{PO}_4)_2 \cdot 3\text{H}_2\text{O}$	ACP
Mono calcium phosphate	$\text{Ca}(\text{H}_2\text{PO}_4)_2$	MCP
Dicalcium phosphate anhydrous	CaHPO_4	DCPA
Dicalcium phosphate dihydrate	$\text{CaHPO}_4 \cdot 2\text{H}_2\text{O}$	DCPD
Tricalcium phosphate	$\text{Ca}_3(\text{PO}_4)_2$	TCP
Octacalcium phosphate	$\text{Ca}_8\text{H}_2(\text{PO}_4)_6 \cdot 3\text{H}_2\text{O}$	OCP
Hydroxyapatite	$\text{Ca}_{10}(\text{PO}_4)_2(\text{OH})_2$	HAP

The biocompatibilities of calcium phosphates are thought to be due to their chemical and structural similarity to the mineral phase of native bone³. Biomineralized tissues are often found to contain polymorphs and individual minerals whose crystal morphology, size, and orientation are often controlled by the local conditions and, in particular, by organic macromolecules such as proteins and polysaccharides^{1,4}. The processes and materials that control such crystal nucleation and growth are of great interest to materials scientists to learn about the architecture, morphology, and patterning of inorganic materials at all dimensions from the nanoscale to macroscopic scale by mimicking the process of biomineralization⁵⁻⁷. Owing to their small size and high surface area, hydroxyapatite (HA) nanoparticles, are similar to that in bone tissue, effectively interact with living cells^{8,9}. The drawbacks of HA nanoparticles are their instability, associated with migration of nanoparticles to surrounding tissue under the action of blood flow and their low solubility¹⁰. To overcome these, a new development in this field is the biomimetic

Chapter 7

synthesis of nanosized calcium phosphates (mainly HA) in polymer-matrices to produce composites that can initiate osteogenesis when implanted in bony sites¹¹. Polymers with distinct molecular organizations may be used as a template to control the geometry of the apatite, for mimicking that of natural bone¹. The development of organic-inorganic hybrids has been triggered in this field using synthetic and natural polymers. Polysaccharides such as chitosan, alginate and starch are currently being investigated to substitute skin, cartilage, nerves, blood vessels and bone. These natural polymers are biocompatible, abundant in source, have low cost and can be modified to host a variety of chemical, physical and biological properties^{12, 13}. Polysaccharides are able to form cross-linked polymer network structures called hydrogels, which are highly hydrated and porous like living tissue. When implanted, these hydrophilic materials allow the permeation of water, metabolic products and chemical signals in the aqueous physiological environment¹⁴. Cellulose, a polysaccharide, is currently used in medicine to produce dialysis membranes, drug coatings and blood coagulants, among many other products. As the primary component of plant cell walls, cellulose is the most abundant natural polymer in the world with an estimated 1010–1011 tons production each year. In biomedical applications, cellulose is used either as regenerated films, fibers or as derivatives (esters, ethers)¹⁴⁻¹⁶. Recently, biomimetic nanocomposites of bacterial cellulose (BC) and HA have been reported^{17,18}. Owing to hydrogen bonding of BC microfibrils, the formed hydroxyapatite / calcium phosphate are deposited and their crystal size increases with increasing reaction time.

In the present study, we have aimed to prepare nanohybrids based on a cellulose derivative. Sodium carboxymethyl cellulose (*Scheme 7.1*), an anionic water-soluble polymer with minimum purity of 99.5%, is widely used in many industrial sectors including food, textiles, paper, adhesives, paints, pharmaceuticals, cosmetics and mineral processing.



Scheme 7.1: Chemical Structure of Sodium Carboxymethyl cellulose (CMC)

Because of its viscosity-increasing properties, aqueous solutions are used to suspend powders intended for topical, oral and / or parenteral applications and as a tablet binder and to stabilize emulsions¹⁹⁻²¹. It has hydroxyl groups (3> per anhydroglucose unit) for lateral hydrogen bonding. Considering, its biodegradability, biocompatibility, non-toxicity, mucoadhesive nature and the carboxyl groups on structure, we expect that CMC can interact with precursors and direct the nucleation and growth of hydroxyapatite to produce bioactive ceramics. Thus, the present study is to prepare nanohybrids of carboxymethyl cellulose (CMC) and hydroxyapatite (HA) nanoparticles and to study the effect of CMC on size, structure and morphology of HA.

7.2. Experimental

7.2.1. Materials

Calcium chloride (CaCl_2), diammoniumhydrogenphosphate ($(\text{NH}_4)_2\text{HPO}_4$) and liquid ammonia were purchased from M/s S.D. Fine Chemicals, Mumbai. Carboxymethyl cellulose (CMC) as sodium salt was obtained from Sigma-Aldrich chemicals.

7.2.2. Synthesis of Nanohybrids

The weighed amounts of polymer and calcium reagent (CaCl_2) were dissolved in aqueous ammonia at 30 °C. After 15 min, the phosphate reagent was added to this solution and stirred for 2 weeks. Prior to precipitation, the solution was allowed to standby for 24 h. The precipitate was washed with deionized water and dried at vacuum oven at 40 °C for 12 h.

Chapter 7

During the reaction, the pH was monitored and adjusted to be 10 by addition of ammonia solution. Portions of prepared samples were also calcined at 1000 °C for 1.5-2 h. Both *as-synthesized* and calcined samples were used for further characterization.

7.2.3. Characterization

The functional group analysis was done using FTIR Spectrum GX Perkin Elmer spectrophotometer, equipped with multiple reflectance accessories for the characterization. Infrared spectra of the samples were recorded in the range of 4000 - 400 cm^{-1} at a resolution of 4 cm^{-1} . A total of 15 scans were used for signal averaging. Solid state ^{31}P Nuclear Magnetic Resonance (NMR) NMR spectra of *as-synthesized* and calcined samples were acquired using high-resolution magic-angle spinning (MAS) Bruker DRX-500 MHz spectrometer with 4mm CP/MAS probe. Thermal gravimetric analysis (TGA) of the samples was done using Perkin Elmer TGA-7 by heating from 50 °C to 900 °C with a heating rate of 10°C min^{-1} under nitrogen with flow rate 20ml min^{-1} .

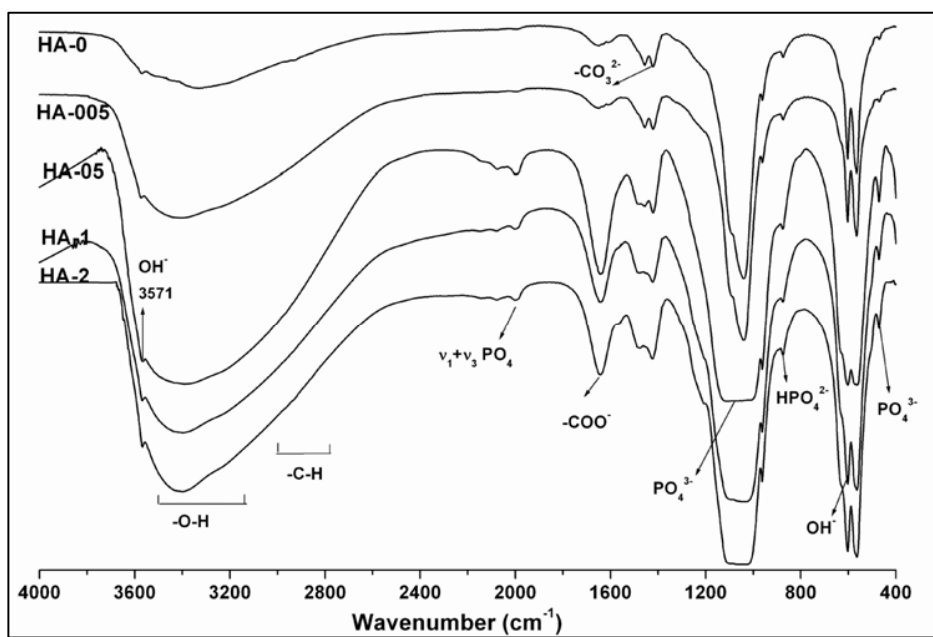
The wide angle X-ray diffraction (WAXD) pattern of sample was obtained using a Rigaku (Japan) X-ray generator (Cu $K\alpha$ radiation with $\lambda = 0.154 \text{ nm}$, 40kV, 80 Am) at room temperature. The diffractograms were obtained in the range from 2° to 60° at scanning speed of 2 °/min. Surface morphology of samples was observed by scanning electron microscopy (Model: Leica Cambridge Stereoscan 440SEM with Phoenix EDAX EDXS). The dispersion of powder sample in isopropanol were stained and dried under vacuum for 24 h at 50°C. The gold-coated samples were scanned under electron microscope. The Ca/P ratio was analyzed by EDAX. The dispersion of sample in isopropanol was dropped on copper grid to obtain ultrathin film of particles. The Transmission electron microscopy (TEM) images were taken using the Jeol – 1200 EX TEM, which was operated with a tungsten electron source at an accelerating voltage of upto 120 kV (resolution: 10 Å; magnification range 5 to 300X).

7.3. Results and Discussion

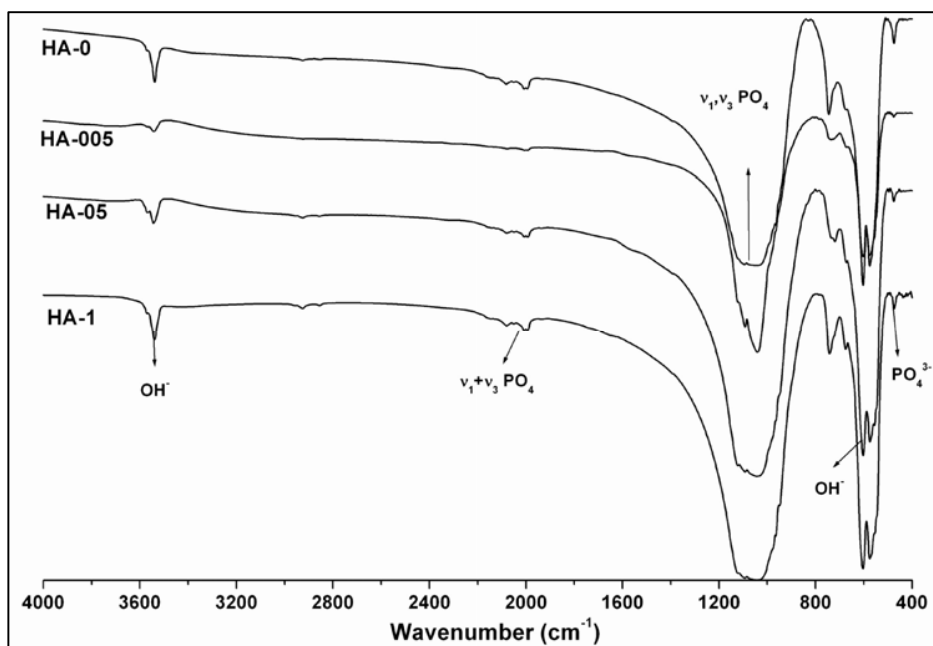
7.3.1. FTIR Spectroscopy

The interactions between carboxymethyl cellulose and hydroxyapatite nanoparticles can be found in *Figure 7.1*, which shows the FTIR spectra of as-synthesized and calcined nanohybrids. In *Figure 7.1a*, the characteristic peaks at 2800-3000 cm^{-1} , 3100-3500 cm^{-1} , 1650-1700 cm^{-1} , and 1100 cm^{-1} , which are assignable for C-H, hydroxyl, carboxylate and C-O- group regions, respectively, indicate the presence of CMC. The absorption bands at 3571 cm^{-1} and 631 cm^{-1} arise from stretching and bending modes of OH^- ions, respectively. The absorbance at 1040 and 1090 cm^{-1} is attributed to (ν_3) phosphate PO_4^{3-} . The other bands at 962 cm^{-1} (for ν_1), 601 and 574 cm^{-1} (for ν_4), and 472 cm^{-1} (for ν_2) are also attributed to unique characteristic vibrations of PO_4 . The weak intensity of bands in 2200 - 1950 cm^{-1} region derives from overtones of bands and combinations of ν_3 and ν_1 phosphate modes. The sharpness of bands, especially at 631, 601 and 574 cm^{-1} indicate a well crystallized HA²².

The 1037 cm^{-1} and 1096 cm^{-1} bands in *Figure 7.1a* and *b* were PO_4^{3-} ν_3 mode and asymmetric HA, respectively. Furthermore, we could see the absorption bands at 1415 and 1450 cm^{-1} and 871 cm^{-1} that are assignable for ν_3 and ν_2 modes of a trace amount of carbonate (CO_3^{2-}) ions. This carbonate, which is designated as B-type carbonate, can replace phosphate PO_4^{3-} ions in the HA lattice (found esp. in human bone)^{23, 24}. However, from these peaks, carbonate ions cannot be completely assigned, because, the symmetric vibrations of CH_2 of CMC can also arise around 1445 cm^{-1} . The weaker intensity (one fifth of ν_3 mode) of ν_2 mode CO_3^{2-} , may also be obscured by HPO_4^{2-} band at 875 cm^{-1} . In calcined samples these peaks were disappeared.



a)



b)

Figure 7.1: FTIR Spectra of a) as-synthesized and b) calcined hydroxyapatite-CMC nanohybrid samples

7.3.2. ^{31}P -NMR Spectroscopy

Figure 7.2 Shows the solid state ^{31}P NMR Spectra of as-synthesized and calcined calcium hydroxyapatite.

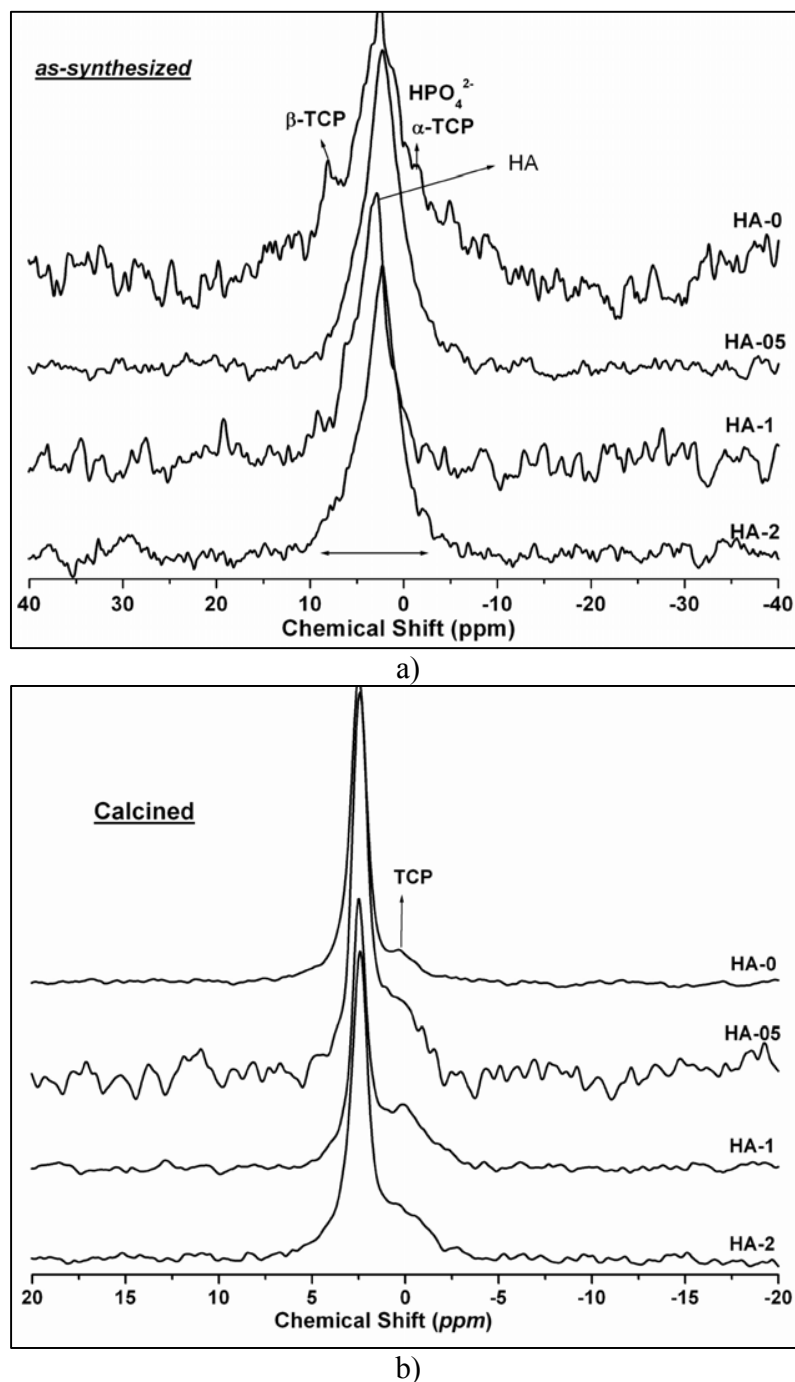


Figure 7.2: ^{31}P -NMR spectra of a) *as-synthesized* and b) calcined hydroxyapatite-CMC nanohybrid samples

The peak at 2.3 - 2.5 ppm, which is typical for hydroxyapatite, can be observed for all the samples. They, however, differ in the line width, and the broadening of peak at foot is also observed for the *as-synthesized* nanohybrids (Figure 7.2a). The broadening of peak is attributed to nanoscale crystalline particles²⁵. The non-protonated calcium phosphates can also contribute a little to the peak intensity. For example, the peak intensity may be contributed by α -tricalcium phosphate at 3.3, 1.8, 0.5 ppm, β -tricalcium phosphate at -0.5, 0.1, 4.2 and 5 ppm and poorly crystallized HA at 3.3 ppm. These were observed for HA-0, whereas, for other samples, the distinction is difficult. However, for calcined samples the peak at 0.2 ppm is observed, which can be assigned for tricalcium phosphates (TCP).

7.3.3. Thermogravimetric Analysis (TGA)

Figure 7.3 shows the TGA thermograms of as-synthesized nanohybrids.

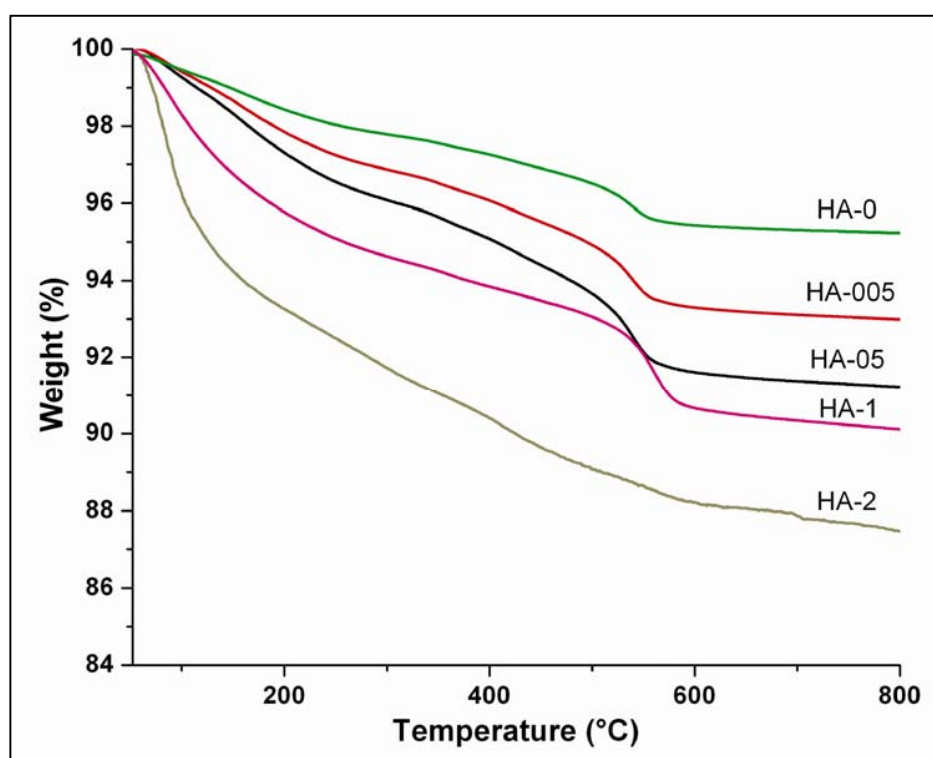


Figure 7.3: Thermograms hydroxyapatite-CMC nanohybrids

The observed weight loss from 75 °C to 550 °C under nitrogen atmosphere can be attributed to dehydration of water molecules present / adsorbed in the crystals, carbon dioxide evolution from carbonate defects of calcium phosphates and decomposition of carboxymethyl cellulose. The untreated HA-0 itself has shown ~3.6 % weight loss. The overall weight loss (%) is linear with CMC content. Since the nanohybrids were thoroughly washed with deionized water for several times while filtration, the strongly adsorbed /bound CMC molecules contributed to the additional weight loss. Similar features were observed with the composite of HA and other polysaccharides ²⁶.

7.3.4. Wide Angle X-Ray Diffraction (WAXD)

Figure 7.4 shows the WAXD patterns of as-synthesized and calcined nanohybrids. The characteristic peaks at $2\theta \sim 10.8, 18.8, 25.8, 31.7$ (with maximum intensity), $32.9, 34.0, 39.8, 46.83, 49.4,$ and 53.1° are attributed to hydroxyapatite. Their corresponding $d_{2\theta}$ values and hkl indices are in with corresponding JCPDS data (Card no: 9-432) reported for hexagonal HA. The broadening at foot of peak at $2\theta \sim 31.7^\circ$ for as-synthesized samples can be correlated to nanocrystal formation. For the calcined samples, these peaks are thin and sharp. Table 7.2, which shows the $d_{2\theta}$ values and hkl indices of the peaks observed for both as-synthesized and calcined HA-05 samples. The additional peaks can be correlated to phase change and the presence of non-protonated calcium phosphates. During calcination (700-1000 °C), amorphous hydroxyapatite can be decomposed to give tricalcium phosphates²⁷, which is in reasonable agreement with corresponding ³¹P-NMR spectra. However, this dehydration is reversible, while cooling, it results in hydroxyapatite ²⁸. The crystallite size, D (nm) was calculated using the following Scherer formula ²⁹;

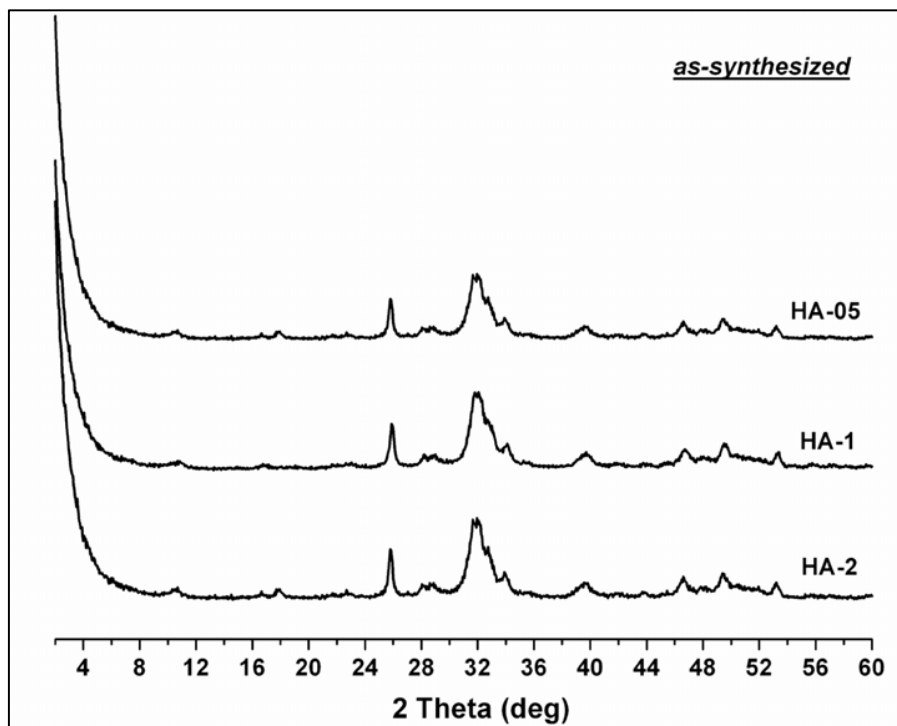
$$D = k\lambda / \beta_{1/2} \cos \theta$$

Where k is Scherer constant (0.9~1), λ wavelength (in angstrom), and θ diffraction angle. The corrected value of $\beta_{1/2}$ is calculated by Warren's equation

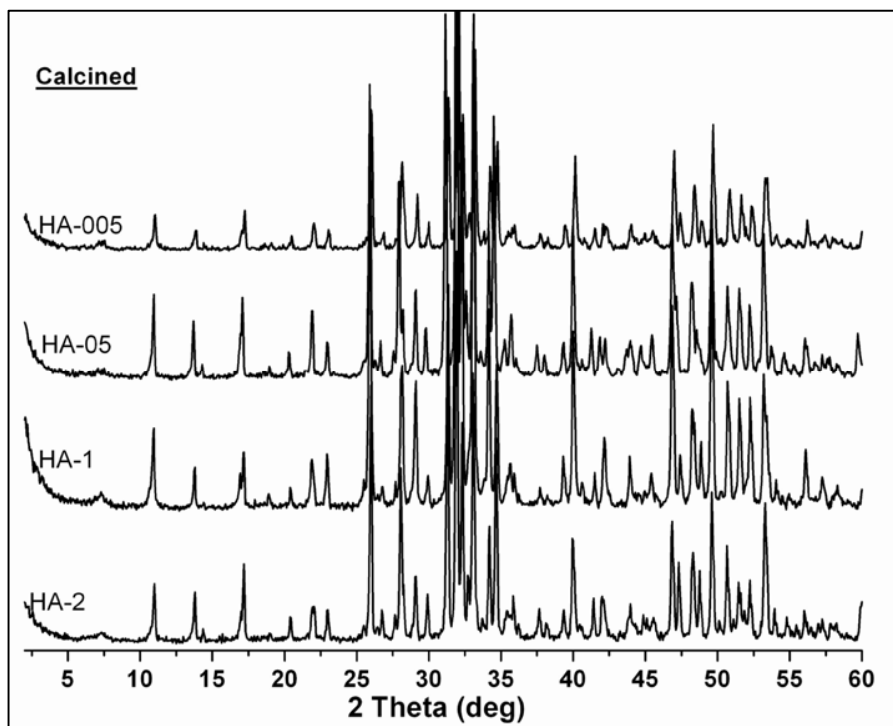
$$\beta_{1/2} = \sqrt{B^2 - b^2}$$

Where, B is full width at half maximum intensity and b is instrument factor.

Table 7.3 shows the effect of CMC content on the crystallite size of HA in both as-synthesized and calcined samples.



a)



b)

Figure 7.4: WAXD patterns of spectra of a) as-synthesized and b) calcined hydroxyapatite-CMC nanocomposite samples

Table 7.2: The observed 2θ ($^\circ$), d-values and corresponding indices from WAXD pattern of as-synthesized and calcined samples of HA-05

Diffraction angle 2θ ($^\circ$)	$d_{2\theta}$ (nm)	Indices (hkl)	Diffraction angle 2θ ($^\circ$)	$d_{2\theta}$ (nm)	Indices (hkl)
10.85	0.815	100	35.44	0.253	301
16.87	0.525	101	39.73	0.226	310
18.84	0.471	110	41.98	0.215	311
21.75	0.408	200	43.84	0.206	113
22.84	0.389	111	46.68	0.194	222
25.35	0.351	201	48.06	0.189	312
25.86	0.344	002	49.46	0.184	213
28.11	0.317	102	51.25	0.178	410
28.92	0.308	210	52.06	0.175	402
31.77	0.281	211	53.16	0.172	004
32.18	0.278	112	55.87	0.164	322
32.90	0.272	300	59.93	0.154	420
34.04	0.263	202			

Table 7.3: Crystallite size of as-synthesized and calcined hydroxyapatite nanoparticles

CMC Content (%)	As-synthesized (nm)	Calcined (nm)
0	60 ± 5	78 ± 4
0.05	29 ± 5	49 ± 4
0.5	26 ± 4	48 ± 4
1	21 ± 3	48 ± 4
2	18 ± 3	48 ± 4

With increasing content of CMC, the crystallite size decreases. After calcination, regardless of CMC content the crystallite size is increased, which can be attributed to the sintering and densification phenomena at higher temperature³⁰. The nanoparticles, which are thermodynamically unstable, are generally stabilized by CMC molecules as aggregates.

Chapter 7

Because of their higher reactivity, during calcination as the organic molecules decompose, HA nanoparticles are densified to result bigger crystals³¹.

7.3.5. Scanning Electron Microscopy (SEM) and Energy Dispersive X-ray Analysis (EDAX)

SEM images of as-synthesized and calcined samples of HA-05 and for HA-1 can be found in *Figure 7.5*.

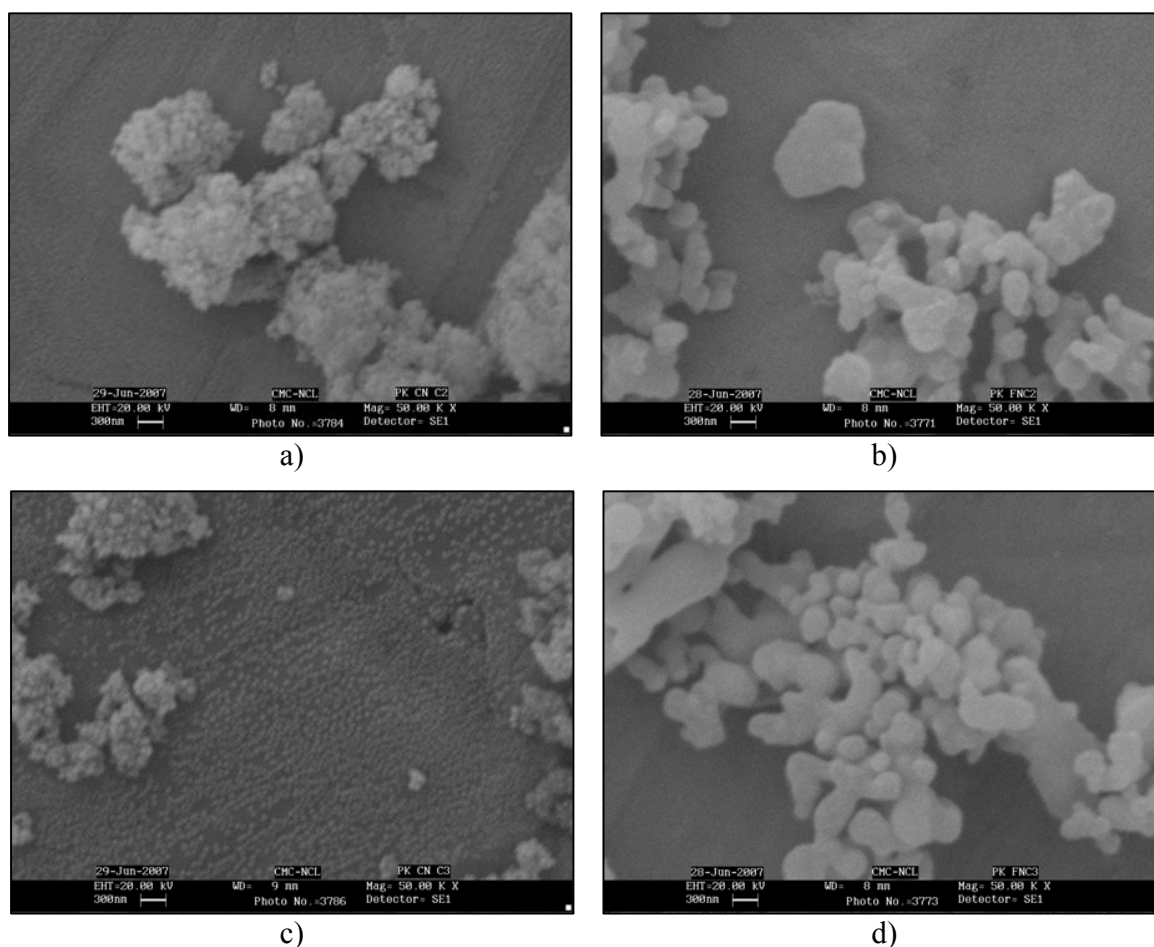


Figure 7.5: Scanning electron micrographs (SEM) of a) as-synthesized and calcined HA-05 (50x magnification)

In as-synthesized samples, the nanoparticles are embedded / surrounded by CMC molecules to form agglomerate whose size is about 100 – 300 nm. These agglomerates show rough and interconnected porous surface. It is reported that the interconnected

porous, rough surface and the flexibility of macromolecular chains in biological solutions are necessary to improve the contact between the tissue and particles, by promoting penetration of the polymeric chains into the tissue to form a strong bonding, leading to an increase in the adhesion strength^{32, 33}. As FTIR spectra results suggest the presence of CMC in as-synthesized nanohybrids, the agglomeration of nanoparticles might be due to CMC molecules. After calcination, particles are bigger in size and smoother on the surface than that of as-synthesized ones. As mentioned above, the increase in particle size can be attributed to the sintering of HA nanoparticles at higher temperature.

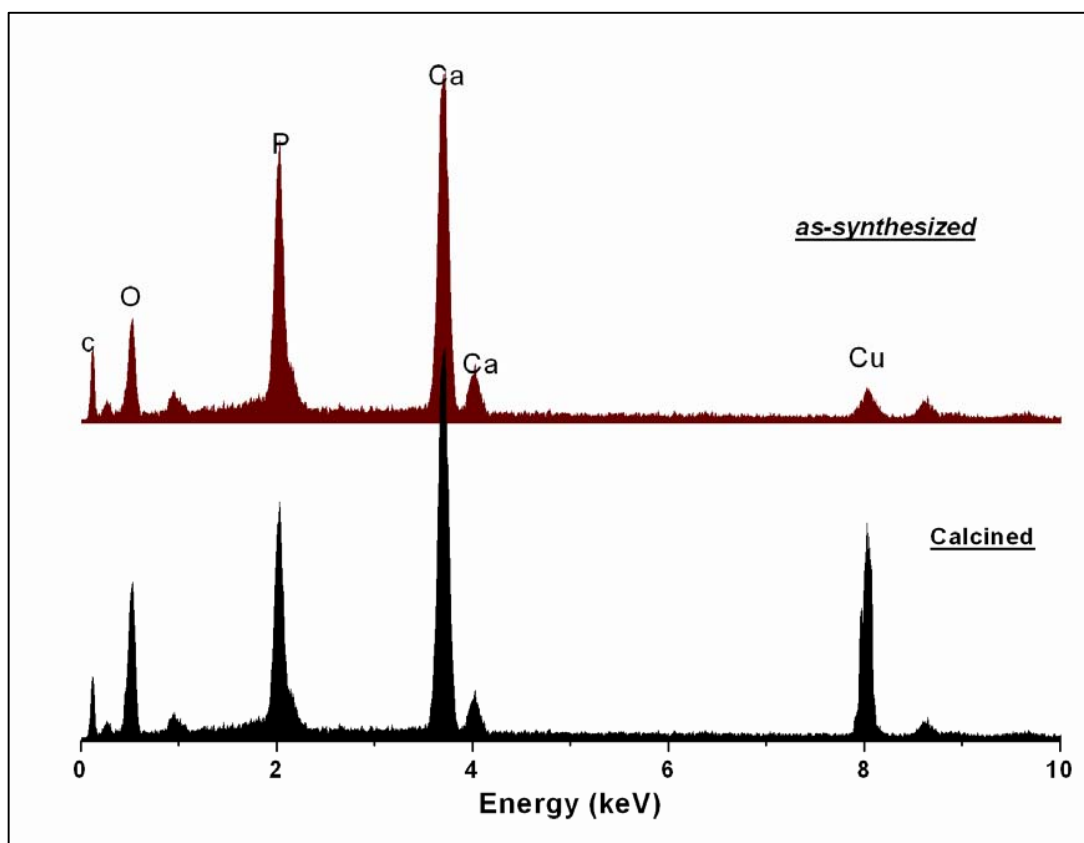


Figure 7.6: EDAX spectra of as-synthesized and calcined HA-05

Figure 7.6 shows the EDAX graph of the as synthesized and calcined sample of HA-05. The Ca/P ratios for as-synthesized and calcined sample were about 1.45 and 1.67, respectively. This also confirms the formation of hydroxyapatite precipitates.

7.3.6. Transmission Electron Microscopy (TEM)

The bright field TEM images of as-synthesized and calcined samples are shown in *Figure 7.7*

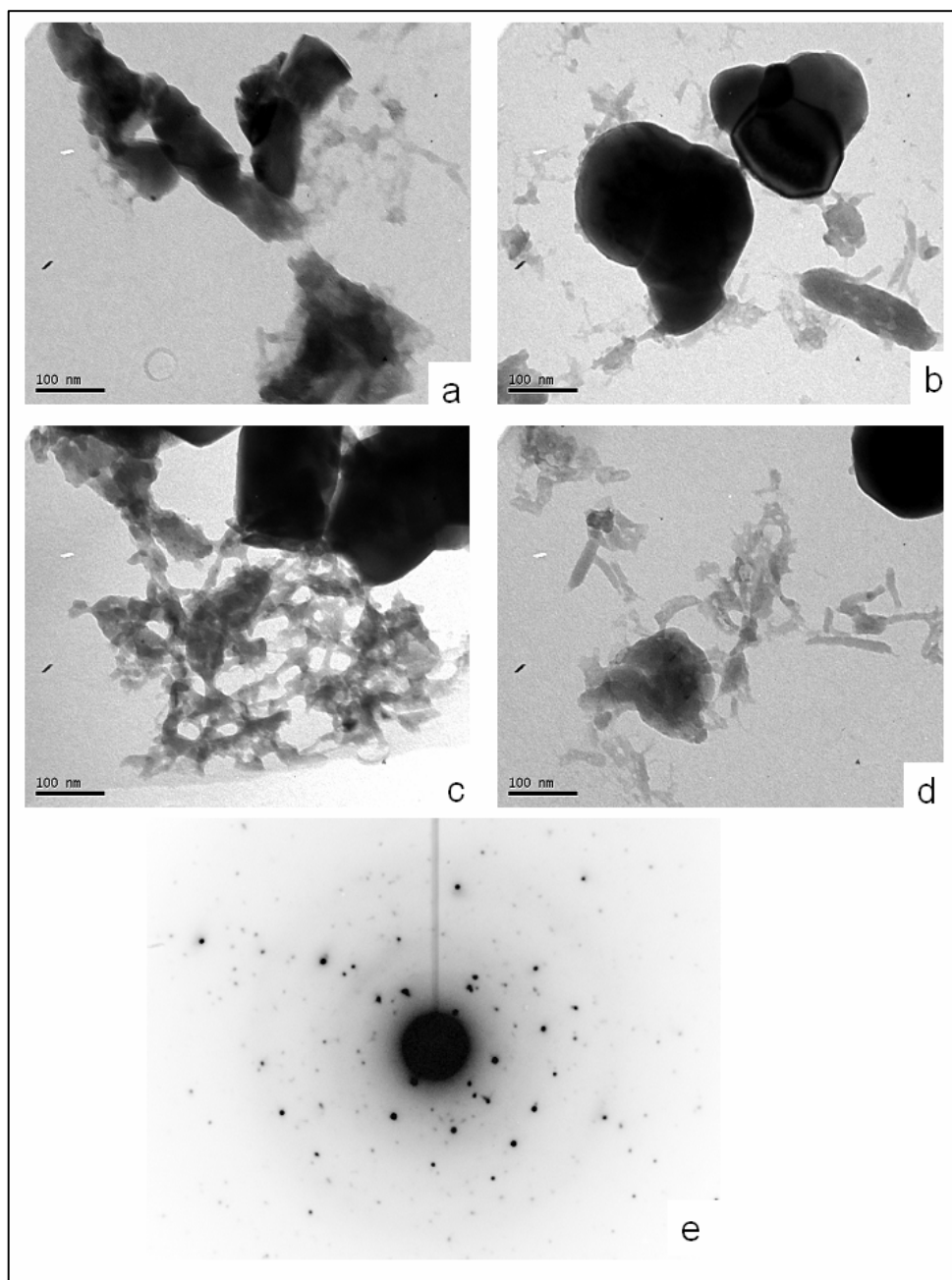
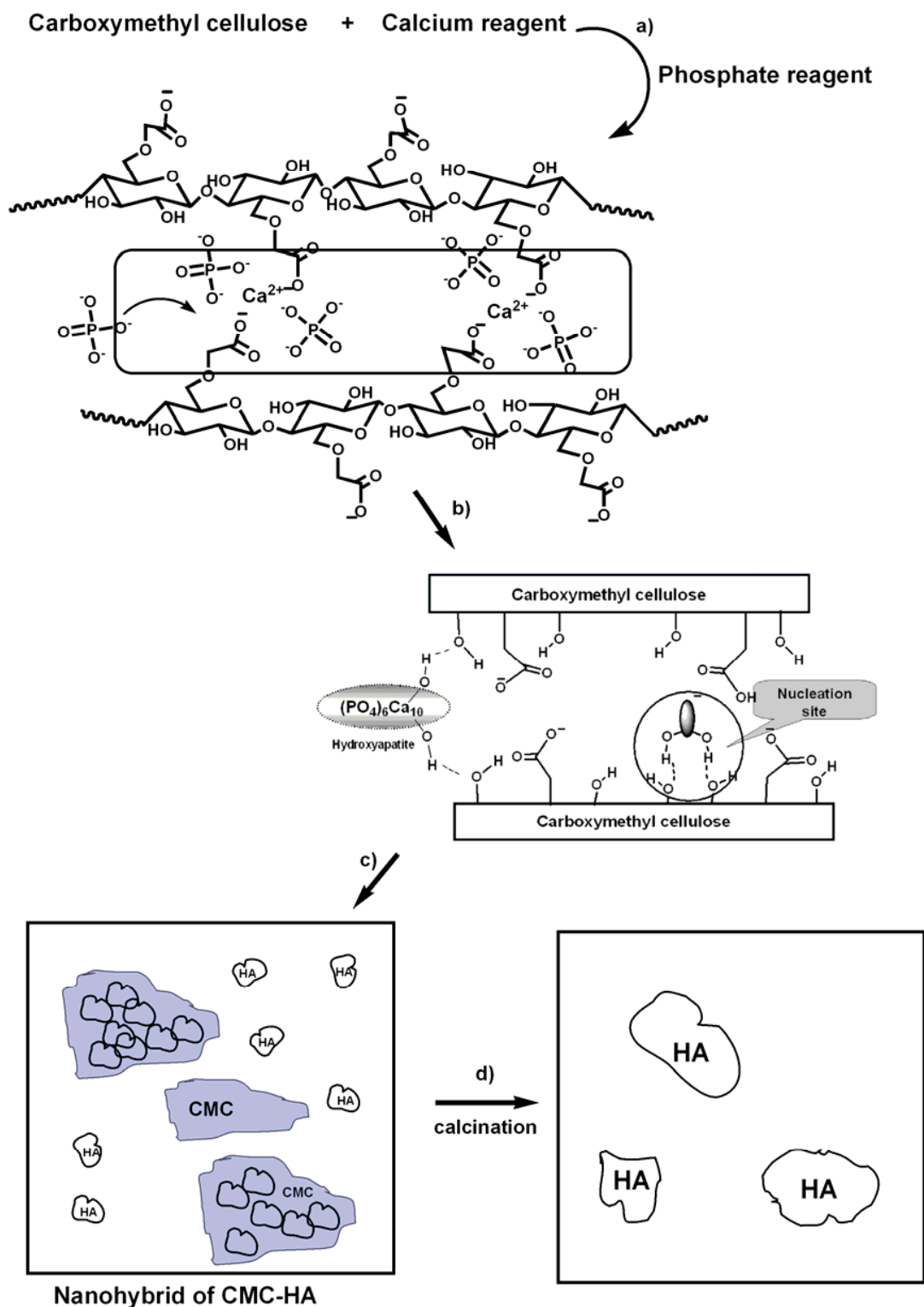


Figure 7.7: Bright field TEM images of a) as-synthesized HA-005, b) calcined HA-005, c) as-synthesized HA-05, d) as-synthesized HA-01 and e) electron diffraction of HA-05

Chapter 7

The as-synthesized nanohybrids can be seen as the agglomerates of nanoparticles in the CMC matrix whereas smooth and bigger HA particles are seen in calcined samples. In the as-synthesized samples, the agglomeration of HA nanoparticles can be explained by interactions of carboxymethyl cellulose, HA and its precursors with each other. *Scheme 7.2* shows the nucleation and induction of hydroxyapatite crystallization on CMC. First, the added calcium ions (Ca^{2+}) are absorbed by carboxyl groups of CMC molecules (step a). Later, phosphate ions react with calcium ions to form calcium phosphates including hydroxyapatite. Owing to intra- and intermolecular hydrogen bondings of CMC, they can act as a template for these reactions. The nuclei of HA crystals can be stabilized by hydrogen bonding between hydroxyl groups of HA and CMC as shown in *Scheme 7.2* step b) and further growth of crystals result in agglomeration. According to Murray et. al., [34], the formation of nanostructures in presence of macromolecules can be attributed to slower growth on the existing nuclei. It is well known that by systematic adjustment of the reaction parameters, such as reaction time, temperature, concentration, and the selection of reagents, surfactants (stabilizer) or polymers matrix can be used to control the size, shape, and quality of nanoparticles³⁵. Tailoring the ratio of the concentration of reagents to that of organic molecules (surfactants) provides another control over nanoparticle size, because high stabilizer-to-reagent concentrations favor the formation of a smaller nuclei and a smaller nanoparticles size. As it was seen in *Table 7.3*, with increasing concentration of CMC, crystallite size of nanoparticles decreases (18 ± 3 nm, for 2 % CMC content). During nanoparticle growth, the polymer chains in solution adsorb reversibly to the surfaces of the particles, providing a dynamic organic shell (capping layer) that stabilizes the nanoparticles in solution and mediates their growth. Macromolecules, which can bind more tightly to the surface of nanoparticles or provide a greater steric hindrance, could slow the rate of addition of materials to the nanoparticle, resulting in smaller size. In the present study, the used macromolecule, CMC has carboxyl groups approximately 0.9 per anhydroglucose unit (AGU) and they are distributed randomly. Thus, the nucleation site might also be distributed through the matrix randomly. In solution, CMC may be present as elongated coils²¹. According to Kun model,³⁶ hypothetical length of linear portion is around 13-18 nm, which (consists of approximately 25 AGUs) can be closer to size of HA nanoparticles.



Scheme 7.2: Schematic representation of nucleation and induction of hydroxyapatite crystals by carboxyl groups of CMC.

However, because of amorphous nature of CMC and randomly distributed nucleation sites, the obtained nanoparticles may have undefined shape. *Figure 7.7e* shows the electron diffraction pattern of HA-05, where discrete crystalline pattern and moiré fringes can be observed. The aggregates of hydroxyapatite nanocrystals caused by CMC matrix might induce moiré fringes. Similar observation was earlier reported by Chang et. al ³⁷ for gelatin / hydroxyapatite. Since the agglomeration of hydroxyapatite caused by water-soluble, biopolymers like carboxymethyl cellulose, the prepared nanohybrids can show improved solubility and biocompatibility in biological media.

7.4. Conclusion

In the present study, the nanohybrids of carboxymethyl cellulose (CMC) and hydroxyapatite (HA) nanoparticles have been prepared by co-precipitation method at room temperature. Fourier transform infrared spectroscopy, ³¹P-NMR spectroscopy and wide-angle X-ray diffraction measurements have shown the formation CMC-nanohybrids. TG analysis revealed that content of CMC in nanohybrids is linear with initial input. Scanning electron microscopy with energy dispersive X-ray analysis and transmission electron microscopy (TEM) revealed that nanohybrids are formed as aggregates of HA nanoparticles embedded in CMC chains. The morphological aspects of calcined samples have shown the sintering capacity of HA nanoparticles. Possible mechanism for interaction between HA and CMC, nucleation and growth is discussed. Thus, we can summarize that the nanohybrids hydroxyapatite nanoparticles can be prepared for mimicking the process of nucleation and growth in nature using biodegradable and biocompatible macromolecules like CMC.

References

1. Stupp S.I.; Braun P.V., *Science*, **1997**, 277, 1242.
2. Kokubo T.; Kim H.M.; Kawashita M., *Biomaterials* **2003**, 24, 2161–2175.
3. Skrtic D.; Antonucci J.M.; Eanes E.D, *J. Res. Natl. Inst. Stand. Technol.* **2003**, 108, 167
4. Lowenstam H. A., Weiner S., *On Biomineralization*, Oxford University Press, New York, **1989**.
5. Mann S, *Nature* **1988**, 332, 119.
6. Berman A.; Ahn D.J.; Lio, A.; Salmeron M.; Reichert A.; Charych D, *Science* **1995**, 269, 515.
7. Falini G.; Albeck S.; Weiner S.; Addadi L., *Science* **1996**, 271, 67.
8. Doi Y.; Horiguchi T, *J. Biomed. Mater. Res.* **1996**, 31, 43
9. Webster T.J.; Siegel R.W.; Bizios R, *Biomaterials*, **2000**, 21, 1803
10. Miyamoto Y.; Shikawa K.I. *Biomaterials*, **1998**, 19, 707
11. Lee I.; Han S.W.; Choi H.J.; Kim K, *Adv Mater* **2001**, 13, 1617
12. Dumitru S.; Vidal P.F.; Chronet E, In: *Polysaccharides in medicinal applications*, Ed, Dumitru S., Marcel Dekker, New York **1996**, 87.
13. Won C.Y.; Chu C.C. In *Biomaterials and bioengineering handbook*, Ed. Wise D.L., Marcel Dekker, New York, **2000**, 355.
14. Miyamoto T.; Takahashi S.; Ito H.; Inagaki H., *J Biomater Res* **1989**, 23, 125
15. Walton A.G.; Blackwell J., *Biopolymers*, Academic Press, New York, **1973**
16. Yang P.Y.; Kokot, S., *J Appl Polym Sci* **1998**, 60, 1137
17. Hutchens S.A.; Benson R.S.; Evans B.R.; O'Neill H.M.; Rawn C.J., *Biomaterials*, **2006**, 26-27, 4661
18. Wan Y.Z.; Hong L.; Jia S.R.; Huang Y.; Zhu Y.; Wang Y.L.; Jiang H.J. *Compos. Sci. Technol*, **2006**, 66, 1825
19. Heinze, T.; Koschella, A. *Macromol. Symp* **2005**, 223, 13
20. Guo, J.-H.; Skinner, G.W.; Harcum, W.W.; Barnum, P.E. *Pharm Sci. Technol. Today* **1998**, 1, 254
21. Kästner, U.; Hoffmann, H.; Dönges, R.; Hilbig, J. *Colloid Surf A: Physicochem. Eng Aspect* **1997**, 123-124, 307
22. Markovic M.; Fowler B.O.; Tung M.S., *J. Res. Natl. Inst. Stand. Technol.*, **2004**, 109, 553
23. Holcomb D.W.; Young. R.A.; *Calcif. Tissue Int.*, **1980**, 31, 189
24. Botha J.; Thorp J.L.; Sponheimer M, *Calcif. Tissue Int.*, **2004**, 74, 162
25. Jäger C.; Welzel T.; Meyer-Zaika W.; Epple M, *Magn. Reson. Chem.* **2006**, 44, 573
26. a) Murugan R.; Rao K.P, *Biomaterials* **2002**, 15, 407, b) Wilson Jr, O.C. Hull J.R. *Mater. Sci. Engg: C*, **2008**, 28, 434
27. Mortier A.; Lemaitre J.; Rouxhet P.G, *J. Mater Sci. Mater Med*, **1989**, 143, 143
28. Bohner M.; Lemaitre J.; Legrand A.P.; d’Espinose de la Caillerie J.-B.; Belgrand P, *J. Mater Sci. Mater Med*, **1996**, 7, 457
29. Klug H.P.; Alexander I.E, *X-ray Diffraction Procedures for polycrystalline and amorphous materials*. 2nd Edn., John Wiley & Sons, New York, **1974**, 618-708
30. Bigi A.; Incerti A.; Roveri N.; Foresti-Serantoni E.; Mongiorgi R.; di Sanseverino L R.; Krajewski A.; Ravaglioli A, *Biomaterials*, **1980**, 1, 140

Chapter 7

31. Arita I.H.; Wilkinson D.S.; Mondragón M.A.; Castaño V.M., *Biomaterials*, **1995**, 16, 403
32. Peppas N.A.; Lustig S.R. *Annals of New York Acad. Sci.*, **1985**, 446, 26
33. Depan D, Kumar A.P, *Acta Biomater* **2008**, communicated.
34. Murray, C.B.; Norris, D.J.; Bawendi, M.G., *J. Am. Chem. Soc.* **1993**, 115, 8706
35. Burda C, Chen X, Narayanan R, El-Sayed M A. *Chem. Rev.*, **2005**, 105, 1025
36. Bikles N.; Segal L, *Cellulose and cellulose derivatives*, John Wiley & Sons, New York, **1974**, Vol 1.
37. Chang M.C.; Ko, C; Doughles W.H., *Biomaerials* **2003**, 24, 2853

8.1. Summary and Conclusions

The present study was focused on the various possibilities of cellulose utilization in structural, semi-structural and biomedical applications. The *Chapter 1* portrays the literature background and motivation for this study and *Chapter 2* describes objectives and approaches focused in the present study. In the first part, which is on the utilization of cellulose fibers as reinforcing materials, three chapters were discussed.

In the *Chapter 3*, the effect of fiber treatments on the mechanical, physical and thermal properties and durability of the natural fiber reinforced composites was examined. The quality of fiber has significantly influenced the properties esp. mechanical properties and durability, which are found to be depending on the chemical components and size of the fiber. For the polyolefins - natural fiber composites, pre-treatment like photo-oxidation is very important for acceptable level of biodegradation. It was summarized that for various applications of natural fiber reinforced composites, the treatments on the fiber have to be optimized depending on their durability requirement.

In the *Chapter 4*, the effect of the incorporation of clay on the properties of cellulose-fiber reinforced composites was discussed. The prepared intercalated nanocomposites have shown the increased mechanical properties (esp. tensile modulus, strength), thermal stability and the resistance towards water absorption. As far durability concerned, the clay-incorporated samples are more susceptible towards photo-oxidation (weathering) than neat polymer and cellulose composites. The biodegradability of photo-irradiated samples is higher than that of non-irradiated ones, which suggest that for the polyolefin – cellulose composites and polyolefin-clay composites, pre-treatment like photo-oxidation is very essential for acceptable level of biodegradation in environment.

The use of cellulose fibers was extended to reinforce and reduce the water absorption properties of the completely biodegradable and hydrophilic polymer matrix in the *Chapter 5*. The reinforcement with microcrystalline cellulose and photo-induced crosslinking resulted in the composite films with reduced water absorption and swelling behavior with increased gel fraction in a polar solvent. The reduction in anti-plasticization by thermal transitions and drastic improvement in tensile properties with increasing photo-irradiation time and cellulose content were observed. It was summarized that combination reinforcement with microcrystalline cellulose and photo-crosslinking of starch matrix has

Chapter 8

improved the physical and mechanical properties of plasticized starch. Since both the polymer matrix and fillers are biodegradable and derived from renewable resources, the prepared composite materials can be coined as ‘green composites’.

The second part of study, the utilization of cellulose esters for nanocomposite preparation, is discussed in *Chapter 6*. The grafting of polyethylene glycol and polylactide and nanoclay reinforcement were found improve tensile properties of the materials. The sequence of incorporating clay has shown significant effect on the crystallographic interactions between matrix and clay and ultimately on modulus, strength, elongation and the toughness. It was summarized the grafting of low molecular biodegradable polymer chains like polyethylene glycol and polylactic acid, and incorporation of nano-clay can improve the materials properties with retained biodegradability.

The third part of study, which is on the use of cellulose derivatives as template materials for biomimetic synthesis of bioceramic nanoparticles for biomedical applications, is discussed in *Chapter 7*. The nanohybrids are formed as aggregates of HA nanoparticles embedded in CMC chains. It was summarized that the nanohybrids hydroxyapatite nanoparticles can be prepared for mimicking the process of nucleation and growth in nature using biodegradable and biocompatible macromolecules like CMC.

The polymeric materials developed using cellulose and its derivatives by various approaches (fiber reinforcement, improvement by nano-scale fillers and photo-crosslinking, internal plasticization) exhibited the advantages of polymeric materials from the renewable resources. These cellulose materials have shown the improved thermal, physical and mechanical properties with controlled degradability, which can be applicable for structural and semi-structural and biomedical applications.

In addition, considering the cost, energy input, carbon dioxide balance and life cycle assessment of both existing synthetic polymers (PP, PE) and biologically degradable materials based on renewable resources may not be a better choice. These are based on renewable, biobased plant and agricultural products that can compete in the markets

currently dominated by petroleum based products. The production of 100% biobased materials as substitute for petroleum-based products is not an economical solution. Of course, the biopolymers certainly offer many ecological advantages. However, the fuel source employed for energy generation is more decisive than the raw materials source for polymer synthesis. If the overall energy demand were satisfied for the largest part from non-fossil sources such as wind energy, solar energy, waterpower and / or nuclear power, polymers based on renewable resources could possess a significantly better balance by comparison to petrochemical synthetic polymers. Thus, a more viable solution would be to combine petroleum and biobased resources to develop a cost-effective product having immense applications. In this concern, cellulose is always proved to be a better sustainable raw material because of its abundant availability, renewability, chemical functionality and their components included during biosynthesis and microfibril hierarchy.

8.2. Future perspectives

Based on the results observed in the present investigation, the further research activities can be extended to study the following aspects;

- The cellulose derivatives can be anchored with polymerizable / curable monomers (acrylates, epoxy monomers) and can be reinforced with nanoscale fillers to have toughness and improved thermal properties and dimensional stability like thermosets.
- The reinforcement of biodegradable polymers by nano-scale cellulose fibers can offer improved thermal and mechanical properties without affecting the biodegradability of polymer matrix.
- The durability of polyolefins-layered silicates nanocomposites can be controlled / improved by modifying the layered silicates with organic modifier anchored with photo-stabilizers (esp. antioxidants).
- The effect of internally plasticized chains (length and grafting efficiency) on the enzymatic biodegradability of cellulose derivatives.
- Regeneration of cellulose fibers filled with nanoscale fillers (e.g. carbon nanotubes) for geo-textile and electronic applications.

Publications

Research Articles:

- **AP. Kumar**, RP. Singh, BD. Sarwade, Degradability of composites, prepared from ethylene-propylene copolymer and jute fiber under accelerated aging and biotic environments, *Mater. Chem. Phys.* **2005**; 92 (2-3): 458-469
- **AP. Kumar**, D. Depan and RP. Singh Durability of Composites of natural fiber and EP Copolymers under accelerated weathering and composting conditions *J. Thermoplast. Compos. Mater.* **2005**; 18: 489-508
- D. Depan, **AP Kumar**, RP. Singh, Preparation and characterization of novel hybrid of chitosan-g-lactic acid and montmorillonite, *J. Biomedical Mater Res. Part A*, **2006**; 78A (2): 372-382
- **AP. Kumar**, RP. Singh, Novel hybrid of clay, cellulose, and thermoplastics. I. Preparation and characterization of composites of ethylene-propylene copolymer, *J. Appl. Polym. Sci.* **2007**; 104(4): 2672-2682
- **AP. Kumar**, RP. Singh, Biocomposites of Cellulose Reinforced Starch: Improvement of Properties by Photo-induced Crosslinking. *Bioresour. Technol.*, **2008**, (In Press) DOI No: 10.1016/j.biortech.2008.04.045
- D. Depan, **AP. Kumar**, RP. Singh, Cell proliferation and Controlled drug release studies of Nanohybrids based on Chitosan-g-lactic acid and Montmorillonite *Acta Biomater.* **2008**, (Under peer review)
- **AP. Kumar**, KK. Mohaideen, RP. Singh, Biomimetic synthesis of nanohybrids based on calcium hydroxyapatite and carboxymethyl cellulose (CMC) *Mater. Sci. Eng. C: Mater. Biol. Appl.* **2008**, (Under peer review)
- **AP. Kumar**, VV. Kodgire, RP. Singh, Bionanocomposites from cellulose derivatives: Preparation and characterization of nanocomposites from polyethyleneglycolated cellulose ester, **2008**, (Under preparation)

Reviews:

- JK. Pandey, KR. Reddy, **AP. Kumar**, RP. Singh An overview of the degradability of polymer nanocomposites *Polym. Degrad. Stab.* **2005**; 88(2): 234-250
- JK Pandey, **AP. Kumar**, M. Misra, AK. Mohanty, LT. Drzal, RP. Singh, Recent Advances in Biodegradable Nanocomposites *J. Nanosci and Nanotechnol.*, **2005**; 5(4): 497-526(30)
- **AP. Kumar**, D. Depan, RP. Singh, N.S. Tomer, 'Nanoscale particles for Polymer Degradation and Stabilization – Trends and Future Perspectives', *Progress in Polymer Science*, **2008**, (Under peer review)

Symposia / Conferences:

- Presented papers in various national and international conferences including International Seminar Advances in Polymer Technology 2004 (APT-04), International Conference on Polymers - MACRO 2004, IUPAC-International Symposium on IONIC POLYMERIZATION 2005, International conference on nanomaterials for electronics (ICNME-2006) and MACRO 2006 (Polymers for Advanced Technologies).